Crosstalk between tumor microenvironment and HIF-1α-HPIP loop establishes phenotypic plasticity in breast cancer cells: Implications in tumor development and metastasis

Submitted for the degree of

Doctor of Philosophy in Biochemistry

By

Saratchandra Singh Khumukcham

(14LBPH06)

Supervisor

Prof. Bramanandam Manavathi, PhD.,

Department of Biochemistry

School of Life Sciences

University of Hyderabad

Hyderabad-500046, Telangana, India

November 2021

प्रतिष्ठित संस्थान
INSTITUTION OF EMINENCE
राष्ट्रीय अपेक्षाएँ, वैश्विक मानक
National Needs, Global Standards
हैदराबाद विश्वविद्यालय

Bramanandam Manavathi, PhD.,
Professor
Dept. of Biochemistry
School of Life Sciences
University of Hyderabad
Hyderabad, 500046.TS
INDIA

CERTIFICATE

This is to certify that the thesis entitled "***Crosstalk between tumor microenvironment and HIF-1α-HPIP loop establishes phenotypic plasticity in breast cancer cells: Implications in tumor development and metastasis***" submitted to the University of Hyderabad by **Mr. Saratchandra Singh Khumukcham** for the degree of Doctor of Philosophy is based on the studies carried out by him under my supervision. I declare to the best of my knowledge that this has not been submitted earlier for the award of any degree or diploma from any other University or Institution.

08/10/21

Prof. Bramanandam Manavathi, PhD.
Supervisor

Prof. Bramanandam Manavathi, PhD
Department of Biochemistry
School of Life Sciences
University of Hyderabad
Hyderabad-500 046. (TS), INDIA

Head
Department of Biochemistry

8/10/2021

HEAD
Dept. of Biochemistry
SCHOOL OF LIFE SCIENCES
UNIVERSITY OF HYDERABAD
HYDERABAD-500 046.

Dean
School of Life Sciences

DEAN
School of Life Sciences
University of Hyderabad
Hyderabad - 500 046.

प्रतिष्ठित संस्थान
INSTITUTION OF EMINENCE
राष्ट्रीय आवश्यकता, वैश्विक मानक
National Needs, Global Standards
हैदराबाद विश्वविद्यालय

Dept. of Biochemistry
School of Life Sciences
University of Hyderabad
Hyderabad, 500046.
Telangana
INDIA

DECLARATION - I

I, Saratchandra Singh Khumukcham, hereby declare that the work presented in this thesis entitled "***Crosstalk between tumor microenvironment and HIF-1α-HPIP loop establishes phenotypic plasticity in breast cancer cells: Implications in tumor development and metastasis***" is entirely original and was carried out by me under the supervision of Prof. Bramanandam Manavathi in the Laboratory of Molecular and Cellular Oncology, Department of Biochemistry, School of Life Sciences, University of Hyderabad. I further declare that this work is original and has not been submitted earlier in part or full for the award of any degree or diploma from any other university or institution.

Prof. Bramanandam Manavathi, Ph.D.
Supervisor

Prof. Bramanandam Manavathi, PhD
Department of Biochemistry
School of Life Sciences
University of Hyderabad
Hyderabad-500 046. (TS), INDIA

Saratchandra Singh Khumukcham
14LBPH06

Date: 08/10/2021

Place: Department of Biochemistry

University of Hyderabad

Bramanandam Manavathi, PhD.,
Professor
Dept. of Biochemistry
School of Life Sciences
University of Hyderabad
Hyderabad, 500046.TS
INDIA

DECLARATION - II

This is to certify that the thesis entitled "***Crosstalk between tumor microenvironment and HIF-1α-HPIP loop establishes phenotypic plasticity in breast cancer cells: Implications in tumor development and metastasis***" submitted by **Saratchandra Singh Khumukcham** bearing Reg. No. **14LBPH06** in partial fulfilment of the requirements for the Doctor of Philosophy in Biochemistry, is a bonafide research work carried out by him under my guidance and supervision. I also declare that it is free from plagiarism and has not been submitted previously in part or in full to this University or any other University or Institution for the award of any degree or diploma. A report on plagiarism statistics from the University Librarian is enclosed.

Furthermore, prior to submitting his thesis/monograph for adjudication, the student had the following publication(s) including two papers from the thesis, Khumukcham et al., ***BBA Reviews on Cancers,*** 2021 and Khumukcham et al., ***Cancer letters,*** 2021, and provided proof for them in the form of reprints in the relevant field of his study.

i. **Saratchandra Singh Khumukcham**, Vasudevarao Penugurti, Anita Soni, Veena Uppala, Kishore Hari, Mohit Kumar Jolly, Anju Dwivedi, Abdul Salam PK, Chiranjeevi Padala, Srinivasulu Mukta, Triveni B, Bramanandam Manavathi. *A reciprocal feedback loop between HIF-1α and HPIP controls phenotypic plasticity in breast cancer cells.* ***Cancer Letters,*** November, 2021 (Accepted).

ii. **Saratchandra Singh Khumukcham**, Bramanandam Manavathi 2021. *Two decades of a protooncogene HPIP/PBXIP1: Uncovering the tale from germ cell to cancer.* ***Biochim Biophys Acta Rev Cancer. (BBA Reviews on cancer)*** *2021 Jun 5;1876(1):188576.*

iii. **Saratchandra Singh Khumukcham**, V.S.K. Samanthapudi, V. Penugurti, A. Kumari, P.S. Kesavan, L.R. Velatooru, S.R. Kotla, A. Mazumder, and B. Manavathi. 2019. *Hematopoietic PBX-interacting protein is a substrate and an inhibitor of the APC/C-Cdc20 complex and regulates mitosis by stabilizing cyclin B1*. ***The Journal of biological chemistry (JBC)***. 294:10236-10252.

iv. Himadri Medhi*, **Saratchandra Singh Khumukcham***, Bramanandam Manavathi and Pradip Paik. *Effective in vitro delivery of paclitaxel by nanocargo of mesoporous polycaprolactone against triple negative breast cancer cells by minimalizing drug dose.* ***RSC Adv.,*** 2020,10, 24095-24107.

v. Vasudevarao Penugurti, **Saratchandra Singh Khumukcham**, Chiranjeevi Padala, Anju Dwivedi, Karthik Reddy Kamireddy, Srinivasulu Mukta, Triveni Bhopal and Bramanandam Manavathi. 2021. *HPIP protooncogene differentially regulates metabolic adaptation and cell fate in breast cancer cells under glucose stress via AMPK and RNF2 dependent pathways.* ***Cancer Letters.*** 518:243-255.

vi. Srikanth Battu, Sumbul Afroz, Jeevan Giddaluru, Saima Naz, Weishan Huang, **Saratchandra Singh Khumukcham**, Rafiq Ahmad Khan, Saleem Yousuf Bhat, Insaf Ahmed Qureshi, Bramanandam Manavathi, Aleem Ahmed Khan, Avery August, Seyed Ehtesham Hasnain, Nooruddin Khan. 2018. *Amino acid starvation sensing dampens IL-1β production by activating riboclustering and autophagy*. ***Plos Biology***, 16(4): e2005317.

vii. Gajulapalli, V.N., V.S. Samanthapudi, M. Pulaganti, **Saratchandra Singh Khumukcham**, V.L. Malisetty, L. Guruprasad, S.K. Chitta, and B. Manavathi. 2016. *A transcriptional repressive role for epithelial-specific ETS factor ELF3 on oestrogen receptor alpha in breast cancer cells*. ***Biochem J***. 473:1047-1061.

8. Information related to presentation of research work in conferences (recognition and acheivements):

i. ***Visiting scholar for two months to Institute of Physiology, University of Lübeck, Ratzeburger Allee 160 – 23562, Germany*** under the bilateral grant project (Department of Science and Technology - DST (India) and German Academic Exchange Service - DAAD (Germany).

ii. ***Best poster award- The International Congress of Cell Biology (ICCB) 2018***, The Dynamic Cell: Molecules and Networks to form and function, CCMB, Hyderabad, India, June 27th to 31st, 2018.

iii. ***Research Proficiency award, 2019,*** Department of Biochemistry, School of Life Sciences, University of Hyderabad, Hyderabad, Telangana, India.

iv. ***Best Poster presentation award-*** International conference organized jointly by IISC (Indian Institute of Sciences), SickKids Canada and The Hebrew University of Jerusalem, 2019.

Furthermore, the student has completed the following courses to fulfill the coursework requirement for the Ph.D.

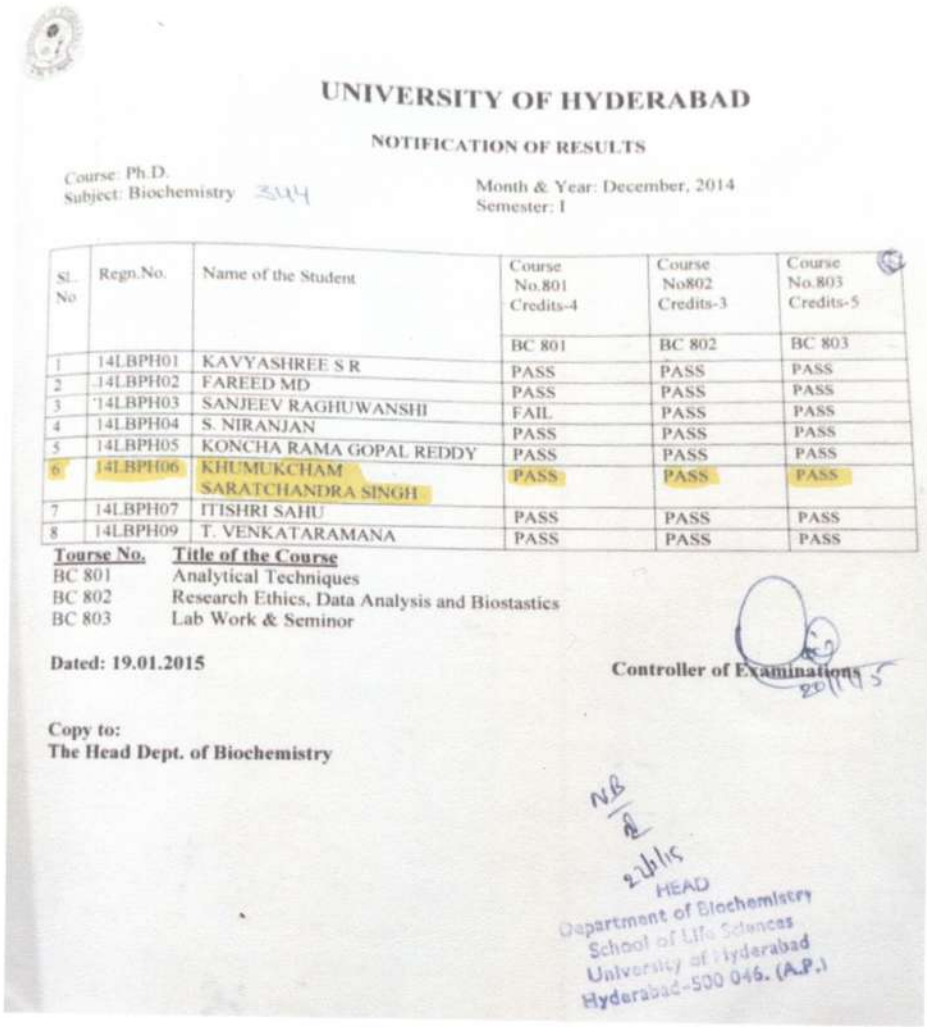

UNIVERSITY OF HYDERABAD

NOTIFICATION OF RESULTS

Course: Ph.D.
Subject: Biochemistry

Month & Year: December, 2014
Semester: I

Sl. No	Regn.No.	Name of the Student	Course No.801 Credits-4	Course No802 Credits-3	Course No.803 Credits-5
			BC 801	BC 802	BC 803
1	14LBPH01	KAVYASHREE S R	PASS	PASS	PASS
2	14LBPH02	FAREED MD	PASS	PASS	PASS
3	14LBPH03	SANJEEV RAGHUWANSHI	FAIL	PASS	PASS
4	14LBPH04	S. NIRANJAN	PASS	PASS	PASS
5	14LBPH05	KONCHA RAMA GOPAL REDDY	PASS	PASS	PASS
6	14LBPH06	KHUMUKCHAM SARATCHANDRA SINGH	PASS	PASS	PASS
7	14LBPH07	ITISHRI SAHU	PASS	PASS	PASS
8	14LBPH09	T. VENKATARAMANA	PASS	PASS	PASS

Tourse No.	Title of the Course
BC 801	Analytical Techniques
BC 802	Research Ethics, Data Analysis and Biostastics
BC 803	Lab Work & Seminor

Dated: 19.01.2015

Controller of Examinations

Copy to:
The Head Dept. of Biochemistry

HEAD
Department of Biochemistry
School of Life Sciences
University of Hyderabad
Hyderabad-500 046. (A.P.)

08/10/21

Supervisor
Prof. Bramanandam Manavathi, PhD
Department of Biochemistry
School of Life Sciences
University of Hyderabad
Hyderabad-500 046. (TS), INDIA

10/2021

Head
Department of Biochemistry

HEAD
Department of Biochemistry
SCHOOL OF LIFE SCIENCES
UNIVERSITY OF HYDERABAD
HYDERABAD-500 046.

Dean
School of Life Sciences

School of Life Sciences
University of Hyderabad
Hyderabad - 500 046.

Acknowledgments

First and foremost, it is my genuine pleasure to express my deep sense of love, thanks and sincerest gratitude to my mentor **Prof. Bramanandam Manavathi** for his continuous support throughout my research with his motivation, enthusiasm, immense knowledge, invaluable guidance, advice and ideas that collectively made my thesis possible. I could not have imagined having a better advisor and mentor for my Ph.D. His attention, moral support and timely suggestions were useful in the preparation of my thesis. It has been a great privilege to have embarked on my journey into the world of science under his supervision. I am always grateful to my supervisor for everything.

I am thankful to my doctoral committee members: Prof. Naresh Babu V Sepuri and Prof. Jagan Pongubala for their insightful comments and invaluable suggestions throughout my PhD work. I would like to thank Prof. Reinhard Depping, University of Luebeck, Institute of Physiology, Dr. Aprotim Mazumder, TIFR, Hyderabad and Dr. Mohit Jolly, Indian Institute of Sciences (IISC), Bangalore, India for their love, support and ideas throughout my PhD journey. I am very thankful to Prof. Srinivasulu Mukta and Prof. Triveni B of MNJ Cancer Hospital Hyderabad, Telangana, India.

I would like to thank the present and former Heads of the Department of Biochemistry (Prof. Krishnaveni Mishra, Prof. Mrinal Kanti Bhattacharyya, Prof. N. Siva Kumar, Prof. O.H. Setty, Prof. K.V.A Ramaiah, Prof. Ramanadham), the present and former Deans of School of Life Sciences (Prof. Dayananda Siddavattam, Prof. KVA Ramaiah, Prof. MNV Prasad, Prof. Pallu Reddanna) for allowing me to use all the central facilities of the department and school.

I would like to thank Dr. Suresh Yenugu for allowing me to use their lab facilities. I thank all faculty members of School of Life Sciences and also thank all the non-teaching staff for their timely help.

I thank my wonderful lab seniors Dr. Vijay, Dr. Oindrilla Dey, Dr. Suresh, Subbu and my present lovely labmates Dr. Chiranjeevi, Vasudev, Anju, Anita, Salam, Sruchytha, Yasaswi, Malte, Venkat and Naresh for making my stay in the lab lively.

I thank all my friends for their love and affection. I have been really privileged to have friends like Sangeeta and Suresh. I thank all those friends who support and encourage during my mom's critical health issues, specially to Sangeeta, Yasaswi and my labmates. They literally supported me all through my ups and downs.

I acknowledge UGC-RGNF (JRF and SRF) for the financial support offered to me.

I also thank all the funding bodies (CSIR, DST, DBT, DBT-CREBB, DST-FIST, UGC-UPE, DST-PURSE) for their financial assistance to BM lab, the department and school.

I would like to thank my family, especially my brother (Subhaschandra Kh) who is my hero, my lovely and our world mom (Anandi Kh), Laxmi Kh, sister (Mina Th) and brother-in-law (Premjit Th) for all the love and support. Their love and care always inspired me to proceed the journey, made me happy and forget the bad times. I dedicate my PhD success to them.

Finally, I thank God Almighty for His shower of blessings throughout and everything is possible because of Him.

ACRONYMS

cDNA - Complementary DNA

CSC - Cancer Stem Cell

CXCR4 - C-X-C chemokine receptor type 4

DAPI - 4’,6-Diamidino-2-Phenylindole

DCIS - Ductal Carcinoma In Situ

DMEM - Dulbecco's Modified Eagle's Medium

DMSO - Dimethyl Sulfoxide

dNTP - Deoxyribonucleotide Triphosphate

E2 - Estrogen Or 17β-Estradiol

ECL - Enhanced Chemiluminescence

ECM - Extra Cellular Matrix

EDTA - Ethylene Diamine Tetra Acetic Acid

EMP - Epithelial To Mesenchyme Plasticity

EMT - Epithelial-Mesenchymal Transition

EPO - Erythropoietin

ER - Estrogen Receptor

ERK - Extracellular-Signal-Regulated Kinases

FA - Focal Adhesions

FAK - Focal Adhesion Kinase

FH - Fumarate Hydratase

GAPDH - Glyceraldehyde-3-Phosphate Dehydrogenase

GSK-3β - Glycogen Synthase Kinase-3β

HCC - Human Hepatocellular Carcinoma

HEK293T - Human Embryonic Kidney 293T Cells

HER2 - Human Epidermal Growth Factor Receptor 2

HPIP/ PBXIP1 - Hematopoietic PBX Interacting Protein Or Pre-B-Cell Leukemia Transcription Factor (PBX)-Interacting Protein

HRE - Hypoxia Response Element

HSC - Hematopoietic Stem Cells

IDC - Invasive Ductal Carcinomas

IgG - Immunoglobulin G

ILC - Invasive Lobular Carcinoma

kDa - Kilo Dalton

LCIS - Lobular Carcinoma In Situ

LDHA - Lactate Dehydrogenase-A

M - Molar

MAPK - Mitogen-Activated Protein Kinase

MAPs - Microtubule-Associated Proteins

MTT - 3-(4,5-Dimethylthiazol-2-Yl)-2,5-Diphenyltetrazolium Bromide

NHEK - Normal Human Epidermal Keratinocytes

OA - Osteoarthritis

OSCC - Oral Squamous Cell Carcinoma

PBS - Phosphate-Buffered Saline

PBX1 - Pre-B-Cell Leukemia Homeobox Protein

PCR - Polymerase Chain Reaction

PDAC - Pancreatic Ductal Adenocarcinoma

PHD - Prolyl Hydroxylase Domain

PI3K - Phosphatidylinositol 3 Kinase

PKCα - Protein Kinase C Alpha

PMSF - Phenyl Methyl Sulfonyl Fluoride

RPM - Rotations Per Minute

RPMI - Roswell Park Memorial Institute Medium

SCD- - Sickle Cell Disease

SDF-1 - Stromal-Derived Factor 1

SDH - Succinate Dehydrogenase

SDS - Sodium Dodecyl Sulfate

SDS-PAGE - SDS-Polyacrylamide Gel Electrophoresis

SMAD - Mothers against decapentaplegic homolog

SRP - Signal Recognition Particle

SRP14 - Signal Recognition Particle 14

Taq - *Thermophilus Aquaticus*

TBS - Tris-Buffered Saline

TBST - Tris-Buffered Saline Tween20

TEX11 - Testis-Expressed 11

TFIS - Transcription Factor Information System

TME - Tumor Microenvironment

TNBC - Triple Negative Breast Cancer

TWIST1 - Twist-related protein 1

VHL - Von Hippel Lindau

ZEB1/2 - Zinc finger E-box-binding homeobox 1/2

Tables of contents

CHAPTER 1 Page no.

CHAPTER 2 Page no.

Chapter 1

1.0. Introduction

1.1. Overview of breast cancer

Cancer is an outcome of abnormal and uncontrolled proliferation of cells having the potential to spread or invade to other body parts. The accumulation of abnormalities in the normal cells directly or indirectly affect cell cycle regulatory machinery that lead to abnormal growth of the cells, reflecting distinguishing behavior from the normal cells. The development of tumor is a multistep process involving accumulation of mutations or genetic alternations resulting continuous proliferation and abnormal growth (Nordling, 1953; Armitage and Doll, 1954). Globally, cancer has become the second most common cause of death. The World Health Organization (WHO) estimates that cancer caused 9.6 million deaths worldwide in 2018. This accounts for one in every six deaths. According to the American Cancer Society, there will be 1.8 million new cancer cases in the United States and 606,520 deaths by 2020. In India, NCRP (India's National Cancer Registry Program) expects to grow to 1.73 million new cases and 0.88 million deaths by 2020 (Gandhi et al., 2017). Among various cancers, breast cancer remains one of the most common malignancies affecting millions of women worldwide, although it exists in man in rare cases (Saunders *et al*., 2009; Gandhi et al., 2017). The incidence of breast cancer is lower in rural areas than in urban areas of the country due to lifestyle, food habits, increased alcohol consumption, use of contraceptives pills, etc. (McTiernan, 2003; Sharma et al., 2010).

Breast is a mammary gland composed of two primary tissues: glandular tissue and stromal tissue. Glandular tissue has grapes like a cluster of glands consisting of hundreds of lobules, which are lined by specialized epithelial cells to produce milk. The lobules are interconnected through small ducts, which eventually join larger ducts to passage the milk through the nipple. Stroma is the supportive tissue comprised of fatty and fibrous connective tissues (Sharma et al., 2010). Breast

cancer may be originated from the cells lining the duct (ductal carcinoma) or in the cells lining the lobules (lobular carcinoma) or other tissues.

1.2. Breast cancer classification based on histology, site and invasiveness

1.2. (a) Ductal Carcinoma In Situ (DCIS)

DCIS is a non-invasive malignancy of the epithelial cells with clonal proliferation and accumulation confined to the basement of the breast ductal system (Allred, 2010; Bane, 2013). It is also known as stage 0 breast cancer or intra-ductal breast cancer. It is the most common type, constituting 90% of non-invasion breast cancer (Sharma et al., 2010). It is considered as very early stage, non-lethal, and highly treatable; however, DCIS is a precursor of invasive breast cancer, which is aggressive cancer and lethal if left untreated or undetected in early-stage (Collins et al., 2005; Sanders et al., 2005). With the advent of new screening technology like mammography, uncommon breast lesions are easily detected, accounting for the increasing incidence of DCIS, approximately 20% of all new breast cancer cases (Leonard and Swain, 2004; Armed Forces Health Surveillance, 2013; Parikh et al., 2018). The DCIS progression to IBC is at least 13% -50% of cases; therefore, it required aggressive and effective therapy or treatment, but DCIS-associated mortality is very low (Sanders et al., 2005; Erbas et al., 2006; Mahoney et al., 2013).

1.2. (b) Lobular Carcinoma In Situ (LCIS)

LCIS is a noninvasive abnormal lobulocentric proliferation or growth of the epithelial cells lining the breast's milk-producing multiples glands (lobules), causing to fill and distort lobular units. It is considered as a marker for the risk factor, precursor for invasive lobular carcinoma (ILC), and evidence suggest that LCIS is a premalignant lesion having potential progression towards invasive carcinoma (Haagensen et al., 1978; Dabbs et al., 2007). LCIS has an 8-10 fold higher risk of developing into ILC than the general population (Page et al., 1991). The probability of progression

to ILC after diagnosed with LCIS was 13%, 26% and 35% by 10, 20 and 35 years, respectively (Bodian et al., 1996).

1.2. (c) Invasive Ductal Carcinoma (IDC)

Invasive ductal carcinoma is also known as infiltrative ductal carcinoma. It begins in the breast's milk ducts and start spreading to the breast's surrounding tissue and further can be metastasized to lymph nodes and other body organs. Approximately 75% - 80% of invasive breast cancers (IBC) are IDC (Li et al., 2005). According to the American Cancer Society, it is reported that in the USA, every year 180,000 women are finding out with invasive breast cancer and 80% of the IBC are DCIS. It is more common to the woman of older age of 55 or more and also affects the man as well.

1.2. (d) Invasive Lobular Carcinoma (ILC)

The second most common type of IBC is ILC. It is originated from the abnormal proliferation of cells lining the lobules and has spread to other parts of the breast tissue. Around 10% of invasive breast cancer are ILC and developed commonly in the older age, especially among post menopause, of 45 to 50 years old women (Li et al., 2000; Li et al., 2003a; Arpino et al., 2004). Based on histology, it can be again divided into different types like medullary carcinoma, papillary carcinoma, tubular carcinoma, cribriform carcinoma and mucinous carcinoma.

1.3. Molecular classification of breast cancer

Localization-based breast cancer classification is not enough to understand the patients' pathological parameters and clinical outcome as it limits targeted therapy. Recent studies on gene expression profiling further led to the identification of five major molecular subtypes of breast cancer (Sorlie et al., 2001; Dai et al., 2015) that gives more in-depth information to provide the best individualized treatment (Perou et al., 2000; van de Vijver et al., 2002; Paik et al., 2004).

1.3. (a) Basal-like breast cancers

The majority of the basal-like breast cancers are TNBC (triple negative breast cancers) and constitute 15-20% of all breast cancers. It lacks the expression of estrogen receptor (ER-), human epidermal growth factor receptor 2 (HER2-) and progesterone receptor negative (PR-) with expression of cytokeratin (CK5/6+) and epidermal growth factor receptor (EGFR+) (Badve et al., 2011). They are very aggressive, high-grade tumor; and associated with frequent mutations in *BRCA1*, *BRCA2* and *P53* genes (Sorlie et al., 2003)**.** There is no option for therapeutic treatment of basal like breast cancers resulting poor survival rate (Carey et al., 2006). Chemotherapy is the only option for the treatment of patients TNBC patients (Cancer Genome Atlas, 2012).

1.3. (b) Luminal A

They are ER (+), PR (+) or PR (-), HER2 (-), CK5/6 (-) and EGFR (-) constituting (35%-40%) of all breast cancers. It has the best prognosis as compared to other subtypes with low mortality as well as low recurrence rates (Al Tamimi et al., 2010; Voduc et al., 2010; Arvold et al., 2011).

1.3. (c) Luminal B

It has ER+ and low or HER2 negative. About 10%-20% of all breast cancers are Luminal B breast cancer (Voduc et al., 2010). They are highly proliferative and have a fairly high survival rate but less than Luminal A tumours (Malhotra et al., 2010; Metzger-Filho et al., 2013; McGuire et al., 2017).

1.3. (d) HER2 overexpressing

This is ER-, PR-, EGFR- and HER2+. It comprises 10% of all breast tumours (Carey et al., 2006). Her2+ tumors are frequently high-grade, very aggressive and associated with poor prognosis (Carey et al., 2006; Parker et al., 2009).

1.3. (e) Claudin-low

This subtype of cancer is characterized by ER-, less expression of genes associated with tight junction of the cells or epithelial cell-cell adhesion like Claudins 3/4/7, E-cadherin and Occludin (Herschkowitz et al., 2007; Malhotra et al., 2010). It is relatively resistant to conventional chemotherapeutic agents and is also linked to poor prognosis (Prat et al., 2010; Prat and Perou, 2011).

In recent years, five years relative survival rates are improving because of advanced treatments with population wide screening. Around 10% of the breast cancers are due to inherited genetic mutation but most of the breast cancer causing factors are associated with reproductive, lifestyle, environments etc. (Rojas and Stuckey, 2016).

1.4. Role of oxygen in diversity and evolution of organisms

Oxygen plays a pivotal role in the evolution of complex organisms (Catling et al., 2005). In the relative absence of oxygen, unicellular organisms relied for their energy on metabolic pathways using CO_2 and SO_4 as electron acceptors (Thannickal, 2009). The most energy-sufficient metabolic pathways were evolved with concomitant increase in the concentration of environmental O_2, and it is the main tipping point for the evolution of complex organisms (Stamati et al., 2011). Oxygen became an integral part of many biochemical pathways replacing anoxic enzymatic reactions in the aerobic organisms. Various complex biochemical networks emerged to adapt to the oxic environment with subsequent development of multicellular organisms (Raymond and Segre, 2006). The oxygen-dependent pathways gradually replaced the anaerobic pathways at different points of the evolution tree. The metabolic network consists of aerobic, generally irreversible, as well as anaerobic counterparts and small molecules called metabolites. The aerobic metabolites that are more rigid and hydrophobic, serve as transmembrane factors to modulate the membrane function favoring complex cellular organizations (Goldfine, 1965; Jiang et al., 2012). Moreover, modifications in the membrane architecture were seen, like extracellular domains of

transmembrane proteins became prominently bigger with limited size and numbers than intracellular domains. It enhanced cellular compartmentalization with proper communication and signaling across the membrane (Acquisti et al., 2007). Thus, many biological events were influenced by oxygen evolution, driving to transforming and expansion of complex multicellular organisms.

The atmospheric oxygen concentration has been fluctuating over time in the earth's evolution, impacting the natural selection of organisms with phenotypic changes. For instance, the oxygen concentration was at its peak during Carboniferous (35%) era with the highest body size, and it remains unchanged as at 21% since last 350 million years (M.Lenton, 2003). In response to low or high oxygen levels, organisms have developed various defense and regulatory mechanisms to adapt and protect the cells. Each era of earth's evolution had various oxygen concentrations with spontaneous development of diverse morphology with effective respiratory system to maximize the organism's survival (Stamati et al., 2011). High atmospheric pressure implicates the development of placenta and maternal atrial diffusion of oxygen. Also, oxygen has a positive effect on body size, metabolism and hatching phenotype etc. For instance, hyperoxia (more than 21%) leads to increased body size in *Drosophila melanogaster* and insects (Frazier et al., 2001; Berner et al., 2007). The hyperoxia treatment (up to 35%) after ambient oxygen leads to early hatching in tree frogs (Warkentin, 2002), 27% of oxygen exposed to alligators resulted in increased body size with positive developmental rate and bone composition, but However, exceeding 27% results in a reduction in body size and a slower pace of development (Berner et al., 2007). Most mammals and birds need optimal oxygen tension and can change the metabolism based on its availability. Many vertebrates such as fish, amphibians, turtles, and reptiles can prolong hypoxia by reducing energy-consuming processes prioritizing essential minimum cellular processes (Berner et al., 2007).

Diving animals can store a large quantity of molecular oxygen as they have higher myoglobin with a low metabolic rate (Ramirez et al., 2007).

Oxygen is a vital component for the development, growth, and survival of multicellular organisms (Stamati et al., 2011). The multicellular organisms have well-established oxygen delivery systems that consist of capturing molecular oxygen and delivery to the target cells (Giaccia et al., 2004). They can sense and respond to low-oxygen with well sophisticated physiological networks to maintain homeostasis. Every cell in tissues requires a particular range of oxygen to perform and maintain proper body function as prolonged exposure to beyond or less oxygen concentration leads to cell death. In adult humans, physiological oxygen levels inside the body fall between 1% to 14% pO_2 (Stamati et al., 2011). Hypoxia is a phenomenon of the non-physiological level of oxygen. Still, its effect can be either positive or negative on the tissue or cells depending on the severity, duration, and context. In mammals, low oxygen (hypoxia) is sensed by the carotid body (CB) (Czyzyk-Krzeska, 1997). The CB comprises clusters of cells (glomeruli) close to blood arteries and nerve fibres. Under hypoxia, the O2-sensitive K+ channels of glomus cells are blocked, causing Ca2+ entry (depolarization), thereby releasing transmitters that activate sensory fibres terminating at the respiratory centre (Lopez-Barneo et al., 2016). Any variation in oxygen concentration drives many physiological signaling involving protein cascades that are important for normal fetal development, angiogenesis, differentiation of cells, maintaining stem cells, pluripotency and embryonic development etc. (Lin et al., 2008; Ivanovic, 2009). However, low-oxygen tension disturbs the internal cellular metabolism and it is associated with many diseases, such as cardiovascular disease, dementia, diabetes and cancer (Eales et al., 2016). Hypoxia modulates the tumor microenvironment and is linked with poor prognosis in several cancers (Muz et al., 2015).

1.5. Development of tumor microenvironment

Our system has evolved with well-developed mechanisms to protect the cells from cancer and other pathological diseases. The niche system of the body system perpetuates a particular range of environment to maintain integrity of the tissue or cells to prevent the creation of cancer cell hallmarks by limiting, and selective barrier such as food supply, oxygen availability, structure of the tissue etc. (Ferraro et al., 2010). Cells are installed with tumor suppressor genes to control an appropriate number of cells via regulating cell division and the organs' size. Cellular suicide programs such as apoptosis and cellular senescence are inherited phenomena in response to aberrant or inappropriate signals among cells (Childs et al., 2014). Effective DNA repair system obviates oncogenic mutation to maintain the genomic integrity and function of the cells (Jeggo et al., 2016). Also, the telomere shortening programs limit the division of cells to control cell population (Victorelli and Passos, 2017). Furthermore, the powerful multifaceted network of immune surveillance system monitors to detect neoplastically abnormal cell and destroy it (Swann and Smyth, 2007). Even though the host system has sophisticated tumor defense mechanisms, it is prone to cancer due to many factors. With the age, the genomic integrity and function deteriorates in the body due to the accumulation of mutations over time. The oxidative damage to DNA by reactive oxidative products derived from cell metabolism and radiation also causes cancer (Adelman et al., 1988). Exposure to natural or artificial carcinogen causes genetic diversity and alteration in cells' population, causing gain or loss of function. For instance, natural carcinogens like aflatoxin B1, Sterigmatocystin, Ochratoxin A cause liver cancer. Many artificial carcinogens such as vinyl chloride, dioxins also cause cancer. Oncogenic virus like human papillomavirus, hepatitis virus B and C and oncogenic bacterium (*Helicobacter pylori*) are known to cause cervical cancer, hepatocellular carcinoma and stomach cancer, respectively (Vandeven and Nghiem, 2014).

The tumor microenvironment (TME) is a heterogeneous milieu that consists of cellular components such as immune-inflammatory cells, neuroendocrine cells, adipose cells, fibroblasts and a non-cellular player, the extracellular matrix (ECM), which comprises of fibronectin, fibrillar collagens, elastin, and laminins (Provenzano et al., 2008; Mammoto et al., 2013). ECM constitutes 60% mass of tumors, which are secreted and dictated by tumor cells (Henke et al., 2019). The interlink dynamic changes of the ECM with respect to microevolution of the tumor, drives cellular functions like cell-cell adhesion, cell migration, cell polarity, and cell proliferation (Paszek et al., 2005; Gritsenko et al., 2012). Initiation of tumor, followed by its progression, dissemination, and colonization to distant organs with acquired cellular traits involve multistep stages with complicated inter or intra-tumoral communication and its surrounding tissues (Gonzalez et al., 2018). The tumor microenvironment is a unique and ambient environment that emerges from the orchestrated molecular talks between tumor cells and surrounding tissues with the ultimate decisive role in driving tumorigenesis (Whiteside, 2008).

Most cancers are originated from a single abnormal cell with selective advantages. The progression of cancer within an individual can be considered as a rapid micro-evolutionary process. The cancer cells' self-proliferating nature jeopardizes the co-ordination among normal cells and escalates a sustainable ecosystem to drive tumorigenesis (Wu et al., 2016). The accumulation of mutation with cell growth and proliferation over time effectuates a more aggressive cancer phenotype (Takahashi et al., 2020). Rapid cancer cell-proliferation and simultaneous pushing of cells away from the blood vessel leads to a desultory creation of microenvironments, known as normoxia (abundant oxygen and nutrients) in the vicinity of the blood vessel, and hypoxia (lack of oxygen and nutrients) distant from the blood vessel, across the tumor. Cancer cells encounter selective restriction for space, nutrients, oxygen for continuous survival and proliferation during this period (Levayer, 2020). Cancer cells prime themselves and acquire hallmarks to dominate via continuous mutational gain

over normal cells. They can cope with the metabolic stress by rewiring the metabolic pathways to support the fast-growing tumor, transforming to more aggressive phenotypes. Unlike normal cells, cancer cell can shunt the glycolysis over TCA cycle (Tricarboxylic acid cycle) for glucose metabolism while directing the glutamine-dependent TCA cycle to replenish its intermediates (Anderson et al., 2018). The upregulation of high affinity glucose transporter proteins like GLUT1 and GLUT 3 enhances glucose uptake and its break down to lactate even under normoxia, a phenomenon known as Warburg effect (de la Cruz-Lopez et al., 2019) is a hallmark of cancer. Lactate is an oncometabolites that alters oncogenic transcription, cell proliferation and drives genes involved in metabolic reprogramming in cancer cells (Dang et al., 2008). It enhances cell migration/ invasion, immune escape and angiogenesis in mice (Dhup et al., 2012). Further, it stabilizes HIF-1α promoting glutamine metabolism via c-MYC dependent upregulation of Glutamine transporter (ASCT2) and Glutaminase (GLS1) (Perez-Escuredo et al., 2016). Besides, TME initiates angiogenesis to overcome the limitation for nutrients and oxygen and triggers metastasis (Makrilia et al., 2009). Thus, cancer cells dominate over normal cells for energy source by driving abnormal uptake of glucose and glutamine and enhanced catabolism provoking tumorigenesis.

1.6. Tumor microenvironment drives phenotypic plasticity: Implication in tumorigenesis and metastasis

Survival of the fittest being its mantra, evolution does its selection over time by eliminating inadaptable organisms or traits through natural selection (Beldade et al., 2011). Organisms have the potential to cope with the heterogeneous environment by rewiring the cellular and biochemical functions. Phenotypic plasticity is the competency of an organism to exhibit different phenotypes when exposed to varying environments (Sergio Pimpinelli, 2019). It is a powerful, inherited transformation in morphological, physiological, or behavioral traits to adapt, protect themselves from predators, and diversify in an ever-changing environment (Fusco and Minelli, 2010; Cohen

et al., 2016) For instance, in the hatching plasticity stimulated by predators in the red-eyed tree frog, if the eggs sense an anomaly, they hatch almost instantaneously instead of doing so in their normal time course (Warkentin, 1995).

Cancer is the outcome of uncontrolled cell growth independent of the body's regulatory system. The evolution of cancer within an individual is a rapid micro-evolutionary process. Cancer cells dominate over systematically fit normal cells through gradual evolution of microenvironment with suitable phenotype and constant selection (Casas-Selves and Degregori, 2011). There are two main phenotypes of cancer: (1) Cell proliferation, which makes a lump of tumor, and (2) Metastasis, where cells break away from tumors and travel through the bloodstream to initiate secondary tumors. The rapid cell proliferation creates many random microenvironments (hypoxia/normoxia) due to the imbalance in supply and consumption of oxygen across the solid tumor, constituting a wide range of pO_2 with 50-60% hypoxia and 50-40% normoxia areas in solid tumor (Vaupel and Mayer, 2007; Kuschel et al., 2012). These intratumoral subsets of microenvironment with different oxygen availability have different patterns of gene expression. Even though TME is often hostile due to the limitation of oxygen and nutrients, as a consequence of continued cell proliferation, cancer cells adapt to this plethora of abnormal stresses by rewiring the cellular function through translational and epigenetic alterations. Hypoxia induces gene amplification, drives progression of malignancy (induction of EMT), resistance to radiation therapy, thus lowering the patient survival rate (Mimeault and Batra, 2013). Prolonged hypoxia initiates angiogenesis, shifting the hypoxia microenvironment back to normoxia following continuous proliferation and so on. This back and forth phenotypic switching between the proliferative and metastatic phenotype under a desultory microenvironment creates phenotypic heterogeneity and tumor progression (Belisario et al., 2020). These phenotypes are mutually exclusive, i.e., having highly proliferative cells with low migration or vice versa, is known as migration/proliferation dichotomy (go or grow mechanism) (Giese et

al., 1996). The oxygen concentration influences the phenotypic plasticity of the tumor cells favoring proliferative phenotype over migration in normoxia and hypoxia trigger transition to invasive phenotype (Hatzikirou et al., 2012).

Hypoxia initiates plasticity and drives heterogeneity in tumors promoting more aggressive and invasive phenotypes. Hypoxia inducible factor-1 (HIF-1) is a heterodimeric transcription factor with HIF-1α (oxygen-responsive subunit) (Semenza and Wang, 1992) and HIF-1β (constitutively expressed subunit) (Ratcliffe et al., 1998; Wang et al., 1995). The HIF-α/β dimer with transcriptional coactivator p300/CBP recruits on the hypoxia response element sequence of the target gene's promoter (Majmundar et al., 2010). The activated heterodimeric protein complex regulates the expression of genes necessary for hypoxic adaptation such as angiogenesis, pH regulation, energy homeostasis, etc. (Semenza and Wang, 1992; Wang et al., 1995). Under normal physiological conditions (normoxia), HIF-1α expression diminishes as it undergoes prolyl hydroxyl dehydrogenase (PHD) induced hydroxylation followed by pVHL-mediated ubiquitination and subsequent 26s proteasome-dependent degradation. The hypoxia-adaptive signaling drives pro-survival, EMT, invasive and metastasis in solid tumors (Schito and Semenza, 2016). Hypoxia promotes EMT in various cancer like prostate, breast, pancreatic, lung, ovarian, myeloma, renal and squamous carcinoma (Scortegagna et al., 2009; Mak et al., 2010; Azab et al., 2012; Salnikov et al., 2012; Huang et al., 2013; Sun et al., 2013b). It is a multifaceted networking system consisting of multistep cellular changes, which drive the transition of highly organized, polar non motile epithelial cells to non-polar spindle shape mesenchymal cells, which have higher motility and aggressive phenotype (Ferrao et al., 2015). Hypoxia-induced EMT has low expression of E-Cad, β-catenin and elevated expression of Vimentin, N-Cad, Smooth muscle antigen (SMA), and CXCR4 (Hsu et al., 2000; Kim et al., 2002; Manotham et al., 2004; Azab et al., 2012;). It is initiated and executed by an orchestrated set of E-box-binding transcription factors like TWIST,

ZEB1/2, SNAIL and SLUG. SNAIL, SLUG and ZEB1/2 transcriptionally represses E-cadherin expression by recruiting to its promoter. HIF-1α, a master regulator of hypoxia, directly modulates many EMT related transcription factors. It transcriptionally activates TWIST and promotes metastasis. High TWIST and HIF-1α expression correlate with the poor prognosis in ovarian cancer, and head and neck cancer patients (Kim et al., 2014; Yang et al., 2008)**.** Similarly**,** HIF-1α induces SNAIL, SLUG, and ZEB1 expression and promotes metastasis (Storci et al., 2010; Zhang et al., 2013; Zhang et al., 2015). TGF-β which is increased under hypoxia, also regulates EMT by activating downstream transcription factors like SMADs, SLUG, SNAIL and TWIST (Tian et al., 2011). It has been reported that HIF-1α regulates TGF-β-SMAD3 pathway in breast cancer (Peng et al., 2018). Additionally, it indirectly regulates EMT transcription factors via FoxM1 signaling pathways and PAFAH1B2 gene (Ma et al., 2018; Tang et al., 2019)**.** It also facilitates the regulatory loop of integrin-linked kinase (ILK) and promotes EMT in breast and prostate cancer (Chou et al., 2015). Hypoxia microenvironment sustains EMT regulatory system through other signaling pathways like Notch and nuclear factor-κB signaling cascades. The Wnt/β-catenin signaling also initiates EMT through GSK3β, which stabilizes SLUG in breast cancer (Wu et al., 2012). Moreover, the cargo exosomes carry EMT inducers such as TGF-β, TNF-α, HDGF (Hepatoma-derived growth factor) and EMT effectors like MMPs and enhances tumor growth and metastasis (Marimpietri et al., 2013; Vella, 2014). For instance, the exosomes derived from prostate cancer promotes differentiation of normal stromal cells into specialized myofibroblasts via TGF-β and accelerate angiogenesis and tumor growth (Webber et al., 2015). When the cancer cells are disseminated and landed on a distant organ, the invasive mesenchymal phenotype with polar spindle-like morphology, changes back to MET, a more proliferative phenotype with apical basal polarity, to initiate secondary tumor (Ferrao et al., 2015).

The EMT abrupts cell-matrix adhesion and breaks down ECM and basement membrane by modulating MMPs (matrix metalloproteinase) activity, and rearrange the intercellular communication to exacerbate metastasis (Thiery, 2002). ECM consists of proteoglycans, non-collagenous glycoproteins, and fibrillar collagens constituting 60% mass of tumors (Hoye and Erler, 2016). The physical force mediated re-alignment of ECM creates routes for the cells' passage (Kai et al., 2019; Winkler et al., 2020). The ECM stiffness drives EMT through translocolization of TWIST1, YAP, and TAZ into the nucleus (Riesterer et al., 2006; Wei et al., 2015)**.** Many proteases such as disintegrin, metalloproteinase MMPs cleaves at cysteine, threonine or serine residues and degrades ECM (Bonnans et al., 2014). During the metastasis (EMT), cancer cells degrade ECM releasing bioactive ECM and ECM-bound factors, which helps in the liberation of cellular constraints and the cells' migration. Total 26 MMPs are known, and they have distinct structural organization with different substrate specificities. MMPs are generated as proenzymes and their activities are controlled by proteolytic regulation of post-translational modification (mature MMPs) and endogenous inhibitors, TIMPs (tissue inhibitor of metalloproteinase) (Jablonska-Trypuc et al., 2016; Quintero-Fabian et al., 2019). MMP-2 and MMP-9 are the MMPs which can hydrolyze gelatin and enhance metastasis (Raeeszadeh-Sarmazdeh et al., 2020).

Cancer cells exhibits Warburg effect and accelerate tumor malignancy (Vaupel et al., 2019). It converts glucose into lactate even in the presence of oxygen and functioning mitochondria (Gatenby and Gillies, 2004). The aerobic glycolysis and lactate formation instigates proliferation, which is acquired by the cancer cells in the early oncogenesis even before the creation of hypoxic microenvironment. The lactate accumulation resulted from Warburg effect, promotes the expression of lactate dehydrogenase and the monocarboxylate transporters (MCT1 and MCT4), which facilitate lactate shuttling between the cancer cells and surrounding microenvironment (Courtnay et al., 2015). MCT4 acts as a lactate exporter, while MCT1 mediates importing of lactate

of cancer cells. Shuttling of lactate between CAFs (cancer associated fibroblasts) and tumor cells accelerates tumor cell proliferation and progression (de la Cruz-Lopez et al., 2019). The hypoxia/normoxia activation of HIF-1α promotes Warburg effect (Vaupel and Multhoff, 2020). The PI3K/Akt/mTOR signaling pathway and HIF-1α are the primary regulators of glycolysis, proliferation and metabolism (Courtnay et al., 2015). The PI3K/AKT signaling cascade enhances glucose import via GLUT1 and modulates phosphofructokinase activity (DeBerardinis et al., 2008). While HIF-1α is induced under hypoxia, however in normoxia, HIF-α subunits undergo ubiquitin-proteasome (26S) mediated degradation (Marxsen et al., 2004). Notwithstandingly, evidence surmounts the existence of non-canonical mechanisms regulating HIF-1α in an oxygen-independent manner (Iommarini et al., 2017). For instance, oncometabolites such as succinate can stabilize HIF-1α in normoxia by inhibiting PHDs (Selak et al., 2005). Also, WSB1 (WB repeat and SOX-box containing protein) stabilizes HIF-1α via ubiquitination of pVHL protein and promotes metastasis (Kim et al., 2015). mTORC1 and increased ROS also enhances normoxic stabilization of HIF-1α (Yan et al., 2014). Oxygen-independent oncogenic signaling such as Mdm2 (mouse double minute 2 homolog) pathway, PI3K (phosphatidylinositol-3-kinase) activation and Hsp90 (heat shock protein 90) also regulate HIF-1α expression (Masoud and Li, 2015). The HIF-1α stabilized under normoxia promotes aerobic glycolysis or Warburg effect by transcriptionally upregulating GLUT1, LDH, etc., and confers tumor growth (Semenza et al., 1994; Courtnay et al., 2015; Nagao et al., 2019).

1.7. Oxygen dependent phenotypic plasticity of cancer cells

Hypoxia is a consequence of rapid cell proliferation in solid tumor. The O_2 concentration in the tumor microenvironment causes a range of phenotypes, such as normoxic cancer cells (proximity to the blood vessel), hypoxic cancer cells (distal to the blood vessel), and necrotic cancer cells (anoxic, 150 µm away from the blood vessel) (Al Tameemi et al., 2019) (fig. 1). Hypoxia is the

prominent feature of most tumors, including breast cancer. Although hypoxia has a cytotoxic effect on normal cells, cancer cells rewire their metabolism to survive under this hostile microenvironment. The reprogramming of tumor metabolism via direct or indirect activation of transcription factors such as HIF-1α, NFkB, CREB, AP1, P53, EGR1, SP1, SP3, etc., enable cells to survive under hypoxia and concomitantly acquires hallmarks of cancer (Cummins and Taylor, 2005). The hypoxic tumor microenvironment facilitates malignancy, metastasis, EMT, propagation of cancer stem cells, chemotherapy resistance with less survival rate and a poor prognosis (Mimeault and Batra, 2013; Yadav et al., 2020; Zhang et al., 2021). HIF-1α is a well-studied and well-characterized transcription factor that mediates diverse biological processes like cell proliferation, cell survival, migration, angiogenesis, etc. (Cummins and Taylor, 2005).

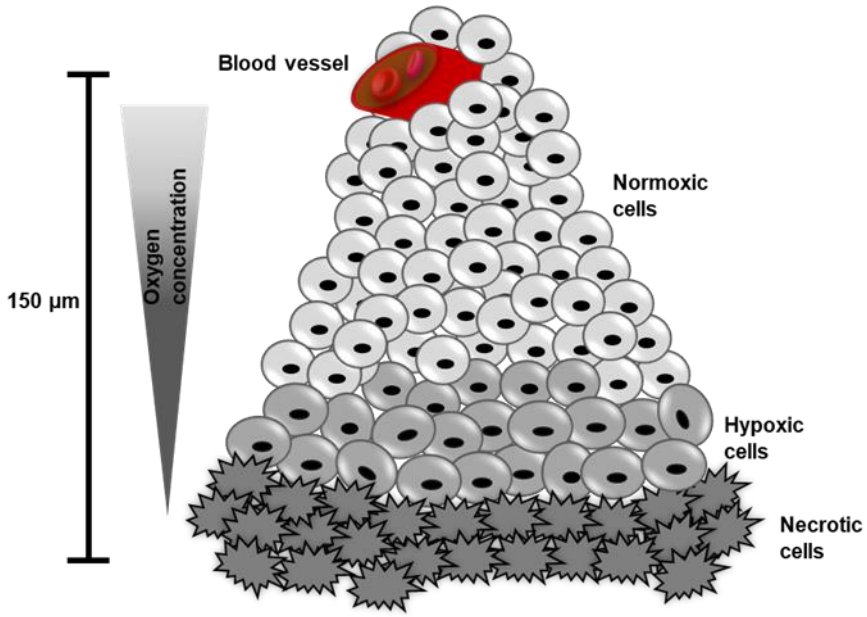

Fig. 1. Schematic illustration of a solid tumor comprises of normoxia or hypoxia regions.

As cancer cells proliferate, it creates normoxic cancer cells (proximity to the blood vessel), hypoxic cancer cells (away from the blood vessel), and necrotic cancer cells (anoxic, 150 µm away from the blood vessel).

Oxygen-dependent phenotypic plasticity in cancer cells is caused by an imbalance of oxygen supply and consumption across the tumor. Solid tumors have a wide range of pO2 levels, including

zones of 50-60% hypoxia and 50-40% normoxia (Vaupel and Mayer, 2007; Kuschel et al., 2012). There is a dynamic microenvironment shift between hypoxia and normoxia through proliferation and angiogenesis or via intratumoral migration of the cells (Fig. 2). The oxygen-dependent cellular plasticity or phenotypic plasticity thus generated in response to dynamic changes in tumor microenvironments (TMEs) endows solid tumors with heterogeneity (Beca and Polyak, 2016; Kong et al., 2020). Under the desultory microenvironment, the two phenotypes, proliferative and metastatic phenotypes, switch dynamically and enhance tumor growth. (Belisario et al., 2020). These two phenotypes are mutually exclusive, i.e., having highly proliferative cells with low migration or vice versa, is known as migration/proliferation dichotomy (go or grow mechanism) (Giese et al., 1996). The tumor cells favor proliferative phenotype over migration in normoxia, but hypoxia triggers the transition to an invasive phenotype (Hatzikirou et al., 2012). However, the molecular mechanisms underlying phenotypic plasticity are largely unknown.

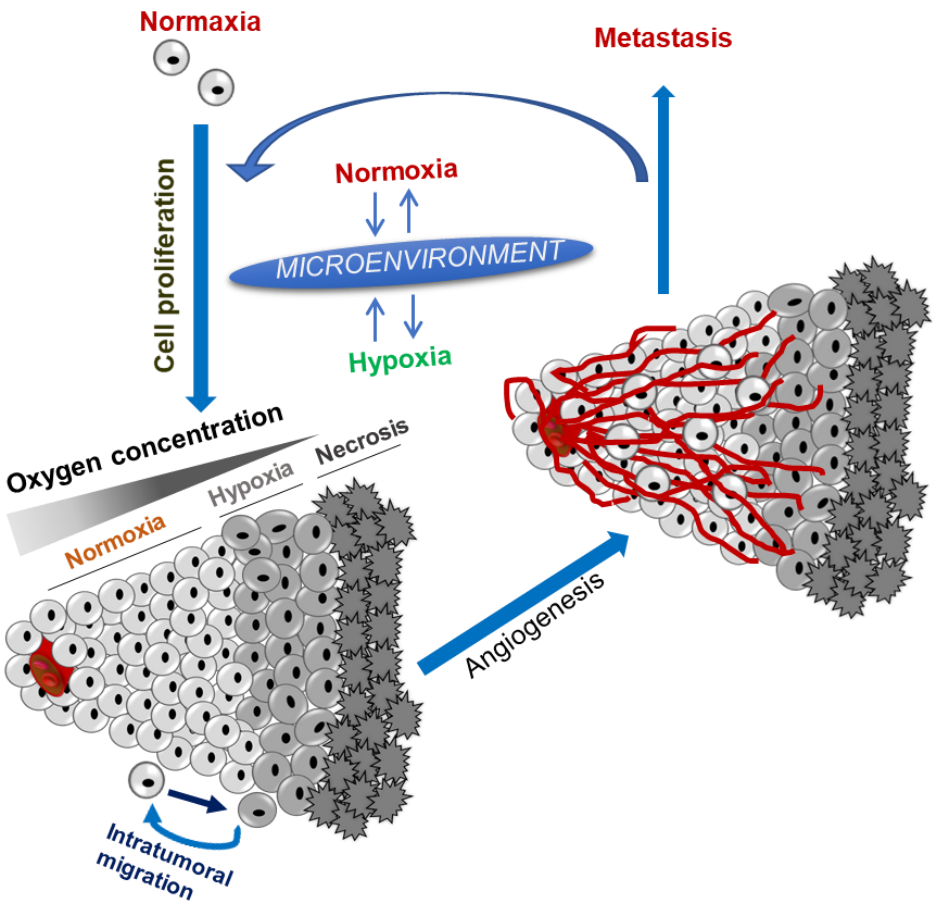

Fig. 2. Dynamics of microenvironment (hypoxia to normoxia or vice versa) promotes tumor progression.

Cells proximal to the blood vessel exhibits proliferative phenotype, while cells away from the blood vessel enhance EMT and metastasis. Prolonged hypoxia initiates angiogenesis, shifting the hypoxia microenvironment back to normoxia reverts proliferative phenotype on cancer cells. Oxygen dependent back and forth phenotypic switching between normoxia and hypoxia may create phenotypic heterogeneity and thus tumor progression.

1.7. (a) Invasive phenotype and HIF-1α under hypoxia

Elevated levels of HIF-1α correlates with tumorigenesis and poor prognosis in a multitude of different types of cancers like breast, colon, gastric, skin, lung, ovarian, prostate, pancreatic and renal carcinoma (Mabjeesh and Amir, 2007; Keith et al., 2011). Under hypoxia, it binds to constitutively expressed, oxygen independent, HIF-1β and forms a heterodimer and modulates

target gene expressions via recruiting on to the HIF responsive elements (HRE) harbor on their promoters. The coactivators CBP and p300, having lysine acetyl-transferase activity, interacts with HIF-1α and enhances the transcriptional activities of the targeted genes like VEGF, EPO (erythropoietin), SDF-1 (stromal-derived factor 1), GLUT1/3, and lactate dehydrogenase-A (LDH-A) and promotes diverse physiological functions, including angiogenesis, erythropoiesis etc. (Bento and Pereira, 2011; Dengler et al., 2014). At normal oxygen levels, prolyl hydroxylase domain (PHD) hydroxylates HIF-1α at proline residues and it is then recognized, and degraded via ubiquitination by von Hippel Lindau (VHL) protein (Fig. 3). HIFs activate transcription of genes that play key roles in critical aspects of cancer biology, including glucose metabolism (Luo et al., 2011), cell immortalization, stem cell maintenance (Wang et al., 2011), epithelial-mesenchymal transition (Mak et al., 2010), vascularization (Liao and Johnson, 2007), genetic instability (Huang et al., 2007), invasion and metastasis (Chan and Giaccia, 2007), pH regulation (Swietach et al., 2007), radiation resistance (Moeller et al., 2007), regulation of angiogenesis, apoptosis, adhesion cell energy, and growth (Esteban et al., 2006; Li et al., 2006; Hirota and Semenza, 2006; Fukuda et al., 2007; Kilic et al., 2007). It induces stem cell markers like NANOG, SOX2, OCT4, CD44, CD133, CD24, and Krüppel-like factor 4 (KLF4) and resists chemo- and radio-therapy (Vermeulen et al., 2008; Zhang et al., 2021). In breast cancer, it is reported that HIF-1α is correlated with the elevated expression of CD44 and underexpression of CD24 (CD44+CD24-/low) and modulates tumor progression and confers poor prognosis of the patients (Oliveira-Costa et al., 2011). It also regulates EMT under hypoxia through transcriptional activation of various EMT target genes including SNAIL, TWIST, SIP1, SLUG, and ZEB1. Other cellular EMT signaling pathways like TGF-β, hedgehog signaling activation, and Wnt/β-catenin pathways are also modulated by HIF-1α under hypoxia (Tam et al., 2020).

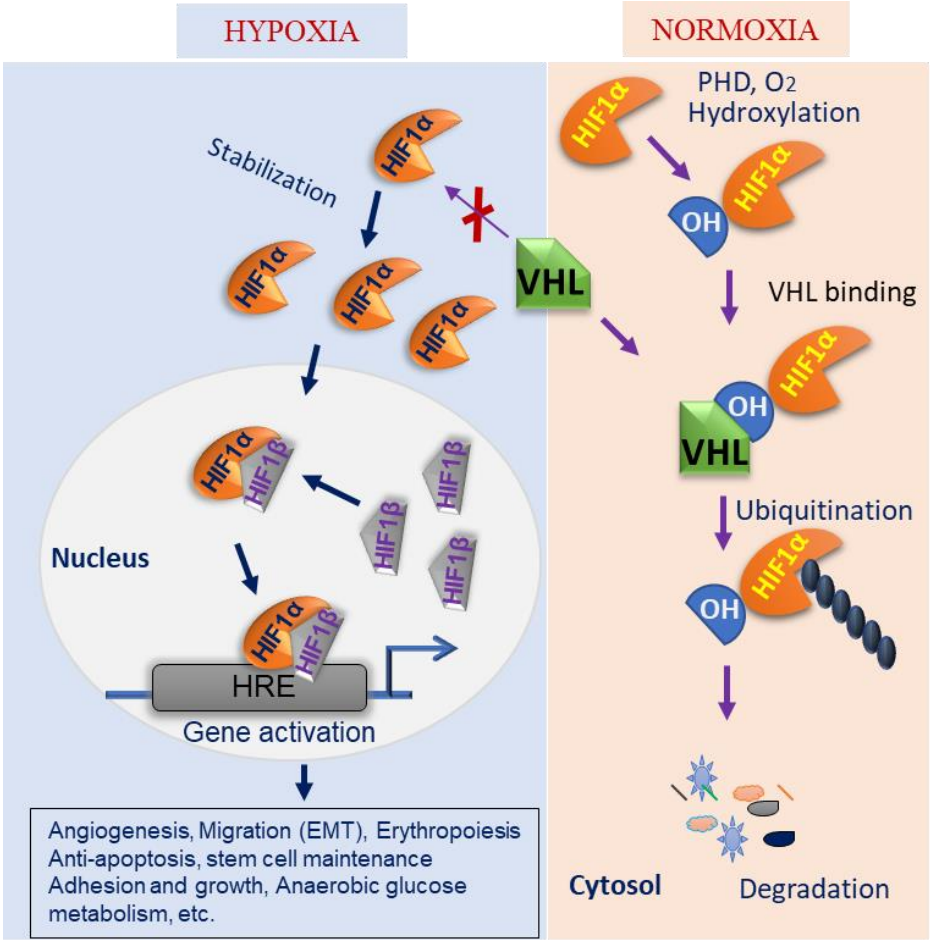

Fig. 3. The fate of HIF-1α.
Under normoxia, HIF-1α is hydroxylated by PHD. The hydroxylated HIF-1α is further recognized by VHL and degraded via ubiquitination. However, in Hypoxia, HIF-1α translocate insides the nucleus and bind with constitutively express HIF-1β and activates many genes thereby enhancing tumorigenesis

1.7. (b) Proliferative phenotype and HIF-1α under normoxia

HIF-1α acts as an oxygen sensor and is degraded under normoxia. Despite, mounting evidence indicates the existence of HIF-1α regulation through oxygen-independent non-canonical signaling pathways (Iommarini et al., 2017). Mutations in two key enzymes of the tricarboxylic acid cycle, SDH (succinate dehydrogenase) and FH (fumarate hydratase) causes accumulation of fumarate and succinate oncometabolites. The oncometabolites block PHDs activity and stabilize HIF-1α under normoxia (Semenza, 2003; Isaacs et al., 2005; Pollard et al., 2005; Selak et al., 2005). Also,

WSB1 (WB repeat and SOX-box containing protein) stabilizes HIF-1α via ubiquitination of pVHL protein and promotes metastasis (Kim et al., 2015). mTORC1 and increased ROS also enhance normoxic stabilization of HIF-1α (Yan et al., 2014). The elevated MYC stabilizes HIF-1α by partially inhibiting the interaction between HIF-1α and the pVHL complex under normoxia (Iommarini et al., 2017). The HIF-1α stabilized under normoxia promotes aerobic glycolysis or Warburg effect by transcriptionally upregulating genes such as GLUT1, LDH, etc., and promotes tumor growth (Semenza et al., 1994; Courtnay et al., 2015; Nagao et al., 2019). Although HIF-1α is upregulated in multiples types of solid tumors and displayed pleiotropic effects (Gladek et al., 2017), the complexity of HIF-1α regulation and its association with cellular plasticity remains elusive.

1.7. (c) Extracellular matrix (ECM) and cancer secretome

Extracellular matrix (ECM) comprises of more than 300 proteins, which regulates tissue homeostasis and organ development (Tam et al., 2020). Collagens are the most abundant components constituting 90% of the ECM (van der Rest and Garrone, 1991) which regulates a network of signals creating tumor microenvironment that modulates cancer cell growth, migration and invasion (Gilkes et al., 2014). Hypoxia promotes fibrogenesis via over deposition of ECM, through HIF-1α and enhances tumorigenesis (Higgins et al., 2007). For instance, HIF-1α regulates P4HA1, P4HA2, PLOD1, and PLOD2 expression promoting ECM modification and tumor progression (Gilkes et al., 2014). Besides collagen deposition, hypoxia stimulates cellular signaling via HIF-1α and degrades ECM to promote cancer cell metastasis. It is associated with the elevation of matrix metalloproteinases expressions such as MMP9 and MMP2 (type IV collagen-degrading enzymes) (Choi et al., 2011; Krishnamachary et al., 2003).

Matrix metalloproteinases (MMPs) belong to endopeptidases family, which play a pivotal role in ECM modelling and EMT processing under hypoxia. Among MMPs, MMP2 and MMP9 degrade

collagen IV, a main component of ECM, enhances cancer cell migration and invasion in various cancer types, and often correlates with poor prognosis of the patients (Kessenbrock et al., 2010; Al-Alem and Curry, 2015). Expression of MMP9/MMP2 is tightly regulated by many factors like cytokines, growth factors, metal ions, oncogenes, and hormones (Van den Steen et al., 2002). It is reported that FMRP, an mRNA binding protein, binds to MMP-9 mRNA and form FMRP containing granule and inhibits translation in hippocampal neurons. It is then translocated from cell body to dendritic synapses where FMRP dissociates from MMP-9 mRNA upon mGluR (metabotropic glutamate receptors) activation. Then MMP9 mRNA associates with active polyribosomes and undergoes de novo protein synthesis (Dziembowska et al., 2012; Janusz et al., 2013). MMP-9 is secreted as a proenzyme containing a proregion adjacent to signal peptide. The cleavage in the proregion activates enzyme activity (Springman et al., 1990). The secretion of MMP9 is linked to its two N-linked glycosylation sites, Asn38 and Asn120 and abrogation of glycosylation retains it in the endoplasmic reticulum (Roth, 2002). The secreted MMP9 can form a complex with CD44 in the cell surface modulating cancer progression in breast cancer (Bourguignon et al., 1998) or can be internalized via interacting with the low-density lipoprotein receptor for its catabolism (Hahn-Dantona et al., 2001). Transcriptional regulation of MMP9 expression is well documented, however, little is known about its post-transcriptional regulation, especially in its translational regulation (Yan and Boyd, 2007).

Secretory proteins have a signal recognition sequence of 6 to 12 amino acids, which is recognized by SRP (Signal Recognition Particle) at the initial translation in the cytoplasm and pauses the translation. The nascent mRNA-ribosome complex with SRP cotranslationally translocate to the rough endoplasmic reticulum's membrane where it interacts with the SRP receptor and resumes the translation (Walter and Blobel, 1981; Saraogi and Shan, 2011).

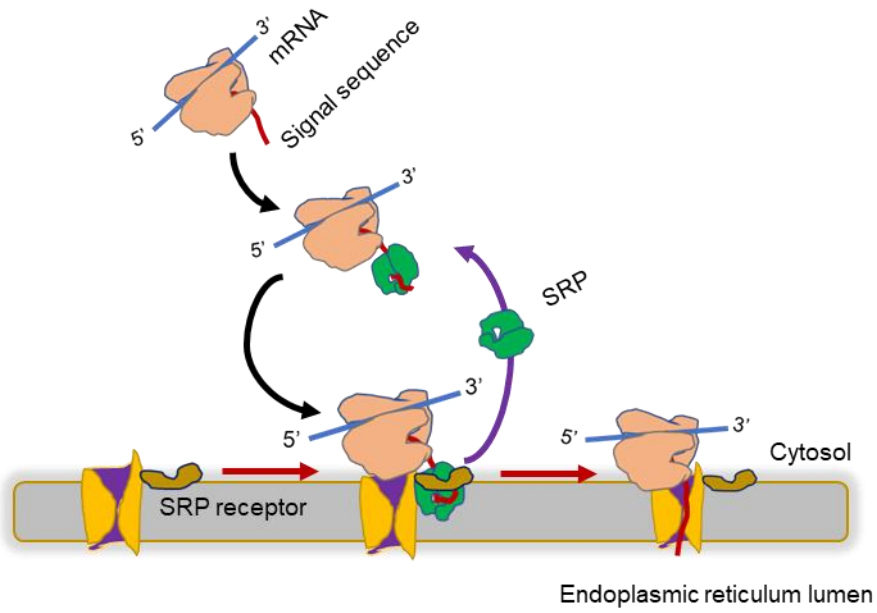

Fig. 4. Classical secretory pathway.

Nascent signaling peptides are recognized, bind by SRP and pause the translation in cytoplasm. The nascent mRNA-ribosome complex with SRP cotranslationally translocated to the rough endoplasmic reticulum's membrane where it interacts with SRP receptor and resume the translation.

The SRP comprises of six proteins (SRP9, SRPP14, SRP68, SRP72, SRP19, and SRP54) and a 300-nucleotide Alu RNA. SRP9/14 subunit interacts with Alu RNA in order to arrest translational elongation while SRP54 subunit interacts with the α-subunit of SRP receptor to resume translation (Siegel and Walter, 1986; Strub et al., 1991). The positively charged patch of lysine residues is essential for the interaction between SRP14 and the Alu RNA (Fig. 4) (Mary et al., 2010). The amount of SRP receptors present on the ER membrane is the limiting factor to determine the rate of translation (Lakkaraju et al., 2008). Despite several reports regarding cancer secretome, the classical secretory pathway and role of SRP in cancer progression remains elusive. So far, only a single report has shown that SRP14 is one of the targeted genes involved in endometrial cancer progression and development (O'Mara et al., 2019). However, the question remains to be addressed is whether dysregulated expression of SRP subunits like SRP9 or 14 causes cancer or its expression

is a consequence of cancer progression. Understanding cancer secretome through classical pathways will dictate a way to explore the molecular mechanistic details to fight cancer.

1.8. Review of literature on PBXIP1/HPIP

1.8. (a) Introduction

Abramovich *et al.*, discovered HPIP as one of the interacting protein partners of PBX1 (pre B cell leukemia homeobox 1) and likewise named it as hematopoietic PBX interaction protein (HPIP). It is also known as pre B-cell leukemia homeobox interacting protein 1 (PBXIP1) (Abramovich et al., 2000). Being an adaptor/scaffold protein, it facilitates physical associations with various signaling proteins like ERα/β, Src, microtubules, etc. (Manavathi et al., 2006). Paramount investigation revealed that HPIP is elevated in more than a dozen cancers and enhances tumorigenesis (Liu et al., 2015; Cao et al., 2017; Wang et al., 2008; Cheng et al., 2019) . Apart from its role in cancer, it is also linked with neuronal development, embryogenesis, and endometrium decidualization of repeated implantation failure in women (Dhaenens et al., 2019). Its expression is elevated in spermatogonial cells and promotes germ cell proliferation. Other physiological disorder-related diseases like renal fibrosis, chronic kidney disease, and Osteoarthritis (OA) (joint cartilage disorder) are linked with upregulation of HPIP (Ji et al., 2019). Two decades have passed since the discovery of HPIP and in unraveling its cellular functions. However, there is a dire need of rigorous empirical studies to address its mechanistic cellular functions because of the myriad of cellular and physiological processes it is associated with. We made a systematic evolutionary tree of HPIP that shows the explorations made so far with respect to its aforementioned cellular activities. HPIP has been investigated for its diverse roles like in hematopoiesis, estrogen signaling-related cellular function, reproduction biology, cancers, etc.

1.8. (b) Background of Pre-B-cell leukemia homeobox interacting protein 1 (PBXIP1 or HPIP)

It was the year 2000 when Abramovich *et al.*, discovered PBXIP1/HPIP. Six years down the line, Manavathi *et al*., had a major breakthrough in elucidating the role of HPIP in tumorigenesis by activation of PI3K/AKT pathway via estrogen signaling. Since then, last 20 years saw a myriad of novel and exciting findings on this protein, so much that we can dedicate the phrase "HPIP biology" to illustrate its significance in the field of life science research (Fig. 5).

HPIP gene is located on chromosome 1 at position q21.3, which is amplified in lung cancer, encoding a protein of 731 amino acid with two functional nuclear localization (485 aa – 505 aa and 695 aa – 720 aa), a nuclear export (443 aa – 731 aa) and microtubules binding sequence (190 aa – 218 aa) (Fig. 6A) (Abramovich et al., 2002; Liu et al., 2015). HPIP predominantly localizes to the cytoskeletal fibers and can shuttle between the cytosol and the nucleus (Abramovich et al., 2002). It was discovered as a PBX1 interacting protein through its PBX1 binding domain sequence (562 aa – 633 aa) and interacts with other PBX families like PBX2 and PBX3 (Abramovich et al., 2000). By consolidating the reported information, we mapped the various domains of HPIP and its responsible interaction sites (Fig. 6A); however, crystal structure of HPIP is not available yet. It has a LXXLL motif or nuclear receptor-interacting motif (615 aa – 619 aa), which interacts with ERα and potentiates estrogen signaling (Manavathi et al., 2006). Also, ERα/β binds on three domains of HPIP, 138 aa – 220 aa, 328 aa – 561 aa, and 562 aa – 731 aa (Wang et al., 2008). It has a RGD domain (421 aa- 423 aa), which is known for FAK activation signaling (Schaller, 2010).

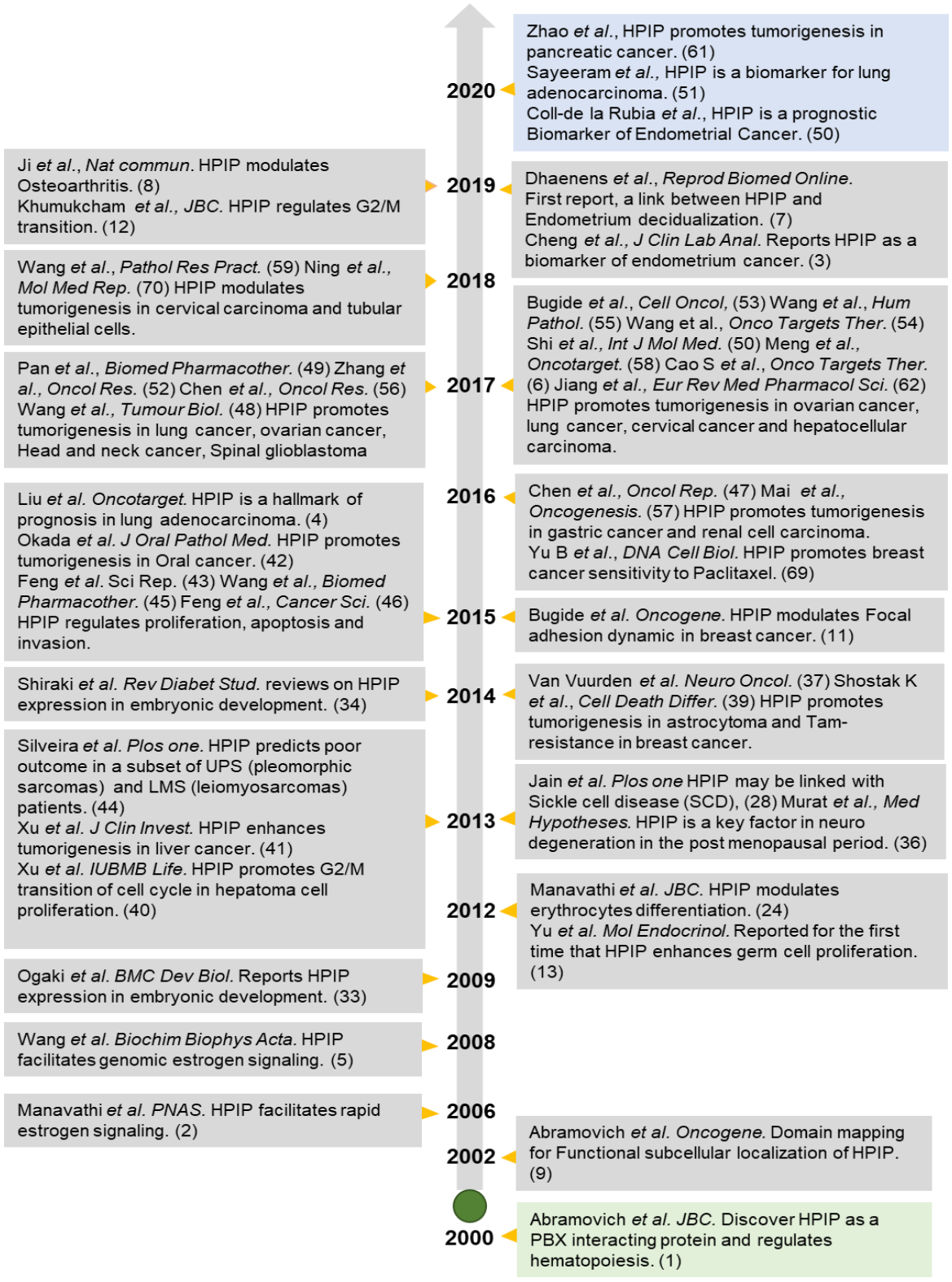

Fig. 5. Evolutionary tree of *HPIP/PBXIP1* gene.

The summary/highlights of *HPIP* since its discovery in the year 2000 and its significance in the field of life science research.

However, Bugedi *et al*., showed that HPIP is activated through direct interaction of its C-terminal sequence (583 aa – 731 aa) with the kinase domain of FAK (Bugide et al., 2015). The conserved consensus sequence D4 domain (335 aa – 338 aa) of HPIP, a stability domain during mitosis, interacts with CDC20 (Khumukcham et al., 2019). Moreover, it interacts with APC3 through another conserved consensus sequence, IR domain (282 aa – 283 aa) that regulates mitosis (Khumukcham et al., 2019). It is shown that the testis-expressed 11 (TEX11) competes with ERβ for binding to the C-terminal region (509 aa – 631 aa) of HPIP (Yu et al., 2012). Recently, one more sequence is reported (362 aa – 541 aa), which interacts with lymphoid enhancer-binding factor 1 (LEF1) during the pathogenesis of osteoarthritis (Ji et al., 2019). Also, Yeast-two hybrid screening shows that HPIP is a interacting partner of AMPK (Moreno et al., 2009). The list of HPIP interacting protein partners, along with their source of information, is mentioned in (Fig. 6B).

A.

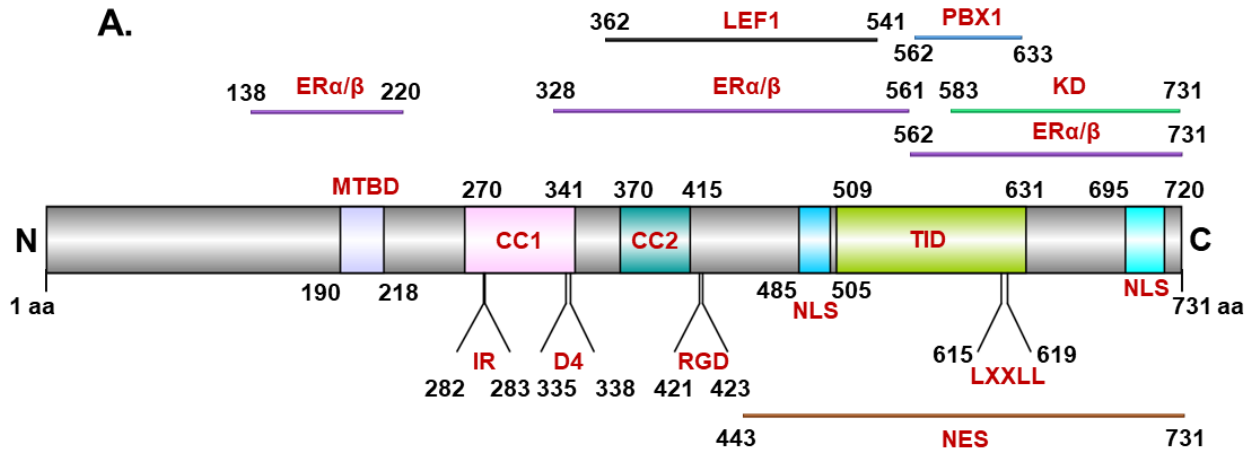

B.

Interaction profile of PBXIP1/HPIP		
Sl. No.	Protein name	Source (Ref)
1	PBX1	Abramovich *et al., 2000* (1)
2	PBX2	Abramovich *et al., 2000* (1)
3	PBX3	Abramovich *et al., 2000* (1)
4	Microtubule	Abramovich *et al., 2000*, Manavathi *et al., 2006* (1,2)
5	p85 subunit of PI3K	Manavathi *et al., 2006* (2)
6	Src kinase	Manavathi *et al., 2006* (2)
7	β-Tubulin	Manavathi *et al., 2006* (2)
8	ERα	Manavathi *et al., 2006*, Wang *et al., 2008* (2,5)
9	ERβ	Wang *et al., 2008 (5)*
10	FAK	Bugide *et al., 2015* (11)
11	Calpain 2	Bugide *et al., 2015* (11)
12	Casein kinase 1α (CK1α)	Mai *et al., 2016* (57)
13	LEF1	Ji *et al., 2019* (8)
14	β-catenine	Ji *et al., 2019* (8)
15	MDM2	Shostak *et al., 2014* (39)
16	TBK1	Shostak *et al., 2014* (39)
17	IKKγ	Shostak *et al., 2014* (39)
18	CDC20	Khumukcham *et al., 2019* (12)
19	MAD2	Khumukcham *et al., 2019* (12)
20	APC3	Khumukcham *et al., 2019* (12)
21	TEX11	Yu *et al., 2012* (13)
22	AMPK	Moreno *et al., 2009* (14)

Fig. 6. Domain architecture of human PBX interacting protein or pre-B-cell leukemia homeobox interacting protein 1 (HPIP or PBXIP1).

A. Analysis of encoded 731 amino acids sequence of HPIP and mapping of its functional domains. (ERα/β binding sites (Purple line), 138 aa – 220 aa, 328 aa – 561 aa, and 562 aa – 731 aa; MTBD (Microtubule binding domain) (light blue) 190 aa – 218 aa; IR motif (Ile-Arg) 282 aa - 283 aa; D4 motif 335 aa – 338 aa; Coil-coiled domains (light pink) (CC1, 270 aa – 341 aa); (green) CC2, 370 aa – 415 aa); RGD motif (Arg-Gly-Asp) 421 aa - 423 aa; LEF1 (lymphoid enhancer-binding factor 1) binding site (black line) 362 aa – 541 aa; NLS (Nuclear localization sequence) (light green) 485 aa – 505 aa and 695 aa – 720 aa; NES (Nuclear export sequence) (brown) 443 aa –731 aa; PBX1

binding site (blue line) 562 aa – 633 aa; TEX11 (Testis-expressed 11) interacting site (lime green) 509 aa – 631 aa; LXXLL motif or nuclear receptor-interacting motif, 615 aa – 619 aa; TID (TEX11 interacting domain), 509-631 aa; KD (kinase domain) (light green line), 583 aa – 731 aa. **B.** List of interacting protein partners of HPIP/PBXIP1 and its source.

1.8. (c) Role of HPIP in hematopoiesis

PBX is a transcription factor that plays a vital role in developing hematopoiesis, while its deregulated expression links to leukemogenesis (DiMartino et al., 2001; Shimamoto et al., 1998). It acts as a coactivator for HOX proteins. PBX-HOX transcription factor complexes are thus formed is essential for the development of hematopoietic stem cells (HSC) (Moens and Selleri, 2006). HPIP is a non-homeoprotein that directly interacts with PBX1 and both are highly expressed (co-expressed) in early hematopoietic progenitor cells enriched with CD34+ population and regulate the primitive stages of hematopoiesis and leukemic transformation (Abramovich et al., 2000). Mechanistic details have shown that HPIP not only interacts with PBX1, but also with proteins of the same family as PBX2 and PBX3. It blocks the recruitment of PBX-HOX heterodimer to the target DNA sequence inhibiting the transcriptional activity of E2A-PBX (Abramovich et al., 2000). Manavathi *et al*., revealed that HPIP is induced in response to erythroid differentiation via erythroid lineage-specific transcription factors GATA-1/2 and mediates transcriptional activation of HPIP in a CTCF (CCCTC-binding factor) dependent manner (Fig. 7A) (Manavathi et al., 2012). The induced HPIP activates PI3K/AKT/GSK3β signaling pathway, which in turn activates GATA1 transcription in a positive feedforward mechanism and regulates erythroid differentiation (Fig. 7A) (Manavathi et al., 2012). The hematopoiesis of sickle cell disease (SCD) is associated with reticulocytosis, erythroid hyperplasia, and HSC development (Grasso et al., 1975; Wu et al., 2005; Leonard et al., 2019). The downregulation of HPIP expression and its inverse correlative expression with miR-1225-3p in SCD further suggests a committed role of HPIP in hematopoiesis which needs to be further extrapolated (Jain et al., 2013).

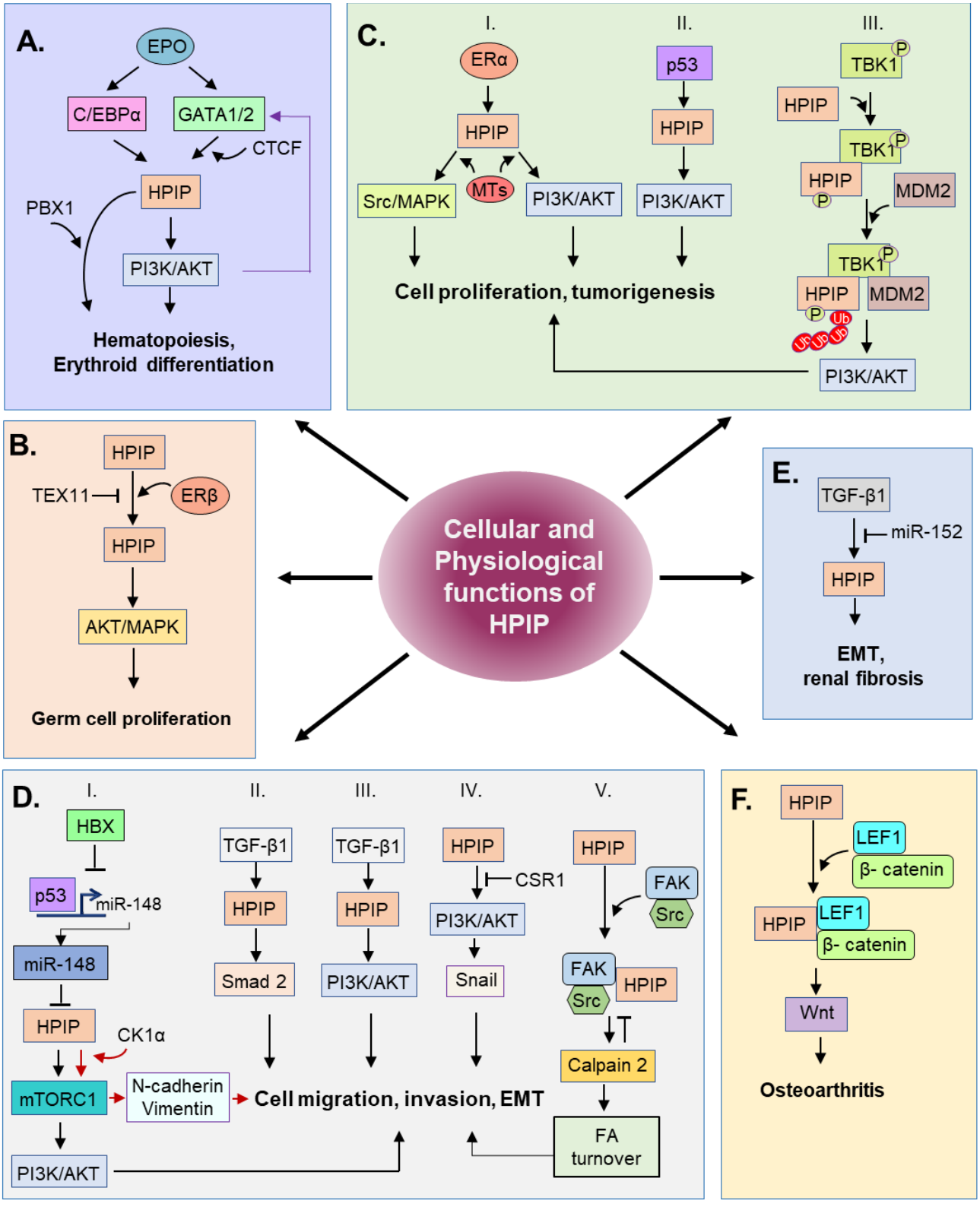

Fig. 7. Generalized cellular and physiological roles of HPIP/PBXIP1.

A. HPIP directly interacts with PBX1 and regulates the primitive stages of hematopoiesis. In response to erythropoietin (EPO), erythroid differentiation inducers, C/EBPα and GATA1 (in a CTCF, CCCTC-binding factor, dependent manner) activate HPIP and regulate erythroid

differentiation through PI3K/AKT signaling pathway. **B.** TEX11 and ERβ compete for HPIP; if TEX11 is more, it replaces ERβ and suppresses germ cell proliferation by inhibiting non-genomic signaling. **C**. (I) The estrogen mediates microtubule scaffold (MTs) multiprotein complex formation, ERα-HPIP-Src-PI3K, activates rapid non-genomic estrogen signaling cascade thereby stimulating AKT/MAPK signaling pathways and promotes tumorigenesis. **C**. (II) In p53-activated epithelial cells, p53 transcriptionally activates HPIP and drives tumorigenesis through HPIP-AKT signaling pathway. **C**. (III) MDM2 degrades HPIP through TBK1 mediated phosphorylation at Serine 147 and activates MDM2-mediated AKT signaling pathway and promotes cell proliferation. **D**. (I) HBX interacts with p53 and inhibits its recruitment to mi-R148a promotor rendering HPIP-mediated cell proliferation or invasion through the pAKT/mTOR signaling pathway. (**Red arrow**) HPIP interacts with CK1α and modulates renal cell carcinoma cell proliferation or EMT via mTOR signaling pathway. **D**. (II) and (III) TGF-β drives EMT through HPIP mediated Smad2 activation or via PI3K/AKT. **D.** (IV) HPIP stabilized Snail via PI3K/AKT pathway and enhances EMT. The cellular stress response 1 (CSR1) inhibits HPIP-mediated PI3K/AKT signaling. **D.** (V) HPIP stimulates MAPK-mediated Calpain2 activation and promotes FA disassembly and turnover, and enhances cell migration. **E.** TGF-β1 induces HPIP mediated EMT in renal fibrosis. **F.** Osteoarthritis (OA) is linked with high expression of HPIP. β-catenin mediated HPIP interaction with LEF1 enhances transcriptional activation of Wnt signaling pathway genes and thus OA pathogenesis.

1.8. (d) Role of HPIP in reproduction and development

Yu *et al*., have shown that mouse spermatogonial stem cells express abundant HPIP that modulates germ cell proliferation by inhibiting the functional interaction between TEX11 and ERβ (Fig. 7B) (Yu et al., 2012). TEX11 is one of the X-linked spermatogenesis genes that are highly expressed in spermatogonia and early spermatocytes (Wang et al., 2001; Adelman and Petrini, 2008). Detailed study shows that formation of ERβ-HPIP-Src-PI3K complex mediates rapid non-genomic signaling and activates AKT and MAPK signaling pathways, promoting germ cell proliferation (Manavathi et al., 2006; Yu et al., 2012). However, if TEX11 expression is more, it replaces ERβ from the complex and suppresses cell proliferation by inhibiting non-genomic signaling (AKT/MAPK signaling) (Fig. 7B). ERβ localizes to the nucleus and promotes genomic signaling by enhancing the transcriptional activity of the estrogen-responsive genes. This study implies that a delicate balance among HPIP, ERβ, and TEX11 levels regulate germ cell proliferation (Yu et al., 2012).

The endometrium is the inner layer of the uterus, which is made up of epithelial cells. It thickens and renews itself periodically every month and sheds during menstruation. However, if a female conceives, it undergoes a series of functional and morphological changes forming a decidual lining for blastocyst implantation known as endometrium decidualization (Okada et al., 2018). Dhaenens *et al*., recently investigated on the proteomes of in-vitro cultured endometrial stromal cells showing that HPIP is down-regulated (7.7-fold) in women with repeated implantation failure compared to normal fertile women upon decidualization (Dhaenens et al., 2019). The mechanism is yet to be reported, but it can be hypothesized that HPIP may be involved in hormonal regulation during endometrium development. The endometrium proliferation and thickening to form a healthy endometrium are regulated by estrogen hormone produced from ovarian granulosa cells (Ng et al., 2020). Further investigation from three independent groups has revealed that HPIP modulates estrogen-mediated signaling and promotes cell proliferation, which strongly supports the possibility of HPIP mediated estrogen signaling during endometrium development (Manavathi et al., 2006; Wang et al., 2008; Yu et al., 2012). Investigating its mechanistic role will be an emerging area to understand pregnancy-related complications in reproduction biology in the near future, which is yet to be reported.

Ogaki *et al*., identified for the first time that HPIP expression is elevated during embryogenesis, particularly in E8.5 mouse embryonic definitive endoderm (DE) and pancreatic buds of E14.5 embryo (pancreatic differentiation) (Ogaki et al., 2011; Shiraki et al., 2014). Also, the chondrocyte specific *HPIP* knockout mice (*HPIP* $^{-/-}$) resulted in proportionate dwarfism during embryonic development (Ji et al., 2019). Interestingly, it is also shown to be upregulated in the astrocytic progenitor cells implying its potential role during human brain development. Besides it being a novel protein that is expressed in hippocampal neurons, and its expression is linked with neuronal degeneration in post-menopausal women (Murat Karamese, 2013; Selina et al., 2015). Further

study shows HPIP as a biomarker for astroglial progenitor cells (Cahoy et al., 2008; van Vuurden et al., 2014). These reports point to the essential roles of HPIP in different stages of reproduction beginning from germ cell proliferation to embryonic development.

1.8. (e) Role of HPIP in estrogen signaling

HPIP is a microtubule binding protein (Abramovich et al., 2000). The endogenous Estrogen receptor (ERα) interacts with microtubules through the LXXLL motif of HPIP. HPIP acts as a scaffold protein holding and recruiting p85 subunits of PI3K and Src kinase to 17 beta-estradiol (E2)-ERα complex (Fig. 7C, I) (Manavathi et al., 2006). The formation of microtubule scaffold signaling molecules complex, ERβ-HPIP-Src-PI3K, activates rapid non-genomic estrogen signaling cascade, thereby stimulating AKT/MAPK signaling pathways and promoting tumorigenesis; however, it negatively regulates transcriptional activity of ERα (genomic estrogen signaling) in the breast cancer cell. Interestingly, when the microtubules are depolarized, it enhances the transcriptional activity of ERα (Manavathi et al., 2006). It means that the microtubules' dynamics have an inherent role in maintaining the homeostasis of estrogen signaling cascades under various physiological signals. Akin to this, Yu *et al*., have reported a mechanism in mouse spermatogonial stem cells where TEX11 competes with estrogen (ERβ) to bind HPIP (Yu et al., 2012). The formation of the ERβ-HPIP-Src-PI3K complex mediates rapid non-genomic signaling and activates AKT/MAPK signaling pathways, promoting germ cell proliferation (Fig. 7B) (Wang et al., 2008; Yu et al., 2012). However, if TEX11 binds with HPIP, it replaces ERβ from the complex, restraining non-genomic signaling but enhancing the estrogen-responsive gene's transcriptional activity (Fig. 7B) (Yu et al., 2012). Moreover, Wang *et al*., have reported that HPIP interacts with ERα or ERβ that compete with each other for binding to HPIP and inhibit the ERα dependent expression of its targeted genes (Wang et al., 2008). However, the effect of HPIP mediated ERα signaling pathways remains controversial. Manavathi *et al*., observed that HPIP negatively regulates the transcriptional activity of ERα; in contrast, Wang *et al*., reported

that HPIP enhances ERα targeted gene expression in MCF7 cells. However, both the team reveals that HPIP activates MAPK and AKT through estrogen signaling cascades. The discrepancy found may be due to the reporter assay experiment with different reporter systems and also the origin of the template DNA for cloned reporters. Concurrently, it is reported that HPIP is a substrate for MDM2, and it prevents the HPIP dependent over activation of AKT in P53-proficient mammary epithelial cells to maintain homeostasis (Fig. 7C, II and III) (Shostak et al., 2014). This study further revealed that HPIP over expression confers taxol resistance in breast cancer cells.

1.8. (f) HPIP is a proto-oncogene

HPIP is a proto-oncogene, which is overexpressed in more than 15 different types of cancers, breast cancer (Manavathi et al., 2006; Wang et al., 2008; Bugide et al., 2015), liver cancer (Xu et al., 2013a; Xu et al., 2013b), oral squamous cell carcinoma (Okada et al., 2015), colorectal cancer (Feng et al., 2015b), pleomorphic sarcomas and leiomyosarcomas (Silveira et al., 2013), thyroid carcinoma (Wang et al., 2015), gastric cancer (Feng et al., 2015a; Chen et al., 2016a), spinal glioblastoma (Wang et al., 2016), lung cancer (Liu et al., 2015; Pan et al., 2016; Shi et al., 2017; Sayeeram et al., 2020), ovarian cancer (Zhang et al., 2016; Bugide et al., 2017; Wang et al., 2017b; Wang et al., 2017c), head and neck cancer (Chen et al., 2016b), renal cell carcinoma (Mai et al., 2016), cervical cancer (Meng et al., 2017; Wang et al., 2018), endometrial cancer (Cheng et al., 2019; Coll-de la Rubia et al., 2020), pancreatic cancer (Zhao et al., 2020), and astrocytoma and ependymoma (van Vuurden et al., 2014). Also, analysis of data sets which are available through Oncomine (Compedia Biosciences, http://www.oncomine.org/) showed a significantly higher expression of HPIP in other cancers types, superficial Bladder cancer, glioblastoma, renal oncocytoma, acute myeloid leukemia (AML), B-cell acute lymphoblastic leukemia (BCALL), cutaneous melanoma (CM), prostate adenocarcinoma (Fig. 8). HPIP promotes tumorigenesis through various signaling cascades like TGF-β1, PI3K/AKT, Wnt, mTOR, and Sonic hedgehog

signaling pathway (Manavathi et al., 2006; Xu et al., 2013a; Pan et al., 2016; Zhang et al., 2016; Ji et al., 2019).

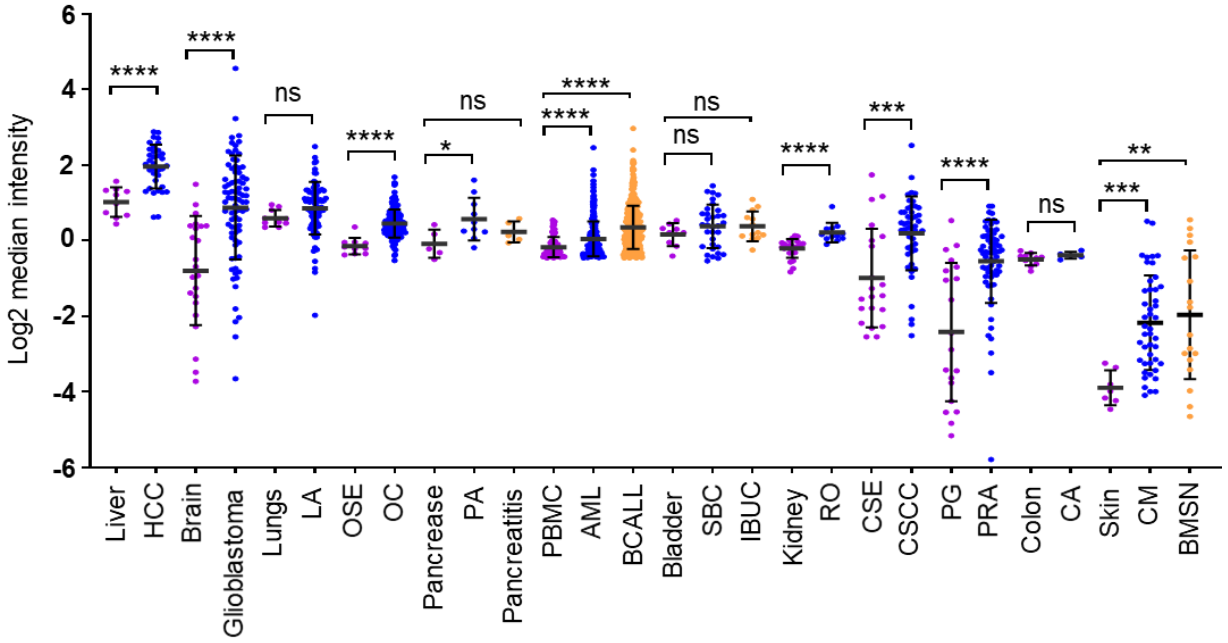

Fig. 8. Analysis of HPIP expression in various cancer types.

Oncomine derived graph showing the high expression of *HPIP* in various types of cancer. (Pink- normal tissue, Blue- cancer tissue. Orange- cancer tissue). (HCC- Hepatocellular Carcinoma, LA- Lungs Adenocarcinoma, OSE- Ovarian Surface Epithelium, OC- Ovarian Carcinoma, PA- Pancreatic Adenocarcinoma, PBMC- Peripheral Blood Mononuclear Cell, AML- Acute Myeloid Leukemia, BCALL- B-Cell Acute Lymphoblastic Leukemia, SBC- Superficial Bladder Cancer, IBUC- Infiltrating Bladder Urothelial Carcinoma, RO- Renal Oncocytoma, CSE- Cervix Squamous Epithelium, CSCC- Cervical Squamous Cell Carcinoma, PG- Prostate Gland, PRA- Prostate Adenocarcinoma), CA- Colon Adenoma, CM- Cutaneous Melanoma, BMSN- Benign Melanocytic Skin Nevus,. Bar represent the mean ± SD (*P < 0.05, **P < 0.01, ***P < 0.001, unpaired Student's t-test).

Since its discovery, our research team was the first to identify HPIP as a part of a scaffold signaling complex consists of ERα, Src, PI3K and HPIP, which activates MAPK/ERK1/2 and AKT signaling pathways in response to estrogen and promotes tumorigenesis (Manavathi et al., 2006). The activated AKT and ERK1/2 further stimulates ERα phosphorylation and drives estrogen-responsive gene expression promoting breast cancer proliferation (Wang et al., 2008). Not only

breast cancer, but HPIP can also promotes proliferation of colorectal cancer cells (Feng et al., 2015b). It activates PI3K/AKT signaling pathway in other cancers such as head and neck squamous cell carcinoma, thyroid cancer, colorectal cancer, human hepatocellular carcinoma, ovarian cancer and drives cancer cell proliferation (Feng et al., 2015b; Wang et al., 2015; Chen et al., 2016b; Bugide et al., 2017; Jiang et al., 2017). In connection with HPIP-mediated AKT signaling, Shostak *et al*., has reported an interesting finding that MDM2 degrades HPIP through TBK1 mediated phosphorylation, which activates MDM2-mediated AKT signaling pathway and promotes cell proliferation in p53-depleted MCF7 cells (Fig. 7C, III) (Shostak et al., 2014). However, in p53-activated epithelial cells, p53 mediated transcriptional activation of HPIP enhances PI3K-AKT signaling pathway. It conveys two possible ways of AKT signaling based on the activity of p53 to drive breast cancer proliferation that needs to be considered during therapeutic administration to the patients (Shostak et al., 2014). In hepatocellular carcinoma, miR148a inhibits HPIP-dependent mTOR signaling pathway, AKT/ERK/FOXO4/ATF5, which enhances cell proliferation (Xu et al., 2013a). miR148a is a transcriptional target of p53. HBX interacts with p53 and suppresses its recruitment to *miR148a* promotor, which renders HPIP-mediated cell proliferation through the pAKT/pERK/mTOR signaling pathway (Xu et al., 2013a). In most cancers, p53 is frequently mutated and loses its function; such cells have a low expression of miR148a as well. So HPIP-mediated AKT signaling intensifies and promotes cell proliferation; however, this finding contradicts Shostak *et al.*, as AKT-mediated signaling happens through MDM2 in p53-mutated cells but not HPIP (Fig. 7C, III) (Shostak et al., 2014). This discrepancy may be due to genotypic plasticity or different epigenetic alternation between cancers. Furthermore, the overexpression of HPIP in HepG2 cells modulates mTOR signaling with elevated Cyclin D1, c-MYC, and promotes cell proliferation (Xu et al., 2013a). c-MYC family is an oncoprotein known as a master regulator of metabolic reprogramming in a broad spectrum of cancers (Dong et al., 2020b). c-MYC regulates 15% of the entire genomic transcription (Li et al., 2003b). As c-MYC is known to be elevated

during HPIP overexpression, further investigation of possible cross-talk between HPIP and c-Myc will be an exciting area to explore in cancer.

HPIP mediates cap-dependent translation, AKT/mTORC1 signaling pathway and enhances cell proliferation in gastric cancer (Chen et al., 2016a). It also regulates cell proliferation and migration through Sonic hedgehog signaling pathway in non-small lung cancer cells (Pan et al., 2016). It involves in astrocytoma and ependymoma, and chondrocyte proliferation (Ji et al., 2019; van Vuurden et al., 2014). Moreover, it modulates renal cell carcinoma cell proliferation through interaction with CK1α, which drives mTOR signaling (Fig. 7D, I) (Mai et al., 2016). Qinong Ye group showed that HPIP promotes liver cancer cells' proliferation by activating the G2-M phase of the cell-cycle (Fig. 9) (Xu et al., 2013b). They report that HPIP regulates the G1/S and G2/M phase transition of the cell cycle in colorectal cancer. At the G1/S phase, it regulates cyclin D1 and cyclin A expression at the transcriptional level; however, at the G2/M phase, post-transcriptionally, it regulates cyclin B1 stability and promotes tumor progression (Feng et al., 2015b) (Fig. 9). Their further investigation in gastric cancer has revealed a similar mechanism of HPIP mediated cell cycle regulation (Feng et al., 2015a) . "How does HPIP regulates cyclin B1 stability and promotes tumor progression?" Cyclin B1 is an essential component that regulates cell cycle progression by controlling G2 to M phase and therefore, its accumulation at late G2 phase is a prerequisite for timely mitotic entry (Gavet and Pines, 2010; Champion et al., 2017). The Cyclin B1 dependent activation of cyclin-dependent kinase 1 (CDK1), and Cdk1–Cyclin B1 complex formation is crucial for G2/M transition (Champion et al., 2017). Khumukcham *et al.*, reported that HPIP stabilizes Cyclin B1 by precluding it from

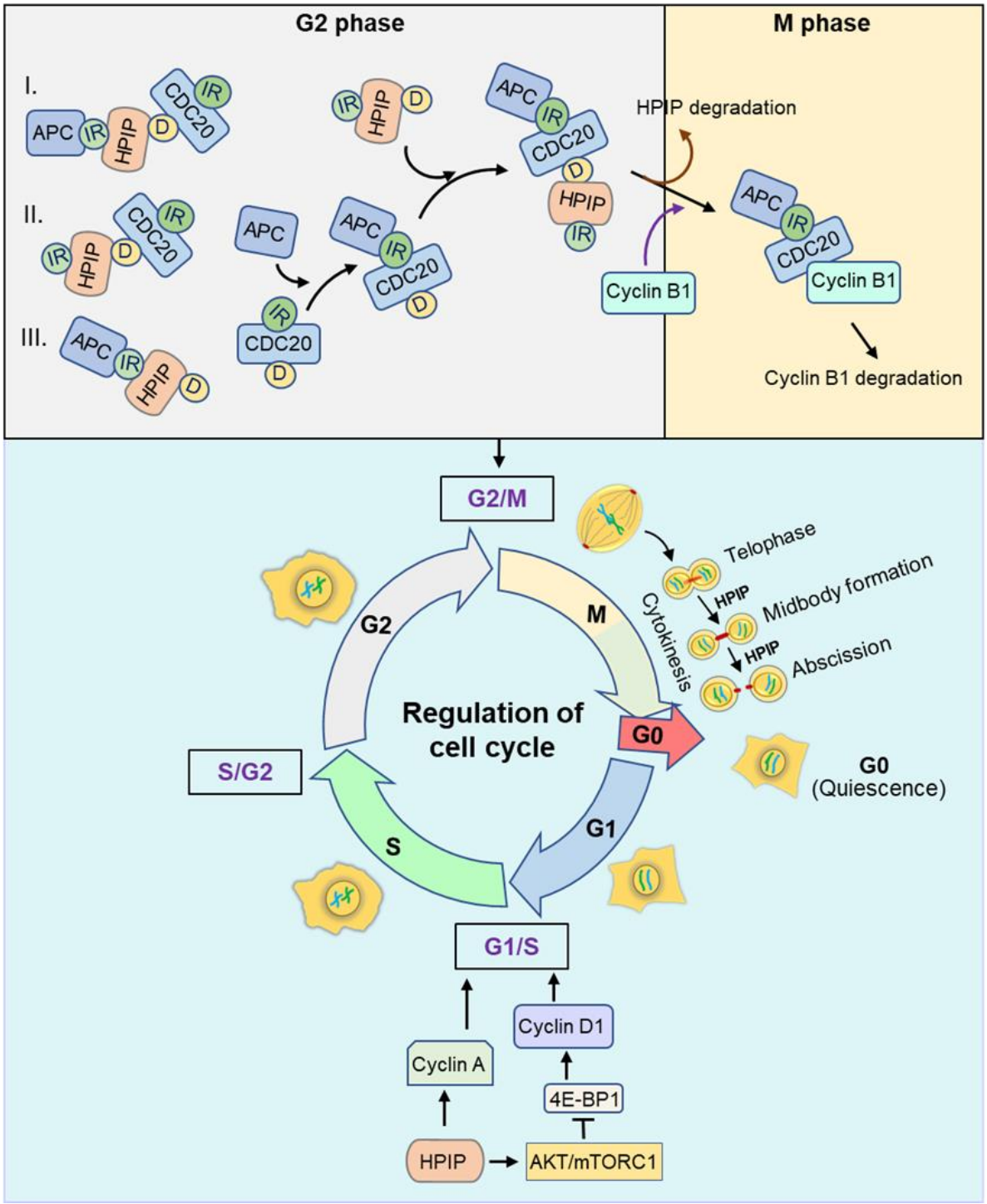

Fig. 9. HPIP-mediated cell cycle checkpoint regulation.

HPIP regulates the G0/G1, G1/S, and G2/M phase transition of the cell cycle. At the G2/M phase, it stabilized cyclin B1 and promotes tumor progression. The D box and IR domains of HPIP create a temporary facultative molecular bridge with APC/C–Cdc20, i.e., I. HPIP-APC, II. APC-HPIP-CDC20, III. HPIP-CDC20 thereby inhibiting the formation of active APC/CDC20 and facilitates temporal and spatial stability of cyclin B1 for timely mitotic entry and cell cycle progression.

Active APC-CDC20 degrades HPIP and Cyclin B1 at the G2/M phase of the cell cycle. HPIP acts as an inhibitor cum a substrate of APC-CDC20. It also regulates cytokinesis and midbody formation. At the G1/S phase, HPIP enhances the expression of cyclin D1 and cyclin A. It promotes cap dependent translation of cyclin D1 by inhibiting 4E-BP1 through AKT/mTORC1 signaling pathway.

APC/Cdc20-mediated ubiquitination and its subsequent proteasomal degradation. HPIP has two domains, the D4 domain which is primarily involved in HPIP stability, and the IR domain which acts as an inhibitor of APC–Cdc20 activity. HPIP is ubiquitinated at lysine 274 by CDC20 during early mitosis. The D box and IR domains of HPIP create a sort of temporary "facultative molecular bridge" with APC/C–Cdc20 and facilitate temporal and spatial stability of cyclin B1 for timely mitotic entry and cell cycle progression (Khumukcham et al., 2019) (Fig. 9). The high expression of both HPIP and Cyclin B1 showed a possible correlation with the malignant behaviors of the cells (Xu et al., 2013b; Chen et al., 2016a). Upon further investigation it was found that HPIP is associated with the mitotic spindle and its depletion causes chromosomal breaks and pre-segregation. Furthermore, HPIP localizes in the midbody and it persists up to abscission formation during cytokinesis. Hence, HPIP depleted cells show defective midbody formation (Khumukcham et al., 2019). The role of HPIP in chromosomal pre-segregation and cytokinesis needs further mechanistic investigation. Besides this, HPIP also promotes cell division in spinal glioblastoma tissues (U87 and U251 cell lines) by regulating G1/S transition (Fig. 9) (Wang et al., 2016). It was recently reported in pancreatic ductal adenocarcinoma (PDAC) cells that HPIP enhances proliferation by promoting G0/G1 to S transition (Fig. 9) (Zhao et al., 2020). Further Chan *et al*., reported that HPIP mediated inactivation of 4E-BP1 through AKT/mTORC1 enhances cap-dependent translation of Cyclin D1 and promotes G1/S transition of cell cycle in gastric cancer cells (Chen et al., 2016a). The discrepancies observed in the role of HPIP-mediated cell cycle checkpoint regulation in different cancers might be due to the differences in the nature and origin of cancers analyzed and also variant genetic backgrounds with diverse signaling networks

associated with each cancer type. Interestingly HPIP suppresses the proliferation of oral squamous cell carcinoma (OSCC) cells while enhancing cell invasion. On the other hand, HPIP inhibits invasion of normal human epidermal keratinocytes (NHEK) but potentiates its proliferation (Okada et al., 2015).

Manavathi *et al.*, reported, for the first time, the role of HPIP in breast cancer cell migration and invasion (Manavathi et al., 2006). The estrogen mediated multiprotein complex formation, ERα-HPIP-Src-PI3K, drives rapid non-genomic ERα signaling and promotes cell migration and invasion (Manavathi et al., 2006). HPIP induces tumor cell migration in astrocytoma and ependymoma, oral squamous cell carcinoma (OSCC), cervical cancer and gastric cancer (van Vuurden et al., 2014; Okada et al., 2015; ; Feng et al., 2015a; Cao et al., 2017). It can also drive cell migration through the Sonic hedgehog signaling pathway in non-small lung cancer cells (Pan et al., 2016). By activating MAPK/ERK1/2 and PI3K/AKT signaling pathways, HPIP modulates EMT (epithelial-mesenchymal transition) and cancer cell migration in various cancers including colorectal cancer, thyroid cancer, head and neck squamous cell carcinoma and ovarian cystadenocarcinoma (Feng et al., 2015b; Wang et al., 2015; Chen et al., 2016b) . The elevated expression of HPIP suppresses E-cadherin (Epithelial marker) while upregulating N-cadherin and Vimentin expression (Mesenchymal markers) (Feng et al., 2015b). Similarly, it regulates EMT in glioblastoma cells (U87 and U251) as knockdown of HPIP reduces N-cadherin, Slug, and MMP2 with high expression of E-cadherin (Wang et al., 2016). Mai *et al*., identified casein kinase 1α (CK1α) as an HPIP-interacting protein. The interaction of CK1α with HPIP promotes EMT via mTOR pathway driving cell migration and invasion in renal cell carcinoma (Fig. 3D, I) (Mai et al., 2016). Similarly, HPIP mediated mTOR pathway increases hepatocellular carcinoma cells' migration and invasion (Figure 7D, I) (Xu et al., 2013a). In ovarian cancer cells, TGF-β also drives EMT through HPIP mediated activation of PI3K/AKT Signaling Pathway (Fig. 7D, III) (Zhang et

al., 2016). Whereas in lung cancer cells, TGF-β induces EMT through HPIP mediated Smad2 activation (Fig. 7D, II) (Shi et al., 2017). In human hepatocellular carcinoma (HCC), cellular stress response 1 (CSR1) inhibits HPIP-mediated PI3K/AKT signaling and suppresses cancer cell migration and invasion (Jiang et al., 2017). Also, in ovarian cancer cells, HPIP modulates PI3K/AKT/GSK-3β pathway which results in Snail stabilization that in turn causes EMT and cancer cell migration and invasion (Fig. 7D, IV) (Bugide et al., 2017). Bugedi *et al.*, reported that HPIP regulates cell adhesion and dynamics in breast cancer cells by modulating FAK activation, focal adhesion disassembly and thus cell migration (Bugide et al., 2015). Focal adhesions (FAs) are multiprotein complexes that serve as mechanical link between cells and extracellular matrix (ECM). They help to anchor cells to the ECM and so their movement is controlled by the dynamic changes in the levels of its component proteins and aids in initiation, maturation and disassembly (Rigiracciolo et al., 2021). Calpain2 is calcium-dependent site-specific protease that cleaves the protein components of FA leading to its disassembly to promote cellular movement (Carragher et al., 2003). Interestingly, HPIP stimulates MAPK-mediated Calpain2 activation and proteolyzes Talin, a FA component, which promotes FA disassembly and turnover, and thus cell migration (Fig. 7D, V) (Bugide et al., 2015). Various independent studies show that HPIP is involved in tumor cell apoptosis. Feng *et al*., reported that diminished HPIP expression leads to apoptosis with elevated apoptosis inducers, PIG3 and BAX along with decrease level of apoptosis inhibitor, BCL2. It also inhibits apoptosis by blocking Caspase-3-mediated cleavage of PARP (Feng et al., 2015b). HPIP inhibits apoptosis in different types of cancers like pancreatic ductal adenocarcinoma (PDAC) cells and glioma cells in a similar fashion (van Vuurden et al., 2014; Zhao et al., 2020). The high expression of HPIP confers cisplatin resistance to ovarian cancer cells (SKOV3) (Bugide et al., 2017), which also has a correlation with platinum resistance in epithelial ovarian cancer (Wang et al., 2017b). It modulates tamoxifen resistance in p53-deficient MCF7 cells (Shostak et al., 2014). However, it sensitizes breast cancer cells (MCF-7 and MDA-MB-231) to paclitaxel, a

hint of clinical value of HPIP as a precision medicine (Yu et al., 2016). Emerging studies have shown that HPIP can be used as a biomarker to predict many cancers' prognoses (Table 1). The elevated expression of HPIP correlates with poorer outcome and poor survival in several cancers like invasive ductal breast carcinoma (Bugide et al., 2015), renal cell carcinoma (Mai et al., 2016), epithelial ovarian carcinoma (Wang et al., 2017c), lung adenocarcinoma (Sayeeram et al., 2020), cervical cancer (Cao et al., 2017), pleomorphic sarcomas and leiomyosarcomas (Silveira et al., 2013), endometrial cancer (Cheng et al., 2019; Coll-de la Rubia et al., 2020), cervical cancer (Meng et al., 2017; Wang et al., 2018) and lung adenocarcinoma (Table 1) (Liu et al., 2015). It is now evident that HPIP may be a good potential biomarker for targeted therapy for several cancers.

Table 1: **PBXIP1/HPIP expression in various cancers.**

Cancer types	PBXIP1/HPIP expression level	Sample type (number of patients)	Method	Prognosis	Reference
Liver	Upregulated	Liver cancer patients- 328	WB, IHC	n/a	Xu *et al.*, 2013b (Xu et al., 2013b)
Breast	Upregulated	Invasive ductal carcinoma patients- 35	IHC	Poor	Bugide *et al.*, 2015 (Bugide et al., 2015)
Oral	Upregulated	Oral squamous cell carcinoma patients- 27	IHC	n/a	Okada *et al.*, 2015 (Okada et al., 2015)
Colorectal	Upregulated	Colorectal cancer patients- 63	IHC	Poor	Feng *et al.*, 2015b (Feng et al., 2015b)
Undifferentiated Pleomorphic sarcomas (UPS) and leiomyosarcomas (LMS)	Upregulated	UPS patients- 20; LMS patients- 17	Array-based comparative genomic hybridization (Array-CGH), qRT-PCR	Poor	Silveira *et al.*, 2013 (Silveira et al., 2013)
Thyroid	Upregulated	Cell lines- K1 and FTC-133	qRT-PCR, WB	n/a	Wang *et al.*, 2015 (Wang et al., 2015)
Gastric	Upregulated	Gastric cancer patients- 103	IHC	n/a	Feng *et al.*, 2015a (Feng et al., 2015a)
Spinal glioblastoma	Upregulated	Intramedullary glioblastoma patients- 5	IHC, qRT-PCR, WB	n/a	Wang *et al.*, 2016 (Wang et al., 2016)
Lung	Upregulated	Lung adenocarcinoma patients (LAP)- 7 for Whole genome sequencing (WGS); LAP- 114 for validation by qRT-PCR; LAP- 313 for disease prognosis assessments	WGS, qRT-PCR	Poor	Liu *et al.*, 2015 (Liu et al., 2015)
		RNA sequencing data sets of Lung adenocarcinoma (TCGA; cBioPortal)	Differential mRNA expression analysis		Sayeeram *et al.*, 2020 (Sayeeram et al., 2020)
		Non-small cell lung cancer (NSCLC)- 11	qRT-PCR		Pan *et al.*, 2016 (Pan et al., 2016)

Ovary	Upregulated	Ovarian cancer patients- 70	IHC	Poor	Bugide *et al.*, 2017 (Bugide et al., 2017)
		Epithelial ovarian cancer (EOC) patients- 145	IHC		Wang *et al.*, 2017a (Wang et al., 2017c)
		EOC patients- 248	IHC		Wang *et al.*, 2017b (Wang et al., 2017b)
		Ovarian cancer cell lines- CAOV3, SKOV3 and HO-8910	qRT-PCR, WB	n/a	Zhang *et al.*, 2016 (Zhang et al., 2016)
Head and Neck	Upregulated	Head-and-neck squamous cell carcinoma cell lines- OSC-20, SNU-1076, HSC-3, and Ca9 -22	qRT-PCR/WB	n/a	Chen *et al*., 2016b (Chen et al., 2016b)
Renal	Upregulated	Renal cell carcinoma patients- 119	IHC	Poor	Mai *et al.*, 2016 (Mai et al., 2016)
Cervical	Upregulated	Cervical cancer patients- 129	IHC	Poor	Meng *et al.,* 2017 (Meng et al., 2017)
		Cervical carcinoma patients- 167	IHC		Wang *et al.,* 2018 (Wang et al., 2018)
		Cervical cancer patients- 119	IHC		Cao *et al*., 2017 (Cao et al., 2017)
Endometrial	Upregulated	Endometrial cancer patients- 113	IHC	Poor	Cheng *et al.,* 2019 (Cheng et al., 2019)
Pancreatic	Upregulated	Pancreatic ductal adenocarcinoma patients- 30	IHC	n/a	Zhao *et al.,* 2020 (Zhao et al., 2020)
Glioma and Astrocytoma	Upregulated	Glial cancer patients (WHO grade I, II, III and IV)- 114	IHC	n/a	van Vuurden *et al.,* 2014 (van Vuurden et al., 2014)

1.8. (g) Role of HPIP in other cellular functions

HPIP expression is elevated in renal fibrosis, a chronic kidney disease, due to lower expression of its inhibitor miR152. In tubular epithelial cell line, HK-2, TGF-β1 induces EMT through HPIP, while miR-152 inhibits it. It implies that HPIP suppression or overexpression of miR-152 could serve as a useful strategy for the treatment of renal fibrosis (Fig. 7E) (Ning et al., 2018).

Osteoarthritis (OA) is a joint cartilage disorder (Chen et al., 2017). A recent report by Ji *et al.*, revealed that HPIP is implicated in osteoarthritis. HPIP is upregulated in OA and its ablation prevents OA development. Furthermore, they unravel an interesting novel mechanism that underlies HPIP causes OA development. They show that β-catenin mediated HPIP interaction with *LEF1* involves transcriptional activation of Wnt signaling pathway genes and thus OA pathogenesis (Fig. 7F) (Ji et al., 2019). "How is HPIP elevated in OA?" Addressing this question will be another input in understanding the physiology of OA and will be an interesting area to explore further. Our lab has reported that CCAAT/enhancer-binding protein-β (C/EBP-α) recruits on HPIPs' promoter, enhancing *HPIP* gene transcription (Manavathi et al., 2012). Also, C/EBPβ is one of the key transactivators in chondrocytes (Hirata et al., 2009). It is expressed in synovial tissues and chondrocytes of rheumatoid arthritis (Pope et al., 1999; Nishioka et al., 2000). It plays a vital role in cartilage degradation by targeting matrix metalloproteinase (MMPs) like MMP-13 in OA. Also, TNF-α and IL-1β activate C/EBP-α (Hirata et al., 2012). Interestingly, knockdown of HPIP diminishes *MMP13, TNFα* and *IL-1β* expression (Ji et al., 2019). Based on the literature, we can hypothesize that C/EBP-α may mediate HPIP elevation in OA (Fig. 7, A and F).

1.9. Analysis of HPIP's Isoform proteins and its possible regulation

1.9. (a) Methodology:

HPIP isoform proteins and their respective RNA sequences are downloaded from NCBI websites and analyzed the promoter sequence of respective isoform proteins to identify the peculiar transcription factors recruited on each transcript using Transcription Factor Information System (TFIS) (Narad et al., 2017). We consider 1.5 kb nucleotide sequence upstream from the starting codon for promotor study.

The expression of HPIP in different cancer types are derived from the different data sets: Dyrskjot bladder 3, Sun Brain, Scotto cervix 2, Skrzpczak colorectal 2, Kimchi Esophagus, Jones Renal, Haferlach leukemia, Warmbach liver, Beer lung, Talantov melanoma, Bonome ovarian, Logsdon pancreas, Wallace prostate, and Detwiller sarcoma which are available in Oncomine (Compedia Biosciences, http://www.oncomine.org/).

1.9. (b) Results and discussion

HPIP has three transcript variants (three isoform proteins). Protein isoform 1 has 1 aa – 731 aa, isoform 2 has 1 aa – 702 aa, and isoform 3 has 1 aa – 576 aa. Twenty-nine (29) and one hundred fifty-six (126) amino acids from N- terminal side of isoform 1 are absent in isoform 2 and isoform 3, respectively (Fig. 10A). All the three transcripts 1, 2, and 3 have distinct and separate starting codon with different 5' UTR but the same 3' UTR sequence. So, we analyzed the immediate upstream sequence of three transcript variants (1.5 kb each) to understand the peculiar transcription factors recruited on each transcript. Using the Transcription Factor Information System (TFIS) (Narad et al., 2017), we found multitudes arrays of motif sequences of different transcription factors (TFs) (Fig. 10B). All three promoters, TP1 (Transcript variant 1 promoter), TP2 (Transcript variant 2 promoter), and TP3 (Transcript variant 3 promoter) have a few

A.

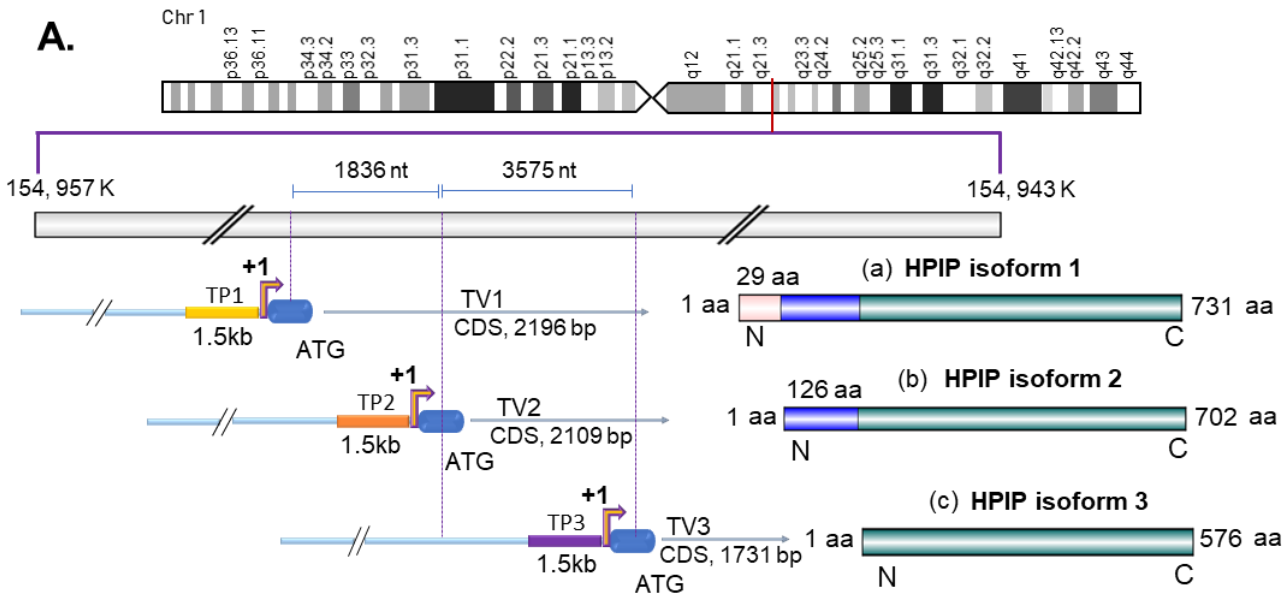

B.

	Transcription Factors (TFs)	Exclusive (specific) TFs	TFs common to TP1/TP2	TFs common to TP2/TP3	TFs common to TP1/TP2/TP3
Transcription variant 1 promoter (TP1)	ERR2, ERR3, ESR2, ETV4, KLF6, LEF1, MECP2, MYF6, NR1I2, NR1I3, NR5A2, PPARA, RARA, RARG, SNAI1, SNAI2, SOX10, SOX15, STF1, UBIP1, VDR	ERR2, ERR3, ETV4, KLF6, NR1I3, NR5A2, PRARA, RARA, RARG, SNAI1, STF1	MYF6, NR1I2, SNAI2, UBIP1, VDR, MYF6		MYF6, UBIP1, VDR
Transcription variant 2 promoter (TP2)	ESR2, GATA6, KLF4, KLF6, LEF1, MAFG, MECP2, MYF6, MZF1, NF2L1, PAX5, SOX10, SOX15, TGIF1, UBIP1, VDR, ZIC1, ZIC2	GATA6, KLF4, MAFG, MZF1, NF2L1, ZIC1, ZIC2		MYF6, PAX5, TGIF1, UBIP1, VDR	
Transcription variant 3 promoter (TP3)	TGIF1, UBIP1, VDR, CDX2, HIC2, HMGA1, MYF6, NKX25, NR1I2, PAX5, PRGR, SNAI2	CDX2, HIC2, HMGA1, NKX25, PRGR			

Fig. 10. Three isoforms of HPIP.

A. Location of *HPIP* gene on chromosome 1 at position q21.3. *HPIP* has three transcript variants (three isoform proteins). All the three transcripts 1, 2, and 3 have distinct and separate starting codons with different 5' UTR but the same 3' UTR sequence. The immediate upstream sequence of three transcript variants (1.5 kb each), transcription variant 1 promoter (TP1), transcription variant 2 promoter (TP2), transcription variant 3 promoter (TP3). The distance between the starting codon of TP1 and TP2, TP2 and TP3 are 1836 nt and 3575 nt respectively. Transcript variant 1/2/3 (TV1/2/3) has coding sequence 2196 bp, 2109 bp, and 1731 bp. Protein isoform 1 has 1 aa – 731 aa, isoform 2 has 1 aa – 702 aa, and isoform 3 has 1 aa – 576 aa. **B.** Identification, using Transcription Factor Information System (TFIS), and categorization of peculiar transcription factors (TFs) recruited onto each transcript's promoter, i.e., TFs exclusive only to each transcription variant promoter, TFs common to both TP1 and TP2, TFs common to both TP2 and TP3, TFs common to all three TP1, TP2, and TP3.

common TFs; TFs MYF6, UBIP1, and VDR (Fig. 10B). Certain TFs are exclusively recruiting to only one promoter (Fig. 10B). For example, Zinc finger protein SNAI1 which is specific to TP1, promotes epithelial to mesenchymal transition (EMT) in many cancers, and enhances tumorigenesis (Kalluri and Weinberg, 2009). The other transcription factor ZIC1, plays a vital role in early neural development, and it is specific to TP2 (Aruga et al., 1994). Similarly, CDX2, which binds only TP3 is crucial for developing intestinal epithelial cells (Saad et al., 2011). To deal with changes in the physiological or cellular environment, TFs drive a cascade of cellular network to maintain homeostasis (Edwards and Myers, 2007; Lambert et al., 2018). Since, three promoters TP1, TP2 and TP3 have different TFs binding sites, characterization and categorization of TFs which are constitutively expressed or conditionally expressed will be interesting to study. The question, "how do these TFs respond to various physiological conditions and regulate the expression of transcripts variants of HPIP?" needs investigation. The investigation and analysis of the expression profile of transcript variants of HPIP in the context of cellular function, and development of an orchestrated signaling network pertaining to each transcript variant will potentially unveil various mechanistic cellular activities.

1.10. Conclusions and future perspectives

It is evident that HPIP can be used as a biomarker for different cancer types and also as a potential biomarker for targeted cancer therapy (Table 1). It plays a vital role in hematopoietic stem cells (HSC) development and erythroid differentiation. HPIP is elevated in rapidly proliferating cells and regulates the cell cycle checkpoint regulation; concurrently, it may be used as a novel proliferation marker. Although comparatively fewer study reports are available on the role of HPIP in germ cell proliferation, endometrium decidualization, and embryogenesis, they have a strong and concrete foundation which can be explored. As HPIP plays a role in estrogen-mediated hormonal signaling and cell proliferation, it may regulate women's menstrual cycles and endometrium cell proliferation. Apparently, HPIP may be linked with conception and pregnancy related complications. Cumulative evidence shows that HPIP may be a promising candidate for neuronal disorder-related diseases, expressed in hippocampal neurons and a marker for astroglial progenitor cells. Further investigation of its role in neuronal development is warranted to be a promising field. Its elevated levels modulate OA pathogenesis and renal fibrosis. Besides, we revealed that HPIP has three transcript variants 1, 2, and 3, with distinct starting codon, different 5’ UTR but same 3’ UTR sequence. The transcript variants promotors' (TP1, TP2, and TP3) have separate sets of TFs, which are common to all (TP1/2/3) or in between two (TP1/2, TP1/3, TP2/3) or exclusively specific to only one promotor. The TFs respond to various physiological conditions and their regulation of different transcript variants of HPIP will enable in understanding the novel cellular and physiological functions of HPIP. Research on HPIP over two decades has uncovered a wide range of roles for HPIP from germ proliferation to cancer, with the advent of new findings every now and then, in disease state and normal cellular activity or physiology (Fig. 5). Now, we can build up a generalized overview of HPIP biology in the context of cancer, neuronal development, embryogenesis, estrogen-related signaling, osteoarthritis, initiation and development of the endometrium, renal fibrosis, and germ cell proliferation (Fig. 7). Nevertheless,

further extensive investigation studies are required to divulge its link with various cellular and physiological functions.

1.11. Rationale, hypothesis and objectives

HIF-1 interacts with the hypoxia response element (HRE, 5'-[R]CGTG- 3' where R is either A or G) harbor on its target genes and promotes their transcription (Bardos and Ashcroft, 2005) and, enhances the adaptive response of cancer cells to oxygen deprivation (Ratcliffe et al., 1998). Since HREs are located on the promoter of HPIP and SRP14, we assumed that a trimolecular cross-talk among HIF-1α, HPIP, and SRP14 may be linked with the potentiality of cancer cells to adapt in a hostile, low-oxygen environment, thereby modulating malignancy and aggressiveness phenotype of cancer cells. It is well documented that HPIP potentiates proliferative phenotype via modulating checkpoints of cell cycle under normoxia (Feng et al., 2015a; Feng et al., 2015b; Khumukcham et al., 2019; Xu et al., 2013b; Zhao et al., 2020). Therefore, we framed the following objectives to characterize the roles of HPIP in cancer cell progression under different microenvironment conditions i.e., hypoxia and normoxia using breast cancer (BC) as a model system.

Objectives:

1. To determine the role of HPIP in hypoxia induced cancer phenotype in BC cells
2. To investigate the role of HPIP in tumorigenesis under normoxia in BC cells, and
3. To evaluate the role of HPIP signalling in microenvironment dependent phenotypic plasticity in BC cells.

Herein, we report a hitherto unknown reciprocal positive feedback mechanism between HPIP and HIF-1α that coordinately controls oxygen dependent phenotypic plasticity in breast cancer cells. Upon hypoxia, HIF-1α induces HPIP expression that drives metastatic phenotype in breast cancer cells. Furthermore, for the first time we reported that involvement of SRP14 in cancer cell invasion.

HIF-1α transcriptionally activates SRP14 and its interaction with HPIP enhances MMP9 synthesis thereby promoting tumor cell migration and metastasis. Conversely, in normoxia, HPIP mediates PI3K/AKT dependent stabilization of HIF-1α, which confers tumor growth phenotype. This is further validated by mathematical formulation of HPIP-HIF-1α feedback loop dynamics. Additionally, we provide clinical evidence supporting the claim that elevated expression of both the proteins, HIF-1α and HPIP, are associated with worse patient survival.

Chapter 2

2.0. Materials and methods

2.1. Collection of patient's (Breast cancer) tumor samples

We collected fresh breast tumor tissues or tissue blocks, non-tumor tissues or tissue block with informed consent after acquiring ethics board approval from the MNJ Institute of Oncology & Regional Cancer Centre, Hyderabad, India. Subsequently, we also obtained IEC, UOH approval to process the samples at University of Hyderabad (UOH) UH/IEC/2016/190. Tissue samples were further processed for IHC and western blotting at the UOH, Telangana.

2.2. Cell culture

HEK293T (Human embryonic kidney cell line), human breast cancer cell lines including MCF7, MDA-MB-231, T47D, MDA-MB-468, ZR-75-1, SKBR-3 and BT-549 cell lines were obtained from NCCS, Pune, India. 4T1 cells are kind gifts by Prof. Ratna Vadlamudi, UT Health Science Center, San Antonio, USA. Cells were maintained in Dulbecco's Modified Eagle's Medium (DMEM, Gibco Life Technologies, USA) containing 10% heat-inactivated fetal bovine serum (FBS, Gibco Life Technologies), 100 U/ml penicillin, and 100 µg/ml streptomycin in a humidified incubator of 5% CO_2 at 37 °C. The other important reagents used in the study were mentioned in Table 1.

Table 1

Reagents used in the study	
Name	**Company/ Catalogue No.**
MG132	Sigma, M7449
Cycloheximide	MP Biomedicals, 100183
MTT	HIMEDIA, TC191
LY-294002	Sigma, L9908
Crystal violet	Sigma, C0775
Propidium Iodide (PI)	Sigma, P4170
Ethidium bromide (ETBR)	HIMEDIA, MB071
Fibronectin	Sigma, F0895
2-NBDG	Cayman chemical company, 11046
Matrigel® Matrix	Corning, 354230
Bouin's solution	Sigma, HT10132
Formaldehyde	Fisher scientific, BP531
Protein A/G PLUS-Agarose	Santa Cruz Biotechnology, sc-2003
Giemsa's stain	HIMEDIA, S011
Protamine sulfate	Sigma, P4020
Puromycin	Sigma, P8833
HIF-1α inhibitor	Santa Cruz Biotechnology, sc-205346
Trypan Blue solution	Sigma, T8154
Acridine Orange/ Propidium Iodide stain	Biosystems, F23001
CoCl2	Sigma, C8661

2.3. Hypoxia induction

For the hypoxic stress, cells were placed in the airtight modular incubator chamber (#5352414 Billups-Rothenberg, USA) with a gas mixture containing 94% nitrogen, 5% carbon dioxide and 1% oxygen for 4 min at the flow rate of 20 liters per min. The chamber was kept inside the incubator used for normoxia conditions (21% O_2, 5% CO_2) to maintain the same temperature. The cells were treated with HIF-1α inhibitor, 30 μM, (SCBT #sc-205346) to inhibit HIF-1α expression when necessary.

Table 2

Plasmid		
Name	**Purposed**	**Source or reference**
shCtrl (pGIPZ)	Siliencing study (Viral transduction)	khumukcham et al., 2019
shHPIP #1 or #2 (pGIPZ)	Siliencing study (Viral transduction)	khumukcham et al., 2019
shSRP14 (pGIPZ)	Siliencing study (Viral transduction)	This study
GFP (pEGFP-C 1)	Overexpression study	Bugedi et al., 2015
GFP SRP 14 (pEGFP-C 1)	Overexpression study	In this study
GFP SRP 14-A5 (pGFH14A5)	Overexpression study	Katharina Strub's lab, Addgene, USA #39543
GFP SRP 14-ΔK (pGFH14A6-12)	Overexpression study	Katharina Strub's lab, Addgene, USA #39543
c-Myc-GSK-3β wt	Overexpression study	Prof. Mien-Chie Hung's lab
c-Myc-GSK-3β KD	Overexpression study	Prof. Mien-Chie Hung's lab
pMNDUS	Overexpression study	Manavathi et al., 2012
pMNDUS-HPIP	Overexpression study	Manavathi et al., 2012
T7 (pCDNA 3.1A)	Overexpression study	Manavathi et al., 2012
pCDNA-HPIP (T7-HPIP)	Overexpression study	Manavathi et al., 2012
pΔR	Lentivirus generation (Viral transduction)	Manavathi et al., 2012
pVSVG	Lentivirus generation (Viral transduction)	Manavathi et al., 2012
pREV	Lentivirus generation (Viral transduction)	Manavathi et al., 2012
pGL3- 2.7 HPIP-luc	Lucuferase assay (promotor binding study)	In this study
pGL3- 2.1 HPIP-luc	Lucuferase assay (promotor binding study)	In this study
pGL3- 1.8 HPIP-luc	Lucuferase assay (promotor binding study)	In this study
pGL3- 0.9 HPIP-luc	Lucuferase assay (promotor binding study)	In this study
pGL3-luc	Lucuferase assay (promotor binding study)	In this study
pLX313-Renilla-Luc	Lucuferase assay (promotor binding study)	Addgene
shRNA sequence		
Name	Sequence	Company/Clone ID
shHPIP#1	ATGTTCTTAGCAGAGAGGC	GE Healthcare Dharmacon, V2LHS_65985
shHPIP#2	AATTCTTTCCCATCTGTCT	GE Healthcare Dharmacon, V3LHS_390144
shSRP14	TCTTCAAGGTGATATAGAC	GE Healthcare Dharmacon, V2LHS_153485

2.4. Plasmid cloning

Genomic DNA (MCF7 cells) was isolated and different deletion constructs of HPIP (pGL3- 2.7 HPIP-luc, pGL3- 2.1 HPIP-luc, pGL3- 0.9 HPIP-luc, pGL3- 0.4 HPIP-luc) promoter were

amplified using Phusion® HF DNA polymerase (BioLabs, #M0530) by PCR using specific primer pairs and digested with HindIII and XhoI enzymes and then ligated to pGL3 basic vector (Promega, USA). SRP14 gene was amplified using the specific primers and digest with XhoI and BamHI enzymes and ligated to pGEFP-C1 vector. The plasmid constructs pGFH14A6-12 or GFP-SRP14-ΔK5 (del 101-113) and pGFH14A5 or GFP-SRP14-A5 (K→A, 96-100) are a gift from Dr. Katharina Strub, Department of Cell Biology, University of Geneva, Switzerland. (Addgene plasmid #39542; Addgene Plasmid #39543). The wild type GSK3β (c-Myc-GSK-3β wt) and kinase-dead mutant of GSK3β (c-Myc-GSK-3β KD) are a gift from Prof. Mien-Chie Hung, Department of Molecular and Cellular Oncology, The University of Texas MD Anderson Cancer Center in Houston, Texas. The details of the primers and source of the plasmids used in the study are listed in Tables, 2 and 3.

2.5. Lentivirus production and infection

Lentivirus was prepared in HEK293T cells (packaging cells) by transfecting lentiviral packaging plasmids along with either pGIPz, pGIPz-shHPIP or pGIPz-shSRP14 plasmids (Table 2) as described previously (Manavathi et al., 2006; Khumukcham et al., 2019). Virus particles were harvested at every 24 h, for three days by changing with fresh DMEM medium. 4T1 or MDA-MB-231 cells were infected with lentivirus using Polybrene (0.8 µg/ml) or Protamine sulfate salt (5 µg/ml). The viral transduced stable clones (shCtrl or shHPIP or shSRP14) were selected with puromycin (Sigma Aldrich, USA). The efficiency of the RNA interference was verified by WB.

2.6. Plasmids and siRNA transfection

Cells were transfected with siRNA or a specific plasmid construct (overexpression study) using Lipofectamine 2000 (Invitrogen, USA) in optiMEM serum-free media in accordance to manufacturer's protocol. After 6 h of transfection, cells were fed with serum containing media for 24 h and cells were cultured in hypoxia at different time points. All the plasmids or shRNA used

in the study are mention in Table 2. Small interference RNA (siRNA) targeting HPIP (Cat No. # M-015428-01), HIF-1α (Cat No. # M-004018-05) and its negative control (mock) used in knockdown experiments were obtained from Dharmacon™ - Horizon Discovery, USA.

Table 3

Gene or promoter	Cloning Primer pair	Restri. Enzyme	Vector name	Cloning name
GFP SRP 14	FP: 5' GATCCTCGAGGTATGGTGTTGTTGGAGAGCGAGC 3'	XhoI	pEGFP-C1	GFP-SRP 14
	RP: 5'GTAGGATCCTTACTGTGCTGCTGTTGCTGCTG 3'	BamHI		
HPIP promoter 2.7 kb	FP: 5' CGAGCTCGAGATTTCTGGGCTGGGGGAGGAAGGCC 3'	XhoI	pGL3	pGL3-2.7 HPIP-luc
	RP: 5' CGTAAGCTTGTCCTGATCCCTCTAACCCAAAGC 3'	HindIII		
HPIP promoter 2.1 kb	FP: 5' CGACCTCGAGAGACTTCCTAGCTTTATGCTGAGTGGGAGAGC 3'	XhoI	pGL3	pGL3-2.1 HPIP-luc
	RP: 5' CGTAAGCTTCAGAGTCTGGGCAGGAGGCCATAG 3'	HindIII		
HPIP promoter 1.8 kb	FP: 5' CGACCTCGAGGAGCAGATTAACCGGGTGCAGGACC 3'	XhoI	pGL3	pGL3-1.8 HPIP-luc
	RP: 5' CGTAAGCTTCAGAGTCTGGGCAGGAGGCCATAG 3'	HindIII		
HPIP promoter 0.9 kb	FP: 5' CGACCTCGAGGAGCAGATTAACCGGGTGCAGGACC 3'	XhoI	pGL3	pGL3-0.9 HPIP-luc
	RP: 5' CGTAAGCTTCAGAGTCTGGGCAGGAGGCCATAG 3'	HindIII		

2.7. Immunoblotting

Total cell extracts were prepared in NP40 lysis buffer (2 mM EDTA , 20 mM Tris pH 8.0, 137 mM NaCl, 10% glycerol, 1% Nonidet P-40, 1X protease inhibitor cocktail) supplemented with 1 mM PMSF, 2 mM NaF, 2 mM Na_3VO_4. To lyse the cancer tissues, samples were snap-frozen in liquid nitrogen and crushed with pestle and mortar and dissolved in lysis buffer. Protein concentration was determined using RC reagent kit method (Bio-Rad, USA) and 100-120 µg of protein lysates were loaded, resolved by SDS-PAGE and transferred to nitrocellulose membrane (Pall Corporation, USA). Western blotting (WB) was performed according to the standard protocol using protein-specific primary antibodies mentioned in Table 4. After incubation with HRP-conjugated secondary antibodies (GE Healthcare, USA), blots were developed using ECL detection reagents (GE Healthcare, USA) in a Chemidoc imaging system (BIO-RAD, USA) or Fusion FX, Vilber Lourmat. The band intensities were measured using Fiji-ImageJ and normalized to the band intensity of β-actin and plotted the graph.

2.8. Co-Immunoprecipitation (CO-IP) analysis

CO-IP was performed as described previously (Khumukcham et al., 2019). Briefly, cell extracts were incubated with primary antibody overnight at 4 ^{o}C and the protein-antibody complexes were pulled down by adding and incubating with agarose A/G beads for an additional 1 h. The beads were washed and subjected to SDS-PAGE, then transferred to nitrocellulose membrane and immunoblotted with antibodies mentioned in Table 4.

2.9. Immunofluorescence assay

MDA-MB-231 cells were cultured and incubated under hypoxia on coverslips in six-well plates (1×10^4 cells/well). The cells were fixed (2% paraformaldehyde), permeabilized using pre-chilled acetone and methanol (1:3) and cells were blocked with 3% BSA. The cells were incubated with antibodies overnight at 4 °C, washed and incubated 1 h with fluorescent-labeled secondary antibodies at RT. The coverslips were mounted on slides with DAPI (Thermo-scientific, USA) and observed using confocal microscope (Model -NLO710, Carl Zeiss, Germany). To quantify the colocalization of HPIP with SRP14, pixel intensity correlation measurement was performed using Fiji software (Image J/Fiji-Coloc2 plugin).

Table 4

Antibody	Company	Catalogue no.	WB dilution	IF dilution	IHC dilution	IP/ChIP dilution
β-Tubulin	CST	2146S	1 µl : 4000 µl			
β- Actin	CST	4967S	1 µl : 1000 µl			
GAPDH	CST	2118S	1 µl : 1000 µl			
GFP	Sigma Aldrich	G1544	0.5 µl : 1000 µl			
T7 tag	Novagen	69522	1 µl : 5000 µl			
SRP14	Abcam	ab138827	2 µl : 1000 µl	1 µl : 100 µl	2 µl : 100 µl	
Flag	CST	8146	1 µl : 1000 µl			4 µl : 1 mg of protein
HIF1α	NOVUS	NB100-449	1 µl : 2000 µl		2 µl : 100 µl	5 µl : 1 mg of protein, 1 µl : 50 µl (CHIP)
Acetyl-Histone H3(K9)	CST	9649	1 µl : 1000 µl			1 µl : 50 µl (CHIP)
Dimethyl-Histone H3(K9)	CST	4658	1 µl : 1000 µl			1 µl : 50 µl (CHIP)
P300	CST	54062	1 µl : 1000 µl			1 µl : 50 µl (CHIP)
C-PARP	CST	5625T	1 µl : 1000 µl			
C-Caspase 9	CST	7237T	1 µl : 1000 µl			
C-Caspase 3	CST	9661T	1 µl : 1000 µl			
vimentin	SCBT	SC-6260	2 µl : 1000 µl			
P53	SCBT	sc-393031	2 µl : 1000 µl			
Snail	SCBT	SC-10432	2 µl : 1000 µl			
MMP2	CST	87809T	1 µl : 1000 µl			
MMP9	CST	13667T	1 µl : 1000 µl			4 µl : 1 mg of protein
TIMP3	CST	5673T	1 µl : 1000 µl			
TIMP2	CST	5738T	1 µl : 1000 µl			
GLUT1	SCBT	sc-377228	2 µl : 1000 µl			
VEGF	SCBT	sc152	2 µl : 1000 µl			
C-MYC	CST	18583S	1 µl : 1000 µl			
PAKT T308	CST	13038T	1 µl : 1000 µl			
PAKT S473	CST	4060T	1 µl : 1000 µl			
AKT(pan)	CST	C67E7	1 µl : 1000 µl			
E-cadherin	SCBT	SC-7870	2 µl : 1000 µl			
L9	SCBT	SC-100828	2 µl : 1000 µl			
PE anti-human CD44	Biolegend	338807	2 µl : 100 µl			
PerCP/Cy5.5 anti-human CD24	Biolegend	311115	2 µl : 100 µl			
HPIP/PBXIP1	Sigma Aldrich	HPA006949	NA	NA	NA	3 µl : 1 mg of protein
HPIP/PBXIP1	Sigma Aldrich	SAB1407783	1 µl : 1000 µl	1 µl : 100 µl		
HPIP/PBXIP1	Bethyl	A301-628A	1 µl : 2000 µl		2 µl : 100 µl	5 µl : 1 mg of protein
Ubiquitin	CST	3933	1 µl : 1000 µl			
Alexa Fluor® 546 Goat anti mouse	Life technologies	A11003	1 µl : 100 µl	1 µl : 100 µl		
Alexa Fluor® 546 Goat anti Rabbit	Life technologies	A11008	1 µl : 100 µl	1 µl : 100 µl		

Santa Cruz Biotechnology (SCBT), Cell signaling Technology (CST)

2.10. Quantitative reverse transcriptase polymerase chain reaction (qRT-PCR)

Total RNA was extracted from cells by TRIzol® Reagent (Life Technologies, USA) following the manufacturer's instruction. The cDNA was synthesized from 1 µg of total RNA using a reverse reaction kit (TaKaRa cDNA synthesis kit, Da-Liang, China) and subjected to qRT-PCR using SYBR Green PCR master mix (Bio-Rad, USA) on Light Cycler@ Roche system, USA. Primer sequences are listed in Table 5. The relative gene expression was calculated after normalization to β-actin as an internal control using 2− ΔΔCT (difference between cycle thresholds) method. Three biological replicates were performed.

Table 5

Gene name	PCR primer
HPIP/PBXIP1	FP: 5' ATGGGTCTTCTGCTGGACAA 3'
	RP: 5' CAGGCTCTGAAGCTCTTCCTT 3'
β - Actin	FP: 5' AGCCATGTACGTAGCCATCC 3'
	RP: 5' CTCTCAGCTGTGGTGGTGAA 3'
MCT4	FP: 5' TGCTGCTGGGCAACTTCTTCTG 3'
	RP: 5' TCAGACACTTGTTTCCGGGGTG 3'
GLUT1	FP: 5' GCA GCACCACAGCGATGAGG 3'
	RP: 5' CGGGCCAAGAGTGTGCTAAAG 3'
LDHA	FP: 5' TCTTGACCTACGTGGCTTGGAAG 3'
	FP: 5' CCATACAGGCACACTGGAATCTC 3'
HIF1α	FP: 5' GTACCCTAACTAGCCGAGGAAGAAC 3'
	RP: 5' CAGGCTGTGTCGACTGAGGAAAG 3'
PFKP	FP: 5' CGGAGTTCCTGGAGCACCTCTC 3'
	RP: 5' AAGTACACCTTGGCCCCCACGTA 3'

2.11. MTT (3-(4,5-Dimethylthiazol-2-yl)-2,5-Diphenyltetrazolium Bromide) assay

MTT assay was performed in 96-well plates in 4T1 or MDA-MB-231 cells following manufacturer's protocol. Cells were treated with MTT (500 µg/ml) for 2 h; media were discarded and dissolved the cells in DMSO. The optical density (OD) was measured at 570 nm and reference wavelength at 650 nm in scanning multi-well spectrophotometer (iMARKTM microplate reader, BIO-RAD, USA) and the percentage of cell proliferation was quantified.

2.12. Acridine Orange (AO) and Propidium Iodide (PI) Staining

MDA-MB-231 or 4T1 cells (shCtrl or shHPIP) were grown under hypoxia or normoxia for 24 h. The cells were trypsinized, washed with PBS and double-stained with PI (10 µg/ml) (Sigma Aldrich, USA) and AO (10 µg/ml) (Sigma Aldrich, USA). Freshly stained cells were observed and analyzed on LUNA-FL™ Dual Fluorescence Cell Counter and calculated the percentage of dead cells from three replicate experiments.

2.13. Trypan Blue assay

Trypan Blue assay was performed using previously reported protocols (Strober, 2015). Briefly, cells were washed, suspended in PBS and mixed with 0.4% trypan blue in 1:1 ratio. After incubation for 3 min, cell viability was monitored using microscope.

2.14. Chromatin immunoprecipitation (ChIP) assay

ChIP assay was performed as described previously (Gajulapalli et al., 2016). Briefly, after exposing the cells to 1% or 21% of oxygen, they were cross-linked, quenched and sonicated. The protein-DNA complexes were immunoprecipitated with respective antibodies and pulled down with protein A/G beads at 4°C for 1 h. Beads were washed, eluted, reversed cross-linked and DNA was extracted by using phenol: chloroform: isoamyl alcohol method. DNA was analyzed by qRT-PCR using the primer mention in Table 6. Using $2^{-\Delta Ct}$ method, the occupancy to DNA fragments was calculated as a percent of input.

Table 6

Name	ChIP primer
HRE 1 (HPIP)	FP: 5' GCCATGAAGGAAGGGACCAGTTGG 3'
	RP: 5' GTCCTGATCCCTCTAACCCAAAGCC 3'
HRE 2 (HPIP)	FP: 5' ATGATAACAAGGGCGGGGGTGG 3'
	RP: 5' GTGCCCTAAGTAACCTCCTGTGG 3'
HRE 3 (HPIP)	FP: 5' GTGCCGACGCTAACACAACAGG 3'
	RP: 5' CCCCCTTCTTTTCATTCAGGCAGG 3'
NS	FP: 5' GAGTGATTCCCTCCCCTATCCC 3'
	RP: 5' CCTCATCACTCTCAGTCTTCATCC 3'
HRE 1 (SRP14)	FP: 5' GCCTAGGTTGCTTCTGGTAACAATG 3'
	RP: 5' GACCGTGATAGCAGATGAGGTG 3'
HRE 2 (SRP14)	FP: 5' AGAGACAGCGTTTCACCGTGTTAG 3'
	RP: 5' ACTCTCCCTAAACGCTGACCTG 3'

2.15. Scratch wound assay

Scratch wound healing assay was performed as described previously (Bugide et al., 2015). Briefly, scraped wounds were created using 10 µl pipette tip in a straight line on confluent monolayer MDA-MB-231 or 4T1 cells (shCtrl or shHPIP). The plates were washed with PBS and the scratch closure was monitored by capturing at 0 h and 24 h under 10X magnification using a bright field microscope (Model IX81, Olympus Singapore). Wound closure was measured in pixel and the graph was plotted as a percentage of wound closure.

2.16. Density gradient ultracentrifugation

MDA-MB-231 cells were cultured to hypoxia for 24 h and lysed the cells in a buffer containing 150 mM KOAc; 5 mM MgOAc; 20 mM Tris-HCL pH 7.5; 0.01% of Triton 100x; peptide inhibitor cocktail (Sigma-Aldrich) and RNAse inhibitor (Sigma-Aldrich) and centrifuged for 7 min in 3,000 rpm followed by 10,000 xg for 5 min. The cell extract (2 mg of protein) was aliquoted and loaded on 10%-40% of sucrose gradients and centrifuged for 254 min at 38,000 rpm. Twenty fractions were collected from the top of the tube to bottom and each fraction was analyzed by WB.

2.17. Yeast Two-Hybrid assay

HPIP gene was cloned into pGBK-7 vector to express as Gal4-DBD and used as bait, while human mammary gland library prepared in pACT2 vector from Takara Bio, USA was used as prey in Y2H genetic screen. As per the manufacturer's instructions we mixed 0.5 ml of Y2HGOLD (PGBK7-HPIP) culture with equal volume of yeast Y187 culture transformed with MATE AND PLATE human mammary cDNA library. After mating, the culture was spread on SD/-Trp (SD-single dropout), SD/-Leu, and SD/-LT/X-aGal/Aerobasidin plates at various dilutions such as 1/10, 1/100, 1/1000 and 1/10000 and incubated at 30^{o}C for 3-5 days. We then calculated the number of screened colonies by counting the colonies from DDO Plates (double dropout). Then we patched out all the blue colonies that grew on DDO/X/A plate onto high stringency QDO/X/A plates (AHLT-Adenine, histidine, Leucine and Tryptophan). All the positive interactions (colonies) were further analyzed by one-one interaction assay. The plasmids were further analyzed by DNA sequencing.

2.18. Luciferase reporter gene assay

Luciferase reporter gene assay was performed as described previously (Gajulapalli et al., 2016). Briefly, cells were transfected with either pGL3-*HPIP*-promoter-Luc or various pGL3-*HPIP*-promoter-Luc (deleted constructs) and pLX313-Renilla-Luc plasmids (internal control) using Lipofectamine 2000 (Invitrogen, USA) reagent. Twenty-four-hour post-transfection, cells were incubated under normoxia or hypoxia for 24 h and luciferase activity was determined using dual luciferase reporter assay kit (Promega, Madison, WI, USA) on a luminometer (Modulus^{TM} single tube multimode reader, Turner BioSystems, Sunnyvale, USA). The Firefly and Renilla luciferase activities were measured and Renilla luc activity was used to normalize Firefly luciferase activity for each sample.

2.19. Flow Cytometry

Apoptosis assay: APC Annexin V apoptosis detection kit with 7-AAD (Biolegend, #640930) was used as per the recommended manufacturer's protocol. Briefly, cells were washed with Biolegend cell staining buffer, resuspended in Annexin V Binding buffer ($1x10^6$ cells/ml) and incubated with APC Annexin V and 7-AAD for 15 min at RT and analyzed by flow cytometer (FACS-Aria; Becton Dickinson).

CD44/CD22 expression: MDA-MB-231 cells were cultured under hypoxia for 24 h. Cells were harvested, fixed (1% paraformaldehyde), blocked (3% BSA) and incubated with PerCP/Cy5.5 anti-human CD24 (Biolegend, San Diego, California, USA) and PE anti-human CD44 (Biolegend, San Diego, California, USA) for 1 h. Samples were acquired on a flow cytometer (FACS-Aria; Becton Dickinson) and data were analyzed using FlowJo software (FlowJo LLC, Ashland, OR, USA).

2.20. Pulse chase experiment

Stably generated (shCtrl or shHPIP) MDA-MB-231 cells ($6 x10^5$) were grown on 35 mm dishes. Next day, cells were culture for 2 h in methionine-free DMEM medium (Sigma Aldrich, USA). The radioactive Methionine (^{35}S-Methionine, 10 µCi/ml) was added and incubated for 24 h at 37 ºC under hypoxia. The cells were lysed in NP40 lysis buffer (137 mM NaCl, 20 mM Tris p^H 8.0, 2 mM EDTA, 1% Nonidet P-40, 10% glycerol, 1X protease inhibitor cocktail) and performed pull-down assay with MMP9 antibody using 300 µg of protein lysate for 1 h. The protein AG beads (30 µl) were added and further incubated for 1 h. After four washes with NP40 lysis buffer for 10 minutes each, beads were loaded with 2xSDS loading dye. Samples were further subjected to WB and blot was exposed to autoradiography film (GE Healthcare), and scanned (Typhon scanner, GE Healthcare).

2.21. *In-vivo tumor* growth and experimental metastasis

The CrTac: NCr-Foxn1nu (NCRNU-F) mice were purchased from Vivo BioTech Ltd., Hyderabad. The animal experiments described in this study were approved by the Institutional Animal Ethics Committee (IAEC), University of Hyderabad (approval no. IAEC/UH/151/2017/12/BM). For *in vivo* metastasis assay, 4T1 cells (shCtrl or shHPIP) were primed under hypoxia for 24 h or grown under normoxia. Five female mice (4-5 week) for each group were injected with 4T1 cells (1×10^6) via tail vein in 100 µl of sterile HBSS buffer. After 20 days of injection, animals were sacrificed, dissected and harvested for lungs. Lungs were weighed, incubated with Bouin's solution and counted the metastatic nodules for each lung. Metastasis nodules were also evaluated by *ex vivo* imaging as cells are GFP positive. The number of metastatic nodules, intensity (fluorescence unit) of the lungs was quantified and plotted.

For *in vivo* tumor growth or tumorigenesis, female mice (4-5 week) were injected subcutaneously to the lower left and right quadrant with 4T1 cells 2×10^6 (shCtrl or shHPIP or siHIF-1α or siHIF-1α plus HPIP) with 100 µL of sterile HBSS buffer with Matrigel (2:1). Tumor sizes (diameter) were measured with a digital caliper. After 15 days of injection, animals were sacrificed, dissected and weighed the tumor tissues. The tumor volume (mm^3) was calculated by the formula: $(Wide)^2$ x Length/2. Tissues and lungs nodules were prepared for histopathology study (paraffin preparation, sectioning, hematoxylin and eosin staining) and analyzed through subsequent microscopic evaluation. All animals were maintained and executed experiments following IAEC guidelines at the University of Hyderabad, India.

2.22. 3D migration assay

As described previously, 3D migration assays were performed (Vinci et al., 2013; Nandi and Brown, 2017). Briefly, 20 µl of MDA-MB-231 or 4T1 cells (shCtrl or shHPIP) consisting of $1x10^3$ cells were grown as hanging drop culture in Petri dishes by inverting the lid for 48 h with proper

humidification inside the incubator. In pre-chilled 96 well-plates, 200 µl of Matrigel was poured and above that, hanging-drop spheroids were carefully embedded. The cellular dissemination was monitor by capturing images at 0 h and 24 h (hypoxia or normoxia) using a bright field microscope (Model IX81, Olympus Singapore). Using Fiji/ImageJ, the out-growth area was determined in each well by subtracting the area at 0 h from the area of 24 h.

2.23. Soft agar assay

A layer of 0.5% base agarose (0.5% agarose in DMEM with 10% FBS) in 35 mm plates were prepared. After solidification, cells (10^4) were mixed with 1 ml of 0.3% agarose (DMEM with 10% FBS) and immediately poured above the bottom layer. The cells were cultured with DMEM (10% FBS along with 100 µM of $CoCl_2$) and incubated in 5% CO_2 incubator at 37 ºC for 2 weeks. The cell colonies were stained with crystal violet (0.005%) and images were acquired and counted with a bright field microscope (Model IX81, Olympus Singapore). Triplicate culture plates were used for each experiment and plotted graph as the percentage of colony number.

2.24. Boyden Chamber assay (cell invasion assay)

The cell invasion assay was performed, as per the manufacturer's protocol, using Corning BioCoat Matrigel invasion chambers (8.0 µm pore size). MDA-MB-231 or 4T1 cells were serum starved for 12 h prior to preceding for the experiment. The cells ($2.5x10^5$) were added to the insert along with serum free media (DMEM) and serum containing media (10% DMEM) with 5 µg/ml of fibronectin was added in the lower compartment of the chamber. After 24 h of incubation under hypoxia or normoxia, cells were fixed with formaldehyde and stained with Giemsa's stain (HIMEDIA, India). The inner side of the insert was swabbed to remove un-invaded cells. The images were captured with a bright field microscope (Model IX81, Olympus Singapore) and the total number of invaded cells was counted and plotted graph as the percentage of invaded cells.

2.25. Lactate secretion assay

The extracellular lactate was measured by spectrophotometric based determination of lactic acid as described previously (L. N. Borshchevskaya, 2016). Briefly, cells were grown in 24 well-plates under hypoxia for 24 h and the culture media were collected by centrifugation to remove the cell debris. The media (50 µl) and 2 ml of 0.2% solution of ferric chloride were mixed and stirred. The absorbance of the developed colored was measured at 390 nm and the solution containing 2 ml of 0.2% solution of ferric chloride was used as a reference. Based on the standard curve of the known lactic acid concentration, the culture media's lactic acid concentration was quantified as micro molar per milligram of protein.

2.26. Immunohistochemistry (IHC)

IHC was performed with the prescribed protocol using Mouse/Rabbit PolyDetector DAB HRP Brown Detection System (catalog# BSB0203). Briefly, 4 µm thick tissues (TNBC) or experimental mouse-derived slides were deparaffinized using xylene and rehydrated in a series of decreasing concentration of ethanol solutions. Epitope retrieval was carried out using citrate buffer in a microwave and slides were blocked with PolyDetector Peroxidase Blocker for 5 min following an additional 1 h blocking with 5% BSA. The slides were incubated with primary antibodies overnight at 4ºC (Table 4), washed and incubated with PolyDetector HRP labels for 45 min. The slides were incubated with DAB substrate-chromogen solution and counterstained with hematoxylin, then dehydrated and mounted (PX Mountant, SRL, #042848). These images were digitally captured using microscope (Model IX81, Olympus Singapore). The IHC profiler plugin for ImageJ (software) was used to digitally score IHC slides as described previously. The scores are given 1 (negative staining), 2 (low positive), 3 (positive) or 4 (high positive) (Varghese et al., 2014) and the data was plotted using violin plot.

2.27. Cycloheximide chasing experiment

Chasing assay was performed as described previously (Khumukcham et al., 2019). Stably expressed shCtrl or shHPIP#1 or shHPIP#2 MDA-MB-231 cells were treated with cycloheximide (25 µg/ml) for the indicated time prior to cell lysis and the extracts were subjected to WB. The band intensities were measured using Fiji-ImageJ and normalized to the band intensity of Actin and plotted graph as percentage of relative protein.

2.28. Ubiquitination assay

Thirty-six hours of post-transfected MDA-MB-231 cells with T7 Vector or T7-HPIP were treated with MG132 (20 µM) for 30 min, harvested and the cell extracts were immunoprecipitated with HIF-1α-specific antibody. Samples were then resolved on SDS-PAGE and immunoblotted using protein-specific antibodies.

2.29. *In-vitro* glucose uptake (Fluorescence microscopic analysis) assay

MDA-MB-231 cells (siCtrl or siHPIP or siHIF-1α or siHIF-1 α plus HPIP) were grown for 24 h in 48 well-plate. Cells were glucose starved for 2 h and then incubated with 2-NBDG (2-(N-(7-Nitrobenz-2-oxa-1,3-diazol-4-yl) Amino)-2-Deoxyglucose) (200 µM) for an additional 30 min at 37 ºC. Plates were rinsed thoroughly with PBS and the intensity of the cells was examined with a fluorescence microscope (Model IX81, Olympus Singapore). From each plate, 5 to 10 random images were taken with the same exposer time and quantified the mean intensity of each field and plotted graph.

2.30. Breast cancer patient data analysis

MMP9 protein sequence was analyzed for signal peptide using SignalP4.1 Server and SecretomeP 2.0a Server (Bendtsen et al., 2004; Petersen et al., 2011). To study the patient's survival for both high and low expression of either *HPIP/HIF-1α* or *SRP14/HIF-1α* was performed using cBioPortal for cancer genomics (https://www.cbioportal.org/) (Gao et al., 2013). In cBioPortal, high or low

mRNA expression of a gene is determined by the number of standard deviations (SD) from the mean. The Kaplan Meier survival curve for co-gene expression was plotted using Breast Invasive Carcinoma (TGCA Nature 2012) as (high expression, *HPIP*: E>0.6, *HIF-1α*: E>0.6) verse (low expression, *HPIP*: E<0.6, *HIF-1α*: E<0.6) and (high expression, *SRP14*: E>0.5, *HIF-1α*: E>0.5) verse (low expression, *SRP14*: E<0.5, *HIF-1α*: E<0.5). The comparative expression of HPIP, SRP14 and HIF-1α in invasive ductal breast carcinoma (IDBC) with normal tissue samples (N) were analyzed using Curtis data sets from Oncomine (https://www.oncomine.org/resource/login.html). The co-expression study of CD44/CD24 with HPIP expression was performed using Bos Breast and Ivshina Breast data sets from Oncomine. High, medium and low expression of HPIP is defined based on the mean values. For Bos Breast data set, we classified as high (>2.218), medium (2.599 -1.79) and low (<1.79), while the mean expression value is 2.218 on the other hand for Ivshina Breast data set, high (>0.01), medium (0.09 - -0.2489) and low (< -0.25), while the mean expression value is -0.23167.

2.31. Mathematical formulation of HPIP-HIF-1α dynamics

Our results show that that HIF-1α transcriptionally activates HPIP (Fig. 11) while HPIP increases the stability of HIF-1α under normoxic conditions, increasing its half-life by about 4 times (Fig. 22, C-D). Thus, HPIP and HIF-1α form an indirect positive feedback loop. The dynamics of this loop can be described by the following equations:

$$\frac{d[HPIP]}{dt} = g_{HPIP} H^{S+}\left(HIF1\alpha, \lambda_{HIF1\alpha,HPIP}, \mathrm{n}_{HIF1\alpha,HPIP}, HIF1\alpha_0\right) - k_{HPIP}[HPIP]$$

$$\frac{d[HIF1\alpha]}{dt} = g_{HIF1\alpha} - k_{HIF1\alpha} H^{S-}\left(HPIP, \lambda_{HPIP,HIF1\alpha}, \mathrm{n}_{HPIP,HIF1\alpha}, HPIP_0\right)[HIF1\alpha]$$

where $[HPIP]$ and $[HIF1\alpha]$ denote the levels of HPIP and HIF-1α respectively; g_{HPIP}, $g_{HIF1\alpha}, k_{HPIP}$ and $k_{HIF1\alpha}$ denote the production and degradation rates of HPIP and HIF-1α

respectively. $H^{S+}\left(HIF1\alpha, \lambda_{HIF1\alpha,HPIP}, \mathrm{n}_{HIF1\alpha,HPIP}\right)$ denotes transcriptional activation of HPIP by HIF-1α, and $H^{S-}\left(HPIP, \lambda_{HPIP,HIF1\alpha}, \mathrm{n}_{HPIP,HIF1\alpha}\right)$ denotes the decreased degradation rate (i.e., larger half-life) of HIF-1α due to HPIP. $H^{S+}\left(HIF1\alpha, \lambda_{HIF1\alpha,HPIP}, \mathrm{n}_{HIF1\alpha,HPIP}\right)$ and $H^{S-}\left(HPIP, \lambda_{HPIP,HIF1\alpha}, \mathrm{n}_{HPIP,HIF1\alpha}\right)$ are shifted Hill functions; shifted Hill functions denoting the effect of X on Y are defined as (a):

$$H^{S}\left(X, \lambda_{X,Y}, n_{X,Y}, X_0\right) = H^{-}\left(X, n_{X,Y}, X_0\right) + \lambda_{X,Y}\left(1 - H^{-}\left(X, n_{X,Y}, X_0\right)\right)$$

where $H^{-}\left(X, n_{X,Y}\right)$ is the inhibitory Hill function, given as (b):

$$H^{-}\left(X, n_{X,Y}, X_0\right) = \frac{X_0^{n_{X,Y}}}{X^{n_{X,Y}} + X_0^{n_{X,Y}}} \quad \text{(b)}$$

where $\lambda_{X,Y}$ denotes the fold-change in production/degradation rate of Y due to X. For $\lambda_{X,Y} > 1$, the shifted Hill functions are represented as H^{S+}, and for $\lambda_{X,Y} < 1$, these functions are represented as H^{S-}. $n_{X,Y}$, the Hill coefficient represents the non-linearity of the interaction between X and Y. X_0, the threshold, is the concentration of X at which the value of inhibitory Hill function is 0.5.

The degradation rates for both HPIP and HIF-1α have been estimated based on first-order kinetics. Our experiments denoted a half-life of 7.5 mins for HIF-1α, thus, the basal degradation rate of HIF-1α, $k_{HIF1\alpha}$, is estimated as ln(2)/7.5 mins = 5.54/h. The half-life of HPIP is estimated based on typical half-life of mammalian proteins, approximately 20 h (Lu et al., 2013). Thus, the basal degradation rate of HPIP k_{HPIP} is ln(2)/20 h = 0.035/h. The production rates for both proteins have been estimated based on characteristic concentrations/levels of signaling proteins in a mammalian cell, i.e. roughly a million molecules (Lu et al., 2013); thus, g_{HPIP} = 10*10^3 molecules/h, and $g_{HIF1\alpha}$ = 300*10^3 molecules/h. Fold-changes have been estimated based on our experimental data – a 3-fold increase in HPIP levels due to HIF-1α (Fig. 11), and a four-fold increase in half-life of

HIF-1α due to HPIP (Fig. 22, C-D); thus, $\lambda_{HIF1\alpha,HPIP}$ = 3; $\lambda_{HPIP,HIF1\alpha}$ = ¼ = 0.25 (considered in terms of fold-change in degradation rate). The Hill coefficient values are $n_{HIF1\alpha,HPIP}$ = $n_{HPIP,HIF1\alpha}$ = 6. The threshold of HIF-1α affecting HPIP ($HIF1\alpha_0$) is considered to be 120*10^3 molecules, and that for HPIP modulating HIF-1α ($HPIP_0$) is considered to be 450*10^3 molecules. The nullcline and stochastic perturbation analysis for the network was carried out in R and the corresponding figures were generated using MATLAB. Bifurcation diagrams were generated using MATCONT (A. Dhooge, 2003). Stochastic simulations involve perturbing the expression levels with normally distributed noise.

We also conducted a sensitivity analysis where we varied the parameters in the model one at a time and re-plotted the bifurcation diagrams (Fig. 23, E-J). Expect for the case of $n_{HIF1\alpha,HPIP}$ = 1,2 and $n_{HPIP,HIF1\alpha}$ = 1, 2; bistability is retained in all cases, suggesting a very robust behavior.

2.32. Statistical analysis

Statistical difference between control samples and test samples were determined by paired or unpaired student's t-test. Significance difference analyses in tumor metastasis, as well as tumor formation (growth), were determined by Mann-Whitney U test or unpaired t test. Statistical analyses were performed using GraphPad Prism. For the Kaplan–Meier curves, Prism software was used, and log-rank analysis was performed. All the experiments were repeated at least twice with triplicate technical replicates. All the data are presented as mean ± SD. P value <0.05 was considered to be statistically significant.

Chapter 3

3.0. Results

3.1. Effect of hypoxia on HPIP gene expression and its functional implications in tumor metastasis

3.1. (a) HPIP expression is induced under hypoxia

HPIP and HIF-1α over expression in various cancers have been reported (Zhong et al., 1999; Bugide et al., 2015; Chen et al., 2016b; Pan et al., 2016; Gladek et al., 2017), however the correlative expression between these proteins and its associated possible risk in breast cancer has not been fully elucidated. Considering the overlapping functions of HPIP and HIF-1α, we analyzed its expression in two breast cancer cell lines (MDA-MB-231 or 4T1) cultured in hypoxia. 4T1 or MDA-MB-231 cells were exposed to hypoxia (1% O_2) for various time points (0 h to 24 h) and HPIP expression was analyzed. A marked increase of HPIP both at protein as well as mRNA levels was observed in these cell lines (Fig. 11, A-F). HIF-1α is a transcriptional regulator that involves in cellular adaptation to hypoxic stress (Hirota and Semenza, 2006). To explore whether HIF-1α mediates hypoxia-induced upregulation of HPIP expression, MDA-MB-231 cells were treated with either Methyl 3-[[2-[4-(2-adamantyl) phenoxy] acetyl] amino]-4-hydroxybenzoate, a HIF-1α inhibitor, or silenced endogenous HIF-1α expression by transfecting HIF-1α-specific siRNA. As expected, downregulation of HIF-1α expression significantly decreased hypoxia-induced HPIP expression (Fig. 11G). HIF-1α regulates the expression of several genes essential for hypoxic adaptation such as invasion, angiogenesis and tumor progression (Semenza and Wang, 1992; Pugh and Ratcliffe, 2003) by directly interacting with hypoxia response elements (HREs) (Bardos and Ashcroft, 2005). We found three such putative HREs that share homology with HIF-1α consensus binding sequence XCGDG (X=G/C, D=A/T) (HRE1: +392 **5'ACGTG3'** +398, HRE2: -1394 **5'CCGTG3'** -1388 and HRE3: -2104 **5'GCGAG3'** -2099) in HPIP promoter (Fig. 11H). To check the functional activity of these HREs, chromatin immunoprecipitation assay (ChIP) was

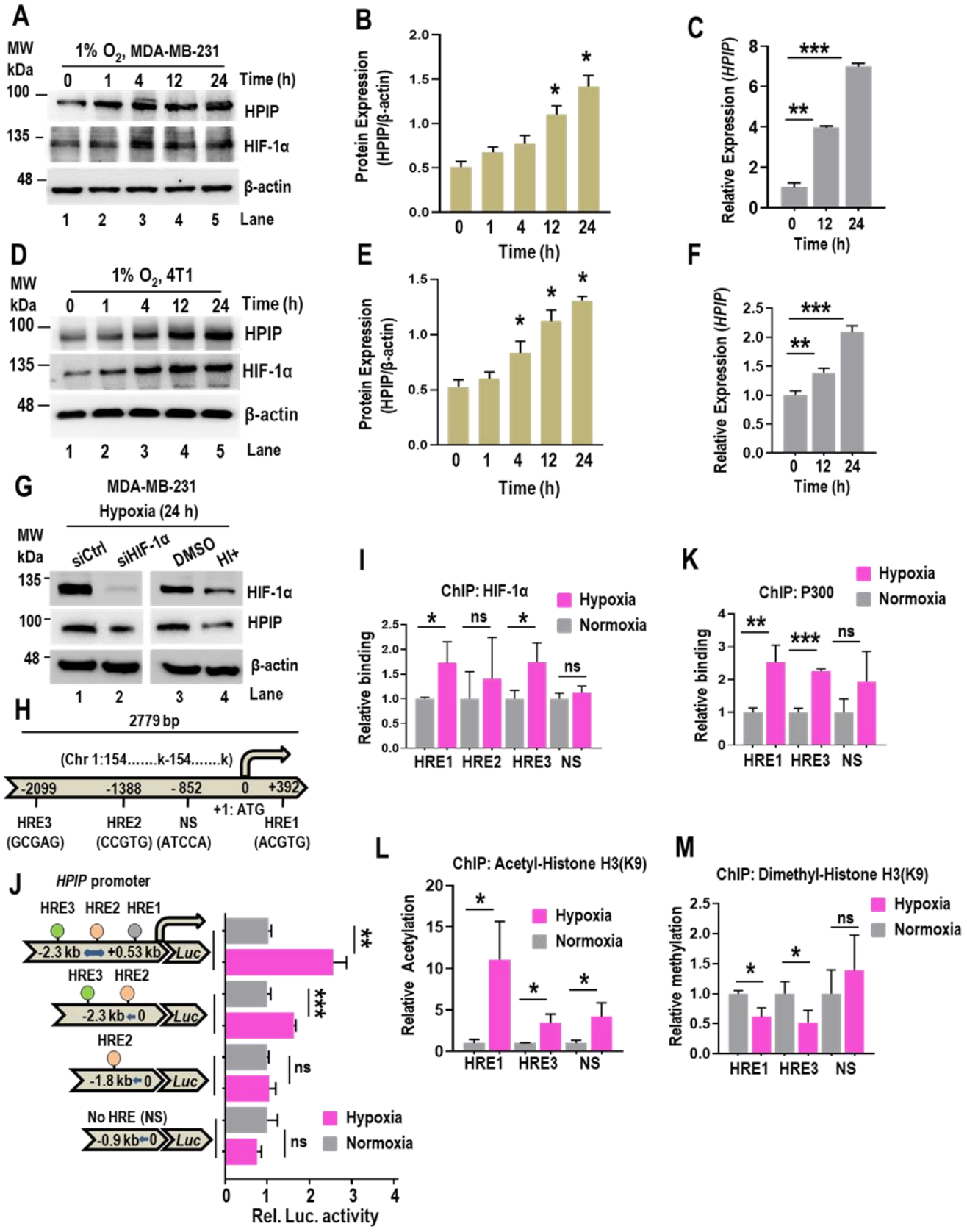
A
MW
kDa
1% O2, MDA-MB-231
0 1 4 12 24 Time (h)
100
135
48
HPIP
HIF-1α
β-actin
1 2 3 4 5 Lane
B
Protein Expression (HPIP/β-actin)
Time (h)
C
Relative Expression (HPIP)
Time (h)
D
1% O2, 4T1
E
F
G
MDA-MB-231
Hypoxia (24 h)
siCtrl
siHIF-1α
DMSO
HI+
H
2779 bp
(Chr 1:154.....k-154.....k)
-2099
-1388
- 852
0
+392
+1: ATG
HRE3 (GCGAG)
HRE2 (CCGTG)
NS (ATCCA)
HRE1 (ACGTG)
I
ChIP: HIF-1α
Hypoxia
Normoxia
Relative binding
HRE1 HRE2 HRE3 NS
K
ChIP: P300
HRE1 HRE3 NS
J
HPIP promoter
-2.3 kb ⟷ +0.53 kb
-2.3 kb ⟵ 0
-1.8 kb ⟵ 0
-0.9 kb ⟵ 0
Luc
No HRE (NS)
Rel. Luc. activity
L
ChIP: Acetyl-Histone H3(K9)
Relative Acetylation
M
ChIP: Dimethyl-Histone H3(K9)
Relative methylation

Fig. 11. *HPIP* is a hypoxic response gene. MDA-MB-231 (**A, B, C**) or 4T1 (**D, E, F**) cells were exposed to hypoxia at indicated time points and cell lysates were analyzed by western blotting (WB) (**A, D**) and HPIP quantification graph from 3 independent experiments (**B, E**) and qRT-PCR (**C, F**). (**G**) MDA-MB-231 cells, transfected with siCtrl, siHIF-1α or treated with HI+ (HIF-1α inhibitor), were cultured in hypoxia for 24 h and cell lysates were analyzed by WB. β-actin was used as an internal control. (**H**) A schematic representation of HPIP promoter (2.76 kb) indicating the location of hypoxia response elements (HRE1, HRE2, HRE3; NS-nonspecific). (**I, J, K, L, M**) MDA-MB-231 cells were incubated under hypoxia or normoxia for 24 h and subjected to various analysis. (**I**) ChIP assay was performed using indicated antibody and co-precipitated DNA samples were subjected to qRT-PCR using HRE1, HRE2, HRE3 and NS (nonspecific) specific primers. (**J**) Luciferase activity was determined in MDA-MB-231 cells using different deleted constructs of human HPIP promoter with HRE1, HRE2 and HRE3 and, are fused to Luc gene. (**K, L, M**) ChIP assays were performed using indicated antibodies and co-precipitated DNA samples were subjected to qRT-PCR using HRE1, HRE3 and NS (nonspecific) specific primers. The relative protein enrichment at specific HRE's was quantified and normalized with normoxia condition. Bar represents the mean ± SD (*P<0.05, **P<0.01, ***P<0.001, unpaired Student's t-test, n=3).

performed using HIF-1α antibody. As shown in Fig. 11I, HIF-1α was enriched onto HRE1 and HRE3 under hypoxia as compared to normoxia. To validate the ChIP data, a series of *HPIP* promoter deletions containing HRE1, HRE2, and HRE3 were cloned into pGL3-Luc vector and assayed the reporter activity. Concomitantly, reporter assay revealed that *HPIP* promoter which harbors both HRE's 1&3, but not HRE2, are active in response to hypoxia as loss of these HRE's abrogated it (Fig. 11J).

It has been reported that histone acetylation occurs on HIF-1α-dependent gene promoters by the recruitment of p300/CBP, which acts as a coactivator for HIF-1α (Johnson et al., 2008; Ruas et al., 2005). So, we next investigated the association of p300 as well as histone modifications in HPIP promoter. p300 binding was strongly augmented onto HRE's 1 and 3, but not onto HRE 2, in response to hypoxia as compared to normoxia (Fig. 11K). In accordance with the binding of p300, relative histone acetylation at H3K9 is increased at HRE's 1 and 3, while histone dimethylation at H3K9, an inactive chromatin marker, decreases in HRE's 1 and 3 (Fig. 11, L and M). Together

these findings indicated that *HPIP* is a hypoxia response gene, and its expression is HIF-1α-dependent.

3.1. (b) HPIP expression is required for the survival of breast cancer cells in response to hypoxia

In solid tumors like breast tumors, increased tumor size led to deprivation of oxygen and nutrients in cancer cells. Furthermore, it has been well established that hypoxia in solid tumors facilitates survival advantage to cancer cells to escape from this hostile microenvironment (Wang et al., 2017a). Since HPIP is a hypoxia response gene with a proto-oncogene activity, we ascertained that HPIP might promote cancer cell survival by antagonizing apoptosis under hypoxic stress. Accordingly, AO/PI or trypan blue assay revealed that silencing of endogenous HPIP markedly decreases the cell viability upon hypoxia but no significant difference in normoxia (Fig. 12, A-D). Similar results were also observed in 4T1 cells, a mouse adenocarcinoma cell line that exhibits TNBC (Triple negative breast cancer) like properties similar to MDA-MB-231 cells (Fig. 12, E-H). Furthermore, HPIP silencing (stable clones using shRNA) significantly reduced anchorage-independent growth ability of MDA-MB-231 cells, under hypoxia (Fig. 13, A and B) or 4T1 cells (Fig. 13, C and D). Consistent with these results, FACS based Annexin V assay showed increased apoptosis upon HPIP silencing by these clones cultured under hypoxia but not in normoxia (Fig. 13, E-G). Moreover, western blot analysis of HPIP silenced MDA-MB-231 or 4T1 cells showed an elevated level of apoptosis markers such as cleaved PARP as well as cleaved Caspase 3/9 in hypoxia but not in normoxia (Fig. 13, H and I). Together these data suggest that HPIP confers breast cancer cell survival and anchorage independent growth under hypoxic stress by antagonizing apoptosis.

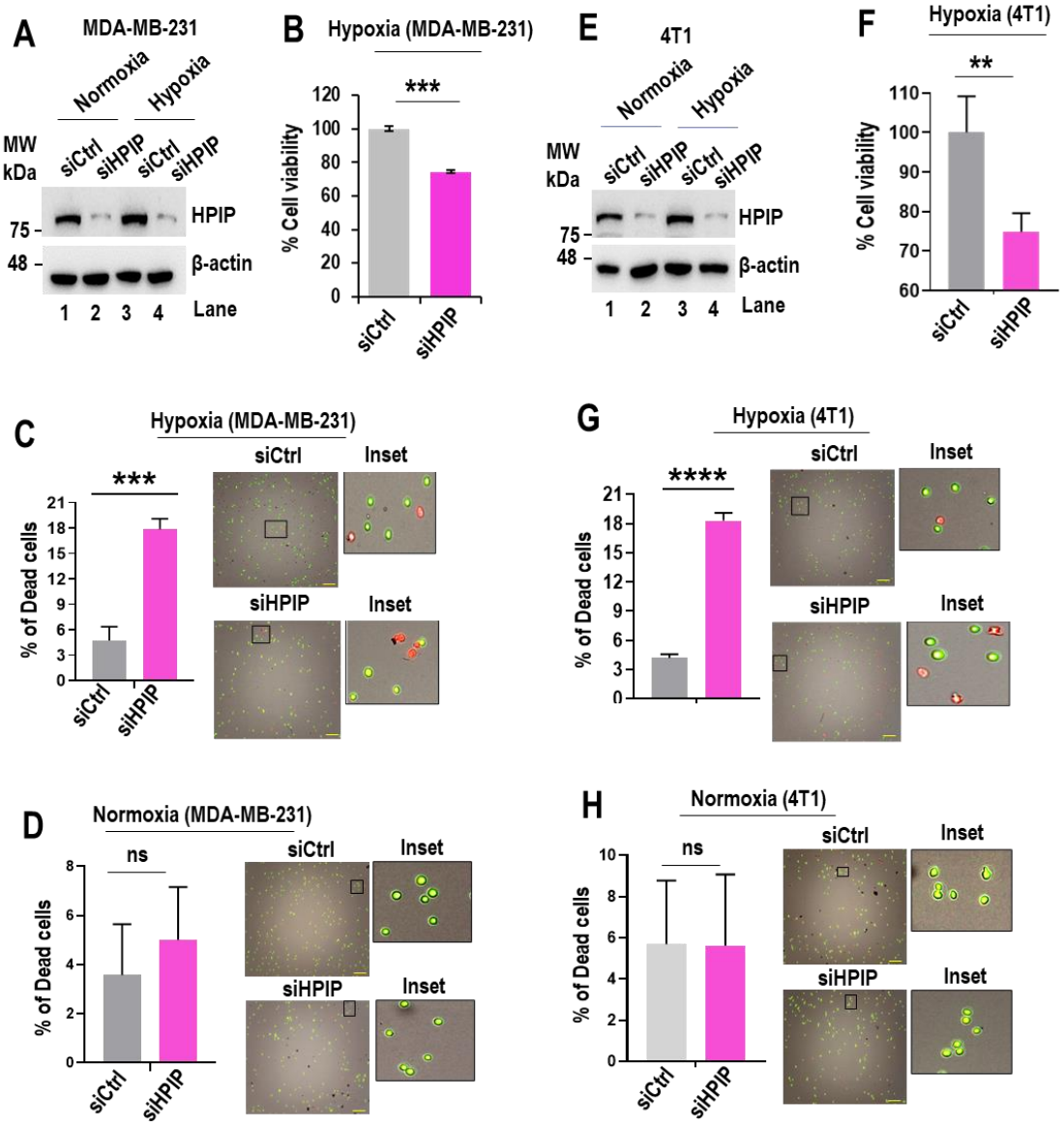

Fig. 12. HPIP expression is required for survival of breast cancer cells in hypoxia.

MDA-MB-231 cells (**A, B, C, D**) or 4T1 cells (**E, F, G, H**) transfected with either si/shCtrl or si/shHPIP were exposed to hypoxia for 24 h and were subjected to various functional analyses. (**A, E**) WB confirming knockdown of HPIP. (**B, F)** Post transfected (24 h) MDA-MB-231 or 4T1 cells with siCtrl or siHPIP were cultured in hypoxia for an additional 24 h. Trypan blue assay was performed and plotted as percentage of viable cells. Cells were exposed to hypoxia (C**, G**) or normoxia (**D, H**) and performed cell viability assay by staining with AO/PI and quantified. Bar represents the mean ± SD (Scale bar: 100 µm. *P<0.05, **P<0.01, ***P<0.001, ***P<0.001, unpaired Student's t-test. n=3).

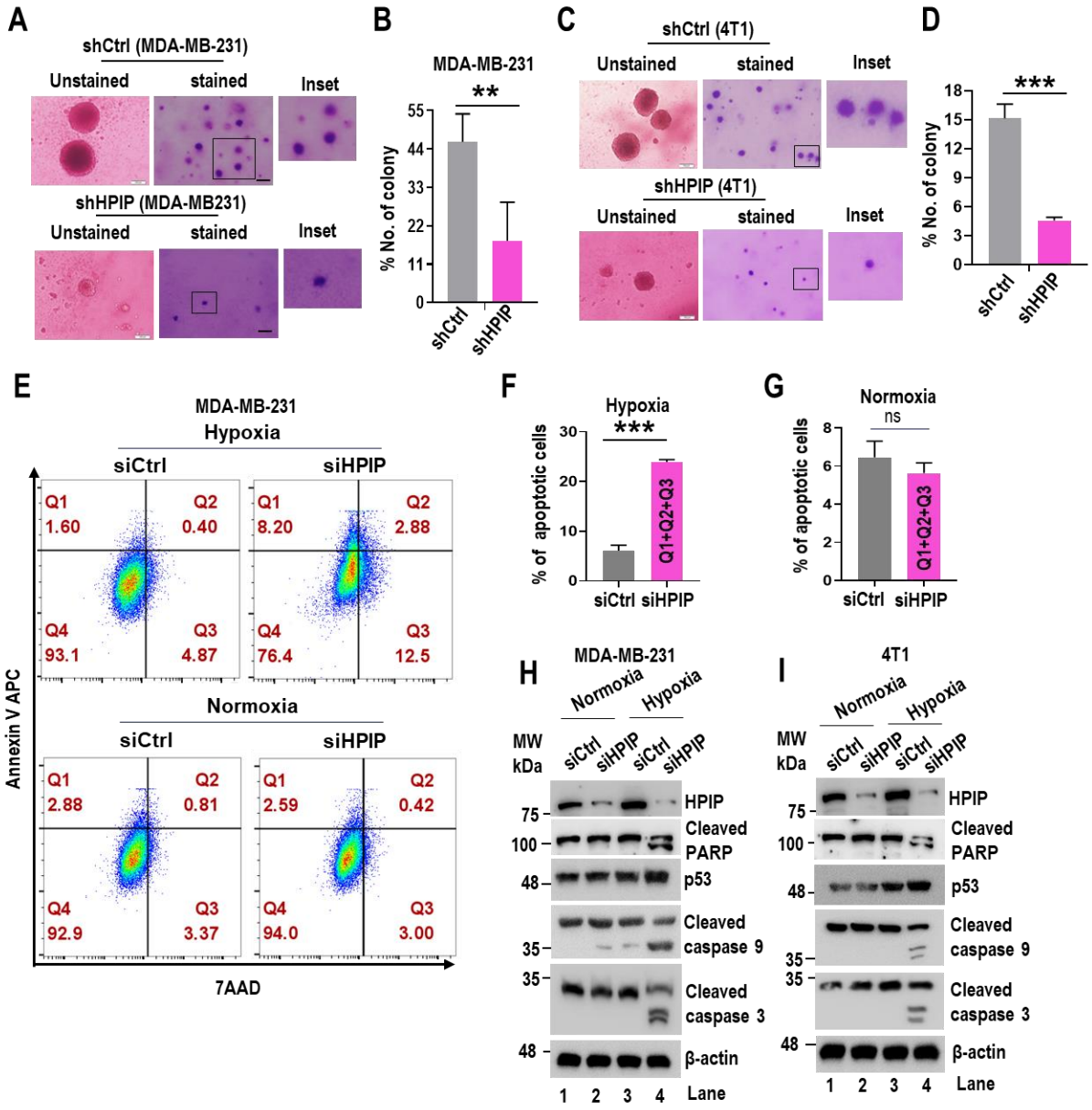

Fig. 13. HPIP expression is required for survival of breast cancer cells in hypoxia. MDA-MB-231 cells (**A, B, E, F, G, H**) or 4T1 cells (**C, D, I,**) transfected with either si/shCtrl or si/shHPIP were exposed to hypoxia or normoxia for 24 h and were subjected to various functional analysis. (**A-D**) Anchorage independent growth was assessed, stained and imaged, and (**B, D**) colonies were counted. (**E**) Apoptosis assay by FACS using Annexin V APC and 7AAD. (**F, G**) Stained samples were analyzed and data were plotted, (n=2) (**H, I**) WB analysis of expression of apoptotic markers. β-actin was used as an internal control. Bar represents the mean ± SD (Scale bar: 100 µm. *P<0.05, **P<0.01, ***P<0.001, ***P<0.001, unpaired Student's t-test. n=3).

3.1. (c) HPIP promotes invasion, EMT, cancer stem cell features and metastasis of breast cancer cells in response to hypoxia

In addition to modulating cell survival, hypoxic microenvironment is also known to increase the aggressiveness of cancer cells by enhancing metastatic potential (Hirota and Semenza, 2006; Chan and Giaccia, 2007). We therefore investigated whether HPIP has any role in hypoxia induced cancer cell migration, invasion, EMT and metastasis. First our 3D migration assay or scratch wound assay demonstrated a significant decrease in cell migration activity upon HPIP silencing in MDA-MB-231 (Fig. 14, A - D) or 4T1 cells (Fig. 14, E - H) cultured in hypoxia. Furthermore, under hypoxia, HPIP silencing significantly reduced invasion capacity of MDA-MB-231 (Fig. 14, I and J) or 4T1 cells (Fig. 14, K and L) cultured in hypoxia. In concordance, HPIP silencing decreased EMT, which is characterized by elevated levels of E-Cadherin while decreased expression of Vimentin and Snail (Fig. 14, M and N). MDA-MB-231 cells also have been shown to display EMT (Huang et al., 2020). Since $CD44^{+}/CD24^{-}$ enriched population of mammary cancer stem cells (MaCSCs) represent as one of the characteristic features of TNBC cells, we evaluated the effect of HPIP silencing on $CD44^{+}/CD24^{-}$ MaCSCs in response to hypoxia. We found a significant loss of $CD44^{+}/CD24^{-}$ population upon HPIP silencing in MDA-MB-231 cells (Fig. 15, A and B). The co-expression study of CD44/CD24 with HPIP expression from Oncomine using Bos Breast data sets also showed a significant correlative expression of HPIP with CD44 but not CD24 (Fig. 15C).

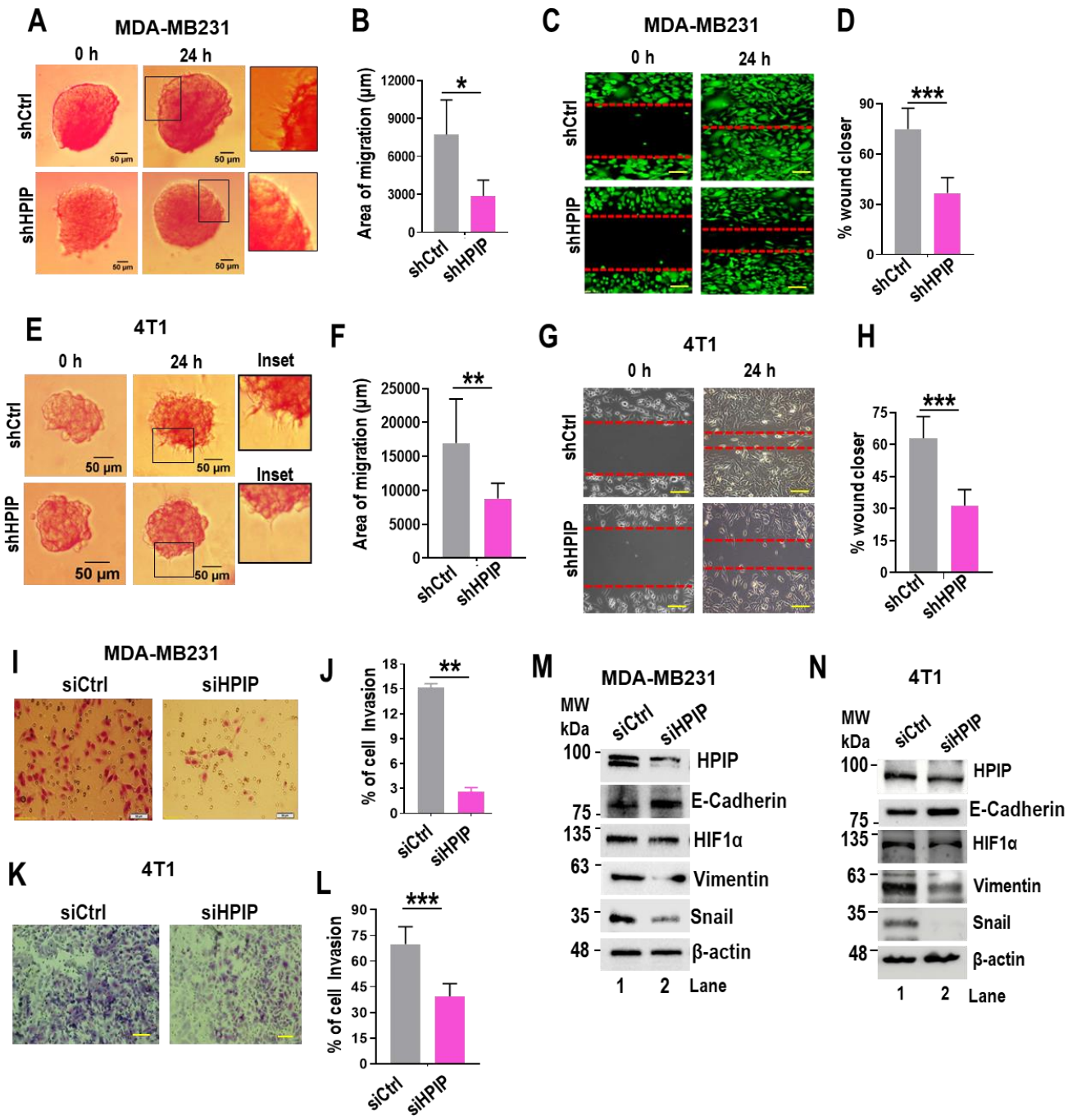

Fig. 14. HPIP promotes invasion, EMT, cancer stem cell features and metastasis in TNBC cells under hypoxic stress.

HPIP silenced cells of MDA-MB-231 (**A, B**) or 4T1(**E, F**) were assessed for 3D migration assay. The disseminated cells from the spheroids following 24 h of exposure to hypoxia (**A, E**) (scale: 100 µm) and invading areas were measured (**B, F**). (**C, D, G, H**) A straight line was scraped in fully confluent monolayer cells (shCtrl or shHPIP), incubated under hypoxia, and the percentage of migrated cells was calculated. Representative microscopy images (fluorescent or phase-

contrast) were taken after wound was created at the indicated time points and the percentage of wound closure was quantified (**C, D**) MDA-MB-231 and (**G, H**) 4T1 cells. MDA-MB-231 (**I, J, M**) or 4T1 (**K, L, N**) cells were transfected with siCtrl or siHPIP and cultured in hypoxia for 24 h. (**I, K**) Invaded cells through Boyden's chambers were fixed, permeabilized and stained, scale: 100 µm, and (**J, L**) determined the percentage of invaded cells. (**M, N**) EMT marker proteins were analyzed by WB using β-actin as an internal control. Data represents mean ± SD, N=3 (*P<0.05, **P<0.01, ***P<0.001, unpaired Student's t-test).

To further confirm the *in vivo* involvement of HPIP in tumor invasion, we utilized HPIP stably knocked down 4T1 clones. After exposure to hypoxia for 48 h, ~ $1x10^6$ cells (shCtrl or shHPIP) were injected intravenously into nude mice via tail vein. After 21 days, we monitored the lung metastasis by counting the number of metastatic nodules and quantified the relative fluorescence units (RFU). Mice injected with control shRNA transfected 4T1 cells displayed prominent lung metastasis, whereas the lung metastatic ability was significantly suppressed in shHPIP-treated cells (Fig. 15, D-G). Interestingly, hypoxia derived metastatic nodules are significantly more than normoxia (Fig. 15, E and F; P<0.05). Histological analysis of lung sections further showed metastatic nodules of shCtrl-4T1 injected nude mice had more compact, highly dense and larger in size as compare to shHPIP-4T1 injected nude mice (Fig. 15, G-H). Taken together our data suggest that HPIP is required to potentiate cell migration, invasion and also *in vivo* lung metastasis of breast cancer cells under hypoxia.

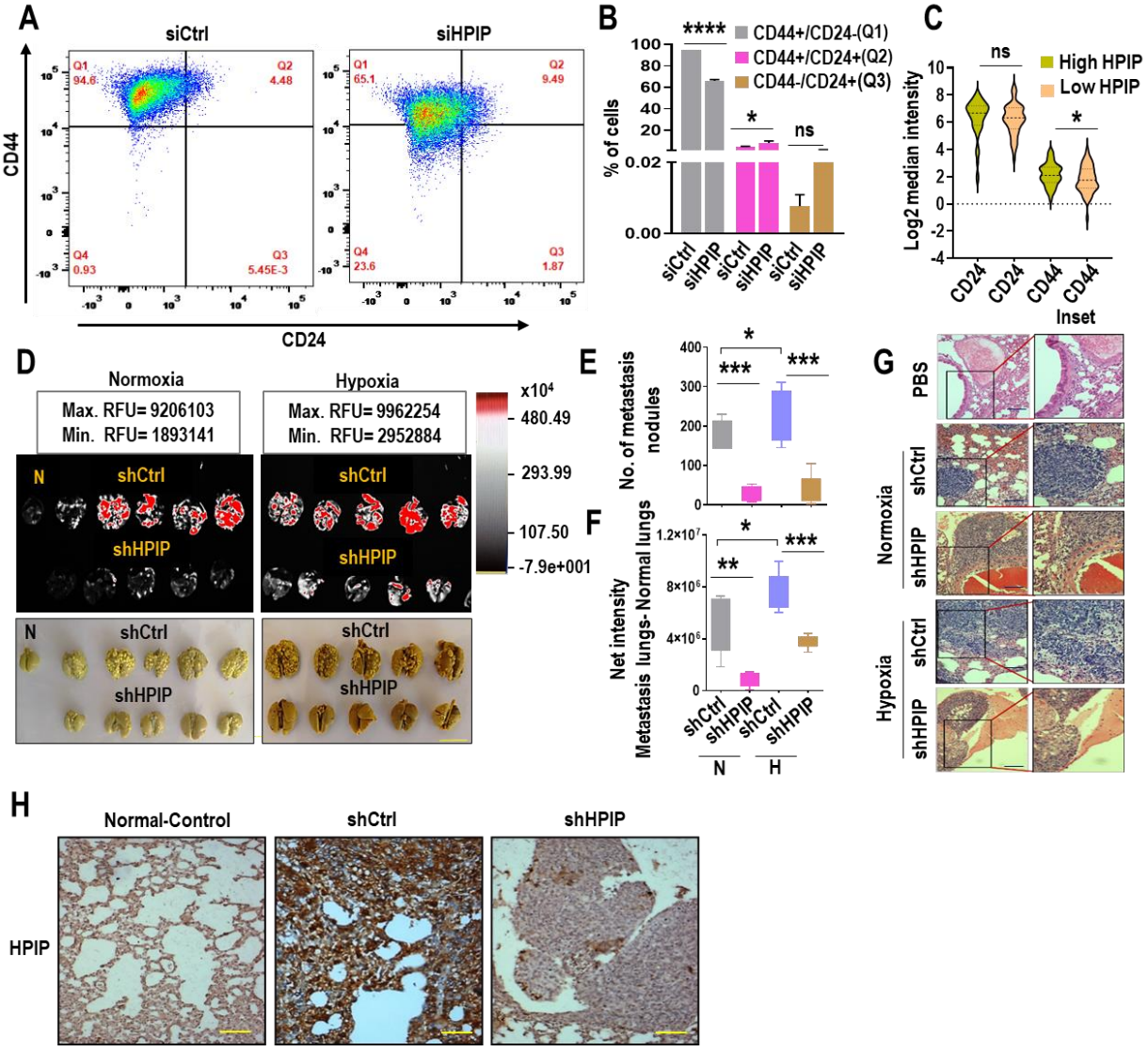

Fig. 15. HPIP promotes invasion, EMT, cancer stem cell features and metastasis in breast cancer cells in response to hypoxic stress.

HPIP silenced cells (MDA-MB-231) were cultured under hypoxia for 24 h. (**A**) Flow cytometry analysis of expression of CD24 and CD44 and (**B**) measured the percentages of population fractions, (*P<0.05, ****P<0.0001, Two-way ANOVA test). (**C**) Oncomine derived correlative expression of HPIP with CD24 or CD44 using Bos Breast data set. **(D-H)** 4T1 cells (shCtrl or shHPIP) were exposed to normoxia or hypoxia for 24 h and injected via tail vein of nude mice. (**D**) **Upper**, gross picture of fluorescence green tumors (shCtrl or shHPIP) (**D**), **lower**, Pictorial representation of lungs with metastatic nodules, scale bar: 1 cm. (**E**) metastatic nodules were counted and (**F**) Quantified and compared the net fluorescence unit. (**G**) H and E staining showing more compact and highly dense lung nodules in control (shCtrl) as compared to shHPIP. (**H**) Paraffin lung tissue derived from tail vein injected animals (shCtrl or shHPIP or PBS) was subjected to immunohistochemical staining of HPIP. Scale bar: 100 µm. Number of mice used per

group, N = 5. Data represents mean ± SD (*P<0.05, **P<0.01, ***P<0.001, unpaired Student's t-test).

3.1. (d) HPIP modulates MMP2/9 protein synthesis in response to hypoxia via SRP14-dependent pathway

Overwhelming evidence support that matrix metalloproteinases (MMPs) regulate cancer cell migration, invasion and metastasis (Deryugina and Quigley, 2006). Furthermore, elevated MMP levels have been shown to be associated with metastasis and poor prognosis in several types of cancer (Nelson et al., 2000). We ascertained whether HPIP-induced invasive and metastasis phenotypes in breast cancer cells were due to matrix metalloproteinases (MMPs). Interestingly, HPIP silencing significantly decreased MMP9 expression at protein level, yet no significant changes at RNA level indicating that, MMP9 might be subjected to either proteasomal degradation or translational defects (Fig. 16, A and B). Treatment of cells with MG132, a proteasomal inhibitor, did not restore MMP9 expression and also TIM2 and TIM3, inhibitors of MMPs, in HPIP depleted cells, which ruled out the possibility of involvement of proteasomal pathway in HPIP regulated MMP9 synthesis (Fig. 16C). We next analyzed MMP9 synthesis by pulse chase experiment using [S^{35}] methionine. As compared to control cells, HPIP depleted cells showed a marked decrease in MMP9 synthesis (Fig. 16D). SignalP4.1 and SecretomeP 2.0a analysis of MMP9 suggested that it carries a signal peptide and, after protein synthesis on endoplasmic reticulum (ER) by ribosomes, it follows the classical secretory pathway for its secretion (Fig. 16E). Since majority of the biological functions are carried out by protein complexes rather as individual components (Spirin and Mirny, 2003), we followed yeast to hybrid (Y2H) genetic approach to identify HPIP interacting partners. We found SRP14 (signal recognition particle) as one of the interacting partners of HPIP (Fig. 16F). SRP14 is a part of signal recognition particle (SRP)-ribonucleoprotein (RNP) complex that involves in protein synthesis on ER membrane (Akopian et al., 2013).

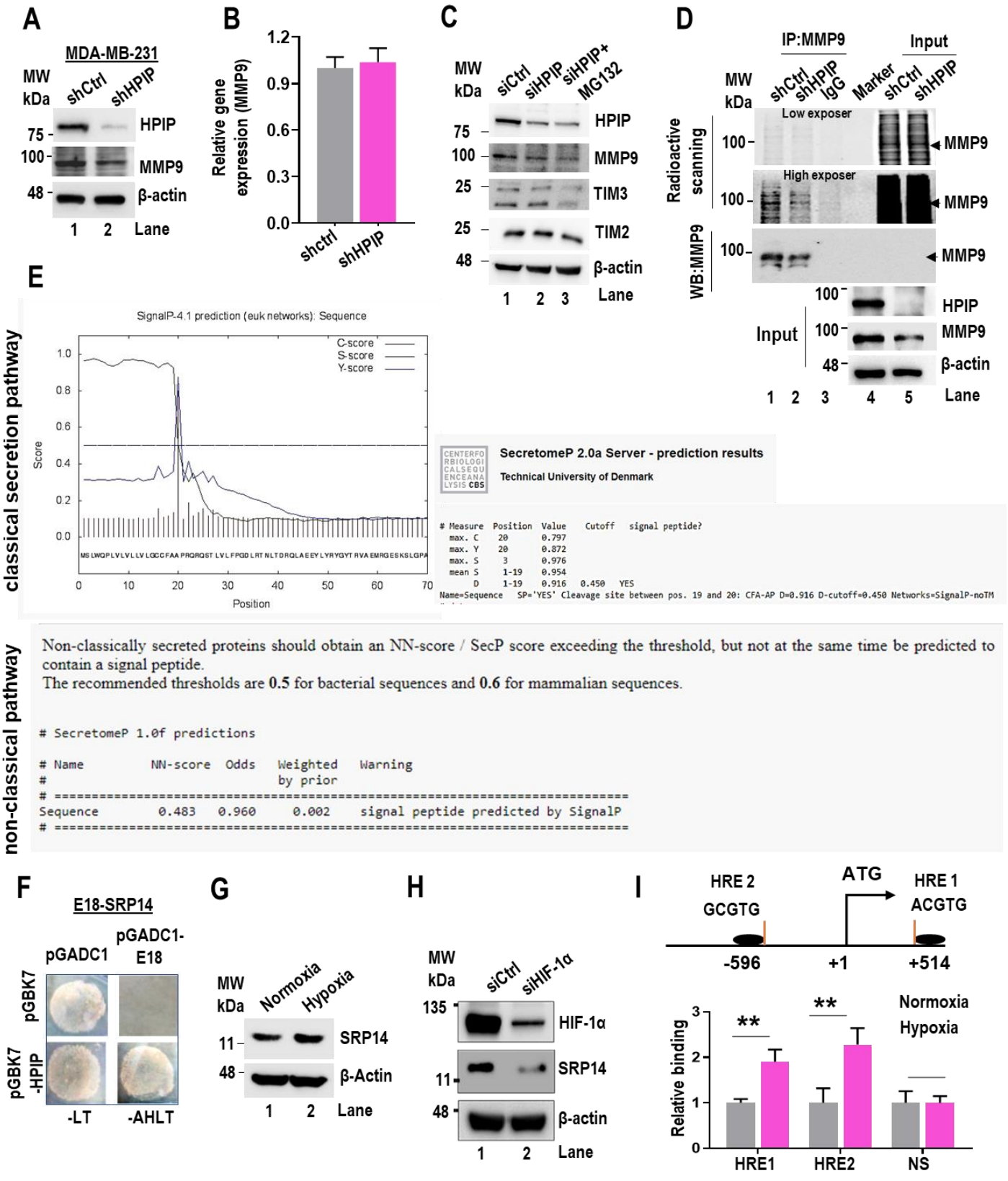
A
MDA-MB-231
MW kDa
shCtrl
shHPIP
75
100
48
HPIP
MMP9
β-actin
1 2 Lane
B
Relative gene expression (MMP9)
1.2
0.9
0.6
0.3
0.0
shctrl
shHPIP
C
MW kDa
siCtrl
siHPIP
siHPIP+ MG132
75
100
25
25
48
HPIP
MMP9
TIM3
TIM2
β-actin
1 2 3 Lane
D
IP:MMP9
Input
MW kDa
shCtrl
shHPIP
IgG
Marker
shCtrl
shHPIP
Radioactive scanning
Low exposer
High exposer
100
100
100
MMP9
MMP9
MMP9
WB:MMP9
Input
100
100
48
HPIP
MMP9
β-actin
1 2 3 4 5 Lane
E
classical secretion pathway
SignalP-4.1 prediction (euk networks): Sequence
C-score
S-score
Y-score
Score
Position
MS LWQP LVLVL LV LGCC FAA PRQRQST LVL FPGD LRT NLTDRQLA EEY LYRYGYT RVA EMRGESKSLGPA
SecretomeP 2.0a Server - prediction results
Technical University of Denmark
Measure Position Value Cutoff signal peptide?
max. C 20 0.797
max. Y 20 0.872
max. S 3 0.976
mean S 1-19 0.954
D 1-19 0.916 0.450 YES
Name=Sequence SP='YES' Cleavage site between pos. 19 and 20: CFA-AP D=0.916 D-cutoff=0.450 Networks=SignalP-noTM
non-classical pathway
Non-classically secreted proteins should obtain an NN-score / SecP score exceeding the threshold, but not at the same time be predicted to contain a signal peptide.
The recommended thresholds are 0.5 for bacterial sequences and 0.6 for mammalian sequences.
SecretomeP 1.0f predictions
Name NN-score Odds Weighted by prior Warning
Sequence 0.483 0.960 0.002 signal peptide predicted by SignalP
F
E18-SRP14
pGADC1
pGADC1-E18
pGBK7
pGBK7-HPIP
-LT
-AHLT
G
MW kDa
Normoxia
Hypoxia
11
48
SRP14
β-Actin
1 2 Lane
H
MW kDa
siCtrl
siHIF-1α
135
11
48
HIF-1α
SRP14
β-actin
1 2 Lane
I
HRE 2
GCGTG
ATG
HRE 1
ACGTG
-596
+1
+514
Relative binding
**
**
Normoxia
Hypoxia
HRE1
HRE2
NS

Fig. 16. HPIP modulates MMP2/9 protein synthesis in response to hypoxia via SRP14-dependent pathway.

Cells were cultured in hypoxia for 24 h and performed the indicated experiments. (**A, B**) MDA-MB-231 cells transfected with shCtrl or shHPIP were analyzed by (**A**) WB (**B**) qRT-PCR. (**C**) siCtrl or siHPIP, were subjected to MG132 (25 µM) treatment for 8 h and lysates were analyzed by WB. (**D**) Pulse-chase experiment: MDA-MB-231 cells (shCtrl or shHPIP) cultured under hypoxia for 24 h were chased with ^{35}S-methionine and extracts were preceded for Immunoprecipitation with MMP9 antibody followed by WB and autoradiography. (**E**) Analysis of MMP9 protein sequence to identify signal peptide using SignalP 4.1 Server and SecretomeP 1.0 Server. (F) Y2H analysis shows interaction of HPIP and SRP14. (**G**) MDA-MB-231 cells exposed to hypoxia or normoxia for 24 h were subjected to WB. (**H**) Post transfected (24 h) cells with siCtrl or siHIF-1α were exposed to hypoxia (24 h), then cell lysates were analyzed by WB. (**I**) **Upper**, A schematic representation of SRP14 promoter indicating the location of HIF-1α binding sites (HRE1, HRE2). (**I**) **Lower**, ChIP assay with HIF-1α antibody. Co-precipitated DNA samples were subjected to qRT-PCR using HRE1, HRE2 and NS (nonspecific) specific primers. The relative binding capacity of HIF-1α is quantified and normalized with normoxic samples. Bar represents the mean ± SD, N=3 (**P<0.01, unpaired Student's t-test).

Generally, proteins synthesized by ER ribosomes are destined for secretion (Karamyshev et al., 2020). Given these premises, we hypothesized that HPIP might regulate MMP9 synthesis by modulating SRP14 function. First, we studied SRP14 expression in breast cancer cells in response to hypoxia. Interestingly, we found that SRP14 expression is also induced by hypoxia stress and depletion of HIF-1α markedly downregulated its expression in MDA-MB-231 cells (Fig. 16, G and H). Careful perusal of *SRP14* gene promoter revealed that it harbors two HRE elements in it (Fig. 16I). Concomitantly, chromatin immunoprecipitation assay (ChIP) confirmed HIF-1α recruitment onto *SRP14* promoter (Fig. 16I). Next, CoIP analysis confirmed the *in vivo* interaction of HPIP with SRP14 (endogenous) in MDA-MB-231 cells (Fig. 17A). Similarly, HPIP and SRP14 also interacts in transiently co-transfected MDA-MB-231 cells with pMNDUS-HPIP and GFP-SRP14 (Fig. 17B). Further analysis of cellular fractions by sucrose gradient centrifugation revealed the enrichment of HPIP and SRP14 in ribosomal fraction (14th and 17th fractions, which are enriched with L9 ribosomal protein) (Fig. 17C). Additionally, protein domain mapping analysis identified lysine rich region located between 96-113 aa in SRP14 is required for interacting with

HPIP as wtSRP14 could interact with HPIP but not SRP14A5 or SRP14-ΔK5 (Fig. 17D). CoIP analysis further demonstrated an increased interaction of HPIP with SRP14 in MDA-MB-231 cells cultured in hypoxia as compared to normoxia (Fig. 17, E and F). Earlier studies reported the localization of SRP14 into stress granules along with 40s ribosomes in response to certain physiological stresses (Berger et al., 2014). Despite HPIP is predominantly a cytoplasmic protein, confocal imaging showed a significant colocalization of HPIP with SRP14 in the stress granules of MDA-MB-231 cells (Fig. 17, G and H).

After establishing the physical interaction and cellular colocalization of HPIP and SRP14 in MDA-MB-231 cells, we next focused on their functional interaction in the context of cancer cell invasion and MMP9 synthesis. While HPIP knockdown suppressed MMP9 expression and invasion of cells, the ectopic expression of GFP-SRP14 failed to restore it (Fig. 18, A-C). Likewise, the ectopic expression of T7-HPIP in depleted SRP14 cells could not restore the invasion ability of the cells (Fig. 18, D-F). Further, in agreement with our domain mapping studies, C-terminal mutants of SRP14 were defective in stimulating MMP9 synthesis (Fig. 18G). Together these data suggested the physical interaction of HPIP with SRP14 is essential for MMP9 synthesis and thus, breast cancer cell invasion in response to hypoxia.

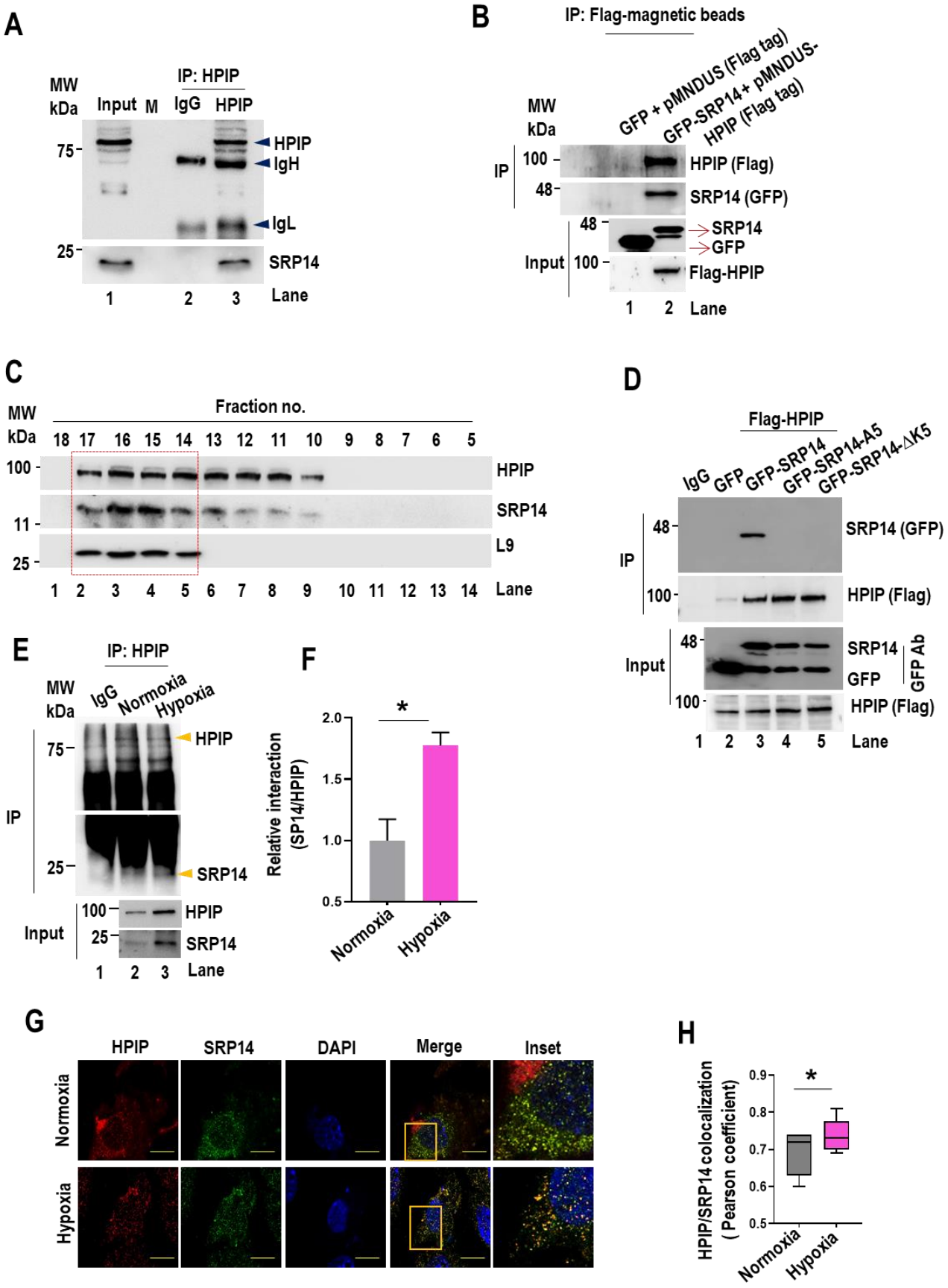
A
IP: HPIP
MW
kDa
Input
M
IgG
HPIP
75
25
HPIP
IgH
IgL
SRP14
1
2
3
Lane
B
IP: Flag-magnetic beads
GFP + pMNDUS (Flag tag)
GFP-SRP14+ pMNDUS-HPIP (Flag tag)
MW
kDa
IP
100
48
HPIP (Flag)
SRP14 (GFP)
Input
48
100
SRP14
GFP
Flag-HPIP
1
2
Lane
C
Fraction no.
MW
kDa
18 17 16 15 14 13 12 11 10 9 8 7 6 5
100
11
25
HPIP
SRP14
L9
1 2 3 4 5 6 7 8 9 10 11 12 13 14
Lane
D
Flag-HPIP
IgG
GFP
GFP-SRP14
GFP-SRP14-A5
GFP-SRP14-ΔK5
IP
48
100
SRP14 (GFP)
HPIP (Flag)
Input
48
100
SRP14
GFP
GFP Ab
HPIP (Flag)
1 2 3 4 5
Lane
E
IP: HPIP
MW
kDa
IgG
Normoxia
Hypoxia
IP
75
25
HPIP
SRP14
Input
100
25
HPIP
SRP14
1 2 3
Lane
F
Relative interaction (SP14/HPIP)
2.0
1.5
1.0
0.5
*
Normoxia
Hypoxia
G
HPIP
SRP14
DAPI
Merge
Inset
Normoxia
Hypoxia
H
HPIP/SRP14 colocalization (Pearson coefficient)
0.9
0.8
0.7
0.6
0.5
*
Normoxia
Hypoxia

Fig. 17. HPIP modulates MMP2/9 protein synthesis in response to hypoxia via SRP14-dependent pathway.

(**A**) MDA-MB-231 cells extracts derive from hypoxia were subjected to CoIP using HPIP antibody and analyzed by WB. (**B**) Post co-transfection (36 h) of MDA-MB-231 cells with Flag-HPIP and GFP-SRP14 or Flag and GFP vectors were lysed following co-immunoprecipitation with anti-Flag antibody and analyzed by WB. (**C**) Cellular extracts of MDA-MB-231 cells were subjected to sucrose gradient centrifugation and collected fractions were analyzed by WB. (**D**) Post co-transfection (36 h) of MDA-MB-231 cells with Flag-HPIP and GFP-SRP14, GFP-SRP14-A15, GFP-SRP14-ΔK5 or pEGFP-C1 plasmid constructs were harvested, co-immunoprecipitated with anti-Flag antibody and analyzed by WB. (**E**) MDA-MB-231 cells cultured in hypoxia or normoxia for 24 h were lysed following co-immunoprecipitation with HPIP antibody and analyzed by WB and (**F**) The relative interaction between HPIP and SRP14 was quantified (ratio between the intensities of SRP14 and HPIP protein bands). (**G**) MDA-MB-231 cells cultured in hypoxia or normoxia for 24 h were immune-stained and imaged, scale bar: 10 μm, and (**H**) localization (Pearson coefficient) of SRP14 and HPIP between hypoxia and normoxia was measured. Data represents mean ± SD (*P<0.05, **P<0.01, unpaired Student's t-test).

3.2. Role of HPIP in tumor development under normoxia

3.2. (a) HPIP enhances Warburg effect under normoxia

We next focused on the functional interaction between HIF-1α and HPIP in normoxia. In normoxia HIF-1α promotes aerobic glycolysis or Warburg effect, which is characterized by enhanced glucose uptake, increased expression of glycolytic enzymes and lactate synthesis etc. and thus confers tumor growth (Semenza et al., 1994; Courtnay et al., 2015; Nagao et al., 2019). Several independent reports showed that HPIP also involves not only in the cellular invasion and migration, but also in cell growth (Chen et al., 2016b; Pan et al., 2016; Khumukcham et al., 2019). This raised the possible existence of a crosstalk between the two proteins in cell growth regulation by controlling Warburg effect. To test this hypothesis, we first measured the rate of cell proliferation and colony forming ability of either HPIP or HIF-1α depleted MDA-MB-231 cells. As shown in Fig. 19, A-C, depletion of either HPIP or HIF-1α significantly reduced cell

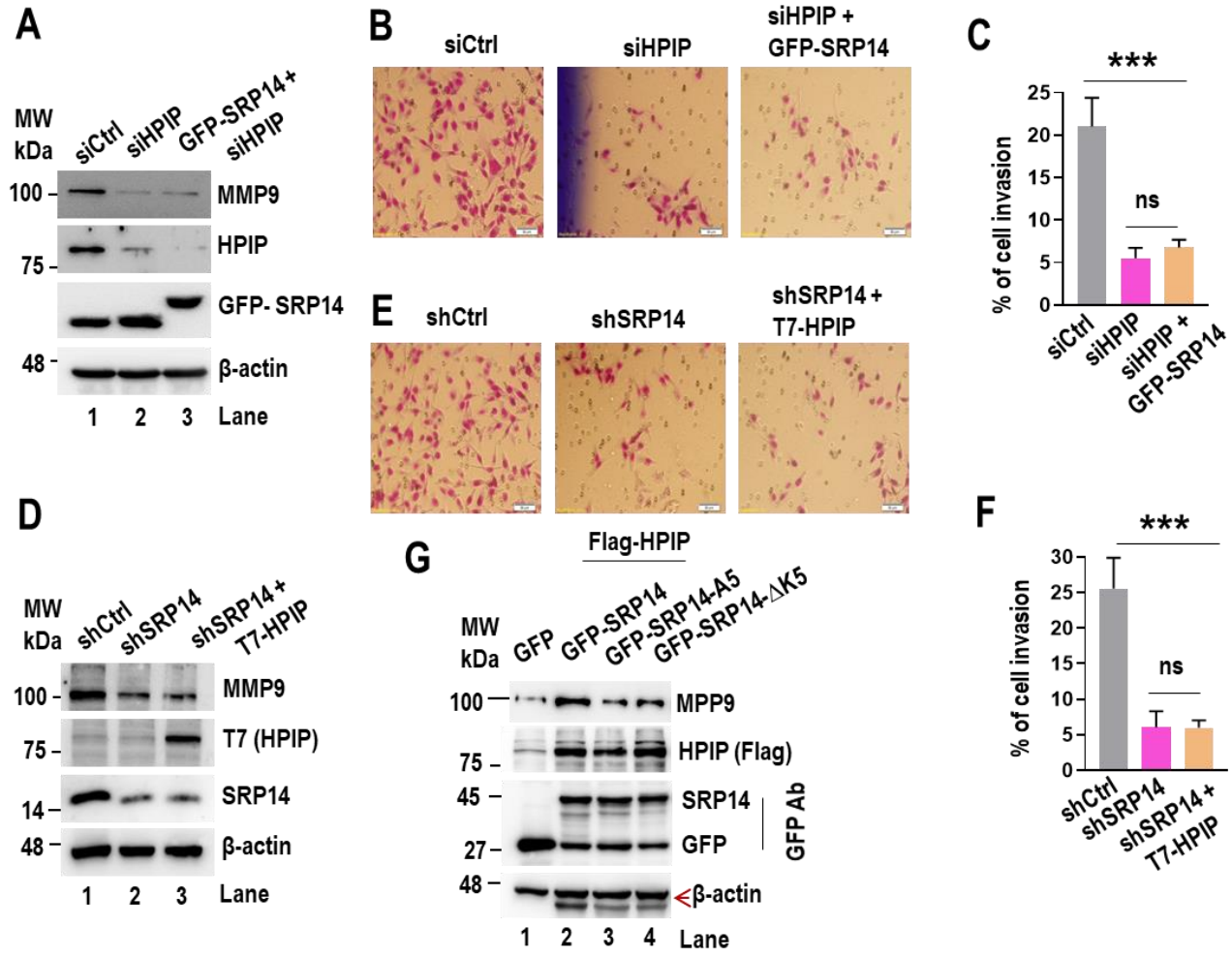

Fig. 18. HPIP modulates MMP2/9 protein synthesis in response to hypoxia via SRP14-dependent pathway. (**A-F**) MDA-MB-231 cells transfected with (**A, B, C**) siCtrl, siHPIP or siHPIP+GFP-SRP14 or (**D, E, F**) shCtrl, shSRP14 or shSRP14+T7-HPIP were cultured under hypoxia for 24 h and perform WB (**A, D**) and invasion assay (**B-F**). The invaded cells were fixed, permeabilized and stained (**B, E**) and (**C, F**) percentage of invaded cells was quantified. (**G**) Post co-transfection (36 h) of MDA-MB-231 cells with Flag-HPIP and GFP-SRP14, GFP-SRP14-A15, GFP-SRP14-ΔK5 or pEGFP-C1 plasmid constructs were harvested and analyzed by WB. β-actin was used as an internal control in all WB. Data represents mean ± SD (*P<0.05, **P<0.01, unpaired Student's t-test), scale bar: 100 μm.

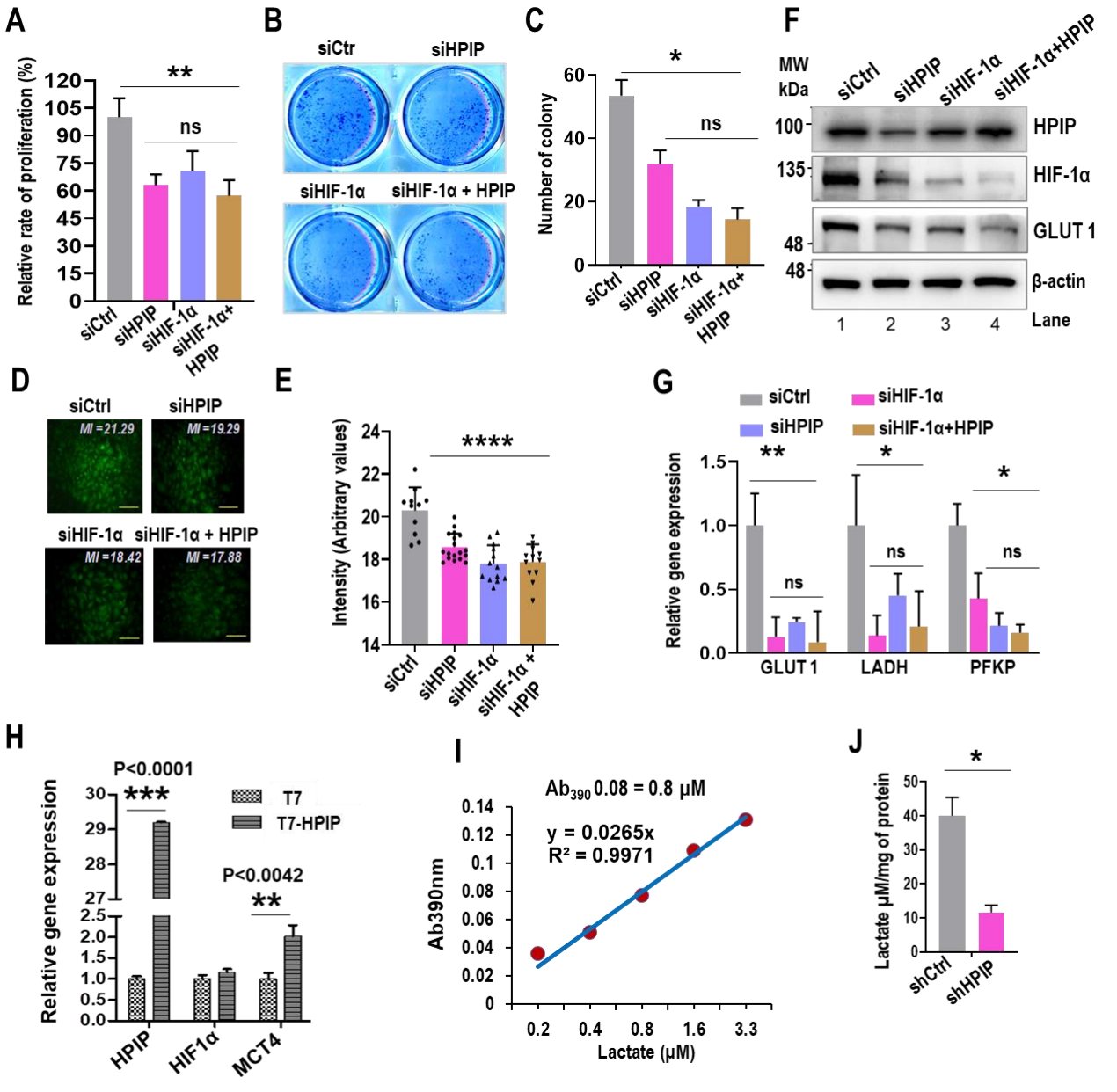

Fig. 19. HPIP promotes Warburg effect and confers cell growth on TNBC cells under normoxia.

(**A-G**) MDA-MB-231 cells were transfected with siCtrl, siHPIP, siHIF-1α or siHIF-1α plus HPIP. (**A**) Proliferation assay (MTT assay), and (**B**) Colony formation assay was performed, and representative images were shown, and (**C**) colony numbers were quantified. (**D**) Glucose uptake assay was performed by incubating with 2-NBDG (200 µM) for 30 min and imaged, scale bar: 100 µm, and (**E**) The mean intensity was quantified. (**F**) Cell's lysates were subjected to WB using following antibodies: anti-HPIP, -HIF-1α, and -GLUT1. β-actin was used as an internal control. (**G**) qRT-PCR analysis of few glycolytic genes (*GLUT1*, *LADH*, and *PFKP*). (**H**) Post transfected (36 h) MDA-MB-231 cells with T7 or T7-HPIP were analyzed by qRT-PCR. β-actin was used as

an internal control. (**I**) Standard graph derived from a spectrophotometrically measured known concentration of lactate. (**J**) Lactate released was measured from cultured media of MDA-MB-231 cells (shCtrl or shHPIP) that are exposed to hypoxia and analyzed by the spectrophotometric method and normalized by total protein. Data represents mean ± SD, N=3 (*P<0.05, **P<0.01, ***P<0.001, unpaired Student's t-test), ns-not significant.

proliferation as well as colony number, but not able to rescue the effect even after the ectopic overexpression of HPIP in HIF-1α depleted cells. We next measured the Warburg effect under similar experimental conditions. While silencing of either HPIP or HIF-1α significantly decreased glucose uptake by MDA-MB-231 cells (Fig. 19, D-F) and also expression of *GLUT1*, *LDHA* and *PFKP* (Fig. 19G), but could not rescue the effect even after the ectopic overexpression of HPIP in HIF-1α depleted cells.

In contrast to normal cells, cancer cells are mainly dependent on the substrate label phosphorylation, aerobic glycolysis, converting the glucose to lactate to meet the energy required for uncontrolled cell proliferation (de Souza et al., 2011; Pinheiro et al., 2012). Since lactate accumulation induces apoptosis, cancer cells move the lactate out of the cancer cells by MCT4 for continuous conversion of pyruvate to lactate to maintain the uninterrupted flow of glycolysis (Pinheiro et al., 2012). As expected, while ectopic expression of HPIP enhanced MCT4 expression (Fig. 19H), its depletion significantly reduced the lactate secretion (Fig. 19, I and J).

To further confirm the overlapping functions of HPIP and HIF-1α in the context of oncogenesis, we performed tumor xenograft studies in nude mouse model using 4T1 cells. In support of the *in vitro* data, mice injected with shCtrl-4T1 clones displayed prominent tumor growth; the other mice injected with either shHPIP or siHIF-1α had significantly smaller tumors. Moreover, the mice injected with 4T1 cells that are transfected with HIF-1α and T7-HPIP could not restore the tumor growth (Fig. 20, A-D). *In vivo* imaging of the dissected tumors from the mice showed GFP autofluorescence emerging out of the cells (Fig. 20, E and F). Further, histological analysis of

tumor sections showed higher cell density in shCtrl-4T1/nude mice as compare to the rest of the groups (Fig. 20G). In support of the *in vitro* data, GLUT1 expression in tumor samples also shown its reduced expression in HPIP or HIF-1α knocked down condition and also HPIP ectopic expression failed to restore it in HIF-1α depleted cells (Fig. 20H). Taken together our data suggested that HPIP enhances Warburg effect through HIF-1α under normoxia.

3.2. (b) HPIP stabilizes HIF-1α under normoxia in breast cancer cells

We next investigated the mechanism underlying the dependence of HIF-1α on HPIP in normoxic regulation of cell growth and tumorigenesis. Under normoxia conditions PHD hydroxylates HIF-1α and, hydroxylated protein is subsequently recognized by pVHL leading to the ubiquitination and then proteasome-dependent degradation (Jaakkola et al., 2001). Intriguingly, few reports pitch in regarding the stability of HIF-1α under normoxia (Yoo et al., 2006; Doe et al., 2012; Kim et al., 2015; Iommarini et al., 2017). We ascertained if HPIP could regulate HIF-1α under normoxia and evaluated the endogenous HIF-1α expression by altering the expression of HPIP. The depletion of HPIP expression in MDA-MB-231 cells profoundly decreases HIF-1α protein, but not it's mRNA suggesting the possible role of ubiquitination in the regulation of HIF-1α (Fig. 21, A and B). Analysis of the expression of HPIP and HIF-1α in a panel of breast cancer cells cultured in normoxia showed a positive correlation, except in T47D and ZR75 (Figure 21, C and D). This raised the possibility of regulation of HIF-1α by HPIP in these cells. We therefore evaluated the endogenous HIF-1α expression by altering the expression of HPIP in MCF-7 cells. The ectopic overexpression of HPIP in MCF-7 cells (HPIP low/HIF-1α low) enhanced HIF-1α expression (Fig. 21E). Additionally, under normoxia, ectopic expression of T7-HPIP in HEK239T cells (endogenous abundance of both HPIP and HIF-1α proteins is very low) elevated HIF-1α protein, while its mRNA levels were unaltered (Fig. 21, F and G). Interestingly, HIF-1α is readily

ubiquitinated in control cells, while T7-HPIP ectopic expression markedly reduced it (Fig. 21H; lane's 2 vs 3).

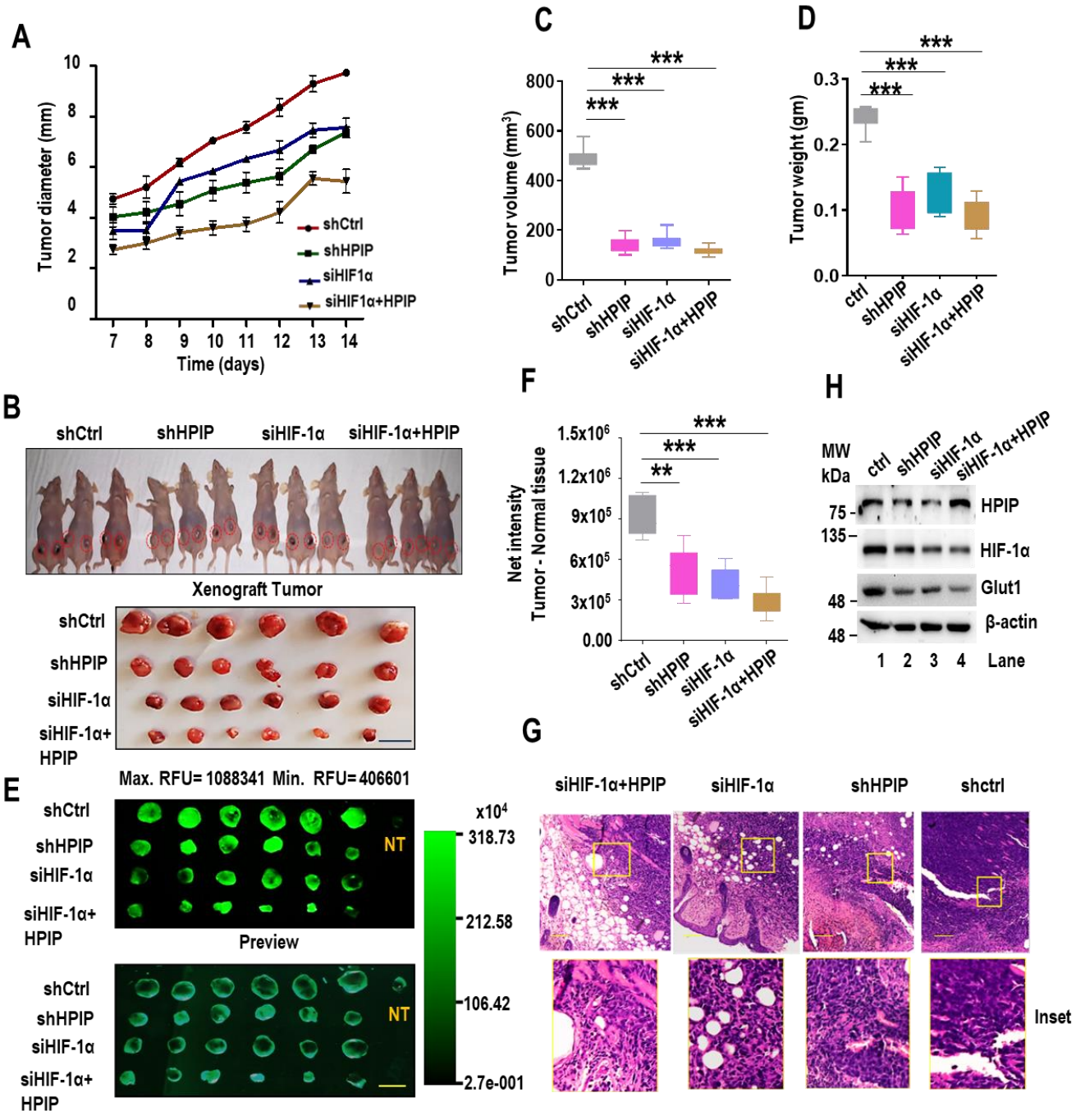

Fig. 20. HPIP promotes Warburg effect and confer cell growth on TNBC cells under normoxia.

(**A-H**) Stably generated 4T1 cells (shCtrl or shHPIP) were transfected with siCtrl, siHIF-1α or siHIF-1α plus Flag-HPIP as indicated, injected subcutaneously in nude mice along with Matrigel and kept for 15 days monitoring up to 15 days and (**A**) measured the diameter of tumors. Animals were sacrificed and excised the tumors. (**B**) **Upper panel**, physical appearance of nude mice, (**B**) **Lower panel**, image of excised tumors. Scale bar: 1 cm. Quantification of (**C**) Tumor volumes and (**D**) excised tumor's weight. (**E**) Quantification and comparison of net fluorescence unit derived from In-vivo imaging of the tumor tissue, **upper**, fluorescence image of the tumors, **lower**, a preview of the tumors. Scale bar: 1 cm (**F**) net fluorescence was measured (n= 3 per group on both planks). (**G**) Image of H and E staining. Scale bar: 100 cm (**H**) Tumor tissues were subjected to WB using β-actin as an internal control. Data represents mean ± SD (*P<0.05, **P<0.01, ***P<0.001, unpaired Student's t-test), ns-not significant.

We next measured the half-life of endogenous HIF-1α in HPIP silencing MDA-MB-231 cells following cycloheximide, a protein translation inhibitor, treatment. As expected, the half-life of HIF-1α was substantially longer in control cells (30 min) as compared to HPIP silencing clones #shHPIP1 or #shHPIP2 (7.5 min), but MG132, a proteasomal inhibitor, treatment abrogated HIF-1α degradation suggesting that HPIP inhibits proteasome-mediated degradation of HIF-1α (Fig. 22, A-D). HPIP is predominantly a cytoplasmic protein that is known to regulate PI3K/AKT pathway (Manavathi et al., 2006) and also reported that PI3K/AKT activation is required for HIF-1α stabilization (Joshi et al., 2014). Given these premises, we rationalized that HPIP may regulate HIF-1α stabilization via PI3K/AKT pathway. Accordingly, ectopic expression of HPIP activated AKT, measured by pAKT at T308, and enhanced HIF-1α protein levels, either in HEK293T or MDA-MB-231 cells (Fig. 22, E and F). Consistent with this data, specific inhibition of PI3K by LY290002 results in marked decrease in HIF-1α levels (Fig. 22G). We did not observe any significant change in HIF-1α hydroxylation after HPIP depletion suggesting that HPIP-mediated HIF-1α stability is VHL-independent (Fig. 22H). Since GSK3β, one of the downstream targets of AKT, is known to destabilize HIF-1α via direct phosphorylation (Mennerich et al., 2014), we ascertained if HPIP enhances HIF-1α stability by inhibiting GSK3β. Consistent with earlier

reports, we also observed a marked decrease in HIF-1α levels upon ectopic expression of GSK3β-wt but not with GSK3β-KD (kinase dead) (Fig. 22I, lane 3 and 5). As expected, HIF-1α levels were restored upon ectopic expression of HPIP in GSK3β (wt/KD) transfected cells (Fig. 22I, lane 2 and 4). Together, these data suggest that HPIP regulates normoxic stabilization of HIF-1α in breast cancer cells via PI3K/AKT/GSK3β axis.

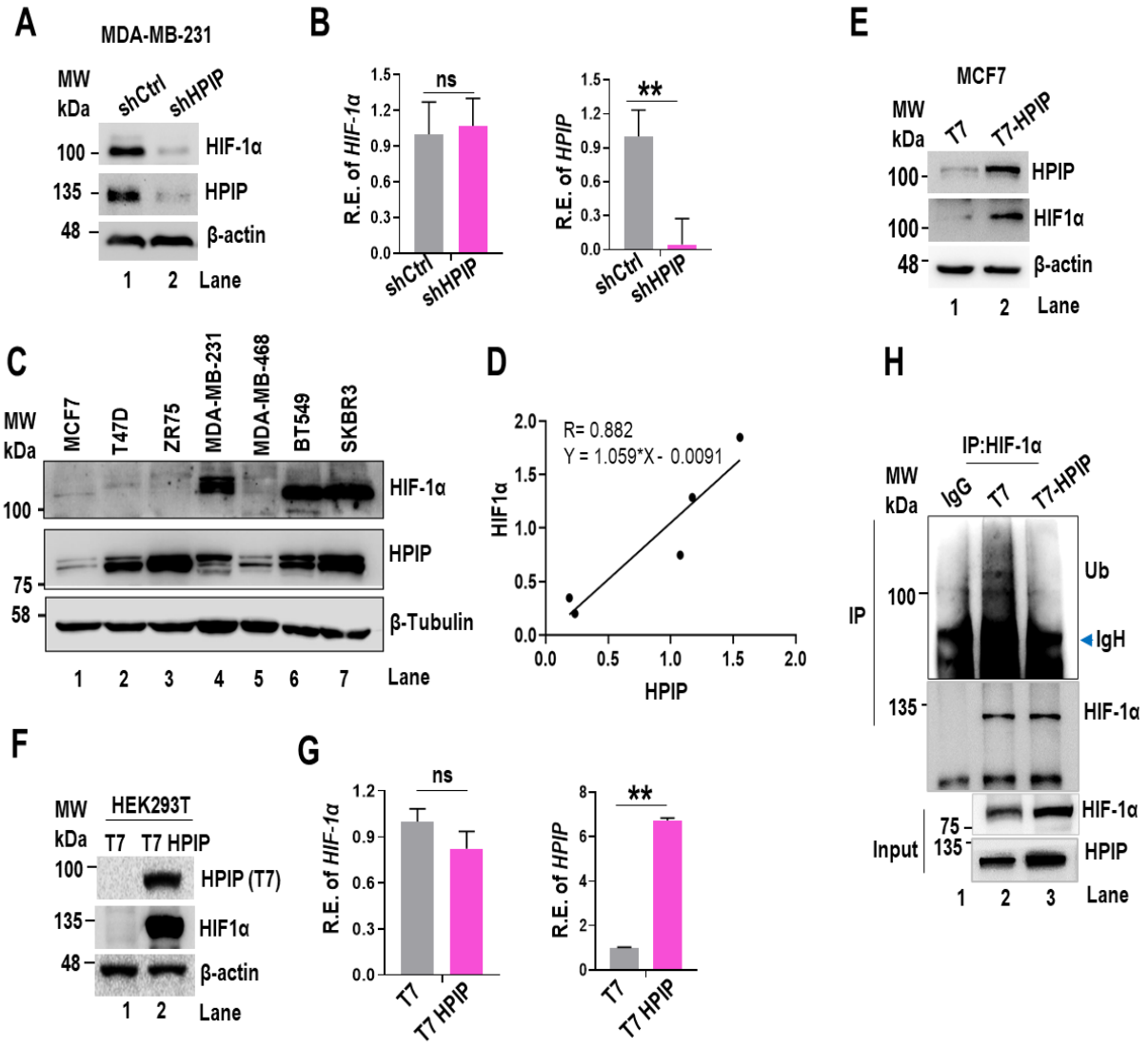

Fig. 21. HPIP stabilizes HIF-1α under normoxia in TNBC cells.

(**A**, **B**) MDA-MB-231 with shCtrl or shHPIP were harvested and analyzed by (**A**) WB and (**B**) qRT-PCR, **left**, relative expression (R.E.) of HIF-1α, **right**, relative expression (R.E.) of HPIP. β-actin was used as an internal control. (**C**) WB analysis of various breast cancer cell lines as indicated with HPIP and HIF-1α antibodies and β-Tubulin as an internal control. (**D**) The band intensities were measured and the correlative expression (Pearson R) between HPIP and HIF-1α was quantified (excluding T47D and ZR75) (**P<0.01). **(E**) Post transfection (36 h) of MCF-7 cells with T7 or T7-HPIP plasmids were harvested and analyzed by WB (**F, G**) Post transfection (36 h) of HEK293T cells with T7 or T7-HPIP plasmid were harvested and analyzed by (**F**) WB and qRT-PCR (**G**) **left**, HIF-1α, **right**, HPIP. β-actin was used as an internal control. (**H**) MDA-MB-231 cells were transfected (24 h) with T7 or T7-HPIP plasmids followed by immunoprecipitation with HIF-1α antibody and then analyzed by WB. Data represent mean ± SD, N=3 (**P<0.01, unpaired Student's t-test).

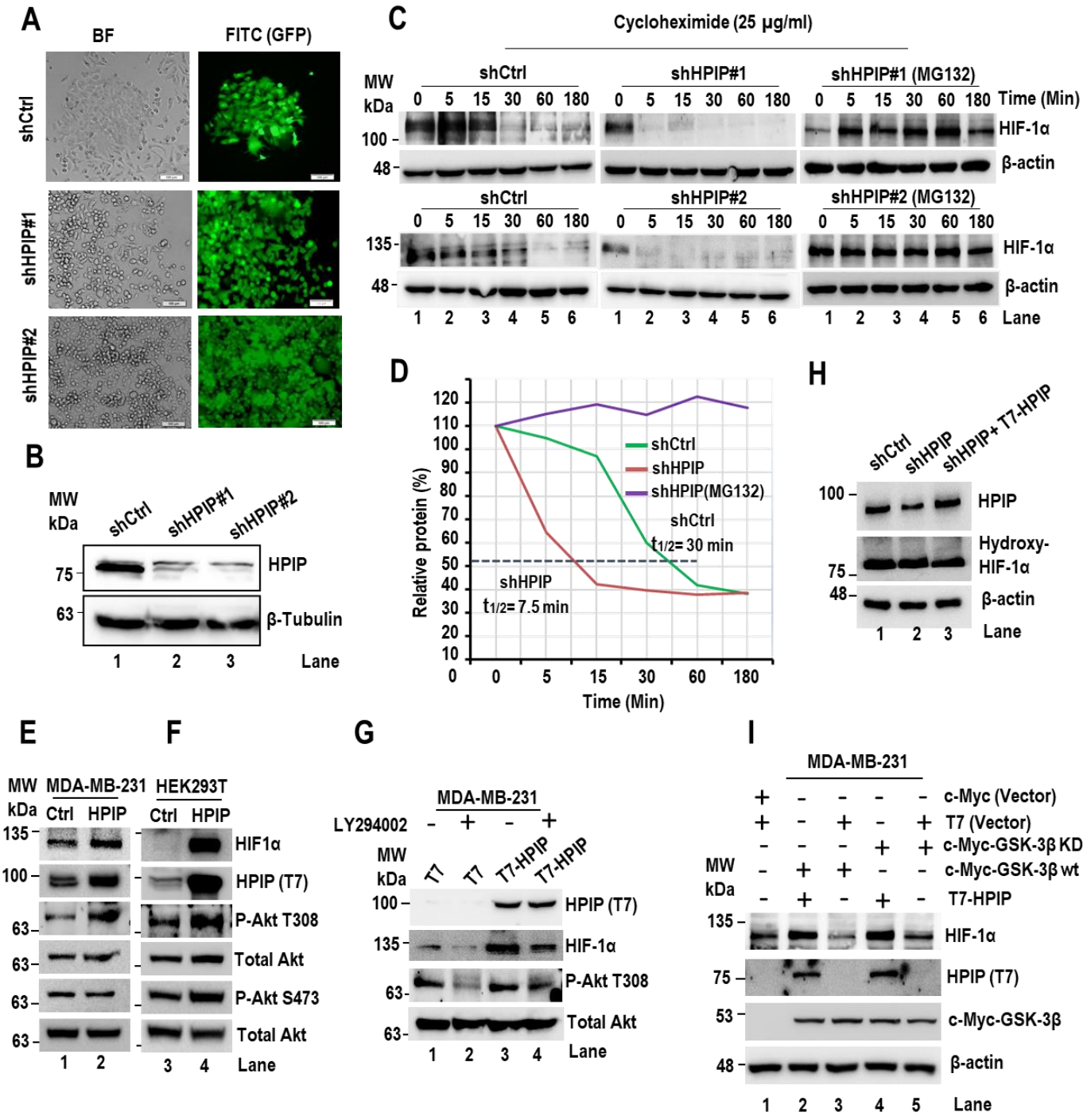

Fig. 22. HPIP stabilizes HIF-1α under normoxia in TNBC cells.

(**A, B**) Representative images of stably generated MDA-MB-231 cells (shCtrl, shHPIP#1 or shHPIP#2) by lentiviral transduction method, scale bar: 100 μm. (**B**) Cell lysates were analyzed by WB using Tubulin as an internal control. (**C**) Cycloheximide chase assay, MDA-MB-231 (shCtrl and shHPIP) cells were treated with or without MG132 at indicated time points and cell extracts were analyzed by WB as indicated. (**D**) Quantification and measurement of half-life ($t_{½}$ min) of HIF-1α. (**E-F**) Cells were transfected with T7 or T7-HPIP plasmids and WB was

performed using extracts of (**E**) MDA-MB-231 and (**F**) HEK293T. (**G**) Transfected MDA-MB-231 cells with T7 or T7-HPIP plasmids were treated with or without LY294002 (PI3K inhibitor) and performed WB. (**H**) Cells transfected with shCtrl, shHPIP or shHPIP plus T7-HPIP were analyzed by WB using β-actin as an internal control. (**I**) Effect of co-transfection of pcDNA vector (T7) or pcDNA-HPIP (T7-HPIP) and c-Myc-GSK-3β wt (wild type) or c-Myc-GSK-3β KD (Kinase dead) on HIF-1α in MDA-MB-231 cells as demonstrated by WB. β-actin is used as an internal control. Data represent mean ± SD (**P<0.01, unpaired Student's t-test, n=3).

3.3. Role of HPIP in oxygen-dependent plasticity of breast cancer cells

3.3. (a) Mathematical modeling in concert with cell proliferation/invasion index studies suggest phenotypic plasticity between HPIP^{low}/ HIF-1α^{low} and HPIP^{high}/HIF-1α^{high} cell states in breast cancer cells

Integrating our quantitative experimental data of HIF-1α (Western blot, RT-PCR and half-life analysis), we constructed a quantitative mathematical model to characterize the dynamics of the feedback loop by HPIP and HIF-1α. HIF-1α can transcriptionally activate HPIP (Fig. 11), while HPIP stabilizes HIF-1α by modulating its half-life (Fig. 22). This feedback loop can give rise to bistability in the system, i.e., cells can attain HPIP^{low}/ HIF-1α^{low} or HPIP^{high}/HIF-1α^{high} states (shown by two solid circles in Fig. 23A, left), and can switch between these states stochastically (Fig. 23A, right) once cells cross a specific 'tipping point' or threshold (shown by hollow circle in Fig. 23A, left). These simulations suggest that mutual reinforcement between HPIP and HIF-1α can stabilize the HPIP^{high}/ HIF-1α^{high} state. In support of these predictions, we also observed cells expressing HPIP^{high}/ HIF-1α^{high} while transitioning from epithelial to mesenchymal phenotype upon switching the microenvironment gradually from normoxia to hypoxia (O_2 %: 21 to 1) (Fig. 23B). Interestingly, we also observed that switch from a HPIP^{low}/ HIF-1α^{low} to a HPIP^{high}/ HIF-1α^{high} state can be driven by increasing the abundance of either HPIP or HIF-1α (Fig 23, C and D). This observation suggests that cells can maintain high levels of HIF-1α even under normoxic conditions, when HPIP stabilizes HIF-1α. Also, in hypoxic conditions when HIF-1α is upregulated, HPIP levels can be upregulated and maintained. Sensitivity analysis shows the

robustness of these predictions upon parameter variation, indicating that this phenotypic switching emerges from the topology of the HPIP/HIF-1α feedback loop (Fig. 23, E-J).

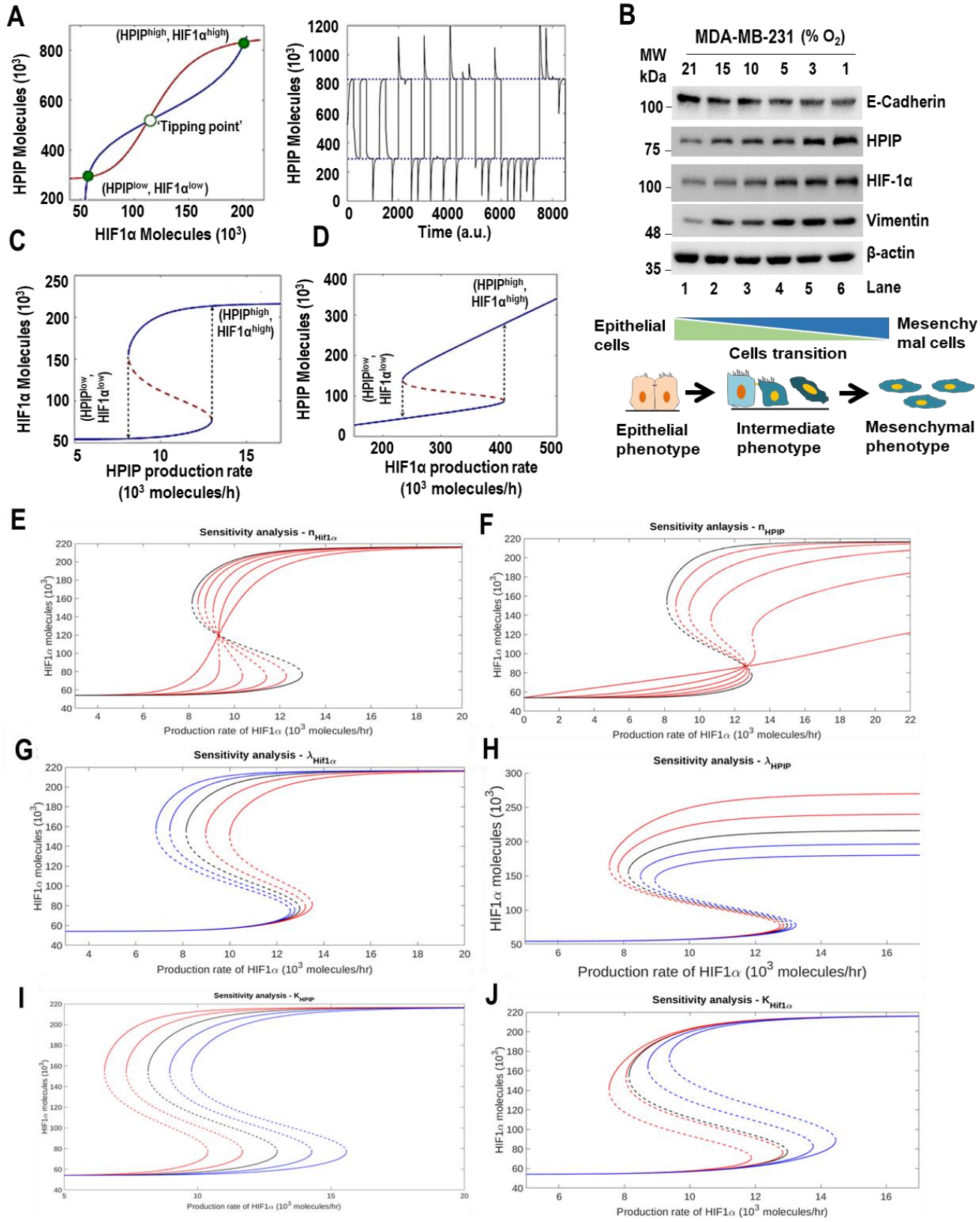

Fig. 23. Mathematical modeling in concert with proliferation/invasion index studies suggest phenotypic plasticity between (HPIPlow/ HIF-1αlow) and (HPIPhigh/ HIF-1αhigh) cell states. (**A**) (**left**) Nullcline simulations for the mathematical model, where red curve represents the change in HPIP levels upon changing HIF-1α, and blue curve represents the change in HIF-1α levels upon changing HPIP. The solid green circles represent the two possible stable steady states (phenotypes) – ($HPIP^{low}$/ $HIF\text{-}1\alpha^{low}$), ($HPIP^{high}$/ $HIF\text{-}1\alpha^{high}$). The hollow circle indicates an unstable state. (**right**) stochastic simulations showing cells switching between these states (indicated by dotted blue lines). (**B**) MCF7 cells were incubated for 24 h at different concentrations of O_2 as indicated and performed WB using β-actin as an internal control. (**C**) Bifurcation diagram showing how cells in ($HPIP^{low}$/ $HIF\text{-}1\alpha^{low}$) state can switch to ($HPIP^{high}$/ $HIF\text{-}1\alpha^{high}$) state upon increasing HPIP production rate. Solid curves reflect stable states; dotted red lines indicate unstable states. (**D**) Same as (**C**) but with varying HIF-1α production rate. (**E-J**) Effect of variation in different parameters on the bistability in the system. (**E**) and (**F**) are varied from 6 (black) to 1; decreasing bistable region with decreasing n is seen. (**G**), (**H**), (**I**) and (**J**) are varied from the model values (black) by +10%, +20% (blue) and -10%, -20% (red). Bistability is retained in all cases.

Based on these predictions, we further argued that HPIP may display functional preference toward cancer cells to establish the cellular plasticity in response to switching of microenvironments i.e., from normoxia to hypoxia or vice-versa. To test this hypothesis, we measured cell proliferative index at normoxia (PI^N) or hypoxia (PI^H) and cell invasion index at normoxia (INI^N) or hypoxia (INI^H) as well as cell migration index at normoxia (MI^N) or hypoxia (MI^H) by culturing MDA-MB-231 cells at respective condition following HPIP knockdown. Indeed, as compared to control, HPIP silencing results in a significant loss of proliferative index by these cells when switched from hypoxic to normoxic microenvironment ($PI^H=0.95\pm0.1$ vs. $PI^N=0.72\pm0.1$) ($p<0.001$) (Fig. 24, A and B). On the other hand, regarding cell migration and invasion indices, we observed an inverse effect by these cells under similar stress conditions. Upon HPIP silencing, MDA-MB-231 cells exhibited a significant loss of invasion index ($INI^N=0.50\pm0.0$ vs. $INI^H=0.37\pm0.0$) as well as migration index ($MI^N=0.33\pm0.0$ vs. $MI^H=0.14\pm0.0$) when switching from normoxic to hypoxic microenvironment ($p<0.01$) (Fig. 24, C-F). Similarly, depletion of HPIP expression in 4T1 cells shows a significant loss of migration index ($MI^N=0.53\pm0.02$ vs. $MI^H=0.32\pm0.01$) (Fig. 24, G and H). In supporting these data, we also observed a correlative spatial expression of HIF-1α and HPIP

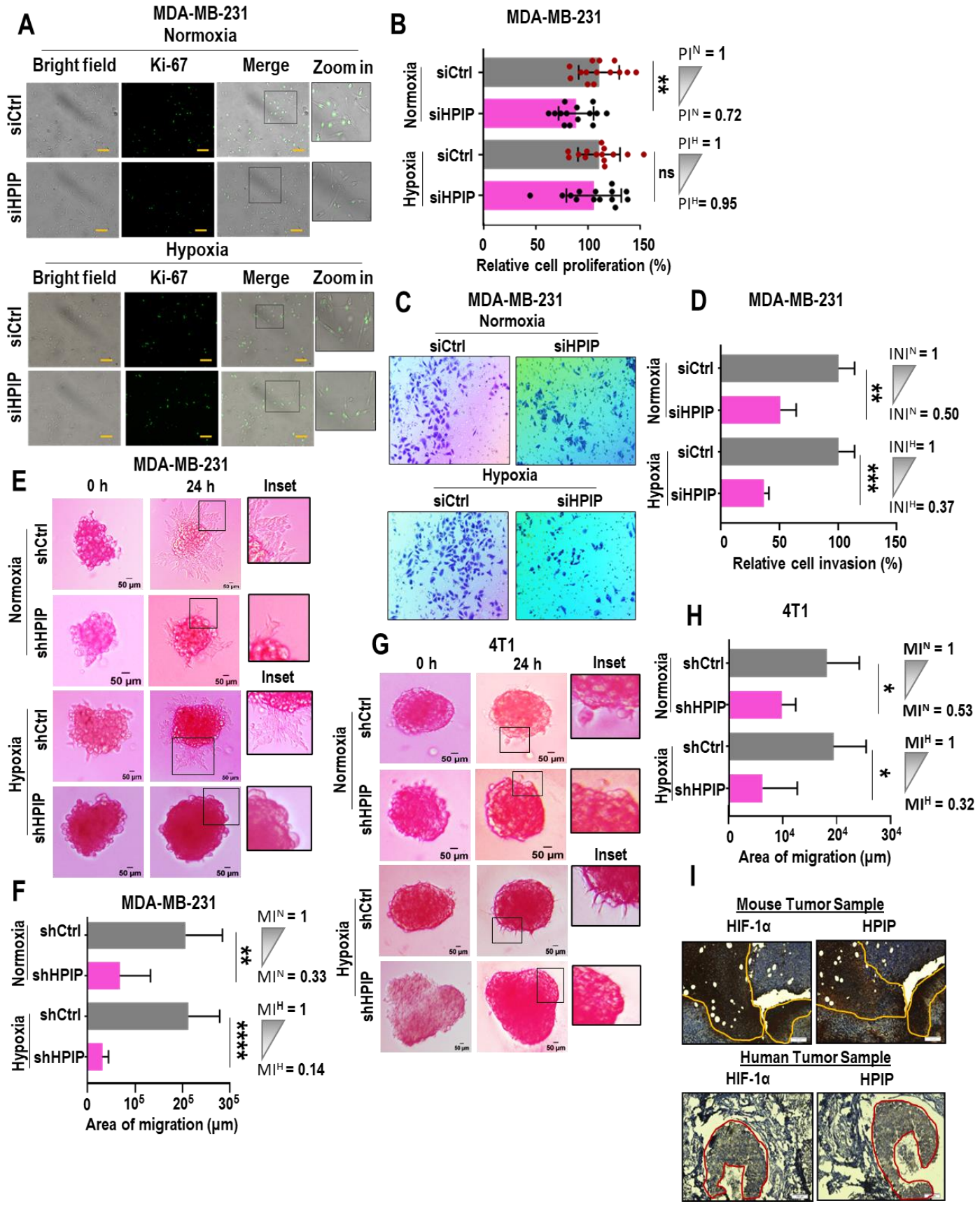
A
MDA-MB-231
Normoxia
Bright field
Ki-67
Merge
Zoom in
siCtrl
siHPIP
Hypoxia
B
MDA-MB-231
Normoxia
siCtrl
siHPIP
Hypoxia
siCtrl
siHPIP
**
ns
PI^N = 1
PI^N = 0.72
PI^H = 1
PI^H= 0.95
0
50
100
150
Relative cell proliferation (%)
C
MDA-MB-231
Normoxia
siCtrl
siHPIP
Hypoxia
siCtrl
siHPIP
D
MDA-MB-231
Normoxia
siCtrl
siHPIP
Hypoxia
siCtrl
siHPIP
**
***
INI^N = 1
INI^N = 0.50
INI^H= 1
INI^H= 0.37
0
50
100
150
Relative cell invasion (%)
E
MDA-MB-231
0 h
24 h
Inset
Normoxia
shCtrl
shHPIP
Hypoxia
shCtrl
shHPIP
50 µm
Inset
F
MDA-MB-231
Normoxia
shCtrl
shHPIP
Hypoxia
shCtrl
shHPIP
**
****
MI^N = 1
MI^N = 0.33
MI^H = 1
MI^H = 0.14
0
10^5
20^5
30^5
Area of migration (µm)
G
4T1
0 h
24 h
Inset
Normoxia
shCtrl
shHPIP
Hypoxia
shCtrl
shHPIP
50 µm
Inset
H
4T1
Normoxia
shCtrl
shHPIP
Hypoxia
shCtrl
shHPIP
*
*
MI^N = 1
MI^N = 0.53
MI^H = 1
MI^H = 0.32
0
10^4
20^4
30^4
Area of migration (µm)
I
Mouse Tumor Sample
HIF-1α
HPIP
Human Tumor Sample
HIF-1α
HPIP

Fig. 24. Mathematical modeling in concert with proliferation/invasion index studies suggest phenotypic plasticity between (HPIPlow/ HIF-1αlow) and (HPIPhigh/ HIF-1αhigh) cell states. (**A-B**) MDA-MB-231 cells were exposed to hypoxia or normoxia (siCtrl or siHPIP) for 24 h and performed Immunofluorescence assay using Ki-67 and measured the Ki-67 positive cells and plotted as the relative percentage of cell proliferation. (**C**) The Invaded cells were fixed, permeabilized, stained and imaged, scale bar: 100 µm, and (**D**) measured the relative percentage of invaded cells and invasion index (INI) (siCtrl vs siHPIP) in hypoxia or normoxia. (**E-H**) Disseminated cells (shCtrl or shHPIP) from the spheroids cultured under hypoxia or normoxia, scale bar: 50 µm, were evaluated for migration index (MI) and quantified (**D, E**) MDA-MB-231 (**G, H**) 4T1. (**I**) Spatial protein expression of HIF-1α and HPIP in tumor by IHC in orthotopically derived tumor with 4T1 cells and Human breast tumor samples, scale bar: 100 µm. Data represents mean ± SD (**P<0.01, ***P<0.001, ****P<0.0001, unpaired Student's t-test).

in subcutaneously transplanted mouse derived cancer tissue (upper panel) as well as human TNBC patient's tissue sample (lower panel) (Fig. 24I). Collectively, our results suggest the existence of phenotypic plasticity behavior between $HPIP^{low}$/ $HIF\text{-}1\alpha^{low}$ and $HPIP^{high}$/ $HIF\text{-}1\alpha^{high}$ states that can happen in normoxic or hypoxic condition.

3.4. Correlative expression of HPIP, SRP14 and HIF-1α in breast cancer patient's tumor tissues

In order to correlate the reciprocal regulation of HPIP and HIF-1α with clinical samples, we analyzed their expression in TNBC samples by western blotting (N=10). The data revealed a significantly higher expression of HPIP and HIF-1α in TNBC samples than adjacent breast tissue (Fig. 25, A and B). Similarly, SRP14 expression was also elevated in TNBC samples. Consistent with this data, immunohistochemical (IHC) analysis also revealed a significantly elevated level of HPIP, SRP14 and HIF-1α in TNBC samples over adjacent breast tissue (Fig. 25, C and D). Supporting this data, analysis of TCGA database showed a significantly higher expression of HPIP, SRP14 and HIF-1α in invasive ductal breast carcinomas (IDBC) (N=1556) over normal breast tissue (N=144) (p<0.0001) (Fig. 25E).

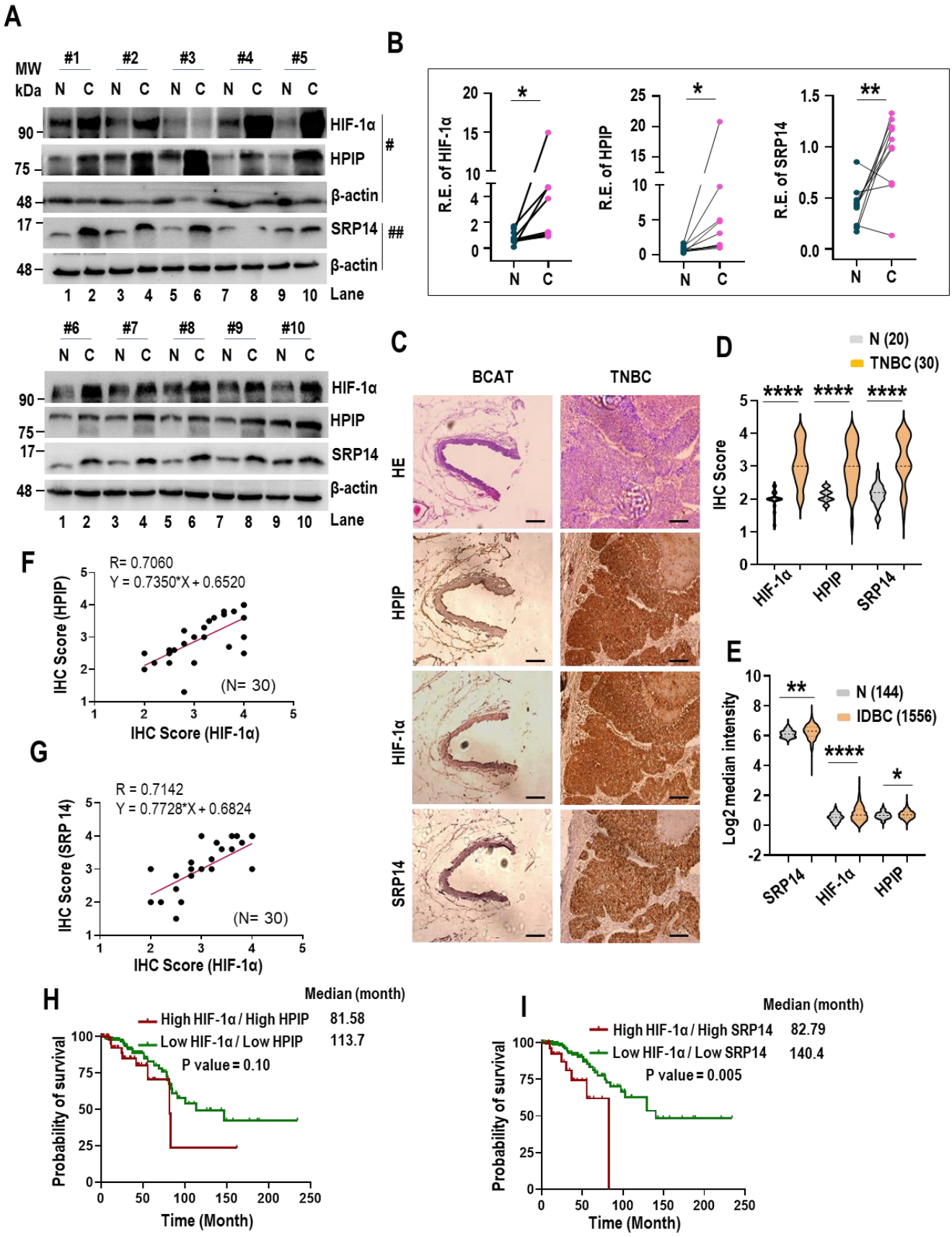
A
MW
kDa
#1
#2
#3
#4
#5
N C N C N C N C N C
90
75
48
17
48
HIF-1α
HPIP
β-actin
SRP14
β-actin
#
##
1 2 3 4 5 6 7 8 9 10 Lane
#6
#7
#8
#9
#10
N C N C N C N C N C
90
75
17
48
HIF-1α
HPIP
SRP14
β-actin
1 2 3 4 5 6 7 8 9 10 Lane
B
R.E. of HIF-1α
R.E. of HPIP
R.E. of SRP14
*
*
**
N C
N C
N C
C
BCAT
TNBC
HE
HPIP
HIF-1α
SRP14
D
N (20)
TNBC (30)
IHC Score
****
****
****
HIF-1α
HPIP
SRP14
E
Log2 median intensity
**
****
*
N (144)
IDBC (1556)
SRP14
HIF-1α
HPIP
F
R= 0.7060
Y = 0.7350*X + 0.6520
IHC Score (HPIP)
(N= 30)
IHC Score (HIF-1α)
G
R = 0.7142
Y = 0.7728*X + 0.6824
IHC Score (SRP 14)
(N= 30)
IHC Score (HIF-1α)
H
Median (month)
High HIF-1α / High HPIP 81.58
Low HIF-1α / Low HPIP 113.7
P value = 0.10
Probability of survival
Time (Month)
I
Median (month)
High HIF-1α / High SRP14 82.79
Low HIF-1α / Low SRP14 140.4
P value = 0.005
Probability of survival
Time (Month)

Fig. 25. Expression of HPIP/SRP14 correlate with HIF-1α in TNBC patients.

(**A, B**) Patient's tumor samples (TNBC) (denoted as C) along with corresponding adjacent normal tissue (ANT) (denoted as N) were lysed and subjected to WB as indicated. (**B**) Expression of HPIP, HIF-1α or SRP14 was quantified and the expression between tumor samples with adjacent normal tissue was compared. [n= 10 (C) and (N) each, paired Student's t-test, *P<0.05, **P<0.01) (**C**) Paraffin TNBC and ANT were subjected to H and E staining or immunohistochemical staining with indicated antibodies, scale bar: 100 μm and (**D**) IHC score for each sample were determined and compared between TNBC and ANT for all three proteins as indicated. (TNBC= 30 and ANT= 20, unpaired Student's t-test, ****P<0.0001). (**E**) Oncomine derived expression analysis of HPIP, SRP14 and HIF-1α in invasive ductal breast carcinoma (IDBC) as compared to normal tissue (N). (IDBC= 1556 and N=144, unpaired Student's t-test, *P<0.05, **P<0.01, ****P<0.0001). Data represent mean ± SD. (**F, G**) IHC score derives from TNBC samples (**D**) were used to analyze the correlative expression (Pearson R) between (**F**) HPIP and HIF-1α (**G**) SRP14 and HIF-1α. (****P<0.0001, Two-tailed test). (**H, I**) The Kaplan Meier survival curve for high and low co-gene expression, (**H**) between high HPIP/HIF-1α and low HPIP/HIF-1α (**I**) between high SRP14/HIF-1α and low SRP14/HIF-1α. (**P<0.001, Log-rank (Mantel-Cox) test).

Furthermore, we found a significant correlative expression of HPIP or SRP14 with HIF-1α in TNBC samples (N=30) (R=0.70 and 0.71, respectively) (Fig. 25, F and G). Patient survival analysis by Kepler-Meier plot further indicated a significant loss of survival in patients with high HPIP or SRP14 and high HIF-1α vs. low HPIP or SRP14 and low HIF-1α (p<0.1 and 0.005, respectively) (Fig. 25, H and I). Together these compelling data suggest that expression of HPIP or SRP14 correlates with HIF-1α in TNBC samples and confers poor survival rate of breast cancer patients.

3.5. Discussion

In this study, we show that breast cancer cells display phenotypic plasticity upon switching from hypoxic to normoxic microenvironments or vice-versa by employing a reciprocal positive feedback regulation of HPIP and HIF-1α. We propose a model wherein, under hypoxia, HIF-1α induces *HPIP* expression which ensures cancer cell survival and metastasis; conversely, in normoxia, HPIP stabilizes HIF-1α and confers Warburg effect and cell growth on breast cancer

cells (Fig. 27). HPIP has been shown to play pleiotropic roles as it is involved in cell proliferation, differentiation, migration and invasion that are coupled with cell cycle regulation, EMT or anti-apoptosis processes (Manavathi et al., 2012; Bugide et al., 2015; Pan et al., 2016; Wang et al., 2016; Chen et al., 2016b; Khumukcham et al., 2019). Despite HPIP playing these diverse functions, it remains largely unknown whether HPIP influences phenotype plasticity in cancer cells in response to changing microenvironments from hypoxia to normoxia or vice-versa, which prevail in solid tumors. Although hypoxia causes cytotoxicity in normal cells, it provides selective advantage to the cancer cells in solid tumors via HIF-1α to become more aggressive clones that acquire features like metastatic ability, chemo-resistance, tumor recurrence etc. (Semenza, 2000; Melillo, 2007). Our study shows that HPIP is induced in response to hypoxia in a HIF-1α-dependent manner and is implicated in cell survival, migration, invasion, EMT and stemness in breast cancer cells. The EMT and cancer stem cell (CSC) phenotype represents the characteristic feature of an epithelial to mesenchyme plasticity (EMP), which drives tumor metastasis and chemoresistance (Tsai and Yang, 2013; Elshamy and Duhe, 2013; Jia et al., 2019; Lu and Kang, 2019; Williams et al., 2019; Dong et al., 2020a;). We observed that HPIP is required for the expression of EMT markers and cancer stem cell phenotype under hypoxia. In support of this, *in vivo* tumor xenograft studies further demonstrated that HPIP is required for lung metastasis in breast cancer cells. These observations support the point that HPIP confers EMT and CSC phenotype, thereby increasing metastatic potential on breast cancer cells under hypoxia by controlling EMP. Under normoxia our findings revealed that HPIP foster Warburg effect and cell growth on breast cancer cells. Decreased lactate synthesis and down regulation of glucose importer GLUT1, LDH etc. upon HPIP silencing is an indication of suppressed Warburg effect. Moreover, *in vivo* tumor xenograft studies further demonstrated that HPIP facilitates tumor growth progression in normoxia. Our very recent findings showed an induced expression of HPIP under energy (glucose) stress in breast cancer cells (Penugurti et al., 2019). HPIP promotes breast cancer

cell survival under acute glucose stress by modulating glutaminolysis through interaction with MYC oncogene. In contrast, cancer cells undergo apoptosis in chronic glucose stress by RNF2-mediated ubiquitination of HPIP and concomitant proteolysis by the 26-proteasome pathway. The present study revealed that HPIP is induced under hypoxia and contributes to cancer cell survival. Moreover, the HPIP gene is first appeared in Danio rerio (Zebrafish) (Fig. 26). It implies that HPIP has been evolved as a stress response gene in the higher eukaryotes as it doesn't express in lower organisms. In support of these findings proliferative and invasive index studies revealed that HPIP drives cell growth over invasion of breast cancer cells cultured in normoxia and an inverse effect in hypoxia. These microenvironment-dependent dual functional natures of HPIP allows cancer cells to display cellular plasticity in regulating diverse cellular functions and thus phenotypic heterogeneity in solid tumors. Mechanistically we found that HPIP executes two distinct mechanisms to establish phenotypic plasticity in breast cancer cells. In hypoxia, HPIP potentiates MMP9 protein expression by interacting with SRP14 dependent protein translation. SRP14 is an integral part of signal recognition particle (SRP) that is essential for targeting of nascent polypeptide containing ribosomes onto endoplasmic reticulum (Akopian et al., 2013). SRP consists of SRP9, SRP14, SRP19, SRP54, SRP68 and SRP72 and a single 300 nucleotide 7S RNA. Among these, SRP9/14 are complexed with *Alu* RNA. Under certain physiological stresses, SPR14 localizes to stress granules that are enriched with mRNA, ribosomal machinery and signaling proteins and, promotes cell survival (Berger et al., 2014). We found that HPIP interacts with C-terminal region of SRP14 and colocalizes to stress granules in hypoxia. It is very intriguing as it provided the molecular clue for HPIP-mediated MMPs expression under hypoxia. Loss of expression of MMP by C-terminal defective mutant of SRP14 in presence of HPIP further implies physical interaction of HPIP with SRP14 is essential for MMPs expression.

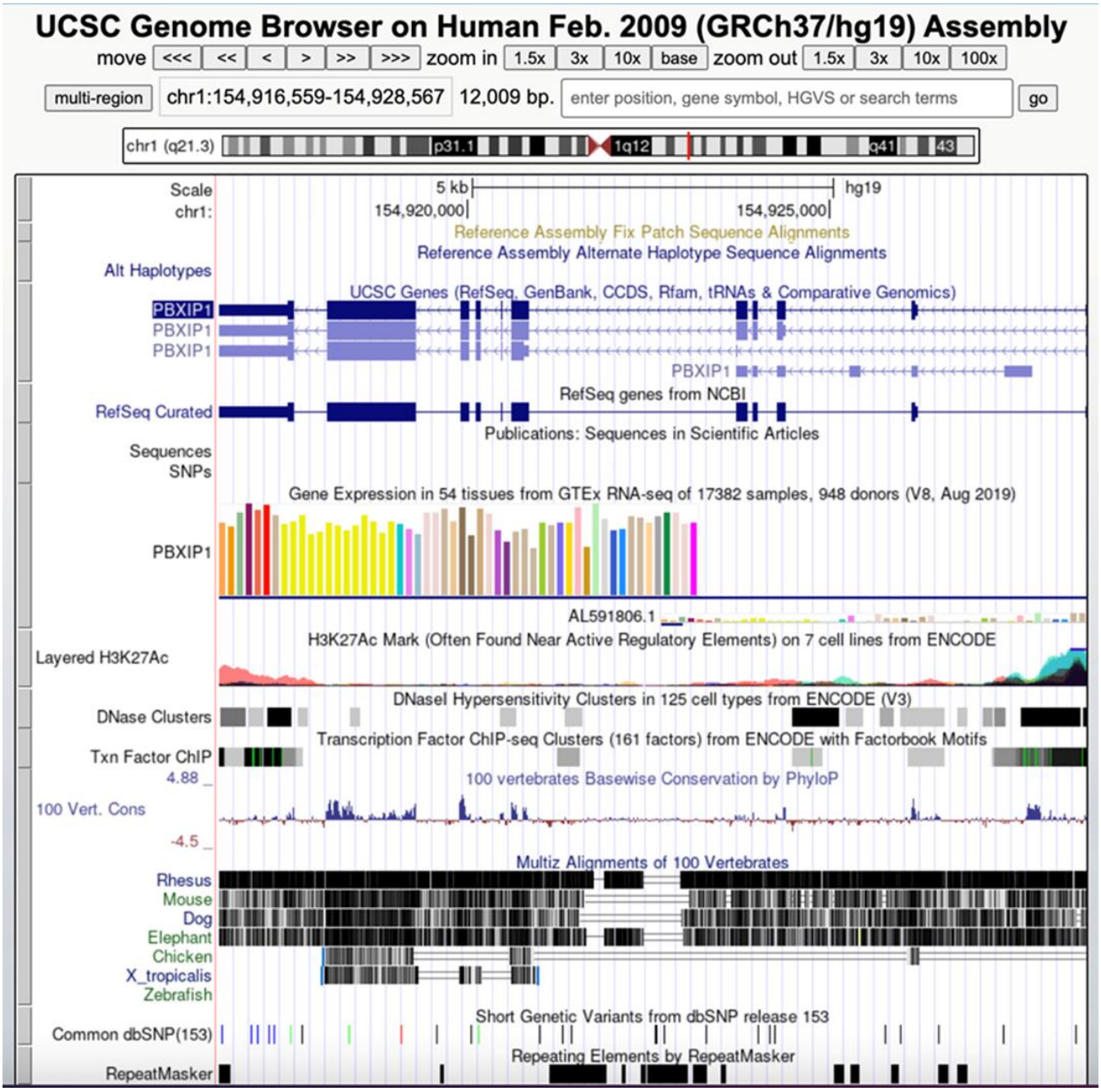

Fig. 26. HPIP (PBXIP1) gene map on chromosome 1q21.3. Comparison of *HPIP* gene among various species, including money, mouse, dog, elephant, chicken, frog and zebrafish.

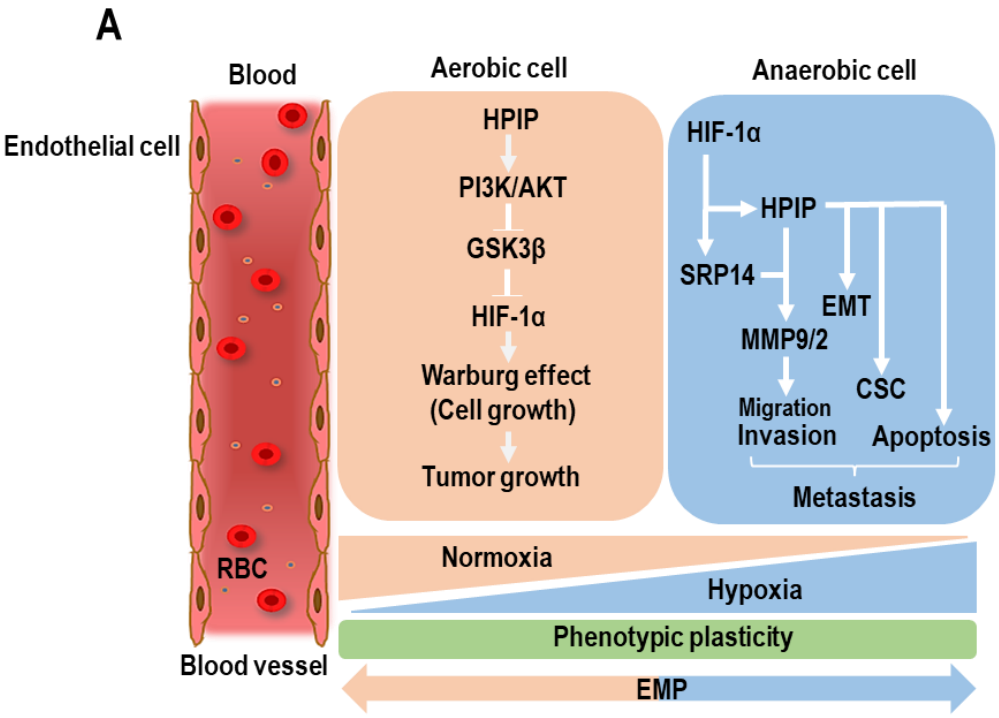
A
Blood
Aerobic cell
Anaerobic cell
Endothelial cell
HPIP
PI3K/AKT
GSK3β
HIF-1α
Warburg effect
(Cell growth)
Tumor growth
HIF-1α
HPIP
SRP14
EMT
MMP9/2
CSC
Migration
Invasion
Apoptosis
Metastasis
RBC
Blood vessel
Normoxia
Hypoxia
Phenotypic plasticity
EMP

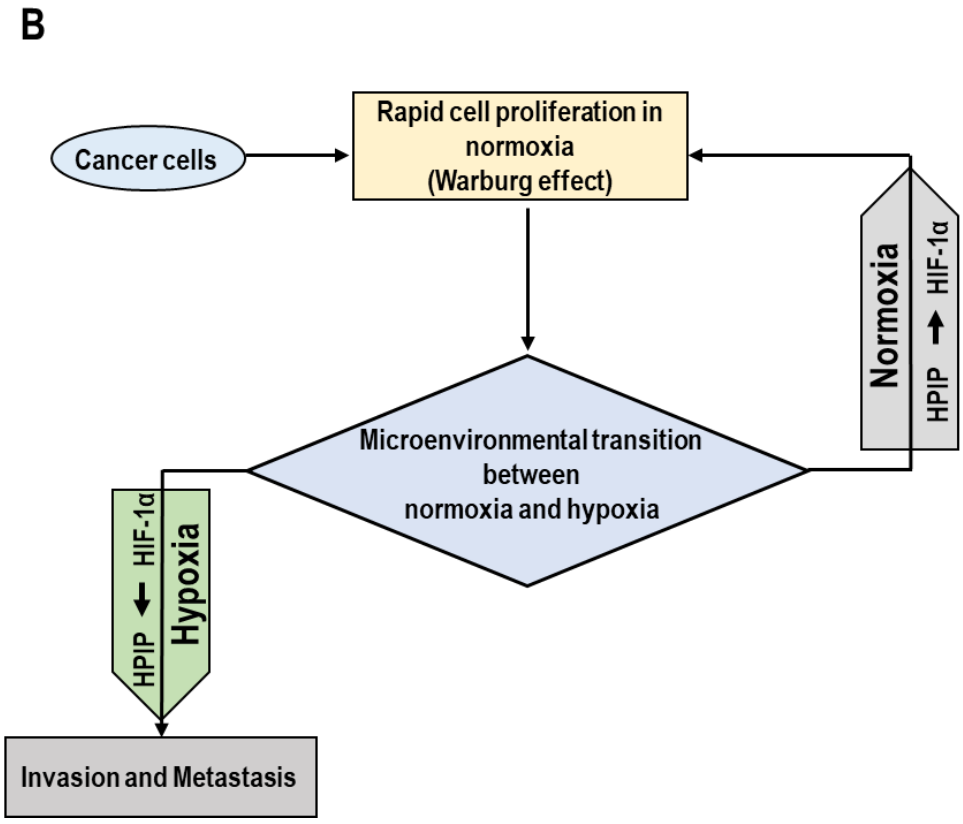
B
Cancer cells
Rapid cell proliferation in
normoxia
(Warburg effect)
Normoxia
HIF-1α
HPIP
Microenvironmental transition
between
normoxia and hypoxia
HPIP
HIF-1α
Hypoxia
Invasion and Metastasis

Fig. 26. Proposed model depicting reciprocal positive feedback regulation between HPIP and HIF-1α which controls phenotypic plasticity of breast cancer cells in response to microenvironment switch from hypoxia to normoxia or vice-versa.

(**A**) In solid tumors, cancer cells display phenotypic plasticity by regulating epithelial to mesenchymal plasticity (EMP) in response to microenvironment switch, i.e., normoxia to hypoxia. In aerobic cell, proximal to the blood vessel, HPIP stabilizes HIF-1α through PI3K/AKT-GSK3β signaling axis and promotes tumor growth. Vice-versa in anaerobic cell, away from the blood vessel, HIF-1α upregulates HPIP (also SRP14), which in turn causes cell migration/invasion and metastasis. HPIP promotes EMT, CSC (cancer stem cell) features while antagonizing apoptosis. (**B**) Flowchart depicts HIF-1α-HPIP loop regulating phenotypic plasticity in breast cancer cells. Under normoxia, HPIP stabilizes HIF-1α and promotes Warburg effect thereby enhancing rapid cancer cell proliferation. As cancer cells proliferate the cells distant from blood vessel become hypoxic cells. The transition from normoxia to hypoxia drives hypoxia induced HPIP upregulation via HIF-1α and promotes cancer cell invasion and metastasis.

In addition to this mechanistic evidence, clinical studies further implied an elevated expression of both HPIP and SRP14 positively correlating with HIF-1α in breast cancer patients. Furthermore, their expression indicates an unfavorable prognosis and poor survival of breast cancer patients. Together, these findings point that HIF-1α-HPIP-SRP pathway attributes metastatic potential on breast cancer cells in hypoxia.

Interestingly, our findings revealed that in normoxia HPIP confers cell growth via Warburg effect on breast cancer cells by enhancing HIF-1α stability. In normoxia, HIF-1α undergoes PHD dependent hydroxylation and subsequent ubiquitination by pVHL followed by proteasome-mediated degradation (Jaakkola et al., 2001). Various proteins like NQO1, MTA1, and TRAF6 have been reported to stabilize HIF-1α via direct interaction with it (Yoo et al., 2006; Sun et al., 2013a; Oh et al., 2016). Unlike these proteins, PI3K/AKT pathway regulates HIF-1α stability by inhibiting GSK3β-mediated phosphorylation. In support of the earlier reports combined with the present investigation that HPIP activates PI3K/AKT pathway (Manavathi et al., 2006; Wang et al., 2008; Chen et al., 2016b; Bugide et al., 2017), our findings imply that HPIP stabilizes HIF-1α by inhibiting GSK3β via PI3K/AKT activation. Cancer cells prefer glycolysis for its energy

generation and synthesis of cellular building blocks in aerobic conditions, Warburg effect, which is potentiated by HIF-1α and promotes cell growth and tumorigenesis (Vander Heiden et al., 2009; Doherty and Cleveland, 2013). Our findings indeed demonstrate HPIP dependent HIF-1α mediated expression of GLUT1, LDH, PFPK and lactate synthesis thereby increasing tumor growth progression in breast cancer cells.

In the tumor microenvironment, tumor cells might switch its cellular states dynamically from quiescence to proliferative, stem cells to non-stem cells and proliferative to invasive, and vice versa, while maintaining a dynamic equilibrium (Gupta et al., 2011). The cellular plasticity has been a conserved property in living systems as the regulation of cell-state decisions is critical for the survival (Gupta et al., 2011; Zellmer and Zhang, 2014). Emerging studies report that within individual tumors, cancer cells frequently exist in several possible phenotypic states and often exhibit diverse functional properties such as tumor-seeding ability, drug resistance etc., (Lapidot et al., 1994; Smalley and Ashworth, 2003; Singh et al., 2004; Li et al., 2007; Stingl and Caldas, 2007). Additionally, these cellular states of cancer cells are also found to be related to both tumor type and grade, and therefore impact on the treatment outcomes (Woodward et al., 2007; Li et al., 2008; Gupta et al., 2009). In support of the earlier reports our findings, revealed that breast cancer cells display phenotypic plasticity in response to varied environmental stresses. We provide the evidence that breast cancer cells show transition from proliferation^{high}-invasion^{low} to invasion^{high}-proliferation^{low} state as they switch from normoxia to hypoxia microenvironment or vice versa in a HPIP-HIF-1α dependent manner. In concordance with our experimental data, mathematical modeling predictions also support that in hypoxic conditions, when HIF-1α is upregulated, HPIP levels can be upregulated and maintained. Sensitivity analysis shows the robustness of these predictions upon parameter variation, indicating that this phenotypic switching emerges from the topology of HPIP/HIF-1α feedback loop (Figure 23, E-J). In unstable environments, organisms constantly change their behavior as part of the adaptation in order to survive. Moreover, bet-

hedging strategies appeared to prevail in order to ensure the survival of clonal populations under unfavorable environments via phenotypic switching or diversity (Kussell et al., 2005; Kussell and Leibler, 2005). Our results indeed suggest a phenotypic plasticity between $HPIP^{low}$/$HIF\text{-}1\alpha^{low}$ and $HPIP^{high/}HIF\text{-}1\alpha^{high}$ states that can happen in normoxic or hypoxic conditions.

3.6. Conclusion

Our findings highlight HPIP-HIF-1α loop in control of phenotypic plasticity displayed by breast cancer cells in response to varied microenvironment stresses such as normoxia and hypoxia. Phenotypic plasticity endows with cancer cells to procure tumorigenic adaptation in response to tumor microenvironment. Upon hypoxia, HIF-1α induces *HPIP* expression that drives metastatic phenotype in breast cancer cells, however under normoxia; HPIP stabilizes HIF1α, which confers tumor growth phenotype. The novel target genes of HIF-1α, *HPIP* and *SRP14*, interact and enhance MMP9 translation thereby promoting invasion and metastasis under hypoxia. On the other hand, HPIP stabilizes HIF-1α through PI3K/AKT/GSK3β signaling axis and promotes Warburg effect to support breast cancer cell growth. Thus, HIF-1α -HPIP loop drives suitable micro-environment dependent phenotype of the cancer cells which is conducive for proliferation (Warburg effect) or metastasis and intensifies tumor progression in breast cancer. Therefore, the HIF-1α-HPIP pathway may be a therapeutic target for breast cancer.

References:

A. Dhooge, W.G., Yu. A. Kuznetsov. 2003. MATCONT: A MATLAB package for numerical bifurcation analysis of ODEs. *ACM Trans Math Softw.* 29:141–164.

Abramovich, C., E.A. Chavez, P.M. Lansdorp, and R.K. Humphries. 2002. Functional characterization of multiple domains involved in the subcellular localization of the hematopoietic Pbx interacting protein (HPIP). *Oncogene*. 21:6766-6771.

Abramovich, C., W.F. Shen, N. Pineault, S. Imren, B. Montpetit, C. Largman, and R.K. Humphries. 2000. Functional cloning and characterization of a novel nonhomeodomain protein that inhibits the binding of PBX1-HOX complexes to DNA. *The Journal of biological chemistry*. 275:26172-26177.

Acquisti, C., J. Kleffe, and S. Collins. 2007. Oxygen content of transmembrane proteins over macroevolutionary time scales. *Nature*. 445:47-52.

Adelman, C.A., and J.H. Petrini. 2008. ZIP4H (TEX11) deficiency in the mouse impairs meiotic double strand break repair and the regulation of crossing over. *PLoS Genet*. 4:e1000042.

Adelman, R., R.L. Saul, and B.N. Ames. 1988. Oxidative damage to DNA: relation to species metabolic rate and life span. *Proc Natl Acad Sci U S A*. 85:2706-2708.

Akopian, D., K. Shen, X. Zhang, and S.O. Shan. 2013. Signal recognition particle: an essential protein-targeting machine. *Annual review of biochemistry*. 82:693-721.

Al-Alem, L., and T.E. Curry, Jr. 2015. Ovarian cancer: involvement of the matrix metalloproteinases. *Reproduction*. 150:R55-64.

Al Tameemi, W., T.P. Dale, R.M.K. Al-Jumaily, and N.R. Forsyth. 2019. Hypoxia-Modified Cancer Cell Metabolism. *Frontiers in cell and developmental biology*. 7:4.

Al Tamimi, D.M., M.A. Shawarby, A. Ahmed, A.K. Hassan, and A.A. AlOdaini. 2010. Protein expression profile and prevalence pattern of the molecular classes of breast cancer--a Saudi population based study. *BMC cancer*. 10:223.

Allred, D.C. 2010. Ductal carcinoma in situ: terminology, classification, and natural history. *Journal of the National Cancer Institute. Monographs*. 2010:134-138.

Anderson, N.M., P. Mucka, J.G. Kern, and H. Feng. 2018. The emerging role and targetability of the TCA cycle in cancer metabolism. *Protein Cell*. 9:216-237.

Armed Forces Health Surveillance, C. 2013. Incident diagnoses of breast cancer, active component service women, U.S. Armed Forces, 2000-2012. *Msmr*. 20:25-27.

Armitage, P., and R. Doll. 1954. The age distribution of cancer and a multi-stage theory of carcinogenesis. *British journal of cancer*. 8:1-12.

Arpino, G., V.J. Bardou, G.M. Clark, and R.M. Elledge. 2004. Infiltrating lobular carcinoma of the breast: tumor characteristics and clinical outcome. *Breast cancer research : BCR*. 6:R149-156.

Aruga, J., N. Yokota, M. Hashimoto, T. Furuichi, M. Fukuda, and K. Mikoshiba. 1994. A novel zinc finger protein, zic, is involved in neurogenesis, especially in the cell lineage of cerebellar granule cells. *J Neurochem*. 63:1880-1890.

Arvold, N.D., A.G. Taghian, A. Niemierko, R.F. Abi Raad, M. Sreedhara, P.L. Nguyen, J.R. Bellon, J.S. Wong, B.L. Smith, and J.R. Harris. 2011. Age, breast cancer subtype approximation, and local recurrence after breast-conserving therapy. *Journal of clinical oncology : official journal of the American Society of Clinical Oncology*. 29:3885-3891.

Azab, A.K., J. Hu, P. Quang, F. Azab, C. Pitsillides, R. Awwad, B. Thompson, P. Maiso, J.D. Sun, C.P. Hart, A.M. Roccaro, A. Sacco, H.T. Ngo, C.P. Lin, A.L. Kung, R.D. Carrasco, K. Vanderkerken, and I.M. Ghobrial. 2012. Hypoxia promotes dissemination of multiple myeloma through acquisition of epithelial to mesenchymal transition-like features. *Blood*. 119:5782-5794.

Badve, S., D.J. Dabbs, S.J. Schnitt, F.L. Baehner, T. Decker, V. Eusebi, S.B. Fox, S. Ichihara, J. Jacquemier, S.R. Lakhani, J. Palacios, E.A. Rakha, A.L. Richardson, F.C. Schmitt, P.H. Tan, G.M. Tse, B. Weigelt, I.O. Ellis, and J.S. Reis-Filho. 2011. Basal-like and triple-negative breast cancers: a critical review

with an emphasis on the implications for pathologists and oncologists. *Modern pathology : an official journal of the United States and Canadian Academy of Pathology, Inc*. 24:157-167.
Bane, A. 2013. Ductal carcinoma in situ: what the pathologist needs to know and why. *International journal of breast cancer*. 2013:914053.
Bardos, J.I., and M. Ashcroft. 2005. Negative and positive regulation of HIF-1: a complex network. *Biochim Biophys Acta*. 1755:107-120.
Beca, F., and K. Polyak. 2016. Intratumor Heterogeneity in Breast Cancer. *Advances in experimental medicine and biology*. 882:169-189.
Beldade, P., A.R. Mateus, and R.A. Keller. 2011. Evolution and molecular mechanisms of adaptive developmental plasticity. *Mol Ecol*. 20:1347-1363.
Belisario, D.C., J. Kopecka, M. Pasino, M. Akman, E. De Smaele, M. Donadelli, and C. Riganti. 2020. Hypoxia Dictates Metabolic Rewiring of Tumors: Implications for Chemoresistance. *Cells*. 9.
Bendtsen, J.D., L.J. Jensen, N. Blom, G. Von Heijne, and S. Brunak. 2004. Feature-based prediction of non-classical and leaderless protein secretion. *Protein engineering, design & selection : PEDS*. 17:349-356.
Bento, C.F., and P. Pereira. 2011. Regulation of hypoxia-inducible factor 1 and the loss of the cellular response to hypoxia in diabetes. *Diabetologia*. 54:1946-1956.
Berger, A., E. Ivanova, C. Gareau, A. Scherrer, R. Mazroui, and K. Strub. 2014. Direct binding of the Alu binding protein dimer SRP9/14 to 40S ribosomal subunits promotes stress granule formation and is regulated by Alu RNA. *Nucleic acids research*. 42:11203-11217.
Berner, R.A., J.M. Vandenbrooks, and P.D. Ward. 2007. Evolution. Oxygen and evolution. *Science*. 316:557-558.
Bodian, C.A., K.H. Perzin, and R. Lattes. 1996. Lobular neoplasia. Long term risk of breast cancer and relation to other factors. *Cancer*. 78:1024-1034.
Bonnans, C., J. Chou, and Z. Werb. 2014. Remodelling the extracellular matrix in development and disease. *Nat Rev Mol Cell Biol*. 15:786-801.
Bourguignon, L.Y., Z. Gunja-Smith, N. Iida, H.B. Zhu, L.J. Young, W.J. Muller, and R.D. Cardiff. 1998. CD44v(3,8-10) is involved in cytoskeleton-mediated tumor cell migration and matrix metalloproteinase (MMP-9) association in metastatic breast cancer cells. *J Cell Physiol*. 176:206-215.
Bugide, S., D. David, A. Nair, N. Kannan, V.S. Samanthapudi, J. Prabhakar, and B. Manavathi. 2015. Hematopoietic PBX-interacting protein (HPIP) is over expressed in breast infiltrative ductal carcinoma and regulates cell adhesion and migration through modulation of focal adhesion dynamics. *Oncogene*. 34:4601-4612.
Bugide, S., V.K. Gonugunta, V. Penugurti, V.L. Malisetty, R.K. Vadlamudi, and B. Manavathi. 2017. HPIP promotes epithelial-mesenchymal transition and cisplatin resistance in ovarian cancer cells through PI3K/AKT pathway activation. *Cellular oncology*. 40:133-144.
Cahoy, J.D., B. Emery, A. Kaushal, L.C. Foo, J.L. Zamanian, K.S. Christopherson, Y. Xing, J.L. Lubischer, P.A. Krieg, S.A. Krupenko, W.J. Thompson, and B.A. Barres. 2008. A transcriptome database for astrocytes, neurons, and oligodendrocytes: a new resource for understanding brain development and function. *J Neurosci*. 28:264-278.
Cancer Genome Atlas, N. 2012. Comprehensive molecular portraits of human breast tumours. *Nature*. 490:61-70.
Cao, S., J. Sun, S. Lin, L. Zhao, D. Wu, T. Liang, and W. Sheng. 2017. HPIP: a predictor of lymph node metastasis and poor survival in cervical cancer. *Onco Targets Ther*. 10:4205-4211.
Carey, L.A., C.M. Perou, C.A. Livasy, L.G. Dressler, D. Cowan, K. Conway, G. Karaca, M.A. Troester, C.K. Tse, S. Edmiston, S.L. Deming, J. Geradts, M.C. Cheang, T.O. Nielsen, P.G. Moorman, H.S. Earp, and R.C. Millikan. 2006. Race, breast cancer subtypes, and survival in the Carolina Breast Cancer Study. *Jama*. 295:2492-2502.

Carragher, N.O., M.A. Westhoff, V.J. Fincham, M.D. Schaller, and M.C. Frame. 2003. A novel role for FAK as a protease-targeting adaptor protein: regulation by p42 ERK and Src. *Curr Biol*. 13:1442-1450.
Casas-Selves, M., and J. Degregori. 2011. How cancer shapes evolution, and how evolution shapes cancer. *Evolution (N Y)*. 4:624-634.
Catling, D.C., C.R. Glein, K.J. Zahnle, and C.P. McKay. 2005. Why O2 is required by complex life on habitable planets and the concept of planetary "oxygenation time". *Astrobiology*. 5:415-438.
Champion, L., M.I. Linder, and U. Kutay. 2017. Cellular Reorganization during Mitotic Entry. *Trends Cell Biol*. 27:26-41.
Chan, D.A., and A.J. Giaccia. 2007. Hypoxia, gene expression, and metastasis. *Cancer Metastasis Rev*. 26:333-339.
Chen, B., J. Zhao, S. Zhang, Y. Zhang, and Z. Huang. 2016a. HPIP promotes gastric cancer cell proliferation through activation of cap-dependent translation. *Oncol Rep*. 36:3664-3672.
Chen, D., J. Shen, W. Zhao, T. Wang, L. Han, J.L. Hamilton, and H.J. Im. 2017. Osteoarthritis: toward a comprehensive understanding of pathological mechanism. *Bone Res*. 5:16044.
Chen, Y., R. Zhao, Q. Zhao, Y. Shao, and S. Zhang. 2016b. Knockdown of HPIP Inhibits the Proliferation and Invasion of Head-and-Neck Squamous Cell Carcinoma Cells by Regulating PI3K/Akt Signaling Pathway. *Oncology research*. 24:153-160.
Cheng, L., T. Zhao, S. Li, Y. Wang, H. Fei, and F. Meng. 2019. Overexpression of HPIP as a biomarker for metastasis and prognosis prediction in endometrial cancer patients. *J Clin Lab Anal*. 33:e22959.
Childs, B.G., D.J. Baker, J.L. Kirkland, J. Campisi, and J.M. van Deursen. 2014. Senescence and apoptosis: dueling or complementary cell fates? *EMBO Rep*. 15:1139-1153.
Choi, J.Y., Y.S. Jang, S.Y. Min, and J.Y. Song. 2011. Overexpression of MMP-9 and HIF-1alpha in Breast Cancer Cells under Hypoxic Conditions. *Journal of breast cancer*. 14:88-95.
Chou, C.C., H.C. Chuang, S.B. Salunke, S.K. Kulp, and C.S. Chen. 2015. A novel HIF-1alpha-integrin-linked kinase regulatory loop that facilitates hypoxia-induced HIF-1alpha expression and epithelial-mesenchymal transition in cancer cells. *Oncotarget*. 6:8271-8285.
Cohen, K.L., M.A. Seid, and K.M. Warkentin. 2016. How embryos escape from danger: the mechanism of rapid, plastic hatching in red-eyed treefrogs. *J Exp Biol*. 219:1875-1883.
Coll-de la Rubia, E., E. Martinez-Garcia, G. Dittmar, A. Gil-Moreno, S. Cabrera, and E. Colas. 2020. Prognostic Biomarkers in Endometrial Cancer: A Systematic Review and Meta-Analysis. *J Clin Med*. 9.
Collins, L.C., R.M. Tamimi, H.J. Baer, J.L. Connolly, G.A. Colditz, and S.J. Schnitt. 2005. Outcome of patients with ductal carcinoma in situ untreated after diagnostic biopsy: results from the Nurses' Health Study. *Cancer*. 103:1778-1784.
Courtnay, R., D.C. Ngo, N. Malik, K. Ververis, S.M. Tortorella, and T.C. Karagiannis. 2015. Cancer metabolism and the Warburg effect: the role of HIF-1 and PI3K. *Molecular biology reports*. 42:841-851.
Cummins, E.P., and C.T. Taylor. 2005. Hypoxia-responsive transcription factors. *Pflugers Arch*. 450:363-371.
Czyzyk-Krzeska, M.F. 1997. Molecular aspects of oxygen sensing in physiological adaptation to hypoxia. *Respir Physiol*. 110:99-111.
Dabbs, D.J., M. Kaplai, M. Chivukula, A. Kanbour, A. Kanbour-Shakir, and G.J. Carter. 2007. The spectrum of morphomolecular abnormalities of the E-cadherin/catenin complex in pleomorphic lobular carcinoma of the breast. *Applied immunohistochemistry & molecular morphology : AIMM*. 15:260-266.
Dai, X., T. Li, Z. Bai, Y. Yang, X. Liu, J. Zhan, and B. Shi. 2015. Breast cancer intrinsic subtype classification, clinical use and future trends. *American journal of cancer research*. 5:2929-2943.
Dang, C.V., J.W. Kim, P. Gao, and J. Yustein. 2008. The interplay between MYC and HIF in cancer. *Nat Rev Cancer*. 8:51-56.

de la Cruz-Lopez, K.G., L.J. Castro-Munoz, D.O. Reyes-Hernandez, A. Garcia-Carranca, and J. Manzo-Merino. 2019. Lactate in the Regulation of Tumor Microenvironment and Therapeutic Approaches. *Front Oncol*. 9:1143.

de Souza, A.C., G.Z. Justo, D.R. de Araujo, and A.D. Cavagis. 2011. Defining the molecular basis of tumor metabolism: a continuing challenge since Warburg's discovery. *Cellular physiology and biochemistry : international journal of experimental cellular physiology, biochemistry, and pharmacology*. 28:771-792.

DeBerardinis, R.J., J.J. Lum, G. Hatzivassiliou, and C.B. Thompson. 2008. The biology of cancer: metabolic reprogramming fuels cell growth and proliferation. *Cell Metab*. 7:11-20.

Dengler, V.L., M. Galbraith, and J.M. Espinosa. 2014. Transcriptional regulation by hypoxia inducible factors. *Crit Rev Biochem Mol Biol*. 49:1-15.

Deryugina, E.I., and J.P. Quigley. 2006. Matrix metalloproteinases and tumor metastasis. *Cancer metastasis reviews*. 25:9-34.

Dhaenens, L., S. Lierman, L. De Clerck, E. Govaert, D. Deforce, K. Tilleman, and P. De Sutter. 2019. Endometrial stromal cell proteome mapping in repeated implantation failure and recurrent pregnancy loss cases and fertile women. *Reprod Biomed Online*. 38:442-454.

Dhup, S., R.K. Dadhich, P.E. Porporato, and P. Sonveaux. 2012. Multiple biological activities of lactic acid in cancer: influences on tumor growth, angiogenesis and metastasis. *Curr Pharm Des*. 18:1319-1330.

DiMartino, J.F., L. Selleri, D. Traver, M.T. Firpo, J. Rhee, R. Warnke, S. O'Gorman, I.L. Weissman, and M.L. Cleary. 2001. The Hox cofactor and proto-oncogene Pbx1 is required for maintenance of definitive hematopoiesis in the fetal liver. *Blood*. 98:618-626.

Doe, M.R., J.M. Ascano, M. Kaur, and M.D. Cole. 2012. Myc posttranscriptionally induces HIF1 protein and target gene expression in normal and cancer cells. *Cancer research*. 72:949-957.

Doherty, J.R., and J.L. Cleveland. 2013. Targeting lactate metabolism for cancer therapeutics. *The Journal of clinical investigation*. 123:3685-3692.

Dong, B., Z. Qiu, and Y. Wu. 2020a. Tackle Epithelial-Mesenchymal Transition With Epigenetic Drugs in Cancer. *Frontiers in pharmacology*. 11:596239.

Dong, Y., R. Tu, H. Liu, and G. Qing. 2020b. Regulation of cancer cell metabolism: oncogenic MYC in the driver's seat. *Signal Transduct Target Ther*. 5:124.

Dziembowska, M., J. Milek, A. Janusz, E. Rejmak, E. Romanowska, T. Gorkiewicz, A. Tiron, C.R. Bramham, and L. Kaczmarek. 2012. Activity-dependent local translation of matrix metalloproteinase-9. *J Neurosci*. 32:14538-14547.

Eales, K.L., K.E. Hollinshead, and D.A. Tennant. 2016. Hypoxia and metabolic adaptation of cancer cells. *Oncogenesis*. 5:e190.

Edwards, T.M., and J.P. Myers. 2007. Environmental exposures and gene regulation in disease etiology. *Environ Health Perspect*. 115:1264-1270.

Elshamy, W.M., and R.J. Duhe. 2013. Overview: cellular plasticity, cancer stem cells and metastasis. *Cancer letters*. 341:2-8.

Erbas, B., E. Provenzano, J. Armes, and D. Gertig. 2006. The natural history of ductal carcinoma in situ of the breast: a review. *Breast cancer research and treatment*. 97:135-144.

Esteban, M.A., M.G. Tran, S.K. Harten, P. Hill, M.C. Castellanos, A. Chandra, R. Raval, S. O'Brien T, and P.H. Maxwell. 2006. Regulation of E-cadherin expression by VHL and hypoxia-inducible factor. *Cancer Res*. 66:3567-3575.

Feng, Y., L. Li, X. Zhang, Y. Zhang, Y. Liang, J. Lv, Z. Fan, J. Guo, T. Hong, B. Ji, Q. Ji, G. Mei, L. Ding, S. Zhang, X. Xu, and Q. Ye. 2015a. Hematopoietic pre-B cell leukemia transcription factor interacting protein is overexpressed in gastric cancer and promotes gastric cancer cell proliferation, migration, and invasion. *Cancer Sci*. 106:1313-1322.

Feng, Y., X. Xu, Y. Zhang, J. Ding, Y. Wang, X. Zhang, Z. Wu, L. Kang, Y. Liang, L. Zhou, S. Song, K. Zhao, and Q. Ye. 2015b. HPIP is upregulated in colorectal cancer and regulates colorectal cancer cell proliferation, apoptosis and invasion. *Sci Rep*. 5:9429.

Ferrao, P.T., A. Behren, R.L. Anderson, and E.W. Thompson. 2015. Editorial: Cellular and Phenotypic Plasticity in Cancer. *Front Oncol*. 5:171.

Ferraro, F., C.L. Celso, and D. Scadden. 2010. Adult stem cels and their niches. *Adv Exp Med Biol*. 695:155-168.

Frazier, M.R., H.A. Woods, and J.F. Harrison. 2001. Interactive effects of rearing temperature and oxygen on the development of Drosophila melanogaster. *Physiol Biochem Zool*. 74:641-650.

Fukuda, R., H. Zhang, J.W. Kim, L. Shimoda, C.V. Dang, and G.L. Semenza. 2007. HIF-1 regulates cytochrome oxidase subunits to optimize efficiency of respiration in hypoxic cells. *Cell*. 129:111-122.

Fusco, G., and A. Minelli. 2010. Phenotypic plasticity in development and evolution: facts and concepts. Introduction. *Philos Trans R Soc Lond B Biol Sci*. 365:547-556.

Gajulapalli, V.N., V.S. Samanthapudi, M. Pulaganti, S.S. Khumukcham, V.L. Malisetty, L. Guruprasad, S.K. Chitta, and B. Manavathi. 2016. A transcriptional repressive role for epithelial-specific ETS factor ELF3 on oestrogen receptor alpha in breast cancer cells. *The Biochemical journal*. 473:1047-1061.

Gandhi, A.K., P. Kumar, M. Bhandari, B. Devnani, and G.K. Rath. 2017. Burden of preventable cancers in India: Time to strike the cancer epidemic. *Journal of the Egyptian National Cancer Institute*. 29:11-18.

Gao, J., B.A. Aksoy, U. Dogrusoz, G. Dresdner, B. Gross, S.O. Sumer, Y. Sun, A. Jacobsen, R. Sinha, E. Larsson, E. Cerami, C. Sander, and N. Schultz. 2013. Integrative analysis of complex cancer genomics and clinical profiles using the cBioPortal. *Science signaling*. 6:pl1.

Gatenby, R.A., and R.J. Gillies. 2004. Why do cancers have high aerobic glycolysis? *Nat Rev Cancer*. 4:891-899.

Gavet, O., and J. Pines. 2010. Activation of cyclin B1-Cdk1 synchronizes events in the nucleus and the cytoplasm at mitosis. *J Cell Biol*. 189:247-259.

Giaccia, A.J., M.C. Simon, and R. Johnson. 2004. The biology of hypoxia: the role of oxygen sensing in development, normal function, and disease. *Genes Dev*. 18:2183-2194.

Giese, A., M.A. Loo, N. Tran, D. Haskett, S.W. Coons, and M.E. Berens. 1996. Dichotomy of astrocytoma migration and proliferation. *Int J Cancer*. 67:275-282.

Gilkes, D.M., G.L. Semenza, and D. Wirtz. 2014. Hypoxia and the extracellular matrix: drivers of tumour metastasis. *Nat Rev Cancer*. 14:430-439.

Gladek, I., J. Ferdin, S. Horvat, G.A. Calin, and T. Kunej. 2017. HIF1A gene polymorphisms and human diseases: Graphical review of 97 association studies. *Genes Chromosomes Cancer*. 56:439-452.

Goldfine, H. 1965. The evolution of oxygen as a biosynthetic reagent. *J Gen Physiol*. 49:Suppl:253-274.

Gonzalez, H., C. Hagerling, and Z. Werb. 2018. Roles of the immune system in cancer: from tumor initiation to metastatic progression. *Genes Dev*. 32:1267-1284.

Grasso, J.A., A.L. Sullivan, and L.W. Sullivan. 1975. Ultrastructural studies of the bone marrow in sickle cell anaemia. I. The structure of sickled erythrocytes and reticulocytes and their phagocytic destruction. *Br J Haematol*. 31:135-148.

Gritsenko, P.G., O. Ilina, and P. Friedl. 2012. Interstitial guidance of cancer invasion. *J Pathol*. 226:185-199.

Gupta, P.B., C.M. Fillmore, G. Jiang, S.D. Shapira, K. Tao, C. Kuperwasser, and E.S. Lander. 2011. Stochastic state transitions give rise to phenotypic equilibrium in populations of cancer cells. *Cell*. 146:633-644.

Gupta, P.B., T.T. Onder, G. Jiang, K. Tao, C. Kuperwasser, R.A. Weinberg, and E.S. Lander. 2009. Identification of selective inhibitors of cancer stem cells by high-throughput screening. *Cell*. 138:645-659.

Haagensen, C.D., N. Lane, R. Lattes, and C. Bodian. 1978. Lobular neoplasia (so-called lobular carcinoma in situ) of the breast. *Cancer*. 42:737-769.

Hahn-Dantona, E., J.F. Ruiz, P. Bornstein, and D.K. Strickland. 2001. The low density lipoprotein receptor-related protein modulates levels of matrix metalloproteinase 9 (MMP-9) by mediating its cellular catabolism. *J Biol Chem*. 276:15498-15503.

Hatzikirou, H., D. Basanta, M. Simon, K. Schaller, and A. Deutsch. 2012. 'Go or grow': the key to the emergence of invasion in tumour progression? *Math Med Biol*. 29:49-65.

Henke, E., R. Nandigama, and S. Ergun. 2019. Extracellular Matrix in the Tumor Microenvironment and Its Impact on Cancer Therapy. *Front Mol Biosci*. 6:160.

Herschkowitz, J.I., K. Simin, V.J. Weigman, I. Mikaelian, J. Usary, Z. Hu, K.E. Rasmussen, L.P. Jones, S. Assefnia, S. Chandrasekharan, M.G. Backlund, Y. Yin, A.I. Khramtsov, R. Bastein, J. Quackenbush, R.I. Glazer, P.H. Brown, J.E. Green, L. Kopelovich, P.A. Furth, J.P. Palazzo, O.I. Olopade, P.S. Bernard, G.A. Churchill, T. Van Dyke, and C.M. Perou. 2007. Identification of conserved gene expression features between murine mammary carcinoma models and human breast tumors. *Genome biology*. 8:R76.

Higgins, D.F., K. Kimura, W.M. Bernhardt, N. Shrimanker, Y. Akai, B. Hohenstein, Y. Saito, R.S. Johnson, M. Kretzler, C.D. Cohen, K.U. Eckardt, M. Iwano, and V.H. Haase. 2007. Hypoxia promotes fibrogenesis in vivo via HIF-1 stimulation of epithelial-to-mesenchymal transition. *J Clin Invest*. 117:3810-3820.

Hirata, M., F. Kugimiya, A. Fukai, S. Ohba, N. Kawamura, T. Ogasawara, Y. Kawasaki, T. Saito, F. Yano, T. Ikeda, K. Nakamura, U.I. Chung, and H. Kawaguchi. 2009. C/EBPbeta Promotes transition from proliferation to hypertrophic differentiation of chondrocytes through transactivation of p57. *PLoS One*. 4:e4543.

Hirata, M., F. Kugimiya, A. Fukai, T. Saito, F. Yano, T. Ikeda, A. Mabuchi, B.R. Sapkota, T. Akune, N. Nishida, N. Yoshimura, T. Nakagawa, K. Tokunaga, K. Nakamura, U.I. Chung, and H. Kawaguchi. 2012. C/EBPbeta and RUNX2 cooperate to degrade cartilage with MMP-13 as the target and HIF-2alpha as the inducer in chondrocytes. *Hum Mol Genet*. 21:1111-1123.

Hirota, K., and G.L. Semenza. 2006. Regulation of angiogenesis by hypoxia-inducible factor 1. *Crit Rev Oncol Hematol*. 59:15-26.

Hoye, A.M., and J.T. Erler. 2016. Structural ECM components in the premetastatic and metastatic niche. *Am J Physiol Cell Physiol*. 310:C955-967.

Hsu, M., T. Andl, G. Li, J.L. Meinkoth, and M. Herlyn. 2000. Cadherin repertoire determines partner-specific gap junctional communication during melanoma progression. *J Cell Sci*. 113 (Pt 9):1535-1542.

Huang, J., X. Yao, J. Zhang, B. Dong, Q. Chen, W. Xue, D. Liu, and Y. Huang. 2013. Hypoxia-induced downregulation of miR-30c promotes epithelial-mesenchymal transition in human renal cell carcinoma. *Cancer Sci*. 104:1609-1617.

Huang, L.E., R.S. Bindra, P.M. Glazer, and A.L. Harris. 2007. Hypoxia-induced genetic instability--a calculated mechanism underlying tumor progression. *J Mol Med (Berl)*. 85:139-148.

Huang, Z., P. Yu, and J. Tang. 2020. Characterization of Triple-Negative Breast Cancer MDA-MB-231 Cell Spheroid Model. *OncoTargets and therapy*. 13:5395-5405.

Iommarini, L., A.M. Porcelli, G. Gasparre, and I. Kurelac. 2017. Non-Canonical Mechanisms Regulating Hypoxia-Inducible Factor 1 Alpha in Cancer. *Front Oncol*. 7:286.

Isaacs, J.S., Y.J. Jung, D.R. Mole, S. Lee, C. Torres-Cabala, Y.L. Chung, M. Merino, J. Trepel, B. Zbar, J. Toro, P.J. Ratcliffe, W.M. Linehan, and L. Neckers. 2005. HIF overexpression correlates with biallelic loss of fumarate hydratase in renal cancer: novel role of fumarate in regulation of HIF stability. *Cancer Cell*. 8:143-153.

Ivanovic, Z. 2009. Hypoxia or in situ normoxia: The stem cell paradigm. *J Cell Physiol*. 219:271-275.

Jaakkola, P., D.R. Mole, Y.M. Tian, M.I. Wilson, J. Gielbert, S.J. Gaskell, A. von Kriegsheim, H.F. Hebestreit, M. Mukherji, C.J. Schofield, P.H. Maxwell, C.W. Pugh, and P.J. Ratcliffe. 2001.

Targeting of HIF-alpha to the von Hippel-Lindau ubiquitylation complex by O2-regulated prolyl hydroxylation. *Science*. 292:468-472.
Jablonska-Trypuc, A., M. Matejczyk, and S. Rosochacki. 2016. Matrix metalloproteinases (MMPs), the main extracellular matrix (ECM) enzymes in collagen degradation, as a target for anticancer drugs. *J Enzyme Inhib Med Chem*. 31:177-183.
Jain, S., M.G. Kapetanaki, N. Raghavachari, K. Woodhouse, G. Yu, S. Barge, C. Coronnello, P.V. Benos, G.J. Kato, N. Kaminski, and M.T. Gladwin. 2013. Expression of regulatory platelet microRNAs in patients with sickle cell disease. *PLoS One*. 8:e60932.
Janusz, A., J. Milek, M. Perycz, L. Pacini, C. Bagni, L. Kaczmarek, and M. Dziembowska. 2013. The Fragile X mental retardation protein regulates matrix metalloproteinase 9 mRNA at synapses. *J Neurosci*. 33:18234-18241.
Jeggo, P.A., L.H. Pearl, and A.M. Carr. 2016. DNA repair, genome stability and cancer: a historical perspective. *Nat Rev Cancer*. 16:35-42.
Ji, Q., X. Xu, L. Kang, Y. Xu, J. Xiao, S.B. Goodman, X. Zhu, W. Li, J. Liu, X. Gao, Z. Yan, Y. Zheng, Z. Wang, W.J. Maloney, Q. Ye, and Y. Wang. 2019. Hematopoietic PBX-interacting protein mediates cartilage degeneration during the pathogenesis of osteoarthritis. *Nature communications*. 10:313.
Jia, D., J.T. George, S.C. Tripathi, D.L. Kundnani, M. Lu, S.M. Hanash, J.N. Onuchic, M.K. Jolly, and H. Levine. 2019. Testing the gene expression classification of the EMT spectrum. *Physical biology*. 16:025002.
Jiang, L., G. Hu, F.F. Chen, X.Y. Du, B. Liu, and C. Liu. 2017. CSR1 suppresses tumor growth and metastasis of human hepatocellular carcinoma via inhibition of HPIP. *Eur Rev Med Pharmacol Sci*. 21:3813-3820.
Jiang, Y.Y., D.X. Kong, T. Qin, X. Li, G. Caetano-Anolles, and H.Y. Zhang. 2012. The impact of oxygen on metabolic evolution: a chemoinformatic investigation. *PLoS Comput Biol*. 8:e1002426.
Johnson, A.B., N. Denko, and M.C. Barton. 2008. Hypoxia induces a novel signature of chromatin modifications and global repression of transcription. *Mutation research*. 640:174-179.
Joshi, S., A.R. Singh, and D.L. Durden. 2014. MDM2 regulates hypoxic hypoxia-inducible factor 1alpha stability in an E3 ligase, proteasome, and PTEN-phosphatidylinositol 3-kinase-AKT-dependent manner. *The Journal of biological chemistry*. 289:22785-22797.
Kai, F., A.P. Drain, and V.M. Weaver. 2019. The Extracellular Matrix Modulates the Metastatic Journey. *Dev Cell*. 49:332-346.
Kalluri, R., and R.A. Weinberg. 2009. The basics of epithelial-mesenchymal transition. *J Clin Invest*. 119:1420-1428.
Karamyshev, A.L., E.B. Tikhonova, and Z.N. Karamysheva. 2020. Translational Control of Secretory Proteins in Health and Disease. *International journal of molecular sciences*. 21.
Keith, B., R.S. Johnson, and M.C. Simon. 2011. HIF1alpha and HIF2alpha: sibling rivalry in hypoxic tumour growth and progression. *Nat Rev Cancer*. 12:9-22.
Kessenbrock, K., V. Plaks, and Z. Werb. 2010. Matrix metalloproteinases: regulators of the tumor microenvironment. *Cell*. 141:52-67.
Khumukcham, S.S., V.S.K. Samanthapudi, V. Penugurti, A. Kumari, P.S. Kesavan, L.R. Velatooru, S.R. Kotla, A. Mazumder, and B. Manavathi. 2019. Hematopoietic PBX-interacting protein is a substrate and an inhibitor of the APC/C-Cdc20 complex and regulates mitosis by stabilizing cyclin B1. *J Biol Chem*. 294:10236-10252.
Kilic, M., H. Kasperczyk, S. Fulda, and K.M. Debatin. 2007. Role of hypoxia inducible factor-1 alpha in modulation of apoptosis resistance. *Oncogene*. 26:2027-2038.
Kim, J.J., S.B. Lee, J. Jang, S.Y. Yi, S.H. Kim, S.A. Han, J.M. Lee, S.Y. Tong, N.D. Vincelette, B. Gao, P. Yin, D. Evans, D.W. Choi, B. Qin, T. Liu, H. Zhang, M. Deng, J. Jen, J. Zhang, L. Wang, and Z. Lou. 2015. WSB1 promotes tumor metastasis by inducing pVHL degradation. *Genes Dev*. 29:2244-2257.

Kim, K., Z. Lu, and E.D. Hay. 2002. Direct evidence for a role of beta-catenin/LEF-1 signaling pathway in induction of EMT. *Cell Biol Int*. 26:463-476.
Kim, K., E.Y. Park, M.S. Yoon, D.S. Suh, K.H. Kim, J.H. Lee, D.H. Shin, J.Y. Kim, M.Y. Sol, and K.U. Choi. 2014. The Role of TWIST in Ovarian Epithelial Cancers. *Korean J Pathol*. 48:283-291.
Kong, D., C.J. Hughes, and H.L. Ford. 2020. Cellular Plasticity in Breast Cancer Progression and Therapy. *Frontiers in molecular biosciences*. 7:72.
Krishnamachary, B., S. Berg-Dixon, B. Kelly, F. Agani, D. Feldser, G. Ferreira, N. Iyer, J. LaRusch, B. Pak, P. Taghavi, and G.L. Semenza. 2003. Regulation of colon carcinoma cell invasion by hypoxia-inducible factor 1. *Cancer Res*. 63:1138-1143.
Kuschel, A., P. Simon, and S. Tug. 2012. Functional regulation of HIF-1alpha under normoxia--is there more than post-translational regulation? *J Cell Physiol*. 227:514-524.
Kussell, E., R. Kishony, N.Q. Balaban, and S. Leibler. 2005. Bacterial persistence: a model of survival in changing environments. *Genetics*. 169:1807-1814.
Kussell, E., and S. Leibler. 2005. Phenotypic diversity, population growth, and information in fluctuating environments. *Science*. 309:2075-2078.
L. N. Borshchevskaya, T.L.G., A. N. Kalinina, and S. P. Sineokii. 2016. Spectrophotometric Determination of Lactic Acid. *Journal of Analytical Chemistry*. 71:755–758.
Lakkaraju, A.K., C. Mary, A. Scherrer, A.E. Johnson, and K. Strub. 2008. SRP keeps polypeptides translocation-competent by slowing translation to match limiting ER-targeting sites. *Cell*. 133:440-451.
Lambert, S.A., A. Jolma, L.F. Campitelli, P.K. Das, Y. Yin, M. Albu, X. Chen, J. Taipale, T.R. Hughes, and M.T. Weirauch. 2018. The Human Transcription Factors. *Cell*. 172:650-665.
Lapidot, T., C. Sirard, J. Vormoor, B. Murdoch, T. Hoang, J. Caceres-Cortes, M. Minden, B. Paterson, M.A. Caligiuri, and J.E. Dick. 1994. A cell initiating human acute myeloid leukaemia after transplantation into SCID mice. *Nature*. 367:645-648.
Leonard, A., A. Bonifacino, V.M. Dominical, M. Luo, J.J. Haro-Mora, S. Demirci, N. Uchida, F.J. Pierciey, Jr., and J.F. Tisdale. 2019. Bone marrow characterization in sickle cell disease: inflammation and stress erythropoiesis lead to suboptimal CD34 recovery. *Br J Haematol*. 186:286-299.
Leonard, G.D., and S.M. Swain. 2004. Ductal carcinoma in situ, complexities and challenges. *Journal of the National Cancer Institute*. 96:906-920.
Levayer, R. 2020. Solid stress, competition for space and cancer: The opposing roles of mechanical cell competition in tumour initiation and growth. *Semin Cancer Biol*. 63:69-80.
Li, C., D.G. Heidt, P. Dalerba, C.F. Burant, L. Zhang, V. Adsay, M. Wicha, M.F. Clarke, and D.M. Simeone. 2007. Identification of pancreatic cancer stem cells. *Cancer research*. 67:1030-1037.
Li, C.I., B.O. Anderson, J.R. Daling, and R.E. Moe. 2003a. Trends in incidence rates of invasive lobular and ductal breast carcinoma. *Jama*. 289:1421-1424.
Li, C.I., B.O. Anderson, P. Porter, S.K. Holt, J.R. Daling, and R.E. Moe. 2000. Changing incidence rate of invasive lobular breast carcinoma among older women. *Cancer*. 88:2561-2569.
Li, C.I., D.J. Uribe, and J.R. Daling. 2005. Clinical characteristics of different histologic types of breast cancer. *British journal of cancer*. 93:1046-1052.
Li, J., M. Shi, Y. Cao, W. Yuan, T. Pang, B. Li, Z. Sun, L. Chen, and R.C. Zhao. 2006. Knockdown of hypoxia-inducible factor-1alpha in breast carcinoma MCF-7 cells results in reduced tumor growth and increased sensitivity to methotrexate. *Biochem Biophys Res Commun*. 342:1341-1351.
Li, X., M.T. Lewis, J. Huang, C. Gutierrez, C.K. Osborne, M.F. Wu, S.G. Hilsenbeck, A. Pavlick, X. Zhang, G.C. Chamness, H. Wong, J. Rosen, and J.C. Chang. 2008. Intrinsic resistance of tumorigenic breast cancer cells to chemotherapy. *Journal of the National Cancer Institute*. 100:672-679.
Li, Z., S. Van Calcar, C. Qu, W.K. Cavenee, M.Q. Zhang, and B. Ren. 2003b. A global transcriptional regulatory role for c-Myc in Burkitt's lymphoma cells. *Proc Natl Acad Sci U S A*. 100:8164-8169.
Liao, D., and R.S. Johnson. 2007. Hypoxia: a key regulator of angiogenesis in cancer. *Cancer Metastasis Rev*. 26:281-290.

Lin, Q., Y. Kim, R.M. Alarcon, and Z. Yun. 2008. Oxygen and Cell Fate Decisions. *Gene Regul Syst Bio*. 2:43-51.
Liu, L., J. Huang, K. Wang, L. Li, Y. Li, J. Yuan, and S. Wei. 2015. Identification of hallmarks of lung adenocarcinoma prognosis using whole genome sequencing. *Oncotarget*. 6:38016-38028.
Lopez-Barneo, J., P. Gonzalez-Rodriguez, L. Gao, M.C. Fernandez-Aguera, R. Pardal, and P. Ortega-Saenz. 2016. Oxygen sensing by the carotid body: mechanisms and role in adaptation to hypoxia. *American journal of physiology. Cell physiology*. 310:C629-642.
Lu, M., M.K. Jolly, H. Levine, J.N. Onuchic, and E. Ben-Jacob. 2013. MicroRNA-based regulation of epithelial-hybrid-mesenchymal fate determination. *Proceedings of the National Academy of Sciences of the United States of America*. 110:18144-18149.
Lu, W., and Y. Kang. 2019. Epithelial-Mesenchymal Plasticity in Cancer Progression and Metastasis. *Developmental cell*. 49:361-374.
Luo, W., H. Hu, R. Chang, J. Zhong, M. Knabel, R. O'Meally, R.N. Cole, A. Pandey, and G.L. Semenza. 2011. Pyruvate kinase M2 is a PHD3-stimulated coactivator for hypoxia-inducible factor 1. *Cell*. 145:732-744.
M.Lenton, T. 2003. 3 - The coupled evolution of life and atmospheric oxygen. *Evolution on planet Earth*:35-53.
Ma, C., Y. Guo, Y. Zhang, A. Duo, Y. Jia, C. Liu, and B. Li. 2018. PAFAH1B2 is a HIF1a target gene and promotes metastasis in pancreatic cancer. *Biochem Biophys Res Commun*. 501:654-660.
Mabjeesh, N.J., and S. Amir. 2007. Hypoxia-inducible factor (HIF) in human tumorigenesis. *Histol Histopathol*. 22:559-572.
Mahoney, M.E., E.J. Gordon, J.Y. Rao, Y. Jin, N. Hylton, and S.M. Love. 2013. Intraductal therapy of ductal carcinoma in situ: a presurgery study. *Clinical breast cancer*. 13:280-286.
Mai, H., X. Xu, G. Mei, T. Hong, J. Huang, T. Wang, Z. Yan, Y. Li, Y. Liang, L. Li, S. Jin, W. You, Y. Ma, L. Chen, and Q. Ye. 2016. The interplay between HPIP and casein kinase 1alpha promotes renal cell carcinoma growth and metastasis via activation of mTOR pathway. *Oncogenesis*. 5:e260.
Majmundar, A.J., W.J. Wong, and M.C. Simon. 2010. Hypoxia-inducible factors and the response to hypoxic stress. *Mol Cell*. 40:294-309.
Mak, P., I. Leav, B. Pursell, D. Bae, X. Yang, C.A. Taglienti, L.M. Gouvin, V.M. Sharma, and A.M. Mercurio. 2010. ERbeta impedes prostate cancer EMT by destabilizing HIF-1alpha and inhibiting VEGF-mediated snail nuclear localization: implications for Gleason grading. *Cancer Cell*. 17:319-332.
Makrilia, N., T. Lappa, V. Xyla, I. Nikolaidis, and K. Syrigos. 2009. The role of angiogenesis in solid tumours: an overview. *Eur J Intern Med*. 20:663-671.
Malhotra, G.K., X. Zhao, H. Band, and V. Band. 2010. Histological, molecular and functional subtypes of breast cancers. *Cancer biology & therapy*. 10:955-960.
Mammoto, T., A. Mammoto, and D.E. Ingber. 2013. Mechanobiology and developmental control. *Annu Rev Cell Dev Biol*. 29:27-61.
Manavathi, B., F. Acconcia, S.K. Rayala, and R. Kumar. 2006. An inherent role of microtubule network in the action of nuclear receptor. *Proceedings of the National Academy of Sciences of the United States of America*. 103:15981-15986.
Manavathi, B., D. Lo, S. Bugide, O. Dey, S. Imren, M.J. Weiss, and R.K. Humphries. 2012. Functional regulation of pre-B-cell leukemia homeobox interacting protein 1 (PBXIP1/HPIP) in erythroid differentiation. *The Journal of biological chemistry*. 287:5600-5614.
Manotham, K., T. Tanaka, M. Matsumoto, T. Ohse, R. Inagi, T. Miyata, K. Kurokawa, T. Fujita, J.R. Ingelfinger, and M. Nangaku. 2004. Transdifferentiation of cultured tubular cells induced by hypoxia. *Kidney Int*. 65:871-880.
Marimpietri, D., A. Petretto, L. Raffaghello, A. Pezzolo, C. Gagliani, C. Tacchetti, P. Mauri, G. Melioli, and V. Pistoia. 2013. Proteome profiling of neuroblastoma-derived exosomes reveal the expression of proteins potentially involved in tumor progression. *PLoS One*. 8:e75054.

Marxsen, J.H., P. Stengel, K. Doege, P. Heikkinen, T. Jokilehto, T. Wagner, W. Jelkmann, P. Jaakkola, and E. Metzen. 2004. Hypoxia-inducible factor-1 (HIF-1) promotes its degradation by induction of HIF-alpha-prolyl-4-hydroxylases. *Biochem J*. 381:761-767.

Mary, C., A. Scherrer, L. Huck, A.K. Lakkaraju, Y. Thomas, A.E. Johnson, and K. Strub. 2010. Residues in SRP9/14 essential for elongation arrest activity of the signal recognition particle define a positively charged functional domain on one side of the protein. *RNA*. 16:969-979.

Masoud, G.N., and W. Li. 2015. HIF-1alpha pathway: role, regulation and intervention for cancer therapy. *Acta Pharm Sin B*. 5:378-389.

McGuire, A., A.J. Lowery, M.R. Kell, M.J. Kerin, and K.J. Sweeney. 2017. Locoregional Recurrence Following Breast Cancer Surgery in the Trastuzumab Era: A Systematic Review by Subtype. *Annals of surgical oncology*. 24:3124-3132.

McTiernan, A. 2003. Behavioral risk factors in breast cancer: can risk be modified? *The oncologist*. 8:326-334.

Melillo, G. 2007. Targeting hypoxia cell signaling for cancer therapy. *Cancer metastasis reviews*. 26:341-352.

Meng, F., H. Liu, S. Liu, and R. Ma. 2017. The clinical significance of HPIP and the associated prognosis in cervical cancer. *Oncotarget*. 8:70262-70270.

Mennerich, D., E.Y. Dimova, and T. Kietzmann. 2014. Direct phosphorylation events involved in HIF-alpha regulation: the role of GSK-3beta. *Hypoxia*. 2:35-45.

Metzger-Filho, O., Z. Sun, G. Viale, K.N. Price, D. Crivellari, R.D. Snyder, R.D. Gelber, M. Castiglione-Gertsch, A.S. Coates, A. Goldhirsch, and F. Cardoso. 2013. Patterns of Recurrence and outcome according to breast cancer subtypes in lymph node-negative disease: results from international breast cancer study group trials VIII and IX. *Journal of clinical oncology : official journal of the American Society of Clinical Oncology*. 31:3083-3090.

Mimeault, M., and S.K. Batra. 2013. Hypoxia-inducing factors as master regulators of stemness properties and altered metabolism of cancer- and metastasis-initiating cells. *Journal of cellular and molecular medicine*. 17:30-54.

Moeller, B.J., R.A. Richardson, and M.W. Dewhirst. 2007. Hypoxia and radiotherapy: opportunities for improved outcomes in cancer treatment. *Cancer Metastasis Rev*. 26:241-248.

Moens, C.B., and L. Selleri. 2006. Hox cofactors in vertebrate development. *Dev Biol*. 291:193-206.

Moreno, D., R. Viana, and P. Sanz. 2009. Two-hybrid analysis identifies PSMD11, a non-ATPase subunit of the proteasome, as a novel interaction partner of AMP-activated protein kinase. *Int J Biochem Cell Biol*. 41:2431-2439.

Murat Karamese, S.A., Ozge Beyza, Gundogdu, Bunyami Unal. 2013. A new hypothesis about hematopoietic Pbx-interaction protein (HPIP): Can it be a key factor in neurodegeneration in the post-menopausal period? *Medical Hypotheses*. 81:470-476.

Muz, B., P. de la Puente, F. Azab, and A.K. Azab. 2015. The role of hypoxia in cancer progression, angiogenesis, metastasis, and resistance to therapy. *Hypoxia*. 3:83-92.

Nagao, A., M. Kobayashi, S. Koyasu, C.C.T. Chow, and H. Harada. 2019. HIF-1-Dependent Reprogramming of Glucose Metabolic Pathway of Cancer Cells and Its Therapeutic Significance. *International journal of molecular sciences*. 20.

Nandi, S., and A.C. Brown. 2017. Characterizing Cell Migration Within Three-dimensional In Vitro Wound Environments. *Journal of visualized experiments : JoVE*.

Narad, P., A. Kumar, A. Chakraborty, P. Patni, A. Sengupta, G. Wadhwa, and K.C. Upadhyaya. 2017. Transcription Factor Information System (TFIS): A Tool for Detection of Transcription Factor Binding Sites. *Interdiscip Sci*. 9:378-391.

Nelson, A.R., B. Fingleton, M.L. Rothenberg, and L.M. Matrisian. 2000. Matrix metalloproteinases: biologic activity and clinical implications. *Journal of clinical oncology : official journal of the American Society of Clinical Oncology*. 18:1135-1149.

Ng, S.W., G.A. Norwitz, M. Pavlicev, T. Tilburgs, C. Simon, and E.R. Norwitz. 2020. Endometrial Decidualization: The Primary Driver of Pregnancy Health. *Int J Mol Sci*. 21.

Ning, Y.X., X.Y. Wang, J.Q. Wang, R. Zeng, and G.Q. Wang. 2018. miR152 regulates TGFbeta1induced epithelialmesenchymal transition by targeting HPIP in tubular epithelial cells. *Mol Med Rep*. 17:7973-7979.

Nishioka, K., S. Ohshima, M. Umeshita-Sasai, N. Yamaguchi, T. Mima, S. Nomura, N. Murata, M. Shimizu, T. Miyake, K. Yoshizaki, M. Suemura, T. Kishimoto, and Y. Saeki. 2000. Enhanced expression and DNA binding activity of two CCAAT/enhancer-binding protein isoforms, C/EBPbeta and C/EBPdelta, in rheumatoid synovium. *Arthritis Rheum*. 43:1591-1596.

Nordling, C.O. 1953. A new theory on cancer-inducing mechanism. *British journal of cancer*. 7:68-72.

O'Mara, T.A., A.B. Spurdle, D.M. Glubb, and C. Endometrial Cancer Association. 2019. Analysis of Promoter-Associated Chromatin Interactions Reveals Biologically Relevant Candidate Target Genes at Endometrial Cancer Risk Loci. *Cancers (Basel)*. 11.

Ogaki, S., S. Harada, N. Shiraki, K. Kume, and S. Kume. 2011. An expression profile analysis of ES cell-derived definitive endodermal cells and Pdx1-expressing cells. *BMC Dev Biol*. 11:13.

Oh, E.T., J.W. Kim, J.M. Kim, S.J. Kim, J.S. Lee, S.S. Hong, J. Goodwin, R.J. Ruthenborg, M.G. Jung, H.J. Lee, C.H. Lee, E.S. Park, C. Kim, and H.J. Park. 2016. NQO1 inhibits proteasome-mediated degradation of HIF-1alpha. *Nature communications*. 7:13593.

Okada, H., T. Tsuzuki, and H. Murata. 2018. Decidualization of the human endometrium. *Reprod Med Biol*. 17:220-227.

Okada, S., T. Irie, J. Tanaka, R. Yasuhara, G. Yamamoto, T. Isobe, C. Hokazono, T. Tachikawa, Y. Kohno, and K. Mishima. 2015. Potential role of hematopoietic pre-B-cell leukemia transcription factor-interacting protein in oral carcinogenesis. *J Oral Pathol Med*. 44:115-125.

Oliveira-Costa, J.P., J.S. Zanetti, G.G. Silveira, D.F. Soave, L.R. Oliveira, V.A. Zorgetto, F.A. Soares, S. Zucoloto, and A. Ribeiro-Silva. 2011. Differential expression of HIF-1alpha in CD44+CD24-/low breast ductal carcinomas. *Diagn Pathol*. 6:73.

Page, D.L., T.E. Kidd, Jr., W.D. Dupont, J.F. Simpson, and L.W. Rogers. 1991. Lobular neoplasia of the breast: higher risk for subsequent invasive cancer predicted by more extensive disease. *Human pathology*. 22:1232-1239.

Paik, S., S. Shak, G. Tang, C. Kim, J. Baker, M. Cronin, F.L. Baehner, M.G. Walker, D. Watson, T. Park, W. Hiller, E.R. Fisher, D.L. Wickerham, J. Bryant, and N. Wolmark. 2004. A multigene assay to predict recurrence of tamoxifen-treated, node-negative breast cancer. *The New England journal of medicine*. 351:2817-2826.

Pan, J., Y. Qin, and M. Zhang. 2016. HPIP promotes non-small cell lung cancer cell proliferation, migration and invasion through regulation of the Sonic hedgehog signaling pathway. *Biomed Pharmacother*. 77:176-181.

Parikh, U., C.M. Chhor, and C.L. Mercado. 2018. Ductal Carcinoma In Situ: The Whole Truth. *AJR. American journal of roentgenology*. 210:246-255.

Parker, J.S., M. Mullins, M.C. Cheang, S. Leung, D. Voduc, T. Vickery, S. Davies, C. Fauron, X. He, Z. Hu, J.F. Quackenbush, I.J. Stijleman, J. Palazzo, J.S. Marron, A.B. Nobel, E. Mardis, T.O. Nielsen, M.J. Ellis, C.M. Perou, and P.S. Bernard. 2009. Supervised risk predictor of breast cancer based on intrinsic subtypes. *Journal of clinical oncology : official journal of the American Society of Clinical Oncology*. 27:1160-1167.

Paszek, M.J., N. Zahir, K.R. Johnson, J.N. Lakins, G.I. Rozenberg, A. Gefen, C.A. Reinhart-King, S.S. Margulies, M. Dembo, D. Boettiger, D.A. Hammer, and V.M. Weaver. 2005. Tensional homeostasis and the malignant phenotype. *Cancer Cell*. 8:241-254.

Peng, J., X. Wang, L. Ran, J. Song, R. Luo, and Y. Wang. 2018. Hypoxia-Inducible Factor 1alpha Regulates the Transforming Growth Factor beta1/SMAD Family Member 3 Pathway to Promote Breast Cancer Progression. *J Breast Cancer*. 21:259-266.

Perez-Escuredo, J., R.K. Dadhich, S. Dhup, A. Cacace, V.F. Van Hee, C.J. De Saedeleer, M. Sboarina, F. Rodriguez, M.J. Fontenille, L. Brisson, P.E. Porporato, and P. Sonveaux. 2016. Lactate promotes glutamine uptake and metabolism in oxidative cancer cells. *Cell Cycle*. 15:72-83.

Perou, C.M., T. Sorlie, M.B. Eisen, M. van de Rijn, S.S. Jeffrey, C.A. Rees, J.R. Pollack, D.T. Ross, H. Johnsen, L.A. Akslen, O. Fluge, A. Pergamenschikov, C. Williams, S.X. Zhu, P.E. Lonning, A.L. Borresen-Dale, P.O. Brown, and D. Botstein. 2000. Molecular portraits of human breast tumours. *Nature*. 406:747-752.

Petersen, T.N., S. Brunak, G. von Heijne, and H. Nielsen. 2011. SignalP 4.0: discriminating signal peptides from transmembrane regions. *Nature methods*. 8:785-786.

Penugurti V, Khumukcham SS, Padala Ch, Dwivedi A, Kamireddy KR, Mukta S, Bhopal T and Manavathi B. 2021. HPIP protooncogene differentially regulates metabolic adaptation and cell fate in breast cancer cells under glucose stress via AMPK and RNF2 dependent pathways. Cancer Letters. 518:243-255.

Pinheiro, C., A. Longatto-Filho, J. Azevedo-Silva, M. Casal, F.C. Schmitt, and F. Baltazar. 2012. Role of monocarboxylate transporters in human cancers: state of the art. *Journal of bioenergetics and biomembranes*. 44:127-139.

Pollard, P.J., J.J. Briere, N.A. Alam, J. Barwell, E. Barclay, N.C. Wortham, T. Hunt, M. Mitchell, S. Olpin, S.J. Moat, I.P. Hargreaves, S.J. Heales, Y.L. Chung, J.R. Griffiths, A. Dalgleish, J.A. McGrath, M.J. Gleeson, S.V. Hodgson, R. Poulsom, P. Rustin, and I.P. Tomlinson. 2005. Accumulation of Krebs cycle intermediates and over-expression of HIF1alpha in tumours which result from germline FH and SDH mutations. *Hum Mol Genet*. 14:2231-2239.

Pope, R.M., R. Lovis, S. Mungre, H. Perlman, A.E. Koch, and G.K. Haines, 3rd. 1999. C/EBP beta in rheumatoid arthritis: correlation with inflammation, not disease specificity. *Clin Immunol*. 91:271-282.

Prat, A., J.S. Parker, O. Karginova, C. Fan, C. Livasy, J.I. Herschkowitz, X. He, and C.M. Perou. 2010. Phenotypic and molecular characterization of the claudin-low intrinsic subtype of breast cancer. *Breast cancer research : BCR*. 12:R68.

Prat, A., and C.M. Perou. 2011. Deconstructing the molecular portraits of breast cancer. *Molecular oncology*. 5:5-23.

Provenzano, P.P., D.R. Inman, K.W. Eliceiri, J.G. Knittel, L. Yan, C.T. Rueden, J.G. White, and P.J. Keely. 2008. Collagen density promotes mammary tumor initiation and progression. *BMC Med*. 6:11.

Pugh, C.W., and P.J. Ratcliffe. 2003. Regulation of angiogenesis by hypoxia: role of the HIF system. *Nature medicine*. 9:677-684.

Quintero-Fabian, S., R. Arreola, E. Becerril-Villanueva, J.C. Torres-Romero, V. Arana-Argaez, J. Lara-Riegos, M.A. Ramirez-Camacho, and M.E. Alvarez-Sanchez. 2019. Role of Matrix Metalloproteinases in Angiogenesis and Cancer. *Front Oncol*. 9:1370.

Raeeszadeh-Sarmazdeh, M., L.D. Do, and B.G. Hritz. 2020. Metalloproteinases and Their Inhibitors: Potential for the Development of New Therapeutics. *Cells*. 9.

Ramirez, J.M., L.P. Folkow, and A.S. Blix. 2007. Hypoxia tolerance in mammals and birds: from the wilderness to the clinic. *Annu Rev Physiol*. 69:113-143.

Ratcliffe, P.J., J.F. O'Rourke, P.H. Maxwell, and C.W. Pugh. 1998. Oxygen sensing, hypoxia-inducible factor-1 and the regulation of mammalian gene expression. *J Exp Biol*. 201:1153-1162.

Raymond, J., and D. Segre. 2006. The effect of oxygen on biochemical networks and the evolution of complex life. *Science*. 311:1764-1767.

Riesterer, O., M. Honer, W. Jochum, C. Oehler, S. Ametamey, and M. Pruschy. 2006. Ionizing radiation antagonizes tumor hypoxia induced by antiangiogenic treatment. *Clin Cancer Res*. 12:3518-3524.

Rigiracciolo, D.C., F. Cirillo, M. Talia, L. Muglia, J.S. Gutkind, M. Maggiolini, and R. Lappano. 2021. Focal Adhesion Kinase Fine Tunes Multifaced Signals toward Breast Cancer Progression. *Cancers (Basel)*. 13.

Rojas, K., and A. Stuckey. 2016. Breast Cancer Epidemiology and Risk Factors. *Clinical obstetrics and gynecology*. 59:651-672.
Roth, J. 2002. Protein N-glycosylation along the secretory pathway: relationship to organelle topography and function, protein quality control, and cell interactions. *Chem Rev*. 102:285-303.
Ruas, J.L., L. Poellinger, and T. Pereira. 2005. Role of CBP in regulating HIF-1-mediated activation of transcription. *Journal of cell science*. 118:301-311.
Saad, R.S., Z. Ghorab, M.A. Khalifa, and M. Xu. 2011. CDX2 as a marker for intestinal differentiation: Its utility and limitations. *World J Gastrointest Surg*. 3:159-166.
Salnikov, A.V., L. Liu, M. Platen, J. Gladkich, O. Salnikova, E. Ryschich, J. Mattern, G. Moldenhauer, J. Werner, P. Schemmer, M.W. Buchler, and I. Herr. 2012. Hypoxia induces EMT in low and highly aggressive pancreatic tumor cells but only cells with cancer stem cell characteristics acquire pronounced migratory potential. *PLoS One*. 7:e46391.
Sanders, M.E., P.A. Schuyler, W.D. Dupont, and D.L. Page. 2005. The natural history of low-grade ductal carcinoma in situ of the breast in women treated by biopsy only revealed over 30 years of long-term follow-up. *Cancer*. 103:2481-2484.
Saraogi, I., and S.O. Shan. 2011. Molecular mechanism of co-translational protein targeting by the signal recognition particle. *Traffic*. 12:535-542.
Sayeeram, D., T.V. Katte, S. Bhatia, A. Jai Kumar, A. Kumar, G. Jayashree, D.S. Rachana, H.V. Nalla Reddy, A. Arvind Rasalkar, R.L. Malempati, and S.D. Reddy. 2020. Identification of potential biomarkers for lung adenocarcinoma. *Heliyon*. 6:e05452.
Schaller, M.D. 2010. Cellular functions of FAK kinases: insight into molecular mechanisms and novel functions. *J Cell Sci*. 123:1007-1013.
Schito, L., and G.L. Semenza. 2016. Hypoxia-Inducible Factors: Master Regulators of Cancer Progression. *Trends in cancer*. 2:758-770.
Scortegagna, M., R.J. Martin, R.D. Kladney, R.G. Neumann, and J.M. Arbeit. 2009. Hypoxia-inducible factor-1alpha suppresses squamous carcinogenic progression and epithelial-mesenchymal transition. *Cancer Res*. 69:2638-2646.
Selak, M.A., S.M. Armour, E.D. MacKenzie, H. Boulahbel, D.G. Watson, K.D. Mansfield, Y. Pan, M.C. Simon, C.B. Thompson, and E. Gottlieb. 2005. Succinate links TCA cycle dysfunction to oncogenesis by inhibiting HIF-alpha prolyl hydroxylase. *Cancer cell*. 7:77-85.
Selina, A.K., K. Murat, K. Emre, M. Ismail, U. Bunyami, and G. Cemal. 2015. The relationship between estrogen receptors and microtubule dynamics in post-menopausal rat brain. *Acta Histochem*. 117:747-751.
Semenza, G.L. 2000. HIF-1: mediator of physiological and pathophysiological responses to hypoxia. *Journal of applied physiology*. 88:1474-1480.
Semenza, G.L. 2003. Targeting HIF-1 for cancer therapy. *Nature reviews. Cancer*. 3:721-732.
Semenza, G.L., P.H. Roth, H.M. Fang, and G.L. Wang. 1994. Transcriptional regulation of genes encoding glycolytic enzymes by hypoxia-inducible factor 1. *The Journal of biological chemistry*. 269:23757-23763.
Semenza, G.L., and G.L. Wang. 1992. A nuclear factor induced by hypoxia via de novo protein synthesis binds to the human erythropoietin gene enhancer at a site required for transcriptional activation. *Mol Cell Biol*. 12:5447-5454.
Sergio Pimpinelli, L.P. 2019. Environmental change and the evolution of genomes: Transposable elements as translators of phenotypic plasticity into genotypic variability. *Functional ecology*.
Sharma, G.N., R. Dave, J. Sanadya, P. Sharma, and K.K. Sharma. 2010. Various types and management of breast cancer: an overview. *Journal of advanced pharmaceutical technology & research*. 1:109-126.
Shi, S., J. Zhao, J. Wang, D. Mi, and Z. Ma. 2017. HPIP silencing inhibits TGF-beta1-induced EMT in lung cancer cells. *Int J Mol Med*. 39:479-483.

Shimamoto, T., K. Ohyashiki, K. Toyama, and K. Takeshita. 1998. Homeobox genes in hematopoiesis and leukemogenesis. *Int J Hematol*. 67:339-350.

Shiraki, N., S. Ogaki, and S. Kume. 2014. Profiling of embryonic stem cell differentiation. *Rev Diabet Stud*. 11:102-114.

Shostak, K., F. Patrascu, S.I. Goktuna, P. Close, L. Borgs, L. Nguyen, F. Olivier, A. Rammal, H. Brinkhaus, M. Bentires-Alj, J.C. Marine, and A. Chariot. 2014. MDM2 restrains estrogen-mediated AKT activation by promoting TBK1-dependent HPIP degradation. *Cell Death Differ*. 21:811-824.

Siegel, V., and P. Walter. 1986. Removal of the Alu structural domain from signal recognition particle leaves its protein translocation activity intact. *Nature*. 320:81-84.

Silveira, S.M., R.A. Villacis, F.A. Marchi, C. Barros Filho Mde, S.A. Drigo, C.S. Neto, A. Lopes, I.W. da Cunha, and S.R. Rogatto. 2013. Genomic signatures predict poor outcome in undifferentiated pleomorphic sarcomas and leiomyosarcomas. *PLoS One*. 8:e67643.

Singh, S.K., C. Hawkins, I.D. Clarke, J.A. Squire, J. Bayani, T. Hide, R.M. Henkelman, M.D. Cusimano, and P.B. Dirks. 2004. Identification of human brain tumour initiating cells. *Nature*. 432:396-401.

Smalley, M., and A. Ashworth. 2003. Stem cells and breast cancer: A field in transit. *Nature reviews. Cancer*. 3:832-844.

Sorlie, T., C.M. Perou, R. Tibshirani, T. Aas, S. Geisler, H. Johnsen, T. Hastie, M.B. Eisen, M. van de Rijn, S.S. Jeffrey, T. Thorsen, H. Quist, J.C. Matese, P.O. Brown, D. Botstein, P.E. Lonning, and A.L. Borresen-Dale. 2001. Gene expression patterns of breast carcinomas distinguish tumor subclasses with clinical implications. *Proceedings of the National Academy of Sciences of the United States of America*. 98:10869-10874.

Sorlie, T., R. Tibshirani, J. Parker, T. Hastie, J.S. Marron, A. Nobel, S. Deng, H. Johnsen, R. Pesich, S. Geisler, J. Demeter, C.M. Perou, P.E. Lonning, P.O. Brown, A.L. Borresen-Dale, and D. Botstein. 2003. Repeated observation of breast tumor subtypes in independent gene expression data sets. *Proceedings of the National Academy of Sciences of the United States of America*. 100:8418-8423.

Spirin, V., and L.A. Mirny. 2003. Protein complexes and functional modules in molecular networks. *Proceedings of the National Academy of Sciences of the United States of America*. 100:12123-12128.

Springman, E.B., E.L. Angleton, H. Birkedal-Hansen, and H.E. Van Wart. 1990. Multiple modes of activation of latent human fibroblast collagenase: evidence for the role of a Cys73 active-site zinc complex in latency and a "cysteine switch" mechanism for activation. *Proc Natl Acad Sci U S A*. 87:364-368.

Stamati, K., V. Mudera, and U. Cheema. 2011. Evolution of oxygen utilization in multicellular organisms and implications for cell signalling in tissue engineering. *J Tissue Eng*. 2:2041731411432365.

Stingl, J., and C. Caldas. 2007. Molecular heterogeneity of breast carcinomas and the cancer stem cell hypothesis. *Nature reviews. Cancer*. 7:791-799.

Storci, G., P. Sansone, S. Mari, G. D'Uva, S. Tavolari, T. Guarnieri, M. Taffurelli, C. Ceccarelli, D. Santini, P. Chieco, K.B. Marcu, and M. Bonafe. 2010. TNFalpha up-regulates SLUG via the NF-kappaB/HIF1alpha axis, which imparts breast cancer cells with a stem cell-like phenotype. *J Cell Physiol*. 225:682-691.

Strober, W. 2015. Trypan Blue Exclusion Test of Cell Viability. *Current protocols in immunology*. 111:A3 B 1-A3 B 3.

Strub, K., J. Moss, and P. Walter. 1991. Binding sites of the 9- and 14-kilodalton heterodimeric protein subunit of the signal recognition particle (SRP) are contained exclusively in the Alu domain of SRP RNA and contain a sequence motif that is conserved in evolution. *Mol Cell Biol*. 11:3949-3959.

Sun, H., X.B. Li, Y. Meng, L. Fan, M. Li, and J. Fang. 2013a. TRAF6 upregulates expression of HIF-1alpha and promotes tumor angiogenesis. *Cancer research*. 73:4950-4959.

Sun, L., H. Li, J. Chen, Y. Iwasaki, T. Kubota, M. Matsuoka, A. Shen, Q. Chen, and Y. Xu. 2013b. PIASy mediates hypoxia-induced SIRT1 transcriptional repression and epithelial-to-mesenchymal transition in ovarian cancer cells. *J Cell Sci*. 126:3939-3947.

Swann, J.B., and M.J. Smyth. 2007. Immune surveillance of tumors. *J Clin Invest*. 117:1137-1146.

Swietach, P., R.D. Vaughan-Jones, and A.L. Harris. 2007. Regulation of tumor pH and the role of carbonic anhydrase 9. *Cancer Metastasis Rev*. 26:299-310.

Takahashi, H., M. Asaoka, L. Yan, O.M. Rashid, M. Oshi, T. Ishikawa, M. Nagahashi, and K. Takabe. 2020. Biologically Aggressive Phenotype and Anti-cancer Immunity Counterbalance in Breast Cancer with High Mutation Rate. *Sci Rep*. 10:1852.

Tam, S.Y., V.W.C. Wu, and H.K.W. Law. 2020. Hypoxia-Induced Epithelial-Mesenchymal Transition in Cancers: HIF-1alpha and Beyond. *Front Oncol*. 10:486.

Tang, C., T. Liu, K. Wang, X. Wang, S. Xu, D. He, and J. Zeng. 2019. Transcriptional regulation of FoxM1 by HIF1alpha mediates hypoxiainduced EMT in prostate cancer. *Oncol Rep*. 42:1307-1318.

Thannickal, V.J. 2009. Oxygen in the evolution of complex life and the price we pay. *Am J Respir Cell Mol Biol*. 40:507-510.

Thiery, J.P. 2002. Epithelial-mesenchymal transitions in tumour progression. *Nat Rev Cancer*. 2:442-454.

Tian, M., J.R. Neil, and W.P. Schiemann. 2011. Transforming growth factor-beta and the hallmarks of cancer. *Cell Signal*. 23:951-962.

Tsai, J.H., and J. Yang. 2013. Epithelial-mesenchymal plasticity in carcinoma metastasis. *Genes & development*. 27:2192-2206.

van de Vijver, M.J., Y.D. He, L.J. van't Veer, H. Dai, A.A. Hart, D.W. Voskuil, G.J. Schreiber, J.L. Peterse, C. Roberts, M.J. Marton, M. Parrish, D. Atsma, A. Witteveen, A. Glas, L. Delahaye, T. van der Velde, H. Bartelink, S. Rodenhuis, E.T. Rutgers, S.H. Friend, and R. Bernards. 2002. A gene-expression signature as a predictor of survival in breast cancer. *The New England journal of medicine*. 347:1999-2009.

Van den Steen, P.E., B. Dubois, I. Nelissen, P.M. Rudd, R.A. Dwek, and G. Opdenakker. 2002. Biochemistry and molecular biology of gelatinase B or matrix metalloproteinase-9 (MMP-9). *Crit Rev Biochem Mol Biol*. 37:375-536.

van der Rest, M., and R. Garrone. 1991. Collagen family of proteins. *FASEB J*. 5:2814-2823.

van Vuurden, D.G., E. Aronica, E. Hulleman, L.E. Wedekind, D. Biesmans, A. Malekzadeh, M. Bugiani, D. Geerts, D.P. Noske, W.P. Vandertop, G.J. Kaspers, J. Cloos, T. Wurdinger, and P.P. van der Stoop. 2014. Pre-B-cell leukemia homeobox interacting protein 1 is overexpressed in astrocytoma and promotes tumor cell growth and migration. *Neuro-oncology*. 16:946-959.

Vander Heiden, M.G., L.C. Cantley, and C.B. Thompson. 2009. Understanding the Warburg effect: the metabolic requirements of cell proliferation. *Science*. 324:1029-1033.

Vandeven, N., and P. Nghiem. 2014. Pathogen-driven cancers and emerging immune therapeutic strategies. *Cancer Immunol Res*. 2:9-14.

Varghese, F., A.B. Bukhari, R. Malhotra, and A. De. 2014. IHC Profiler: an open source plugin for the quantitative evaluation and automated scoring of immunohistochemistry images of human tissue samples. *PloS one*. 9:e96801.

Vaupel, P., and A. Mayer. 2007. Hypoxia in cancer: significance and impact on clinical outcome. *Cancer Metastasis Rev*. 26:225-239.

Vaupel, P., and G. Multhoff. 2020. Revisiting the Warburg effect: historical dogma versus current understanding. *J Physiol*.

Vaupel, P., H. Schmidberger, and A. Mayer. 2019. The Warburg effect: essential part of metabolic reprogramming and central contributor to cancer progression. *Int J Radiat Biol*. 95:912-919.

Vella, L.J. 2014. The emerging role of exosomes in epithelial-mesenchymal-transition in cancer. *Front Oncol*. 4:361.

Vermeulen, L., M.R. Sprick, K. Kemper, G. Stassi, and J.P. Medema. 2008. Cancer stem cells--old concepts, new insights. *Cell Death Differ*. 15:947-958.

Victorelli, S., and J.F. Passos. 2017. Telomeres and Cell Senescence - Size Matters Not. *EBioMedicine*. 21:14-20.

Vinci, M., C. Box, M. Zimmermann, and S.A. Eccles. 2013. Tumor spheroid-based migration assays for evaluation of therapeutic agents. *Methods in molecular biology*. 986:253-266.

Voduc, K.D., M.C. Cheang, S. Tyldesley, K. Gelmon, T.O. Nielsen, and H. Kennecke. 2010. Breast cancer subtypes and the risk of local and regional relapse. *Journal of clinical oncology : official journal of the American Society of Clinical Oncology*. 28:1684-1691.

Walter, P., and G. Blobel. 1981. Translocation of proteins across the endoplasmic reticulum III. Signal recognition protein (SRP) causes signal sequence-dependent and site-specific arrest of chain elongation that is released by microsomal membranes. *J Cell Biol*. 91:557-561.

Wang, D., L. Wang, Y. Zhou, X. Zhao, and H. Xiong. 2016. The involvement of hematopoietic pre-B cell leukemia transcription factor-interacting protein in regulating epithelial-mesenchymal transition of human spinal glioblastoma. *Tumour biology : the journal of the International Society for Oncodevelopmental Biology and Medicine*. 37:5897-5903.

Wang, G.L., B.H. Jiang, E.A. Rue, and G.L. Semenza. 1995. Hypoxia-inducible factor 1 is a basic-helix-loop-helix-PAS heterodimer regulated by cellular O2 tension. *Proc Natl Acad Sci U S A*. 92:5510-5514.

Wang, M., J. Zhao, L. Zhang, F. Wei, Y. Lian, Y. Wu, Z. Gong, S. Zhang, J. Zhou, K. Cao, X. Li, W. Xiong, G. Li, Z. Zeng, and C. Guo. 2017a. Role of tumor microenvironment in tumorigenesis. *Journal of Cancer*. 8:761-773.

Wang, P.J., J.R. McCarrey, F. Yang, and D.C. Page. 2001. An abundance of X-linked genes expressed in spermatogonia. *Nat Genet*. 27:422-426.

Wang, S.C., D.S. Chai, C.B. Chen, Z.Y. Wang, and L. Wang. 2015. HPIP promotes thyroid cancer cell growth, migration and EMT through activating PI3K/AKT signaling pathway. *Biomed Pharmacother*. 75:33-39.

Wang, X., Z. Yang, H. Zhang, L. Ding, X. Li, C. Zhu, Y. Zheng, and Q. Ye. 2008. The estrogen receptor-interacting protein HPIP increases estrogen-responsive gene expression through activation of MAPK and AKT. *Biochimica et biophysica acta*. 1783:1220-1228.

Wang, Y., D. Li, Y. Liu, S. Tian, and X. Chen. 2018. Expression and clinicopathological significance of hematopoietic pre-B cell leukemia transcription factor-interacting protein in cervical carcinoma. *Pathol Res Pract*. 214:1340-1344.

Wang, Y., M. Li, F. Meng, and G. Lou. 2017b. HPIP expression predicts chemoresistance and poor clinical outcomes in patients with epithelial ovarian cancer. *Hum Pathol*. 60:114-120.

Wang, Y., Y. Liu, S.N. Malek, P. Zheng, and Y. Liu. 2011. Targeting HIF1alpha eliminates cancer stem cells in hematological malignancies. *Cell Stem Cell*. 8:399-411.

Wang, Y., F. Meng, Y. Liu, and X. Chen. 2017c. Expression of HPIP in epithelial ovarian carcinoma: a clinicopathological study. *Onco Targets Ther*. 10:95-100.

Warkentin, K.M. 1995. Adaptive plasticity in hatching age: a response to predation risk trade-offs. *Proc Natl Acad Sci U S A*. 92:3507-3510.

Warkentin, K.M. 2002. Hatching timing, oxygen availability, and external gill regression in the tree frog, Agalychnis callidryas. *Physiol Biochem Zool*. 75:155-164.

Webber, J.P., L.K. Spary, A.J. Sanders, R. Chowdhury, W.G. Jiang, R. Steadman, J. Wymant, A.T. Jones, H. Kynaston, M.D. Mason, Z. Tabi, and A. Clayton. 2015. Differentiation of tumour-promoting stromal myofibroblasts by cancer exosomes. *Oncogene*. 34:290-302.

Wei, S.C., L. Fattet, J.H. Tsai, Y. Guo, V.H. Pai, H.E. Majeski, A.C. Chen, R.L. Sah, S.S. Taylor, A.J. Engler, and J. Yang. 2015. Matrix stiffness drives epithelial-mesenchymal transition and tumour metastasis through a TWIST1-G3BP2 mechanotransduction pathway. *Nat Cell Biol*. 17:678-688.

Whiteside, T.L. 2008. The tumor microenvironment and its role in promoting tumor growth. *Oncogene*. 27:5904-5912.

Williams, E.D., D. Gao, A. Redfern, and E.W. Thompson. 2019. Controversies around epithelial-mesenchymal plasticity in cancer metastasis. *Nature reviews. Cancer*. 19:716-732.

Winkler, J., A. Abisoye-Ogunniyan, K.J. Metcalf, and Z. Werb. 2020. Concepts of extracellular matrix remodelling in tumour progression and metastasis. *Nat Commun*. 11:5120.

Woodward, W.A., M.S. Chen, F. Behbod, M.P. Alfaro, T.A. Buchholz, and J.M. Rosen. 2007. WNT/beta-catenin mediates radiation resistance of mouse mammary progenitor cells. *Proceedings of the National Academy of Sciences of the United States of America*. 104:618-623.

Wu, C.I., H.Y. Wang, S. Ling, and X. Lu. 2016. The Ecology and Evolution of Cancer: The Ultra-Microevolutionary Process. *Annu Rev Genet*. 50:347-369.

Wu, C.J., L. Krishnamurti, J.L. Kutok, M. Biernacki, S. Rogers, W. Zhang, J.H. Antin, and J. Ritz. 2005. Evidence for ineffective erythropoiesis in severe sickle cell disease. *Blood*. 106:3639-3645.

Wu, Z.Q., X.Y. Li, C.Y. Hu, M. Ford, C.G. Kleer, and S.J. Weiss. 2012. Canonical Wnt signaling regulates Slug activity and links epithelial-mesenchymal transition with epigenetic Breast Cancer 1, Early Onset (BRCA1) repression. *Proc Natl Acad Sci U S A*. 109:16654-16659.

Xu, X., Z. Fan, L. Kang, J. Han, C. Jiang, X. Zheng, Z. Zhu, H. Jiao, J. Lin, K. Jiang, L. Ding, H. Zhang, L. Cheng, H. Fu, Y. Song, Y. Jiang, J. Liu, R. Wang, N. Du, and Q. Ye. 2013a. Hepatitis B virus X protein represses miRNA-148a to enhance tumorigenesis. *The Journal of clinical investigation*. 123:630-645.

Xu, X., C. Jiang, S. Wang, Y. Tai, T. Wang, L. Kang, Z. Fan, S. Li, L. Li, J. Fu, J. Liu, Q. Ji, X. Wang, L. Wei, and Q. Ye. 2013b. HPIP is upregulated in liver cancer and promotes hepatoma cell proliferation via activation of G2/M transition. *IUBMB Life*. 65:873-882.

Yadav, U.P., T. Singh, P. Kumar, P. Sharma, H. Kaur, S. Sharma, S. Singh, S. Kumar, and K. Mehta. 2020. Metabolic Adaptations in Cancer Stem Cells. *Front Oncol*. 10:1010.

Yan, C., and D.D. Boyd. 2007. Regulation of matrix metalloproteinase gene expression. *J Cell Physiol*. 211:19-26.

Yan, M., M.C. Gingras, E.A. Dunlop, Y. Nouet, F. Dupuy, Z. Jalali, E. Possik, B.J. Coull, D. Kharitidi, A.B. Dydensborg, B. Faubert, M. Kamps, S. Sabourin, R.S. Preston, D.M. Davies, T. Roughead, L. Chotard, M.A. van Steensel, R. Jones, A.R. Tee, and A. Pause. 2014. The tumor suppressor folliculin regulates AMPK-dependent metabolic transformation. *The Journal of clinical investigation*. 124:2640-2650.

Yang, M.H., M.Z. Wu, S.H. Chiou, P.M. Chen, S.Y. Chang, C.J. Liu, S.C. Teng, and K.J. Wu. 2008. Direct regulation of TWIST by HIF-1alpha promotes metastasis. *Nat Cell Biol*. 10:295-305.

Yoo, Y.G., G. Kong, and M.O. Lee. 2006. Metastasis-associated protein 1 enhances stability of hypoxia-inducible factor-1alpha protein by recruiting histone deacetylase 1. *The EMBO journal*. 25:1231-1241.

Yu, B., X. Tian, L. Zhang, and R. Feng. 2016. Hematopoietic PBX-Interaction Protein Promotes Breast Cancer Sensitivity to Paclitaxel Through a Microtubule-Dependent Mechanism. *DNA Cell Biol*. 35:740-745.

Yu, Y.H., F.P. Siao, L.C. Hsu, and P.H. Yen. 2012. TEX11 modulates germ cell proliferation by competing with estrogen receptor beta for the binding to HPIP. *Mol Endocrinol*. 26:630-642.

Zellmer, V.R., and S. Zhang. 2014. Evolving concepts of tumor heterogeneity. *Cell & bioscience*. 4:69.

Zhang, G.Y., A.H. Liu, G.M. Li, and J.R. Wang. 2016. HPIP Silencing Prevents Epithelial-Mesenchymal Transition Induced by TGF-beta1 in Human Ovarian Cancer Cells. *Oncol Res*. 24:33-39.

Zhang, L., G. Huang, X. Li, Y. Zhang, Y. Jiang, J. Shen, J. Liu, Q. Wang, J. Zhu, X. Feng, J. Dong, and C. Qian. 2013. Hypoxia induces epithelial-mesenchymal transition via activation of SNAI1 by hypoxia-inducible factor -1alpha in hepatocellular carcinoma. *BMC Cancer*. 13:108.

Zhang, Q., Z. Han, Y. Zhu, J. Chen, and W. Li. 2021. Role of hypoxia inducible factor-1 in cancer stem cells (Review). *Mol Med Rep*. 23:1.

Zhang, W., X. Shi, Y. Peng, M. Wu, P. Zhang, R. Xie, Y. Wu, Q. Yan, S. Liu, and J. Wang. 2015. HIF-1alpha Promotes Epithelial-Mesenchymal Transition and Metastasis through Direct Regulation of ZEB1 in Colorectal Cancer. *PLoS One*. 10:e0129603.

Zhao, Y.M., G. Yang, L. You, Y. Hu, and Y.P. Zhao. 2020. [Effect of Hematopoietic Pre-B-cell Leukemia Transcription Factor Interacting Protein Knockdown on Proliferation,Cell Cycle and Apoptosis in Pancreatic Cancer Cells]. *Zhongguo yi xue ke xue yuan xue bao. Acta Academiae Medicinae Sinicae*. 42:7-15.

Zhong, H., A.M. De Marzo, E. Laughner, M. Lim, D.A. Hilton, D. Zagzag, P. Buechler, W.B. Isaacs, G.L. Semenza, and J.W. Simons. 1999. Overexpression of hypoxia-inducible factor 1alpha in common human cancers and their metastases. *Cancer Res*. 59:5830-5835.

Publications
(From the Thesis)

BBA - Reviews on Cancer 1876 (2021) 188576

Contents lists available at ScienceDirect

BBA - Reviews on Cancer

journal homepage: www.elsevier.com/locate/bbacan

Review

Two decades of a protooncogene HPIP/PBXIP1: Uncovering the tale from germ cell to cancer

Saratchandra Singh Khumukcham, Bramanandam Manavathi *

Molecular and Cellular Oncology Laboratory, Department of Biochemistry, School of Life Sciences, University of Hyderabad, Hyderabad, Telangana, India

ARTICLE INFO

Keywords:
HPIP/PBXIP1
Proto-oncogene
EMT/Metastasis
Hematopoiesis
Osteoarthritis
Germ cell proliferation
Cell cycle regulation
ERα/β functions

ABSTRACT

Hematopoietic PBX interacting protein (HPIP or pre-B-cell leukemia transcription factor interacting protein (PBXIP1) was discovered two decades ago as a corepressor of pre-B-cell leukemia homeobox (PBX) 1 with a vital functional role in hematopoiesis. Later it emerged as a potential biomarker of poor prognosis and tumorigenesis for more than a dozen different cancers. It regulates aggressive cancer phenotypes, cell proliferation, metastasis, EMT, etc. The anomaly in the regulation of HPIP is linked with physiological disorders like renal fibrosis, chronic kidney disease and osteoarthritis. Scientists have unraveled more than twenty interacting proteins of HPIP and its functional role in various physiological and cellular processes that involves normal neuronal development, embryogenesis, endometrium decidualization, and germ cell proliferation. Over the past 20 years, we have witnessed the emerging role of HPIP and its association with a myriad of cellular activities ranging from germ cell proliferation to cancer aggressiveness, modulating multitude of signaling cascades like TGF-β1, PI3K/AKT, Wnt, mTOR, and Sonic hedgehog signaling pathways. This review will give the current understanding of HPIP, in terms of its diverse functions, theoretical ideas, and further explore cellular links and promising areas that need to be investigated. We also provide a comprehensive overview of the transcript variants of HPIP and distinct sets of transcription factors regulating their expression, which may help to understand the role of HPIP in various cellular or physiological conditions.

1. Introduction

Abramovich et al., discovered HPIP as one of the interacting protein partners of PBX1 (pre B cell leukemia homeobox 1) and likewise named it as hematopoietic PBX interaction protein (HPIP). It is also known as pre B-cell leukemia homeobox interacting protein 1 (PBXIP1) [1]. Being an adaptor/scaffold protein, it facilitates physical associations with various signaling proteins like ERα/β, Src, microtubules, etc. [2]. Paramount investigation reveals that HPIP is elevated in more than a dozen cancers and enhances tumorigenesis [3–6]. Apart from its role in cancer, it is also linked with neuronal development, embryogenesis, and endometrium decidualization of repeated implantation failure in women [7]. Its expression is elevated in spermatogonial cells and promotes germ cell proliferation. Other physiological disorder-related diseases like renal fibrosis, chronic kidney disease, and Osteoarthritis (OA) (joint cartilage disorder) are linked with upregulation of HPIP [8]. Two decades have passed since the discovery of HPIP and in unraveling its cellular functions. However, there is a dire need of rigorous empirical study to address its mechanistic cellular functions because of the myriad of cellular and physiological processes it is associated with. We made a systematic evolutionary tree of HPIP that shows the explorations made so far with respect to its aforementioned cellular activities. HPIP has been investigated for its diverse roles like in hematopoiesis, estrogen signaling-related cellular function, reproduction biology, cancers, etc. In this review we intend to throw lights on the research done so far on HPIP and its functions, discuss further on theoretical ideas and touch upon the promising areas that need to be investigated. We also reveal a comprehensive overview of the transcript variants of HPIP promoter and its distinct sets of transcription factor binding sites, which may help to understand the role of HPIP in various cellular or physiological conditions.

2. Background of Pre-B-cell leukemia homeobox interacting protein 1 (PBXIP1 or HPIP)

It was the year 2000 when Abramovich et al., discovered PBXIP1/HPIP. Six years down the line, Manavathi et al., had a major breakthrough in elucidating the role of HPIP in tumorigenesis by activation of

* Corresponding author.
E-mail address: manavathibsl@uohyd.ac.in (B. Manavathi).

https://doi.org/10.1016/j.bbcan.2021.188576
Received 9 April 2021; Received in revised form 25 May 2021; Accepted 28 May 2021
Available online 5 June 2021

Contents lists available at ScienceDirect

Cancer Letters

journal homepage: www.elsevier.com/locate/canlet

A reciprocal feedback loop between HIF-1α and HPIP controls phenotypic plasticity in breast cancer cells

Saratchandra Singh Khumukcham[1], Vasudevarao Penugurti[1], Anita Soni[1], Veena Uppala[1], Kishore Hari[2], Mohit Kumar Jolly[2], Anju Dwivedi[1], Abdul Salam PK[1], Chiranjeevi Padala[1], Srinivasulu Mukta[3], Triveni B[3], Bramanandam Manavathi[1]*

[1]Molecular and Cellular Oncology Laboratory, Department of Biochemistry, School of Life Sciences, University of Hyderabad, Hyderabad, India.

[2]Center for BioSystems Science and Engineering, Indian Institute of Science, Bangalore, India.

[3]MNJ Cancer Hospital Hyderabad, Telangana, India.

*Correspondence: manavathibsl@uohyd.ac.in

Abstract

While phenotypic plasticity is a critical factor contributing to tumor heterogeneity, molecular mechanisms underlying this process are largely unknown. Here we report that breast cancer cells display phenotypic diversity in response to hypoxia or normoxia microenvironments by operating a reciprocal positive feedback regulation of HPIP and HIF-1α. We show that under hypoxia, HIF-1α induces *HPIP* expression that establishes cell survival, and also promotes cell migration/invasion, EMT and metastatic phenotypes in breast cancer cells. Mechanistic studies revealed that HPIP interacts with SRP14, a component of signal recognition particle, and stimulates MMP9 synthesis under hypoxic stress. Whereas, in normoxia, HPIP stabilizes HIF-1α, causing the Warburg effect to support cell growth. Concurrently, mathematical modelling corroborates this reciprocal feedback loop in enabling cell-state transitions in cancer cells. Clinical data indicate that elevated levels of HPIP and HIF-1α correlate with unfavorable prognosis and shorter survival rates in breast cancer subjects. Together, this data shows a reciprocal positive feedback loop between HPIP and HIF-1α that was unknown hitherto. It unveils how the tumor microenvironment influences phenotypic plasticity that has an impact on tumor growth and metastasis and, further signifies considering this pathway as a potential therapeutic target in breast cancer.

Keywords: Hypoxia, Warburg effect, Metastasis, cell proliferation, tumor microenvironment

Other Publications

Hematopoietic PBX-interacting protein is a substrate and an inhibitor of the APC/C–Cdc20 complex and regulates mitosis by stabilizing cyclin B1

Received for publication, November 15, 2018, and in revised form, April 27, 2019 Published, Papers in Press, May 17, 2019, DOI 10.1074/jbc.RA118.006733

Saratchandra Singh Khumukcham[‡1], Venkata Subramanyam Kumar Samanthapudi[‡1], Vasudevarao Penugurti[‡1], Anita Kumari[‡], P. S. Kesavan[§], Loka Reddy Velatooru[‡], Siva Reddy Kotla[‡], Aprotim Mazumder[§], and Bramanandam Manavathi[‡2]

From the [‡]Department of Biochemistry, School of Life Sciences, University of Hyderabad, Hyderabad 500046, India and the [§]Centre for Interdisciplinary Sciences, Tata Institute of Fundamental Research Hyderabad, Hyderabad 500107, Telangana, India

Edited by Xiao-Fan Wang

Proper cell division relies on the coordinated regulation between a structural component, the mitotic spindle, and a regulatory component, anaphase-promoting complex/cyclosome (APC/C). Hematopoietic PBX-interacting protein (HPIP) is a microtubule-associated protein that plays a pivotal role in cell proliferation, cell migration, and tumor metastasis. Here, using HEK293T and HeLa cells, along with immunoprecipitation and immunoblotting, live-cell imaging, and protein-stability assays, we report that HPIP expression oscillates throughout the cell cycle and that its depletion delays cell division. We noted that by utilizing its D box and IR domain, HPIP plays a dual role both as a substrate and inhibitor, respectively, of the APC/C complex. We observed that HPIP enhances the G_2/M transition of the cell cycle by transiently stabilizing cyclin B1 by preventing APC/C–Cdc20–mediated degradation, thereby ensuring timely mitotic entry. We also uncovered that HPIP associates with the mitotic spindle and that its depletion leads to the formation of multiple mitotic spindles and chromosomal abnormalities, results in defects in cytokinesis, and delays mitotic exit. Our findings uncover HPIP as both a substrate and an inhibitor of APC/C–Cdc20 that maintains the temporal stability of cyclin B1 during the G_2/M transition and thereby controls mitosis and cell division.

Accurate chromosome segregation is essential for proper cell division in normal cells. Two important post-translational modifications, phosphorylation, and ubiquitin-mediated proteolysis during mitosis, play crucial roles in this process (1). The anaphase promoting complex/cyclosome (APC/C),[3] a ubiquitin ligase, controls the cell division by regulating mitosis through ubiquitin-directed proteolysis of key substrates in an ordered fashion to direct progression through the mitotic exit, chromosome segregation, and cytokinesis (2–4). The activity of APC/C is coordinated by two regulatory proteins, Cdc20 and Cdh1, through phase-specific interactions during the cell cycle and promotes cell division with precision and accuracy (5). For example, APC/C–Cdc20 degrades Securin and cyclin B1 at anaphase onset. This ensures Separase activation and proteolysis of Cohesin, which holds pair of sister chromatids together during early mitosis. The spindle assembly checkpoint, which depends on multiprotein complexes including Mad2, BubR1, and Bub3, delays APC/C–Cdc20 activation until all chromosomes are properly aligned at the metaphase plate (6, 7). Perturbation of this checkpoint results in chromosomal abnormality (8).

Entry into mitosis is coordinated by cyclin B1–dependent activation of cyclin-dependent kinase 1 (CDK1) during G_2 phase and form a Cdk1–cyclin B1 complex also known as maturation-promoting factor, which is crucial for G_2/M transition (9). Cyclin B1 accumulates in the nucleus as the cells progress to mitosis, although the activation of CDK1–cyclin B1 is initiated at the cytoplasm (10). Cyclin B1 binding triggers a conformational change in Wee1 phosphorylated and inactive CDK1, restoring the activity in CDK1 (11). The activated CDK1–cyclin B1 complex triggers initiation of chromosome condensation, nuclear envelope breakdown, and mitotic spindle assembly through phosphorylation of its substrates (10). It also phosphorylates APC/C–Cdc20 for its complete activation, but later during mitosis cyclin B1 is degraded by APC/C–Cdc20 (12, 13). Abolishing the degradation of cyclin B1 leads to arrest of cells in mitosis, suggesting timely degradation of cyclin B1 by APC/C, is important for proper cell cycle progression (14, 15). Although transcriptional up-regulation of cyclin B1 and its increased stability of mRNA during the G_2 phase has been described before (16), the role of proteasomal pathway in increased cyclin B1 levels is largely unknown.

Hematopoietic PBX-interacting protein (HPIP, also known as PBXIP1) is a protooncoprotein that has been shown to be overexpressed in several cancer types including infiltrative ductal carcinoma (17), hepatocellular carcinoma (18), glioma (19), and ovarian cancer (20). Previous reports have shown that HPIP promotes cell proliferation by modulating the expression of cyclins during the

This work was supported by Department of Biotechnology, India Grants BT/PR7672/BRB/10/1173/2013, BT/Med/30/SP11273/2015, and BT/PR8764/MED/97/104/2013 and Department of Science and Technology, India Grant SB/SO/BB/013/2013 (to B. M.). The authors declare that they have no conflicts of interest with the contents of this article.

This article contains supporting "Materials and methods," Tables S1 and S2, Figs. S1 and S2, and Videos S1–S13.

[1] These authors contributed equally to this work.

[2] To whom correspondence should be addressed. E-mail: manavbrahma@gmail.com.

[3] The abbreviations used are: APC/C, anaphase-promoting complex/cyclosome; HPIP, hematopoietic PBX-interacting protein; CDK, cyclin-dependent kinase; DT, double thymidine; DMEM, Dulbecco's modified Eagle's medium; DAPI, 4′,6′-diamino-2-phenylindole; SAC, spindle assembly checkpoint; MCC, mitotic checkpoint complex.

RSC Advances

PAPER

View Article Online
View Journal | View Issue

Cite this: *RSC Adv.*, 2020, **10**, 24095

Effective *in vitro* delivery of paclitaxel by nanocargo of mesoporous polycaprolactone against triple negative breast cancer cells by minimalizing drug dose†

Himadri Medhi,‡[a] Saratchandra Singh Khumukcham,‡[b] Bramanandam Manavathi*[b] and Pradip Paik *[ac]

Among the breast cancers, triple negative breast cancer (TNBC) has relatively poor outcomes with a lower survival rate and personalised chemotherapy is the only option available for treatment. Currently in the biomedical domain, nanomaterials with porous morphology have revealed their tremendous possibilities to be used as a nanocarrier in treating cancer by offering void space to encapsulate/entrap biological agents. However, the development of nanocarrier-based targeted therapy with high therapeutic efficacy and fewer side effects to normal cells is always a challenge. Here, we have developed nanocargos based on biodegradable mesoporous PCL (polycaprolactone) of approx. diameter of 75 nm by template removal synthesis techniques. Succeeding the comparative analysis of the nanocarriers, the efficiencies of core shell PCL-mZnO (PZ) and mesoporous PCL (HPZ) to deliver paclitaxel (Taxol/T) into breast cancer cells, is investigated. We found that HPZ nanocapsules have less cytotoxicity and drug loading efficiency of about 600 μg mg^{-1}. The Taxol-loaded nanoparticles (T-HPZ) have exhibited more cytotoxicity than Taxol alone treated cancer cells. Furthermore, T-HPZ treated MDA-MB231 cells are accumulated at G2/M phase of the cell cycle and eventually undergo apoptosis. In support of this, anchorage independent growth of MDA-MB231 cells are significantly inhibited by T-HPZ treatment. Together, our findings suggest that T-HPZ-based paclitaxel (Taxol/T) loaded nanoparticles provide a novel therapeutic option in the treatment of TNBC.

Received 20th May 2020
Accepted 13th June 2020

DOI: 10.1039/d0ra04505e

rsc.li/rsc-advances

Introduction

Breast cancer is one of the most frequently arising cancers among women with a transience rate of ~15%. Among the breast cancer types, triple negative breast cancer (TNBC) is highly invasive in nature and has a lower survival rate.[1] TNBC is characterized by the lack of expression of three main receptors such as estrogen receptor (ER), progesterone receptor (PR), and the human epidermal growth factor receptor 2 (HER2).[1] Due to this, TNBC is resistant to the conventional therapies such as trastuzumab, tamoxifen and aromatase inhibitors, which are routinely used in breast cancer treatment. TNBC accounts for 15–20% of all breast cancers with a poor prognosis and high mortality of over 50% as compared to the other subtype of breast cancers.[2,3] Chemotherapy is the only principle treatment and effective option for TNBC.[4,5] However, treatment associated with this mode is accompanied with myriad side effects as the accessible anticancer drugs not only affect the malignant cells but also damage the healthy cells surrounding the malignant cells. Therefore, continuous efforts are being made in this field to improve the therapeutic efficiency of drugs carrying fewer side effects.[6–8] The biodegradable 'polymer based nano-sized capsules' are becoming more promising as a drug delivery cargo[9–13] because of their advantages over the other nanomaterials used for delivery applications.[14] The polymer nanocapsules are engineered by encapsulating the drugs or other biomolecules on the surface or inside of the nanoparticle by chemical or physical approaches.[15,16] The engineered nanodrugs formulation thus designed are delivered to the site of interest, and after delivery, these nanocarriers effortlessly degrade in the physiological environment.[17]

Polycaprolactone (PCL) is one of the dexterous polymers that exhibits amalgamation of biodegradable and biocompatible properties, which makes it complimentary for all the biological applications.[6,7] Moreover, it is approved by the FDA (Food and

[a]*School of Engineering Sciences and Technology, University of Hyderabad, Hyderabad 500046, India*

[b]*Department of Biochemistry, School of Life Sciences, University of Hyderabad, Hyderabad 500046, India. E-mail: manavbrahma@gmail.com*

[c]*School of Biomedical Engineering, Indian Institute of Technology, BHU, Varanasi 221 005, India. E-mail: paik.bme@iitbhu.ac.in; pradip.paik@gmail.com*

† Electronic supplementary information (ESI) available: Fig. S1–S3. See DOI: 10.1039/d0ra04505e

‡ These authors contributed equally.

Cancer Letters 518 (2021) 243–255

Contents lists available at ScienceDirect

Cancer Letters

journal homepage: www.elsevier.com/locate/canlet

HPIP protooncogene differentially regulates metabolic adaptation and cell fate in breast cancer cells under glucose stress via AMPK and RNF2 dependent pathways

Vasudevarao Penugurti [a], Saratchandra Singh Khumukcham [a], Chiranjeevi Padala [a], Anju Dwivedi [a], Karthik Reddy Kamireddy [b,d], Srinivasulu Mukta [c], Triveni Bhopal [c], Bramanandam Manavathi [a,*]

[a] Molecular and Cellular Oncology Laboratory, Department of Biochemistry, School of Life Sciences, University of Hyderabad, Hyderabad, 500046, Telangana, India
[b] Molecular and Cellular Biology Laboratory, Baylor College of Medicine, Houston, TX, United States
[c] MNJ Institute of Oncology and Regional Cancer Center, Hyderabad, 500004, Telangana, India
[d] Indian Institute of Chemical Technology, Hyderabad, Telangana, 500007, India

ARTICLE INFO

Keywords:
HPIP
FOXO3a
AMPK
MYC
Cell survival
Apoptosis
Glutaminolysis

ABSTRACT

While cancer cells rewire metabolic pathways to sustain growth and survival under metabolic stress in solid tumors, the molecular mechanisms underlying these processes remain largely unknown. In this study, cancer cells switched from survival to death during the early to late phases of metabolic stress by employing a novel signaling switch from AMP activated protein kinase (AMPK)-Forkhead box O3 (FOXO3a)-hematopoietic PBX1-interacting protein (HPIP) to the ring finger protein 2 (RNF2)-HPIP-ubiquitin (Ub) pathway. Acute metabolic stress induced proto-oncogene *HPIP* expression in an AMPK-FOXO3a-dependent manner in breast cancer (BC) cells. HPIP depletion reduced cell survival and tumor formation in mouse xenografts, which was accompanied by diminished intracellular ATP levels and increased apoptosis in BC cells in response to metabolic (glucose) stress. Glutamine flux (^{13}C-labeled) analysis further suggested that HPIP rewired glutamine metabolism by controlling the expression of the solute carrier family 1 member 5 (SLC1A5) and glutaminase (GLS) genes by acting as a coactivator of MYC to ensure cell survival upon glucose deprivation. However, in response to chronic glucose stress, HPIP was ubiquitinated by the E3-Ub ligase, RNF2, and was concomitantly degraded by the proteasome-mediated pathway, ensuring apoptosis. In support of these data, clinical analyses further indicated that elevated levels of HPIP correlated with AMPK activation in BC. Taken together, these data suggest that HPIP is a signal coordinator during metabolic stress and thus serves as a potential therapeutic target in BC.

1. Introduction

For rapidly dividing cells, such as cancer cells, there is a huge demand for metabolic energy to synthesize various biomolecules. To accomplish this, cancer cells often rewire metabolic pathways to suit their needs [1–3]. As glucose is the main energy and carbon source for rapidly dividing cells, cancer cells rely on glycolysis to generate energy; however, under glucose stress, glutamine is utilized as an anaplerotic substance for ATP generation and to control redox homeostasis, thus ensuring cell survival [1,4,5]. Typically, reduced expression of tumor suppressor genes and increased oncogenic gene expression is observed in cancer cells during metabolic stress as a part of cellular adaptation [6]. For example, oncogenes, such as protein kinase B (AKT), c-MYC (hereafter referred to as MYC), and Ras are overexpressed under metabolic stress to support cancer cell survival [7].

A balance between energy production and consumption dictates cell survival under metabolic stress [8]. Accordingly, in such situations, tumor cells acquire certain adaptations for their survival by suppressing energy-consuming pathways and promoting energy-producing pathways [9]. One such adaptation is the expression of AMP activated protein kinase (AMPK), a metabolic sensor, which is activated in response to a low ATP:AMP ratio in cells [10,11]. For example, AMPK-mediated pyruvate kinase M1 expression is essential for cell survival under hypoglycemic conditions [12] and modulates the expression of

* Corresponding author.
E-mail address: manavathibsl@uohyd.ac.in (B. Manavathi).

https://doi.org/10.1016/j.canlet.2021.07.027
Received 23 April 2021; Received in revised form 27 June 2021; Accepted 19 July 2021
Available online 22 July 2021

The FEBS Journal

FEBS PRESS science publishing by scientists

Hematopoietic PBX-interacting protein is a novel regulator of mammary epithelial cell differentiation

Anju Dwivedi[1], Chiranjeevi Padala[1], Anita Kumari[1], Saratchandra Singh Khumukcham[1], Vasudevarao Penugurti[1], Sinjini Ghosh[2], Aprotim Mazumder[2], Vincent Goffin[3] and Bramanandam Manavathi[1]

1 Department of Biochemistry, School of Life Sciences, University of Hyderabad, India
2 TIFR Centre for Interdisciplinary Sciences, Tata Institute of Fundamental Research Hyderabad, India
3 Institut Necker Enfants Malades (INEM), Inserm U1151/CNRS 8253, Université de Paris, France

Keywords
HPIP; lactogenic differentiation; miR-148a; PI3K-AKT signaling; prolactin signaling

Correspondence
B. Manavathi, Department of Biochemistry, School of Life Sciences, University of Hyderabad, Hyderabad-500046, India
Tel: +914023134546
E-mails: manavathibsl@uohyd.ac.in; manavathi.hcu@gmail.com

(Received 12 March 2021, revised 6 September 2021, accepted 19 October 2021)

doi:10.1111/febs.16242

Hematopoietic PBX-interacting protein (HPIP, also known as PBXIP1) is an estrogen receptor (ER) interacting protein that regulates estrogen-mediated breast cancer cell proliferation and tumorigenesis. However, its functional significance in the context of mammary gland development is unexplored. Here, we report that HPIP is required for prolactin (PRL)-induced lactogenic differentiation *in vitro*. Molecular analysis of HPIP expression in mice revealed its induced expression at pregnancy and lactation stages of mammary gland. Moreover, PRL is a lactogenic hormone that controls pregnancy as well as lactation and induces *Hpip*/*Pbxip1* expression in a signal transducer and activator of transcription 5a-dependent manner. Using mammary epithelial and lactogenic-competent cell lines, we further show that HPIP plays a regulatory role in PRL-mediated mammary epithelial cell differentiation, which is measured by acini formation, β-casein synthesis, and lipid droplet formation. Further mechanistic studies using pharmacological inhibitors revealed that HPIP modulates PRL-induced β-casein synthesis via phosphoinositide 3-kinase (PI3K)/protein kinase B (AKT) activation. This study also identified HPIP as a critical regulator of autocrine PRL signaling as treatment with the PRL receptor antagonist Δ1-9-G129R-hPRL restrained HPIP-mediated PRL synthesis, AKT activation, and β-casein synthesis in cultured HC11 cells. Interestingly, we also uncovered that microRNA-148a (miR-148a) antagonizes HPIP-mediated mammary epithelial cell differentiation. Together, our study identified HPIP as a critical regulator of PRL signaling and revealed a novel molecular circuitry involving PRL, HPIP, PI3K/AKT, and miR-148a that controls mammary epithelial cell differentiation *in vitro*.

Introduction

Mammary glands are highly evolved, specialized exocrine glands made up of lobes, and ducts [1]. The alveoli (hollow cavities) in mammary glands are lined with milk-secreting cuboidal cells and are surrounded by myoepithelial cells. The alveolus undergoes development and differentiation under the control of

Abbreviations
AKT, protein kinase B; bPRL, bovine prolactin; HPIP, hematopoietic PBX-interacting protein; JAK2, Janus kinase 2; miR-148a, microRNA-148a; PI3K, phosphoinositide 3-kinase; PRL, Prolactin; PRLR, prolactin receptor; PTEN, phosphatase and tensin homolog deleted on chromosome 10; STAT5, signal transducer and activator of transcription 5.

PLOS BIOLOGY

RESEARCH ARTICLE

Amino acid starvation sensing dampens IL-1β production by activating riboclustering and autophagy

Srikanth Battu[1], Sumbul Afroz[1], Jeevan Giddaluru[1], Saima Naz[2], Weishan Huang[3], Saratchandra Singh Khumukcham[4], Rafiq Ahmad Khan[1], Saleem Yousuf Bhat[1], Insaf Ahmed Qureshi[1], Bramanandam Manavathi[4], Aleem Ahmed Khan[2], Avery August[3], Seyed Ehtesham Hasnain[5,6,7], Nooruddin Khan[1]*

1 Department of Biotechnology and Bioinformatics, School of Life Sciences, University of Hyderabad, Hyderabad, Telangana, India, **2** Centre for Liver Research and Diagnostics, Central Laboratory for Stem Cell Research and Translational Medicine, Deccan College of Medical Sciences, Kanchanbagh, Hyderabad, Telangana, India, **3** Department of Microbiology and Immunology, College of Veterinary Medicine, Cornell University, Ithaca, New York, United States of America, **4** Department of Biochemistry, School of Life Sciences, University of Hyderabad, Hyderabad, Telangana, India, **5** JH-Institute of Molecular Medicine, Jamia Hamdard University, Hamdard Nagar, New Delhi, India, **6** Molecular Infection and Functional Biology Laboratory, Kusuma School of Biological Sciences, Indian Institute of Technology, New Delhi, India, **7** Dr Reddy's Institute of Life Sciences, University of Hyderabad Campus, Hyderabad, Telangana, India

* noor@uohyd.ac.in

Citation: Battu S, Afroz S, Giddaluru J, Naz S, Huang W, Khumukcham SS, et al. (2018) Amino acid starvation sensing dampens IL-1β production by activating riboclustering and autophagy. PLoS Biol 16(4): e2005317. https://doi.org/10.1371/journal.pbio.2005317

Academic Editor: Douglas Green, St. Jude Childrens Research Hospital, Memphis, United States of America

Received: January 9, 2018

Accepted: March 5, 2018

Published: April 5, 2018

Data Availability Statement: All relevant data are within the paper and its Supporting information files.

Funding: Department of Biotechnology, Govt. of India http://www.dbtindia.nic.in/ (grant number BT/PR8624/MED/29/798/2013). The funder had no role in study design, data collection and analysis, decision to publish, or preparation of the manuscript. Nano Mission Council, Department of Science and Technology http://nanomission.gov.in/

Abstract

Activation of the amino acid starvation response (AAR) increases lifespan and acute stress resistance as well as regulates inflammation. However, the underlying mechanisms remain unclear. Here, we show that activation of AAR pharmacologically by Halofuginone (HF) significantly inhibits production of the proinflammatory cytokine interleukin 1β (IL-1β) and provides protection from intestinal inflammation in mice. HF inhibits IL-1β through general control nonderepressible 2 kinase (GCN2)–dependent activation of the cytoprotective integrated stress response (ISR) pathway, resulting in rerouting of IL-1β mRNA from translationally active polysomes to inactive ribocluster complexes—such as stress granules (SGs)—via recruitment of RNA-binding proteins (RBPs) T cell–restricted intracellular antigen-1 (TIA-1)/TIA-1–related (TIAR), which are further cleared through induction of autophagy. GCN2 ablation resulted in reduced autophagy and SG formation, which is inversely correlated with IL-1β production. Furthermore, HF diminishes inflammasome activation through suppression of reactive oxygen species (ROS) production. Our study unveils a novel mechanism by which IL-1β is regulated by AAR and further suggests that administration of HF might offer an effective therapeutic intervention against inflammatory diseases.

Author summary

Reduced intake of food (also known as dietary restriction) without malnutrition has been shown to benefit health in humans and animals, including an increase in life expectancy, metabolic fitness, and resistance to acute stress. Recent studies have attributed the benefits

Biochem. J. (2016) **473**, 1047–1061 doi:10.1042/BCJ20160019

A transcriptional repressive role for epithelial-specific ETS factor ELF3 on oestrogen receptor alpha in breast cancer cells

Vijaya Narasihma Reddy Gajulapalli*, Venkata Subramanyam Kumar Samanthapudi*, Madhusudana Pulaganti†, Saratchandra Singh Khumukcham*, Vijaya Lakhsmi Malisetty‡, Lalitha Guruprasad§, Suresh Kumar Chitta† and Bramanandam Manavathi*[1]

*Molecular and Cellular Oncology Laboratory, Department of Biochemistry, School of Life Sciences, University of Hyderabad, Hyderabad 500046, Telangana, India
†Department of Biochemistry, Sri Krishnadevaraya University, Anantapur 515003, Andhra Pradesh, India
‡Department of Biotechnology, Acharya Nagarjuna University, Guntur, Andhra Pradesh, India
§School of Chemistry, University of Hyderabad, Hyderabad 500046, Telangana, India

Oestrogen receptor-α (ERα) is a ligand-dependent transcription factor that primarily mediates oestrogen (E2)-dependent gene transcription required for mammary gland development. Coregulators critically regulate ERα transcription functions by directly interacting with it. In the present study, we report that ELF3, an epithelial-specific ETS transcription factor, acts as a transcriptional repressor of ERα. Co-immunoprecipitation (Co-IP) analysis demonstrated that ELF3 strongly binds to ERα in the absence of E2, but ELF3 dissociation occurs upon E2 treatment in a dose- and time-dependent manner suggesting that E2 negatively influences such interaction. Domain mapping studies further revealed that the ETS (E-twenty six) domain of ELF3 interacts with the DNA binding domain of ERα. Accordingly, ELF3 inhibited ERα's DNA binding activity by preventing receptor dimerization, partly explaining the mechanism by which ELF3 represses ERα transcriptional activity. Ectopic expression of ELF3 decreases ERα transcriptional activity as demonstrated by oestrogen response elements (ERE)-luciferase reporter assay or by endogenous ERα target genes. Conversely ELF3 knockdown increases ERα transcriptional activity. Consistent with these results, ELF3 ectopic expression decreases E2-dependent MCF7 cell proliferation whereas ELF3 knockdown increases it. We also found that E2 induces *ELF3* expression in MCF7 cells suggesting a negative feedback regulation of ERα signalling in breast cancer cells. A small peptide sequence of ELF3 derived through functional interaction between ERα and ELF3 could inhibit DNA binding activity of ERα and breast cancer cell growth. These findings demonstrate that ELF3 is a novel transcriptional repressor of ERα in breast cancer cells. Peptide interaction studies further represent a novel therapeutic option in breast cancer therapy.

Key words: breast cancer, epithelial-specific ETS transcription factor-1 (ESE1/ELF3), oestrogen receptor alpha, transcriptional repression.

INTRODUCTION

The oestrogen receptor alpha (ERα) belongs to a large family of nuclear hormone receptors that mediate oestrogen (17β-oestradiol)-induced mammary epithelial cell proliferation and ductal formation required for mammary gland development [1–4]. Deregulated expression of ERα is therefore implicated in the development of ER-positive breast cancer [5,6]. Approximately 70% of breast tumours are ER-positive and respond well to anti-oestrogen therapy, whereas ER-negative breast tumours are poorly differentiated and display a worse prognosis [7–9]. Although selective ER modulators (SERMs) and anti-oestrogens are effective against ER-positive breast tumours, in many cases metastatic breast tumours eventually become resistant to this treatment [10].

ERα, a ligand-inducible transcription factor, contains three discrete domains namely, a core DNA binding domain (DBD), a hinge region and two activation function (AF1 and AF2) domains. The DBD is involved in recognizing oestrogen response elements (ERE) on ER target genes [1]. The hinge region is a flexible coil that connects DBD and AF2 domain (also known as ligand binding domain, LBD), and is also shown to be involved in ERα dimerization [11,12]. Activation function 1 (AF-1) acts as hormone-independent, whereas activation function 2 (AF2) binds to oestrogen and mediates oestrogen-dependent actions [1]. Upon ligand binding, ERα dimerizes and translocates into nucleus where it binds to EREs on target genes, and elicits transcriptional response [1,13]. However, ERα requires coregulators for its optimal activity [14,15]. Coregulators modulate oestrogen receptor transcriptional activity by modulating the chromatin structure [16–19]. Additional mechanisms also exist for regulating ER transcriptional activity. For instance, transcription factors like activator protein 1 (AP1), Sp1, nuclear factor-κB (NF-κB) and E2F1 can influence ERα-dependent gene transcription through their physical interactions with the receptor [20]. We identified that ELF3, also a transcription factor, is an ERα interacting protein. However, the mechanism by which ELF3 influences ERα action remains largely unknown.

Epithelial-specific ETS transcription factor-1 (ELF3, also known as ESE-1) belongs to a family of ETS (E-twenty six) transcription factors which play a crucial role in various physiological processes [21]. ELF3 is expressed in organs

Abbreviations: AF-1, activation function 1; Co-IP, co-immunoprecipitation; DAPI, 4′,6-diamidino-2-phenylindole; DBD, DNA binding domain; ELF3/ESE1, epithelial-specific ETS transcription factor-1/E74 like ETS transcription factor-3; ERα, oestrogen receptor alpha; ERE, oestrogen response element; ERIPE, ERα-interacting peptide of ELF3; ETS, E-twenty six; GFP, green fluorescent protein; LBD, ligand binding domain; qRT-PCR, quantitative real-time reverse transcription PCR; SERM, selective oestrogen receptor modulator.

[1] To whom correspondence should be addressed (email manavathibsl@uohyd.ernet.in).

Certificates
(Awards and recognitions)

Department of Biochemistry

Award for Research Proficiency to

Khumukcham SS,

Title: Hematopoietic PBX-interacting protein is a substrate and an inhibitor of the APC/c-cdc20 complex and regulates mitosis by stabilizing cyclin B1.

Published in: Journal of Biological Chemistry. 2019.

Prof. Mrinal Kanti Bhattacharyya
Head of Department

Indian Society Of Cell Biology

Sanatchandra KH

is awarded the Professor V C Shah memorial prize for best paper presentation in poster session during the International Congress of Cell Biology organized by CSIR-Centre for Cellular and Molecular Biology, Hyderabad from 27th to 31st January 2018.

Pradeep K. Burma
Secretary

Jagat K. Roy
President

Award Certificate

This is to certify that

Mr./Ms./Dr. Kh. Saratchandra Singh has secured Winner (1st) position

in poster presentation event at

"Phenotypic heterogeneity as a driver of cancer progression"

conference held from 5-6th January, 2019 at the Indian Institute of Science, Bengaluru

Organizing Committee

Funder:

IDRC CRDI Canada

Organizers:

SickKids

האוניברסיטה העברית בירושלים
THE HEBREW UNIVERSITY OF JERUSALEM

הפקולטה לרפואה
FACULTY OF MEDICINE

INDIAN INSTITUTE OF SCIENCE
भारतीय विज्ञान संस्थान

UN UNIVERSITÄT ZU LÜBECK
INSTITUT FÜR PHYSIOLOGIE

Institut für Physiologie, Universität zu Lübeck, Ratzeburger Allee 160,
23562 Lübeck

Dr. Reinhard Depping
Lübeck, den 09.12.2019
Telefon: +49 451 - 3101 7310
Telefax: +49 451 - 3101 7304
E-Mail: Reinhard.Depping@uni-luebeck.de

To whom it may concern

It is our pleasure to confirm that Kh. Saratchandra Singh, was joining our research group at the Institute of Physiology in Lübeck as part of the DST-DAAD project 57452615 to expand his knowledge on CRIPSR based methods.

Kh. Saratchandra Singh started his work here on October 21, 2019 and stayed until December 9, 2019

We are very pleased to have had Kh. Saratchandra Singh here to practice the techniques that are currently used in our laboratory.

The experiments were as follows:

1. Crispr mediated knock out of siva1 in mcf7, a breast cancer cell line.
2. Cloning and characterisation of siva1 promoter

With best regards

Reinhard Depping

प्रतिष्ठित संस्थान
INSTITUTION OF EMINENCE
राष्ट्रीय आवश्यकता, वैश्विक मानक
National Needs, Global Standards
हैदराबाद विश्वविद्यालय

Bramanandam Manavathi, PhD.,
Professor
Dept. of Biochemistry
School of Life Sciences
University of Hyderabad
Hyderabad, 500046.TS
INDIA

CERTIFICATE

This is to certify that the similarity index of this thesis, as evaluated by the librarian of the University of Hyderabad, is 30%. There is a 24% similarity in Saratchandra Singh Khumukcham's publications.

- 24% from the publications mentioned here:

1. **Saratchandra Singh Khumukcham, Bramanandam Manavathi**. "Two decades of a protooncogene HPIP/PBXIP1: Uncovering the tale from germ cell to cancer", Biochimica et Biophysica Acta (BBA) - Reviews on Cancer, 2021. (**22% Similarity**)
2. Vasudevarao Penugurti, **Saratchandra Singh Khumukcham**, Chiranjeevi Padala, Anju Dwivedi et al. "HPIP protooncogene differentially regulates metabolic adaptation and cell fate in breast cancer cells under glucose stress via AMPK and RNF2 dependent pathways", Cancer Letters, 2021. (**1% Similarity)**
3. **Saratchandra Singh Khumukcham**, Venkata Subramanyam Kumar Samanthapudi, Vasudevarao Penugurti, Anita Kumari et al. "Hematopoietic PBX-interacting protein is a substrate and an inhibitor of the APC/C– Cdc20 complex and regulates mitosis by stabilizing cyclin B1", Journal of Biological Chemistry, 2019. (**<1% Similarity)**

- In the current thesis, only ~7% similarity was found from external sources such as internet and other publications. Hence the present thesis considered free of plagiarism.

Prof. Bramanandam Manavathi, PhD.
Supervisor

Prof. Bramanandam Manavathi, PhD
Department of Biochemistry
School of Life Sciences
University of Hyderabad
Hyderabad-500 046. (TS), INDIA

Crosstalk between tumor microenvironment and HIF-1α-HPIP loop establishes phenotypic plasticity in breast cancer cells: Implications in tumor development and metastasis

by Saratchandra Singh Khumukcham

Submission date: 05-Nov-2021 02:36PM (UTC+0530)
Submission ID: 1693759035
File name: Thesis_PhD_Sarat_antipalagirsm.docx (13.6M)
Word count: 19610
Character count: 114092

Crosstalk between tumor microenvironment and HIF-1α-HPIP loop establishes phenotypic plasticity in breast cancer cells: Implications in tumor development and metastasis

ORIGINALITY REPORT

30%	7%	30%	2%
SIMILARITY INDEX	INTERNET SOURCES	PUBLICATIONS	STUDENT PAPERS

PRIMARY SOURCES

1	Saratchandra Singh Khumukcham, Bramanandam Manavathi. "Two decades of a protooncogene HPIP/PBXIP1: Uncovering the tale from germ cell to cancer", Biochimica et Biophysica Acta (BBA) - Reviews on Cancer, 2021 Publication	22%
2	Vasudevarao Penugurti, Saratchandra Singh Khumukcham, Chiranjeevi Padala, Anju Dwivedi et al. "HPIP protooncogene differentially regulates metabolic adaptation and cell fate in breast cancer cells under glucose stress via AMPK and RNF2 dependent pathways", Cancer Letters, 2021 Publication	1%
3	jeccr.biomedcentral.com Internet Source	<1%
4	www.jbc.org Internet Source	<1%

From students own publication

Prof. Bramanandam Manavathi, PhD
Department of Biochemistry
School of Life Sciences
University of Hyderabad
Hyderabad-500 046. (TS), INDIA

From students publication

Prof. Bramanandam Manavathi, PhD
Department of Biochemistry
School of Life Sciences
University of Hyderabad
Hyderabad-500 046. (TS), INDIA

5	www.mdpi.com Internet Source	<1 %
6	www.frontiersin.org Internet Source	<1 %
7	Abdol-Hossein Rezaeian, Chien-Feng Li, Ching-Yuan Wu, Xian Zhang et al. "A hypoxia-responsive TRAF6–ATM–H2AX signalling axis promotes HIF1α activation, tumorigenesis and metastasis", Nature Cell Biology, 2016 Publication	<1 %
8	www.ncbi.nlm.nih.gov Internet Source	<1 %
9	Myron K. Evans, Michael C. Brown, Joseph Geradts, Xuhui Bao et al. "XIAP Regulation by MNK Links MAPK and NFκB Signaling to Determine an Aggressive Breast Cancer Phenotype", Cancer Research, 2018 Publication	<1 %
10	Submitted to Leiden University Student Paper	<1 %
11	link.springer.com Internet Source	<1 %
12	www.nature.com Internet Source	<1 %
13	worldwidescience.org Internet Source	<1 %

14	Submitted to University of Hyderabad, Hyderabad Student Paper	<1 %
15	www.spandidos-publications.com Internet Source	<1 %
16	spandidos-publications.com Internet Source	<1 %
17	www.thno.org Internet Source	<1 %
18	Submitted to The Hong Kong Polytechnic University Student Paper	<1 %
19	www.atsjournals.org Internet Source	<1 %
20	apps.dtic.mil Internet Source	<1 %
21	Saratchandra Singh Khumukcham, Venkata Subramanyam Kumar Samanthapudi, Vasudevarao Penugurti, Anita Kumari et al. "Hematopoietic PBX-interacting protein is a substrate and an inhibitor of the APC/C–Cdc20 complex and regulates mitosis by stabilizing cyclin B1", Journal of Biological Chemistry, 2019 Publication	<1 %

Prof. Bramanandam Manavathi, PhD
Department of Biochemistry
School of Life Sciences
University of Hyderabad
Hyderabad-500 046. (TS), INDIA

22	Piyush B. Gupta, Christine M. Fillmore, Guozhi Jiang, Sagi D. Shapira, Kai Tao, Charlotte Kuperwasser, Eric S. Lander. "Stochastic State Transitions Give Rise to Phenotypic Equilibrium in Populations of Cancer Cells", Cell, 2011 Publication	<1 %
23	Z. Wang, Y. Wu, H. Wang, Y. Zhang et al. "Interplay of mevalonate and Hippo pathways regulates RHAMM transcription via YAP to modulate breast cancer cell motility", Proceedings of the National Academy of Sciences, 2013 Publication	<1 %
24	cancerci.biomedcentral.com Internet Source	<1 %
25	Dehu Chen, Haihua Zhou, Guiyuan Liu, Yinghai Zhao, Gan Cao, Qinghong Liu. "SPOCK1 promotes the invasion and metastasis of gastric cancer through Slug-induced epithelial-mesenchymal transition", Journal of Cellular and Molecular Medicine, 2017 Publication	<1 %
26	Wang, Wenbo, Lei Yang, Liu Hu, Fen Li, Li Ren, Haijun Yu, Yu Liu, Ling Xia, Han Lei, Zhengkai Liao, Fuxiang Zhou, Conghua Xie, and Yunfeng Zhou. "Inhibition of UBE2D3 Expression Attenuates Radiosensitivity of MCF-7 Human	<1 %

Breast Cancer Cells by Increasing hTERT Expression and Activity", PLoS ONE, 2013.
Publication

27	D-S Kim, Y-B Choi, B-G Han, S-Y Park, Y Jeon, D-H Kim, E-R Ahn, J-E Shin, B I Lee, H Lee, K-M Hong, S-Y Kim. "Cancer cells promote survival through depletion of the von Hippel–Lindau tumor suppressor by protein crosslinking", Oncogene, 2011 Publication	<1 %
28	cancerres.aacrjournals.org Internet Source	<1 %
29	pubs.rsc.org Internet Source	<1 %
30	vetsci.org Internet Source	<1 %
31	iovs.arvojournals.org Internet Source	<1 %
32	Emilia Wiechec. "Implications of genomic instability in the diagnosis and treatment of breast cancer", Expert Review of Molecular Diagnostics, 2014 Publication	<1 %
33	José López-Barneo, Patricia González-Rodríguez, Lin Gao, M. Carmen Fernández-Agüera et al. "Oxygen sensing by the carotid body: mechanisms and role in adaptation to	<1 %

hypoxia", American Journal of Physiology-Cell Physiology, 2016
Publication

34	breast-cancer-research.biomedcentral.com Internet Source	<1 %
35	Eva M. Verdugo-Sivianes, Lola Navas, Sonia Molina-Pinelo, Irene Ferrer et al. "Coordinated downregulation of Spinophilin and the catalytic subunits of PP1, PPP1CA/B/C, contributes to a worse prognosis in lung cancer", Oncotarget, 2017 Publication	<1 %
36	Li-Min Xia. "Transcriptional up-regulation of FoxM1 in response to hypoxia is mediated by HIF-1", Journal of Cellular Biochemistry, 02/01/2009 Publication	<1 %
37	bmccancer.biomedcentral.com Internet Source	<1 %
38	journals.plos.org Internet Source	<1 %
39	pharmaceuticalintelligence.com Internet Source	<1 %
40	synapse.koreamed.org Internet Source	<1 %

41	Berger, A., E. Ivanova, C. Gareau, A. Scherrer, R. Mazroui, and K. Strub. "Direct binding of the Alu binding protein dimer SRP9/14 to 40S ribosomal subunits promotes stress granule formation and is regulated by Alu RNA", Nucleic Acids Research, 2014. Publication	<1 %
42	academic.oup.com Internet Source	<1 %
43	downloads.hindawi.com Internet Source	<1 %
44	elifesciences.org Internet Source	<1 %
45	etheses.bham.ac.uk Internet Source	<1 %
46	journals.sagepub.com Internet Source	<1 %
47	Ajeet Kumar Gandhi, Pavnesh Kumar, Menal Bhandari, Bharti Devnani, Goura Kishor Rath. "Burden of preventable cancers in India: Time to strike the cancer epidemic", Journal of the Egyptian National Cancer Institute, 2017 Publication	<1 %
48	en.wikipedia.org Internet Source	<1 %
	gird.cn	

49	Internet Source	<1%
50	mcb.asm.org Internet Source	<1%
51	jcmtjournal.com Internet Source	<1%
52	molecular-cancer.biomedcentral.com Internet Source	<1%
53	www.biomedcentral.com Internet Source	<1%
54	www.jci.org Internet Source	<1%
55	www.scbt.com Internet Source	<1%
56	H. Yagi, W. Tan, P. Dillenburg-Pilla, S. Armando et al. "A Synthetic Biology Approach Reveals a CXCR4-G13-Rho Signaling Axis Driving Transendothelial Migration of Metastatic Breast Cancer Cells", Science Signaling, 2011 Publication	<1%
57	Maciej Suski, Anna Wiśniewska, Aneta Stachowicz, Rafał Olszanecki et al. "The influence of AICAR - direct activator of AMP-activated protein kinase (AMPK) - on liver	<1%

proteome in apoE-knockout mice", European Journal of Pharmaceutical Sciences, 2017
Publication

58	Submitted to Savitribai Phule Pune University Student Paper	<1 %
59	livrepository.liverpool.ac.uk Internet Source	<1 %
60	www.biorxiv.org Internet Source	<1 %
61	"Abstract", Breast Cancer Research and Treatment, 2006 Publication	<1 %
62	Submitted to Aston University Student Paper	<1 %
63	Fahim Ullah Khan, Nana Yaa Gyaama Owusu-Tieku, Xiaoyong Dai, Kewei Liu et al. "Wnt/β-Catenin Pathway-Regulated Fibromodulin Expression Is Crucial for Breast Cancer Metastasis and Inhibited by Aspirin", Frontiers in Pharmacology, 2019 Publication	<1 %
64	doi.org Internet Source	<1 %
65	ijcep.com Internet Source	<1 %

nagoya.repo.nii.ac.jp

66	Internet Source	<1%
67	rupress.org Internet Source	<1%
68	web16.bernama.com Internet Source	<1%
69	www.oncotarget.com Internet Source	<1%

Exclude quotes	On	Exclude matches	< 14 words
Exclude bibliography	On		